The University Of Sheffield.

Polymer Based Inhibition of Quorum Sensing in Gram Negative Bacteria

Rawan Mohammed S Alshalan

The University of Sheffield
Faculty of Medicine, Dentistry and Health
Academic Unit of Oral & Maxillofacial Medicine and Pathology
School of Clinical Dentistry

2022

Acknowledgments

First and foremost, I would like to express my sincere gratitude to my supervisor, Dr Joey Shepherd, for her endless support, encouragement, and guidance during my PhD studies. I feel extremely lucky to be part of her research team. I want to thank prof Graham P Stafford, my second supervisor, for her invaluable contributions and suggestions. A big thank you to all the technical staff who helped me these last four years; Brenka, Jason, Emilia, and Matt. Special thanks to my colleagues in the Micro group. I must express my gratitude to the University of Saud for funding for my doctoral degree. My Mom, whom I missed dearly (Hassah Alsalem), and my sister (Amjad Alshalan).No words to express my deep gratitude to you for supporting me through my studies and life.

Presentations

Oral presentation:

- First year talk titled “Polymer based inhibition of Quorum Sensing in Gram negative Bacteria.” The University of Sheffield School of Clinical Dentistry PGR day, Sheffield, 2020.
- Third year talk titled “Polymer based inhibition of Quorum Sensing in Gram negative Bacteria.” The University of Sheffield School of Clinical Dentistry, Sheffield, 2021.

Poster presentation:

- “Polymer based inhibition of Quorum Sensing in Gram negative Bacteria.” BSODR, at the University of Leads, Leeds,2019.
- **“**Polymer based inhibition of Quorum Sensing in Gram negative Bacteria.” EPSRC CDT in Advanced Biomedical Materials meeting. The University of Sheffield, Sheffield, 2020.
- “Polymer based inhibition of Quorum Sensing in Gram negative Bacteria.” The 8th Global Conference on Polymer and Composite Materials (PCM 2021). Macau, China, 2021 (online).
- “Polymer based inhibition of Quorum Sensing in Gram negative Bacteria.” Cell–Cell Communication in Bacteria: Fundamental and Applied Aspects Meeting, Robinson College, Cambridge, 2022
- “Polymer based inhibition of Quorum Sensing in Gram negative Bacteria.” Early Career Microbiologists (ECM), Forum Summer Conference, The University of Sheffield, Sheffield, 2022.

Prizes:

- First place for the best poster at the “Poster Competition for the Faculty of Medicine,” Dentistry, and Health, PGR day, 2021 (online).

Table of Contents

I. List of figures

II. List of tables

III. Abbreviations

3-oxo-C12-AHL	N -3-oxo-dodecanoyl-L-homoserine lactone
AHL	N-acyl-homoserine lactone
AI	Autoinducer
AMR	antimicrobial resistance
bioassay	Biological assay
Bp	Base pair
C	Carbon
C. violaceum	*Chromobacterium violaceum*
C4-AHL	N -butanoyl-L-homoserine lactone
C6-AHL	N-hexanoyl-l-homoserine lactone
cDNA	Complementary deoxyribonucleic acid
CF	Cystic fibrosis
CFU	Colony forming units
Ct	Threshold cycle
CV	Crystal violet
CV026	*Chromobacterium violaceum* 026
CviR	*Chromobacterium violaceum* QS receptor
DALY	Disability-adjusted life year
DMSO	Dimethyl sulfoxide
DNA	Deoxyribonucleic acid
DNase	Deoxyribonuclease
dNTP	Deoxyribonucleotide triphosphate
E.coli	*Escherichia coli*
ECR	Elastin –Congo red
eDNA	Extracellular DNA
EPS	Extracellular polymeric substances
EU	European Union
Fap	Functional amyloid in Pseudomonas
g	Gravity
Gbps	Glucan-binding proteins
h	Hour
HB-PINIAPAM-HL	Highly branched poly(N-isopropylacrylamide)with homoserine lactone functionalised ending
HHQ	2-heptyl-4-(1H)-hydroxyquinolone
HQNO	2-n-heptyl-4-hydroxyquinolone-N-oxide
AHL	Homoserine lactone
Kb	Kilobase
LasI	*Pseudomonas aeruginosa* AHLs synthase
LasR	*Pseudomonas aeruginosa* QS receptor
LB	Luria-Bertani
LCST	lower critical solution temperature
LuxM	*V. harveyi* AHLs synthase
LuxI	*V fischeri* AHLs synthase
LuxR	*V fischeri* QS receptor
M	Molar
mg	Milligram
mM	Milimolar
mm	Millimeter
nm	Nanometer
ºC	Degree Celcius
OD	Optical density
P. aeruginosa	*Pseudomonas aeruginosa*
PBP	Penicillin-binding protein
PBS	Phosphate buffered saline
PCN	Pyocyanin
PCR	Polymerase chain reaction
pH	Acidity measurement unit
PNIPAM	Poly(N-isopropylacrylamide)

PQS	Pseudomonas quinolone signal
qPCR	Quantitative polymerase chain reaction
QS	Quorum sensing
RhlI	*Pseudomonas aeruginosa* AHLs synthase
RhlR	*Pseudomonas aeruginosa* QS receptor
RNA	Ribonucleic acid
RNase	Ribonuclease
rpm	Rotations per minute
RT-PCR	Reverse transcriptase polymerase chain reaction
SCVP-RAFT	Self-condensing reversible addition fragmentation transfer polymerization
TAE	Tris acetate EDTA
TCA	Trichloroacetic acid
UV	Ultraviolet
V	Volt
V fischeri	*Vibrio fischeri*
VFs	Virulence factors
w/v	Weight by volume
µl	Microlitre

IV. Abstract

Background: Bacterial quorum sensing (QS) is involved in several pathogenic bacterial processes, such as production of tissue-destroying enzymes, pyocyanin, and rhamnolipids, and biofilm formation. QS -mediated infectious diseases caused by bacteria make QS an important target for the development of materials with a novel antibacterial mode of action.

Aim: To evaluate the anti- QS ability of the polymer HB-PINPAM-HL, a hyperbranched poly(NIPAM) polymer with chain ends uniquely functionalised with homoserine lactone ($C_4H_7NO_2$) on two Gram-negative bacteria *Chromobacterium violaceum* CV026 and *Pseudomonas aeruginosa* PAO1.

Method: The polymer HB-PNIPAM-HL was first assessed for inhibition of QS in the model organism *Chromobacterium violaceum* CV026, and then in the pathogen *Pseudomonas aeruginosa* PAO1 indirectly by measuring different virulence factors (VFs). Then, the differential gene expression of bacterial genes involved in QS and VFs pathways regulated by QS systems was directly assessed following treatment with HB-PNIPAM-HL and HB-PNIPAM-succ, an intermediate polymer formed during the process of HB-PNIPAM-HL production. Further analyses of the effects of the polymers on human cells were performed, which included a cytotoxicity assay and a wound healing assay (migration assay). Subsequently, the anti-QS actions of the two polymers were tested in early (2h) and late (24h) *P.aeruginosa* infections in a tissue-based wound infection model.

Results: HB-PNIPAM-HL at 128 μg/ml can significantly reduce production of the violacein pigment in *C.violaceum* CV026 and down-regulate the gene *cviR*, encoding the QS receptor, in addition to three genes directly encoding the violacein genes. HB-PNIPAM-HL incubated with *P.aeruginosa* at 256 μg/ml can significantly reduce the production of several VFs such as protease, elastase, pyocyanin, rhamnolipids and biofilm, anti-QS. There was no cytotoxic effect on either of the cell lines tested at up to 512 μg/ml. In the wound healing assay, there

was no significant delay in cell migration and wound healing at up to 512 μg/ml of HB-PNIPAM-HL, and 256 μg/ml of HB-PNIPAM -succ. In a three-dimensional tissue-engineered human skin wound infection model infected with *P.aeruginosa,* application of HB-PNIPAM-HL at up to 512 μg/ml resulted in less tissue destruction caused by the bacteria when applied 2 hours after infection, but not when applied late, 24 hours after infection.

Conclusion: HB- PNIPAM-HL and HB-PNIPAM -succ show promising anti- QS properties by reducing the virulence and pathogenicity of *P.aeruginosa*. These polymers could be used as an alternative to conventional antibiotics or antibiotic adjacent for wound infections treatment.

Chapter 1: Literature Review

1. Quorum Sensing in Bacteria

Quorum sensing (QS) is a bacterial, density-dependent communication system that initiates and unifies bacterial population behaviours, such as biofilm formation. In 1970, QS was first observed in the symbiotic relationship between the bacteria *Vibrio fischeri* and the *Euprymna scolopes* squid. Once a specific bacterial population density is reached, production of luciferase in *V. fischeri* commences following cell-cell signalling via QS. Luciferase is an enzyme produced by bacteria that catalyses the bioluminescence within the *Euprymna scolopes* squid (Nealson *et al.,* 1970). The *E. scolopes* squid needs the bioluminescent bacterium *V. fischeri* for protection from predators, especially during its nocturnal feeding period, to emits light downwards thus preventing the formation of tell-tale shadows on the seabed This symbiotic relationship begins with the squid ingesting *V. fischeri* from the surrounding seawater, where they are flushed through the squid's mantle cavity and across the surface of the symbiotic light organ, where ciliary movements direct the bacteria into protected zones (Christensen and Visick, 2020). Inside the light organ, *V. fischeri* can increase their population and obtain nutrients such as host-derived lipids and chitin (Ruby, 1996).

Bacteria can survive stressful conditions within a group and through collective behaviour where they would not be able to grow alone, e.g. when exposed to antibiotics, by forming biofilms and antibiotic-degrading enzymes (Yan and Bassler, 2019, Zhao *et al*., 2020). These responses to stress conditions depend on the system QS, where the concentration of signalling molecules, autoinducer (AI), in the environment directly correlates with bacterial population density (Miller *et al.,* 2001).

Bacteria use these low molecular weight AI to communicate efficiently within the community. The term autoinducer come from the bacteria responding to their own signal molecules that they have dispersed (Hense *et al*., 2007). This assumption has been challenged

recently by Smith and Schuster (2022), who found several accessory proteins (*QteE, QslA, and QscR*) in *Pseudomonas aeruginosa* responsible for preventing "autoinducing" or self-sensing. Self-sensing can be defined as the cell density-dependent sensing of signals produced by the same cell. Self-sensing is repressed in bacteria when the density of cells is low. Self-sensing deactivation supports the bimodal expression of genes in bacteria (QS off/on). The bimodal expression is switching the gene expression only when there is enough "quorum" in the environment and switching the expression when the quorum is low. The self-sensing deactivation has been observed in the Gram-positive *Bacillus subtilis* (Brinklov *et al*., 2009), which indicates that stopping self-sensing might be a shared processes between Gram negative and positive bacteria.

The QS communication guided by autoinducer is integral to the survivability of the bacteria within the community. There are four types of AI, which are: autoinducer 1 (AI1), autoinducer 2 (AI2), autoinducer 3 (AI3) and peptides. AI1 is a fatty acid-based signalling molecule used mostly in Gram-negative bacteria (Cao and Meighen, 1989, Rumbaugh *et al*., 1999). AI1 molecules can differ, as some will have shorter or longer carbon chains with or without an acyl side group (**Figure 1, a)**.

AI2 is a universal signalling chemical employed in interspecies communication (**Figure 1 ,b)**. AI 3 is a metabolite exclusively produced by enterohemorrhagic *E. coli* (EHEC), which had an unknown structure for three decades until (Kim *et al*., 2020) identified the structure to be a pyrazine (**Figure 1, c**). Gram-positive bacteria, on the other hand, use peptide signalling molecules rather than fatty acids **(Figure 1, d).**

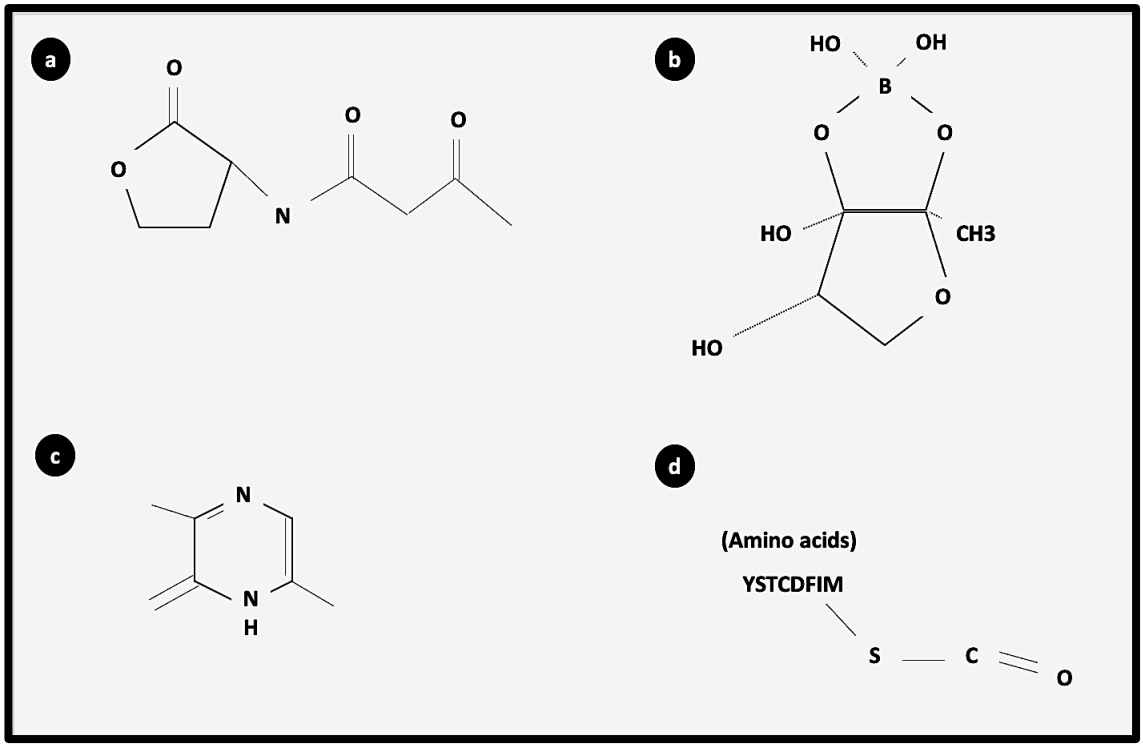

Figure 1: chemical structures of different auto inducers used by bacteria.

(a) Autoinducer 1 (AI1) is a fatty acid signalling molecule used by Gram-negative bacteria. **(b)** Autoinducer 2 (AI2) is a universal signalling molecule used by Gram- negative and positive bacteria. **(c)** Autoinducer 3 (AI3) a pyrazine that exclusively produced by enterohemorrhagic E. coli (EHEC). **(d)** Gram- positives use oligopeptides as a signalling molecule. The peptide signals are composed of 8-9 amino acids and a side chain , that might include a thio-lactone ring (Bassler, 2002).

The dominant QS system in Gram-negative bacteria is the LuxI/LuxR system, which uses AI1 signalling. To explain the QS system, *V.fischeri* will be used as a general example **(Figure 2)** and more details will be given regarding the QS systems in *Pseudomonas aeruginosa* in **section 4.2.** The signal molecules are continuously dispersed into the environment, and the accumulation of these signal molecules indicates that a threshold of bacterial density has been reached. Consequently, a change in the cellular behaviour commences (Downward, 2001). Population density is a condition for initiating gene expression for different QS regulated phenotypes for several reasons. First, the nature of some phenotypes is regulated by QS, which requires a high population density, i.e., biofilm production. Second, high density allows for some individual bacteria to differentiate into subpopulations. This gives

the community a better chance of resistance to any environmental stresses, such as antibiotics (Case *et al*., 2008).

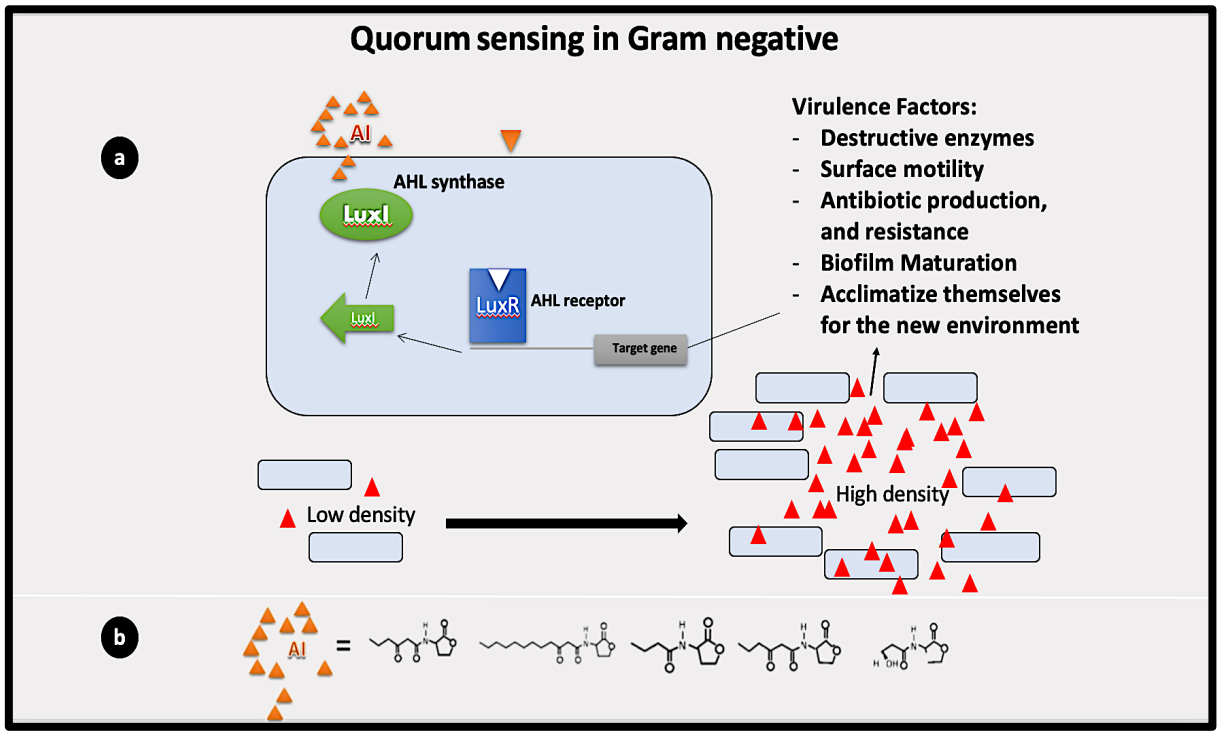

Figure 2: generalized schematic illustration for AHLs based Quorum sensing in most Gram- negative bacteria.

(a) The enzyme LuxI produces AHLs constantly, but only at a certain cell density threshold do AHLs bind to the receptor LuxR, activating the expression of virulence genes. **(b)** AI1 molecules can differ, as some will have a shorter or longer carbon chains with or without an acyl side group.

Engebrecht *et al*. (1983) demonstrated that two regulatory proteins, LuxI and LuxR, control the luminescence in *V.fischeri*. LuxI is a synthase responsible for the production of the AI1-type autoinducer acyl-homoserine lactone (AHL), while LuxR is a receptor and transcriptional activator that interacts directly with the (AI)at the appropriate cell density (and therefore concentration of extracellular AHL) of *V.fischeri.* Initiation of transcriptional pathways begins, which ultimately results in the production of luciferase (Hazan *et al*., 2016). This system can be influenced by several factors that may result in misinformation. For example, the concentration of AI can be higher when the spatial distribution is small, or the concentration of AI can be decreased in the presence of AI sequesters or degrading enzymes, such as acylases, lactonases, and oxidoreductases (Xu *et al*., 2003, LaSarre and Federle, 2013).

This led to the theory that there is another type of bacterial density estimation. Redfield (2002) proposed that QS is not only a density sensing process, but also a diffusion sensing, where the bacteria sense how fast the AI is diffused away and into the environment so that no released products (i.e., protease) are wasted or diluted. Homologues of both proteins, LuxI and LuxR, have been found in several Gram-negative bacteria **(Table 1).**

Table 1: list of some Gram-negative bacteria that use a lux QS homologue

Bacteria	***luxI/luxR*-homologue genes**	Auto inducer	References
Vibrio fischeri	*luxR/luxI*	3-oxo-C6AHL C8-AHL	(Lazdunski *et al*., 2004)
Chromobacterium violaceum	*cviI/cviR*	C6-AHL	(McClean *et al*., 1997a)
Pseudomonas aeruginosa	*lasR/lasI* *rhlR/rhlI* *pqsA/pqsR*	3-oxo-C12AHL C4-AHL 2-heptyl-3-hydroxy-4-quinolone	(Pearson *et al*., 1995) (Case *et al*., 2008)
Agrobacterium tumefaciens	*traI /traR*	3-OH-C8-AHL	(Zhang *et al*., 1993)
Burkholderia cepacia	*cepI/cepR*	C8-AHL	(Lewenza *et al*., 1999)
Erwinia carotovora	*expI /expR*	3-oxo-C6-AHL	(Pirhonen *et al*., 1993) Jones *et al.,* 1993 (Jones *et al*., 1993)

1.2 Quorum Sensing Circuits Components in Gram-negative Bacteria

The Gram-negative complete QS system comprises three components: (LuxI/homologue), an enzyme synthesising the signalling molecule, also known as autoinducer (AI), which binds to a (LuxR/homologue) receptor to form a complex that attaches to a DNA promoter to downregulate or upregulates genes of interest (Fuqua *et al*., 1994). In the sections below, each component will be discussed in detail: the signalling molecules (AI), the enzyme responsible for producing AI, and the QS receptor.

1.2.2 Acyl homoserine lactones (AHLs)

Many Gram-negative bacteria use acyl-homoserine lactones (AHLs) as a signalling molecule. AHLs are "cheap" to produce in terms of energy cost; hence, bacteria can diffuse them constantly into the environment (Redfield, 2002). AHLs consist of a homoserine lactone ring bound to a fatty acid side chain, which can be classified as a short chain (4C-8C) or a long chain (10C-18C) (Churchill *et al*., 2011) **(Figure 3).** Other bacterial AHLs can include some modification e.g., by adding 3-oxo, such as in the case of *P.aeruginosa* AHLs 3-oxo-12C (Pearson *et al*., 1999) **(Figure 3, c).**

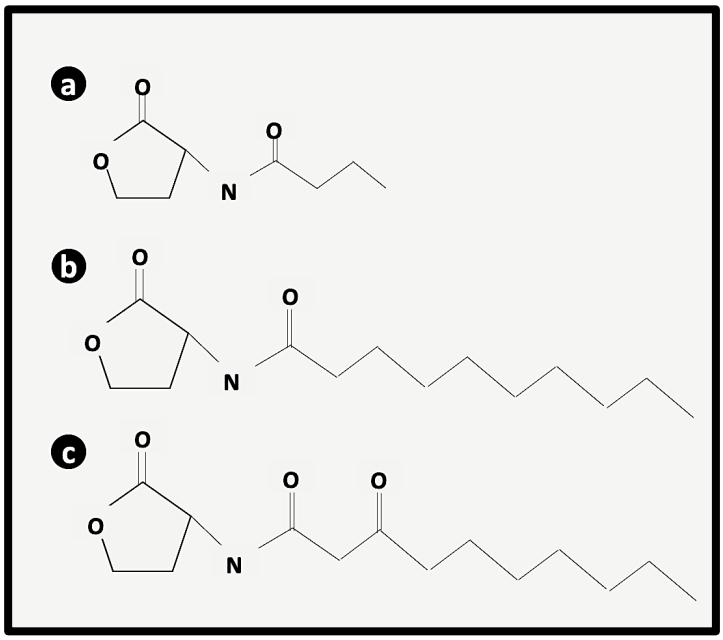

Figure 3: structure of some examples of different AHLs produced by Gram-negative bacteria.

(a) C4-HSL, a short chain AHLs produced by *P.aeruginosa*. **(b)** C10-HSL, a long chain AHLs produced by *Serratia liquefaciens* an environmental bacteria. **(c)** 3-oxo-C12-AHL12, a long chain AHLs with a 3O modification, produced by *P.aeruginosa.*

It is worth mentioning that AHLs are not stable in an alkaline environment (Yates *et al*., 2002, Zhang *et al*., 2019). AHLs are also susceptible to degradation by other enzymes, namely lactonases and acylases (Kalia *et al*., 2011) **(Figure 4**).

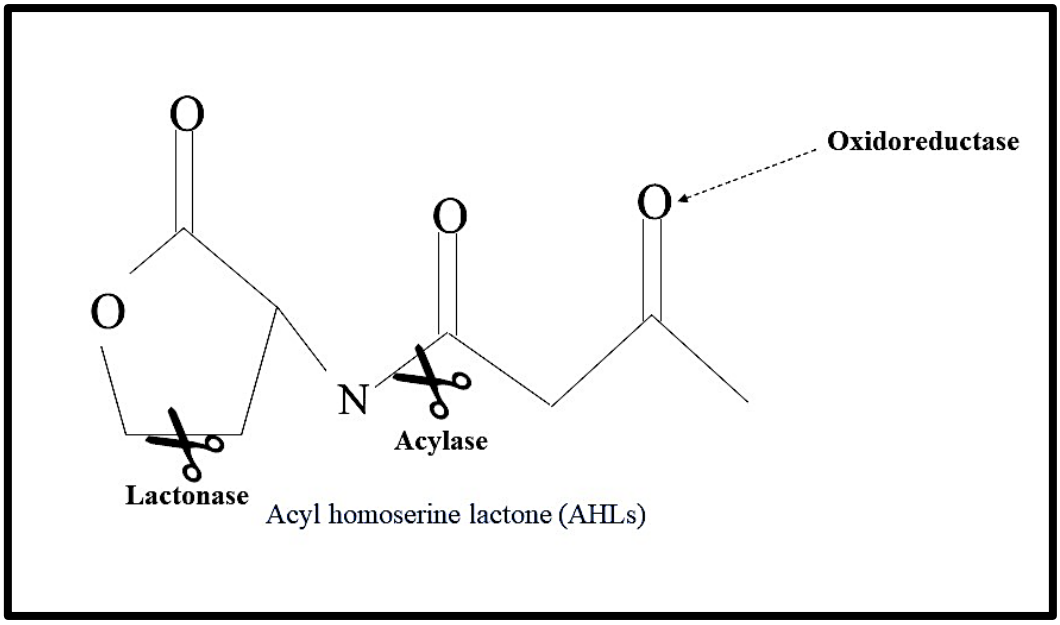

Figure 4: mechanism of several AHLs degrading enzymes.

Lactonase enzyme targets the lactone ring in AHLs and hydrolyse it without affecting the rest of the AHL molecule (Mohammed Sakr *et al*., 2013). On the other hand, acylase hydrolyse the side chain, detaching the chain from the lactone ring (Xu *et al*., 2003). Oxidoreductase can inactivate AHLs by either oxidation or reduction of the side chain. The image was acquired and redesigned from (Chen *et al*., 2013), which is licensed under (CC BY 4.0).

After AHLs are produced, they diffuse to the environment by a passive route or are pumped actively through an efflux pump. For example, in *P.aeruginosa,* C4-AHL diffuses freely through membrane permeability, while 3-oxo-C12-AHL12-AHL is actively diffused out by efflux pumps such as MexAB-OprM (Pearson *et al*., 1999). When AHLs accumulate in the environment, they are bound to the receptor (LuxR) or a homologue, which may be found as transmembrane or in the cytoplasm (see **Chapter 1, section 2.1.3).**

As previously mentioned, several species of Gram-negative bacteria produce one type of signalling molecule. However, in the case of *P.aeruginosa,* more than one AHL are used, which makes for a complex pattern of signal production. This complexity might have an evolutionary benefit for *P.aeruginosa* , but the real reason remains unclear. This is partly because many QS pathways and regulations are difficult to deduce, and many receptors and signals remain to be identified. For instance, the Gram-negative bacteria *E.coli* do not produce AHLs, although a receptor, SdiA, for AHLs has been identified in *E.coli* (Kanamaru *et al*.,

2000) (more will be discussed in **section 1.2.4**). The next **section 1.2.3** will provide a detailed description of AHLs production by a LuxI/homologue.

1.2.3 Acyl-homoserine lactone synthesis (LuxI)

As discussed previously, AHLs in Gram-negative bacteria are produced by the enzyme LuxI/homologue (also known as I protein). A model of AHLs production by a LuxI enzyme in *V.fischeri* was first suggested by Schaefer *et al*. (1996), and has been verified by several studies in different Gram-negative bacteria (Parsek *et al*., 1999, Watson *et al*., 2002, Churchill and Herman, 2008) . To produce the signalling molecules, two substrates of amino acids are recognised, hexanoyl-ACP and S-adenosyl-L-methionine (SAM). The process briefly starts with transporting the hexanoyl group from the ACP to the active site on LuxI. SAM also binds to the active site on LuxI. The hexanoyl group is released from the cysteine to form an amide bond with the amino group of SAM, which results in the release of 5'-Methylthioadenosine. This lactonization reaction results in hexanoyl homoserine lactone **(Figure 5).**

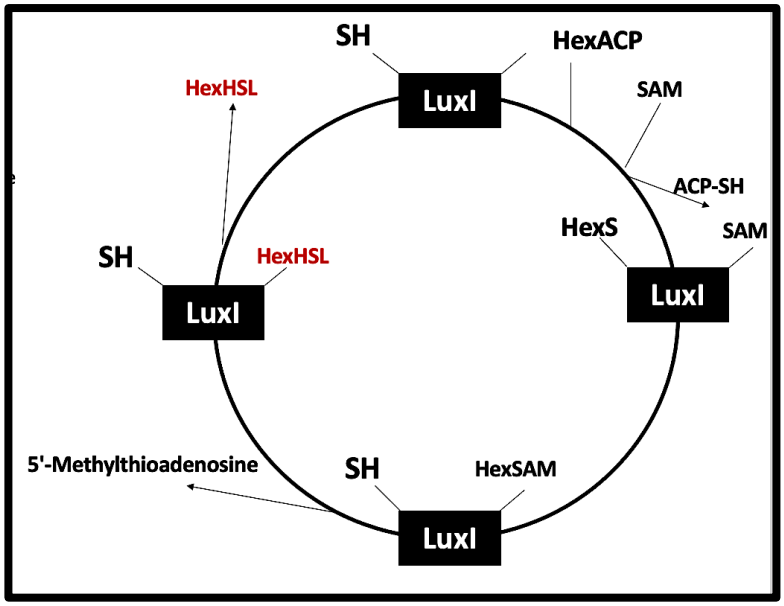

Figure 5: schematic diagram for acyl homoserine lactone (AHLs) synthesis by LuxI/homologue.

SH= hexanoyl acyl carrier protein, HexACP= hexanoyl acyl carrier protein, HexSAM= hexanoyl S-adenosyl-L-methionine, and HexHSL= hexanoyl homoserine lactone.

1.2.4 Acyl-homoserine lactone receptor (LuxR)

LuxR, also known as R protein, is a protein that consists of two domains: a C terminal that is involved in DNA binding, and an N terminal that binds to the auto inducer. In Gram-negative bacteria, there are at least two types of luxR homologue receptors. The first is a cytoplasmic, two-component histidine sensor kinase, such as the lasR, rhlR, and Pqs receptors found in *P. aeruginosa*. The second is a membrane receptor, such as LuxN receptor in *Vibrio harveyi* (Bassler *et al*., 1993).

Bacteria can have multiple LuxR homologue receptors. In *P. aeruginosa*, for example, there are four types of QS receptors (LasR, RhlR, PqsR and QscR) that work together to fine-tune QS regulation. While LasR, RhlR and PqsR work together to regulate several QS phenotypes, QscR can negatively affect the expression QS regulation. This coordination between receptors was demonstrated by Asfahl and Schuster (2018), who observed that the deletion of *qscR* stimulates activation of LasR activation. Another example of receptor fine-tuning is the relationship between RhlR and PqsR. It was reported that RhlR suppresses the activation of pqsR by binding to the las-rhl box located at -513 bp upstream of the PqsR translation start site (Xiao *et al*., 2006).

In the environment, *P.aeruginosa lasR* mutants have been documented and Dekimpe and Deziel (2009) demonstrated that the loss of LasR does not imply the loss of the virulence factors of *P. aeruginosa,* as the *rhl* (the second QS system in *P. aeruginosa*) takes control over QS and expresses pyocyanin. A double mutant of *lasR* and *rhlR*, inhibited the production of pyocyanin, demonstrating the involvement of the *rhl* system in pyocyanin production and coordination between systems in production of virulence factors (Dekimpe and Deziel, 2009).

There are also bacteria that lack one of the components of the QS system, usually the AHLs synthase LuxI. Those systems are referred to as having an incomplete QS circuit. In *P.aeruginosa*, the receptor QscR is referred to as an orphan receptor, as it lacks the synthase

components (Chugani and Greenberg, 2014). Also, incomplete QS circuits can be found in strains of *Escherichia coli*, *Klebsiella spp.* and *Salmonella typhimurium* (Surette *et al*., 1999). These bacteria cannot produce AHLs of their own, due to the lack of the LuxI homologue. However, they do have a LuxR receptor, named SdiA (Smith and Ahmer, 2003). The SdiA receptor can bind to a wide range of AHLs (Almeida *et al*., 2018). The suggestive benefit of only having LuxR homologues is for sensing or "eavesdropping" on AHLs produced by competitive bacteria (Case *et al*., 2008), which have been theorised by Smith (Smith *et al*., 2011) to be used as a competitive advantage for eavesdropping on the polymicrobial environment.

2. Quorum Sensing and Regulation of Virulence Factors in Gram-negative Bacteria (*P.aeruginosa* as a QS Model)

2.1 *Pseudomonas aeruginosa*

P.aeruginosa is an opportunistic Gram-negative pathogen. It is the leading cause of healthcare-associated infections worldwide, accounting for 25% of all ventilator-associated pneumonia in the UK (Masterton *et al*., 2008). The number of reports in the United Kingdom (UK) of *P. aeruginosa* infections has increased by 16% since 2009, with a rate of 8.1 reports per 100 000 of the population (PHE, 2018). The latest report from Public Health England showed that the actual number of reports of *P.aeruginosa* infections in the UK from July 2018 to July 2019 was 28,068 incidents. The World Health Organization (WHO) announced that finding new treatment for *P.aeruginosa* is a priority because it is highly dangerous to humans and new drugs are urgently needed. .In the list of pathogens and under "critical" category, *P.aeruginosa* was named as a priority 1 pathogen (WHO, 2021) **(Table 2).**

Table 2: WHO priority pathogen for which new antibiotics are needed.

Priority 1: CRITICAL
• *Acinetobacter baumannii*, carbapenem-resistant • *Pseudomonas aeruginosa*, carbapenem-resistant • *Enterobacteriaceae*, carbapenem-resistant, ESBL-producing
PRIORITY 2: HIGH
• *Enterococcus faecium*, vancomycin-resistant • *Staphylococcus aureus*, methicillin-resistant, vancomycin-intermediate and resistant • *Helicobacter pylori*, clarithromycin-resistant • *Campylobacter* spp., fluoroquinolone-resistant • *Salmonellae*, fluoroquinolone-resistant • *Neisseria gonorrhoeae*, cephalosporin-resistant, fluoroquinolone-resistant
PRIORITY 3: MEDIUM
• *Streptococcus pneumoniae*, penicillin-non-susceptible • *Haemophilus influenzae*, ampicillin-resistant • *Shigella* spp., fluoroquinolone-resistant

Qu *et al*. (2021) have recognised the increasing number of coinfection in COVID-19 patients with *Pseudomonas aeruginosa*, causing worsening of illness. They noted that *P.aeruginosa* isolated from COVID-19 patients is more virulent with increased production in several QS-regulated phenotypes, such as biofilm, motility, elastase and rhamnolipids. They extrapolate that the environment of patients with COVID-19 allowed for *P.aeruginosa* to be more virulent. In another study by Lansbury *et al*. (2020) it was found that coinfection with *P.aeruginosa* is the second most frequently detected pathogen in patients with COVID-19 patients.

P. aeruginosa is a phenomenal bacterium when it comes to antibiotic resistance (**Table 3**). Some strains possess almost all known mechanisms of resistance, allowing them to be resistant to most antibiotic classes (Yayan *et al*., 2015, Sheikh *et al*., 2019) *P.aeruginosa* intrinsically expresses efflux pumps (Bonomo and Szabo, 2006) and can secrete antibiotic destructive enzymes, such as the AmpC Beta-lactamase (cephalosporinase) (Nordmann and Guibert, 1998)). Furthermore*, P.aeruginosa* inherently has a low permeable outer membrane (Angus *et al*., 1982), due to the low number of OprD proteins (carbapenem- specific porin). These factors make *P.aeruginosa* one of modern medicine's greatest challenges, and the development of non-antibiotic-based treatments a matter of urgency.

Table 3: list of antibiotics with their targets and the proposed *P.aeruginosa* resistance mechanism.

Class of antibiotic	Target	Resistance mechanism	References
Beta – lactams (e.g., Penicillin, Ampicillin, Piperacillin)	Cell wall synthesis	**Enzyme production:** o Production of destructive enzymes that break the amide bond of the Beta-lactam ring .Such enzymes: ESBL and Beta- lactamases classes A, B, C and D. **Overexpression of efflux pumps:** o Efflux systems such as MexA-MexB-OprM. **Loss of permeability:** o The loss of OprD protein **Alteration of targets:** o Alteration of Penicillin – binding protein (PBP), and the production of low affinity PBPs, such as 3s and 4s.	Sykes and Mathew, 1976. Bush *et al.,*1995. Saito *et al.,*1999 ; Quinn *et al.,* 1986 ; Livermore, 2001. Kapoor *et al*., 2017
Fluoroquinolones (e.g., Levofloxacin, Ciprofloxacin, Moxaifloxacin)	Nucleic Acid synthesis : DNA Gyrase	**Overexpression of efflux pumps:** o Mutation in *nalB* gene in the *mexR* locus and *ŋfxc* that results in the overexpression of the multi drug effluxes pumps MexA-MexB-OprM and MexE-MexF-OprNa, respectively. o Over expression of MexA-mexB-OprM pumps. **Loss of permeability:** o The loss of the OprD protein. **Alteration of targets:** o Mutation in the gene *gyrAIgyrB* encoding for the target DNA gyrase (topoisomerase II).	Saito *et al.,* 1999. Livermore, 2001. Kapoor *et al.,* 2017
Aminoglycosides (e.g., gentamicin, tobramycin, streptomycin)	Protein Synthesis: 30S subunit	**Enzyme production:** o The production of antibiotic modifying enzymes, such as aminoglycoside phosphoryl transferases (APHs), aminoglycoside acetyltransferases (AACs), and aminoglycoside adenylyl transferases (AAD). **Loss of permeability:** o To prevent the accumulation of the antibiotic inside the bacterial cell. **Alteration of targets :** o Methylation of 16S rRNA with methylase such as RmtA and RmtD.	Lano-Sotelo *et al*., 2002 Villegas and Mobashery, 2003 Macleod *et al*., 2000; Yokoyama *et al.,* 2003; Doi *et al*., 2006 ;

			Kapoor *et al*., 2017
Chloramphenicol	Protein Synthesis: 50S subunit	**Overexpression of efflux pumps:** o Mutation in *nalB* gene in the *mexR* locus that results in the over expression of the efflux pumps MexA-MexB-OprM. o MexA-mexB-OprM efflux pump **Loss of permeability:** o The loss of the OprD protein	Saito *et al*., 1999. Livermore, 2001. Kapoor *et al*., 2017
Trimethoprim	Nucleic Acid synthesis: Folate synthesis	**Overexpression of efflux pumps:** o Mutation in *nalB* gene in the *mexR* locus, that results in the over expression of MexA-MexB-OprM, a multi drug efflux pumps.	Saito *et al*., 1999. Livermore, 2001. Kapoor *et al*., 2017
Tetracycline (e.g., Doxycycline,Minocycline)	Protein Synthesis: 30S subunit	**Overexpression of efflux pumps:** o Mutation in *nalB* gene in the *mexR* locus that results in the over expression of MexA-MexB-OprM, a multi drug efflux pumps. o MexA-MexB-OprM efflux pumps. **Loss of permeability:** o The loss of OprD protein.	Saito *et al*., 1999. Livermore, 2001. Kapoor *et al*., 2017

2.2 *P.aeruginosa* QS systems

Quorum sensing in *Pseudomonas aeruginosa* is complex, with multiple QS systems regulating different virulence factors (VFs), and many negative and positive feedback loops fine tuning the regulation process. In *P. aeruginosa*, the homologue of the LuxI enzyme is called LasI, which took its name from its role in elastase induction (Pearson *et al*., 1995) and the LuxR homologue is LasR. Both proteins, LasI and LasR, can facilitate the production of several VFs (**Figure 6**). Almost all proteobacteria that produce N-acyl homoserine lactones as signalling molecules rely on the LuxI/LuxR QS system (Case *et al*., 2008). *P. aeruginosa* has three known QS systems **(Figure 6).** LasI/LasR and RhlI/RhlR are the major QS systems in *P. aeruginosa;* LasI and RhlI produce 3-oxo-C12-AHL12-AHL and C4-AHL, respectively. Each of these (AI) binds to their respective receptors (3-oxo-C12-AHL12-AHL with LasR and C4-

AHL with RhlR) to form lasR-3-oxo-C12-AHL12-AHL and RhlI-C4-AHL complexes that then bind to the *las-rhl* boxes that reside within the promoter regions of target genes including those that encode for the signalling molecules used in QS, creating a positive feedback loop (Whitehead *et al*., 2001). Each receptor controls a set of genes that can overlap (Schuster and Greenberg, 2007, Lee and Zhang, 2015a). Not all QS systems in *P.aeruginosa* function simultaneously, but rather in sequence. The complex lasR-3-oxo-C12-AHL12-AHL is formed first, activating the expression of the second QS system genes, rhlI and rhlR. In addition, LasR also activates a third QS system, PqsA/PqsR, that produces 2-heptyl-3-hydroxy-4-quinolone (HHQ). QS is a sophisticated and complex process that can be finely regulated through many forward and feedback loops (Papenfort and Bassler, 2016, Eickhoff and Bassler, 2018).

As previously mentioned, the different QS pathways regulate several VFs, resulting in the premise that disrupting QS can decrease the expression of these VFs. Studies have confirmed this relationship, showing that when QS is disturbed, several virulence factors in *P.aeruginosa* are also disturbed, indirectly affecting bacterial ability to cause diseases (Strateva and Mitov, 2011). Events downstream of LasR binding of AHLs control *P.aeruginosa* virulence factors such as protease (lasA) and Elastase (lasB) (De Kievit and Iglewski, 2000). The second system, RhlI/RhlR with its cognate N-butyryl-l-homoserine lactone (C4-AHL), is involved in the production of secondary metabolites such as pyocyanin (Brint and Ohman, 1995, Latifi *et al*., 1995).

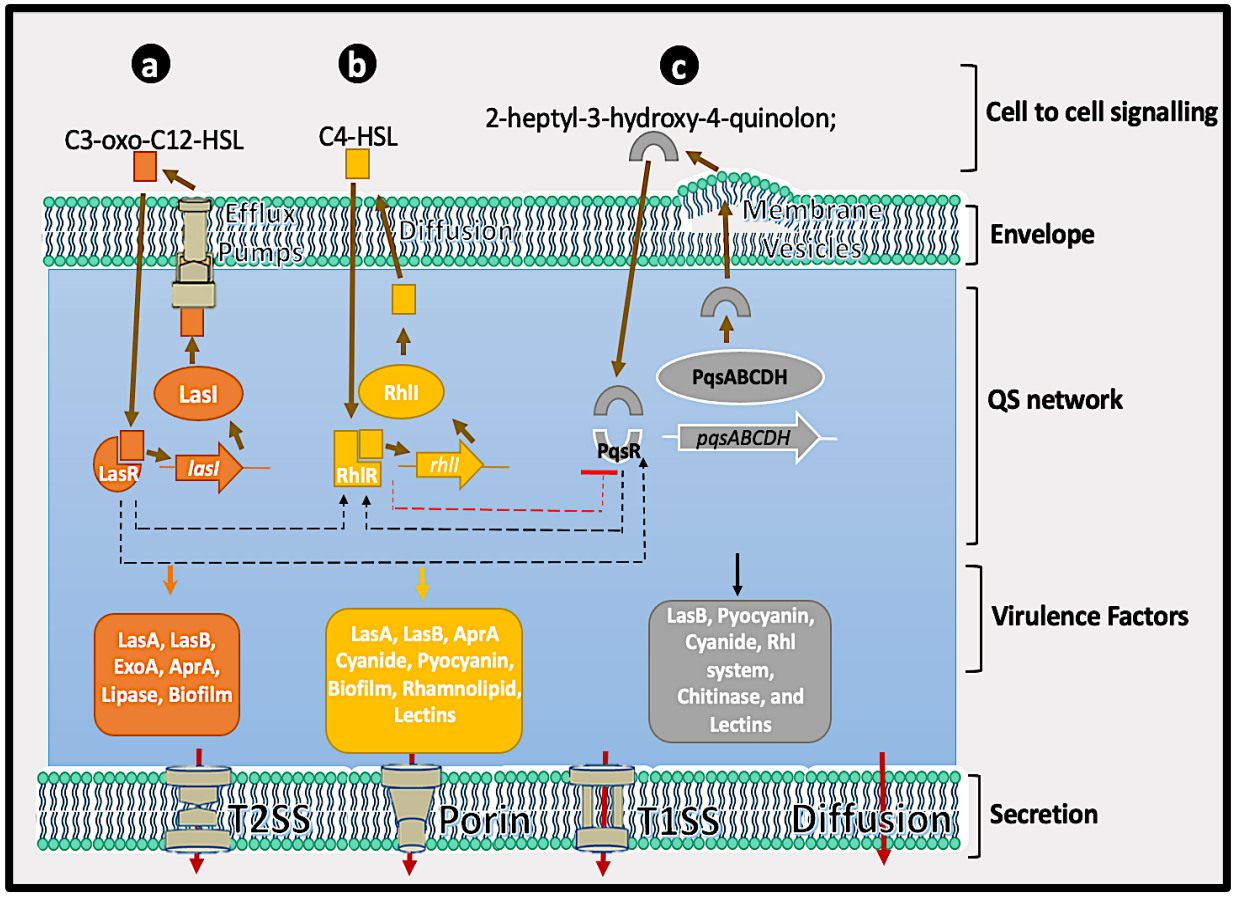

Figure 6: a schematic diagram for *P.aeruginosa* multiple QS systems.

Each system is used to regulate the expression of different virulence factors. Four pathways of QS have been discovered; however, only three are understood, which are: **(a)** *las*,**(b)** *Rhl,* and **(c)** *Pqs*. This comprehensive illustration shows the three complete QS systems and their VFs in *P.aeruginosa* with their dissemination route with 3-oxo-C12-AHL12-HSL disseminated to the environment through efflux pumps and C4-HSL diffused through the membrane, while 2-heptyl-3-hydroxy-4-quinolone is encapsulated in a membrane vesicle. The image was obtained and modified from (Moradali *et al*., 2017) licenced under CC BY-ND 4.0, which allows sharing and customisation.

2.3 *P.aeruginosa* QS regulated virulence factors (VFs)

2.3.1 Biofilm formation

Bacterial biofilm is defined as the aggregation of microbial community that is buried inside a self-produced extracellular matrix, which is comprised of extracellular DNA (eDNA) (Whitchurch *et al*., 2002) extracellular polysaccharides (EPS), and proteins (Frølund *et al*., 1996) Bacterial biofilm can usually be found attached to surfaces. Inside the biofilm architecture, channels allow for distribution of water and nutrients to all parts of the biofilm (Quan *et al*., 2022). Biofilm is formed in four main stages (summarised in **Figure 7**). Bacterial adhesion to a surface is thought to be the first step of biofilm formation; when prevented it can

prohibit the formation of biofilm (Garrett *et al*., 2008). Then the cells are aggregated and attached with the help of appendages and adhesins. Next comes maturation, where the amount of eDNA increases as the biofilm matures and supports the biofilm architecture. After a decrease in nutrients and oxygen and an increase in toxic waste products, some bacteria leave the biofilm and disperse, possibly to begin the cycle of biofilm formation again (Kostakioti *et al*., 2013).

The biofilm matrix of *P.aeruginosa* consists of extra polysaccharides (EPS), proteins and nucleic acids. Each component contributes to the strength of the biofilm formed. The EPS matrix is mostly composed of carbohydrates, namely mannose, galactose, and glucose (Bales *et al*., 2013). The presence of extracellular proteins such as the amyloid like fibres (ALF) inside the biofilm has the essential function of maintaining the rigidity of the biofilm structure (Taglialegna *et al*., 2016). These proteins play the role of connecting the surface of bacterial cells to the extracellular polysaccharides, as the loss of such proteins can have a negative impact on the structure of the biofilm.

In *P.aeruginosa*, three gene clusters are involved in exopolysaccharide synthesis, the *pel* (PA3058-PA3064), *alg* biosynthetic genes (PA3540-PA3551) and the *psl* (PA2231-PA2245) (Wei and Ma, 2013). QS control EPS synthesis by controlling the transcription of the *pel* genes cluster via the *las* system (Sakuragi and Kolter, 2007).

Whitchurch *et al*. (2002) first reported the existence of eDNA in biofilm after an investigation of the effect of DNase I on the biofilm of *P.aeruginosa*. eDNA has been involved in bacterial acquired resistance mechanisms from other innately resistant cells by the swapping of resistance genes through horizontal transfer (Bae *et al*., 2014) QS pathways have been discovered to influence the expression of eDNA (Allesen-Holm *et al*., 2006). Additionally, QS mutants were found to produce reduced levels of eDNA, and biofilms appeared to be flat (Yang *et al*., 2007).

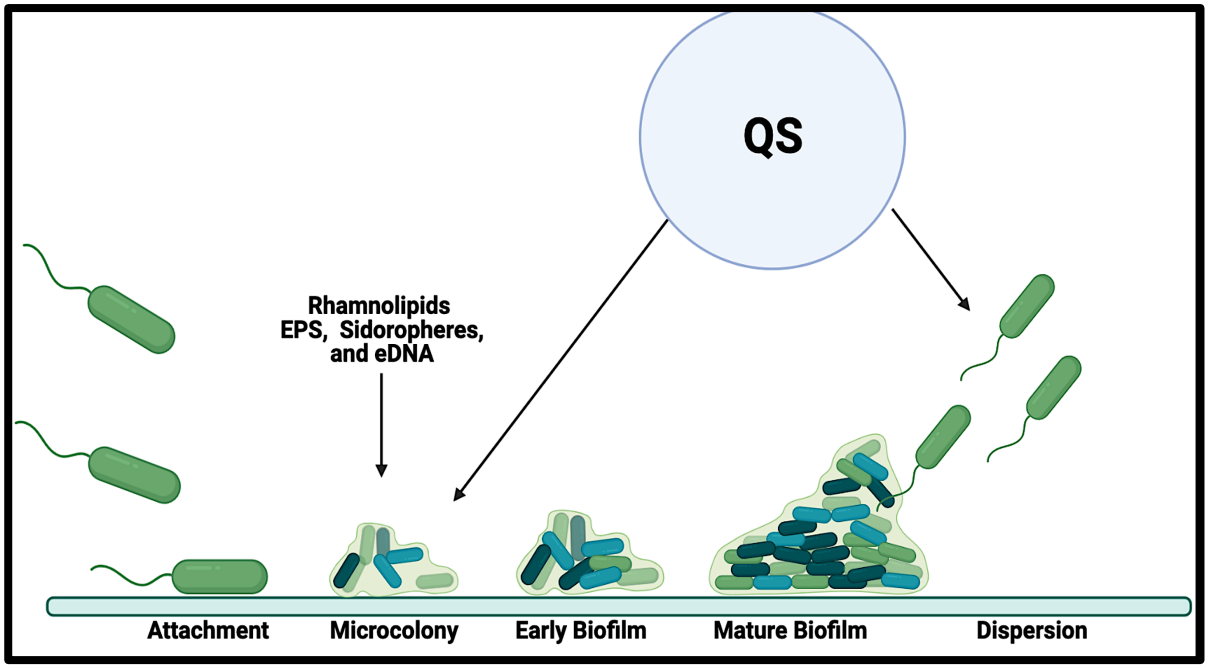

Figure 7: schematic diagram for the bacterial biofilm formation four main steps.

The first step of biofilm formation is the initial interaction with the surface, this interaction being influenced by hydrodynamic, Brownian motion and gravitational forces. Then the cells are aggregated and attached with the help of appendages and adhesins. Next comes maturation, where the amount of eDNA increases as the biofilm matures, helping to support biofilm architecture. After a decrease in nutrients and oxygen and an increase in toxic waste products, some bacteria leave the biofilm and disperse, possibly to begin the cycle of biofilm formation again (Kostakioti *et al*., 2013).

Biofilm can provide many advantages to the individual bacterium. One of these benefits is protection, as the bacteria within the biofilm can find refuge from different harsh environmental conditions, such as a high concentration of antibiotic (Arthur *et al*., 1987, Cochran *et al*., 2000, Costerton, 1984).

2.3.1.1 Biofilm formation promotes resistance to antibiotics

In burn wound infections, 60% of mortality are associated with biofilm formed in wounds (Thomas and Thomas, 2021). Biofilms are estimated to be around 100-1000-fold less sensitive to antibiotics in comparison to planktonic bacteria (Anderl *et al*., 2000). Biofilm resistance to antibiotics can be due several factors. First, the protective coat of the extracellular polysaccharide matrix of the biofilm forms a barrier that hinders the entrance of antibiotics Second, most of the biofilm is water, which can lower the concentration of the antibiotic diffused into the EPS (Stewart, 1996). Moreover, persister cells, a subpopulation in biofilm,

have a slow metabolism rate which hinders antibiotics that require an active metabolism to work (Cochran *et al*., 2000). The fourth factor is the close vicinity of many bacteria that convey intrinsic resistance genes to antibiotics, where the chance of taking up resistance genes are slightly higher (Ma and Bryers, 2013)

2.3.1.2 QS and biofilm formation

QS and biofilm formation are connected, as biofilm formation is one of the virulence factors controlled by QS. Biofilm structure is affected by QS; biofilms formed by *lasI* mutants appear to be flat and fragile (Davies *et al*., 1998). This might be partially explained in the work of Davey *et al*. (2003), where they showed that a mutant in the gene *rhlA* encoding for rhamnolipid, a surfactant, showed similar flat structure. Rhamnolipids are under the control of both QS systems, *las* and *rhl*, which emphasize the connection between QS and biofilm formation (Hentzer *et al*., 2002). Rhamnolipids play a role in maintaining the structure of biofilm, by allowing cavities within the biofilm to exist for better distribution of water and nutrients (Davey *et al*., 2003, Boles *et al*., 2005, Chrzanowski *et al*., 2012) Furthermore, QS can influence biofilm formation by affecting the iron scavenging process. Inhibition in QS can limit the iron needed for growth and thus affect the biofilm formation process (Singh *et al*., 2002).

However, this observation cannot be implemented in all bacteria, as *V. cholerae* and *Staphylococcus aureus* biofilms can be reduced when QS is activated. Autoinducer (AI) production can interfere negatively with initiating biofilm formation in both *V. cholerae* and *S. aureus* (Kim *et al*., 2016). Nevertheless, once the biofilm is mature, QS is re-activated.

QS may influence biofilm antibiotic tolerance through the QS regulator 2-n-heptyl-4-hydroxyquinolone-N-oxide (HQNO), which promotes the release of eDNA. Consequently, the released eDNA plays a role in the structural integrity of the biofilm matrix (Hazan *et al*., 2016).

2.3.2 Protease Enzymes

Most clinically isolated *P.aeruginosa* strains produce proteolytic and elastolytic enzymes. Such enzymes include LasA protease (staphylolytic protease), LasB elastase, and AprA alkaline protease **(Table 4).** These enzymes are important in human infections, in lysing collagen, elastin, immunoglobulins, and complement molecules (Toder *et al*., 1994). The *las* system regulates protease at the late logarithmic and early stationary phase of growth (Whooley and Mcloughlin, 1983). LasA and LasB proteases are some of the secreted VFs under the regulation of QS systems in *P.aeruginosa*. **Table 4** contains examples of key QS-dependent secreted virulence factors produced by *P.aeruginosa* are shown. In the next section the two proteases LasA and LasB are discussed in further detail.

Table 4: key QS-dependent secreted virulence factors produced by *P.aeruginosa.*

Virulence factor	Gene Synthesis	Secretion	Role in pathogenesis	Reference
LasA protease	*lasA*	Sec pathways and T2SS	Tissue invasive, Staphylolytic activity	(Toder *et al*., 1994)
LasB elastase	*lasB*	Sec pathways and T2SS	Lysing collagen, elastin, immunoglobulins, and complement molecules	(Toder *et al*., 1991)
Alkaline Protease	*aprA*	T1SS	Protein degradation, such as laminin and the inactivation of immune cell components	(Laarman *et al*., 2012)
Rhamnolipids	rhlAB and rhlC	Sec pathway and T2SS	An important compound for biofilm formation, inhibits polymorphonuclear neutrophilic cells and ciliary function in lung infections, has cytotoxic ability	(Soberón-Chávez *et al*., 2005) (Nickzad and Déziel, 2014),
Exotoxin A	*toxA*	T2SS	A toxin that targets the protein synthesis in the host cell, resulting in the cell death.	(Michalska and Wolf, 2015)
Pyocyanin	phzA1-G1 and phzA2-G2 operons	T2SS	An important iron carrier that has a cytotoxic effect on host cell	(van‘t Wout *et al*., 2015)

2.3.2.1 LasA protease

LasA protease is a 20-22 kDa polypeptide (Schad and Iglewski, 1988) with a staphylolytic activity, cleaving the pentaglycine bridge within the peptidoglycan in *Staphylococcus aureus* (Brito *et al*., 1989). *P. aeruginosa* lyses *S. aureus* through the secreted LasA protease, giving *P. aeruginosa* access to iron for growth in iron-deficient environments (i.e., at the site of infection) (Mashburn *et al*., 2005). LasA, unlike the LasB protease, has a limited protease action that only targets the Gly-Gly peptide bonds. LasA protease is encoded by the gene *lasA,* which is regulated by the two QS systems in *P.aeruginosa las and rhl* systems.

2.3.2.2 LasB elastase

Elastase is a ~33kDa extracellular zinc metalloproteinase (Teufel and Götz, 1993) with an elastolytic activity that promotes the degradation of elastin and collagen, a compound found in the lungs and skin **(Table 5).** LasB elastase is extensively produced in tissue colonisation (Tümmler and Kiewitz, 1999). The gene *lasB* encodes LasB, and three QS systems, *las, rhl*, and *pqs systems*, are involved in the production of the LasB elastase. Elastase can aid *P.aeruginosa* in evading immune responses by working with alkaline protease to clear the immunogenic flagellin (Casilag *et al*., 2016). Furthermore, the LasB elastase enzyme can degrade many immune cells from innate and adaptive responses, such as immunoglobulin G (IgG), immunoglobulin A and alpha-1 protease (Schultz and Miller, 1974, Döring *et al*., 1981, Parmely *et al*., 1990, Hamood *et al*., 1996). **Table 5** summarises the comparison between lasA and LasB proteases in *P.aeruginosa*

Table 5: a summary of the differences between LasA and LasB protases in *P.aeruginosa.*

	Protease LasA	**Elastase LasB**
QS system	*las & rhl* system	*las, rhl & pqs* systems
Family	*beta-lytic endopeptidase*	t*hermolysin*
Gene	*lasA*	*lasB*
Length	20 kDa	~33 kDa

staphylolytic activity	Yes	No
Autolytic	No	Yes
Protease action	Limited (mainly to Gly3 and Gly2-Ala sequences)	Wide action (cleaves proteins at multiple sites)
Effect on the Host	**Epithelial disruption**, tissue penetration and endothelial damage	Degrades the **extracellular matrix** constituents (e.g., elastin and collagen) of host cells, **inducing tissue injury** and haemorrhage.
Immune system attack strategies	Induce a host inflammatory including human leukocyte elastase and human neutrophil elastase.	Degrade **Tumour necrosis factor-α**, **interferon-γ** and **interleukin-2** and by inactivating **components of the complement system**.

2.3.3 Pyocyanin (PCN)

The competitive success of *P.aeruginosa* is partly due to its production of different exo-secretions in large quantities, including the blue redox-active pyocyanin (PCN). Pyocyanin is a blue-greenish pigment and a member of the phenazine family (Frank and DeMoss, 1959). Pyocyanin is regulated by QS systems in *P.aeruginosa,* namely *rhl, and pqs*. The production of Pyocyanin is a complex process, that is summarised in **Figure 8**.

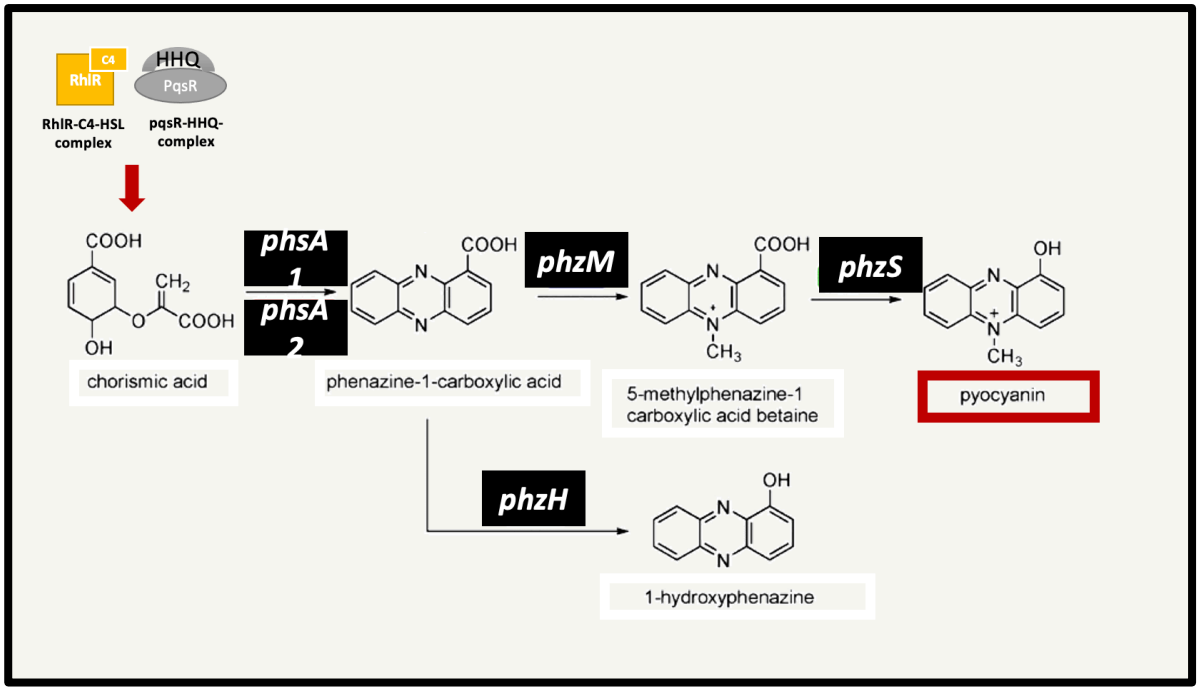

Figure 8: schematic diagram for the biosynthesis process of pyocyanin.

Pyocyanin is regulated by QS systems in *P.aeruginosa,* namely *rhl, and pqs* Both operons, phsA1 and phsA2, will activate the production of phenazine-1-carboxylic acid (PCA) that is converted by the enzymes PhzH, phzM, and phzS to 5-methylphenazine-carboxylic acid betaine then by the enzyme PhzS into pyocyanin (Mavrodi *et al*., 2010).

PCN is involved in necrosis and tissue damage in *P.aeruginosa* lung infection (Lau *et al*., 2004), the cornea (Green *et al*., 2008), and skin (Weinstein and Mayhall, 2003). The toxicity of PCN on epithelial cells is well established; however, the exact pathology of PCN is yet to be explained. Muller *et al*. (2009) concluded that *P.aeruginosa* persistence in wound infection is due to pyocyanin inducing early senescence in mammalian cells, delaying the healing, and repairing process of cells. The ability of PCN to change the function of epithelial cells and modify immune cells might explain chronic *P.aeruginosa* infections (Kanthakumar *et al*., 1994). Moreover, PCN is important for biofilm maturation as it promotes the release of eDNA for the biofilm matrix (see **section 2.3.1.1**), which also plays a part in chronic *P.aeruginosa* infections (Das *et al*., 2013).

2.3.4 Rhamnolipids

Rhamnolipids are a secondary metabolite composed of fatty acids and one or two rhamnoses. Rhamnolipids are produced mainly by *P.aeruginosa*, although other non-pathogenic

pseudomonads have been observed to produce rhamnolipids as well, such as *Pseudomonas putida* (Tuleva *et al*., 2002). *P. aeruginosa* produces rhamnolipids as an active surface agent or "surfactant" to minimise surface tension when they swarm (Deziel *et al*., 2003). Swarming is defined as the mass migration of bacteria across a surface. The term swarming means to move in great number, which, in the case of bacteria, happens in a high cell density, unlike other types of bacterial motility (Kearns, 2010).

Rhamnolipids or Di-rhamnolipids are formed from two kinds of rhamnolipids sugars, L-rhamnosyl-L-rhamnosyl-P-hydroxydecanoyl-p-hydroxydecanoate and L-rhamnosyl-p-hydroxydecanoyl-p-hydroxydecanoate (Lang and Wagner, 2017). **Figure 9** is a simplified illustration of the synthesis pathway of rhamnolipids in *P.aeruginosa*. Rhamnolipids are regulated by two genes, *rhlA* and *rhlB*, which are clustered with the second QS system genes, *rhlR* and *rhlI* (Lazdunski *et al*., 2004). Since surfactants are only effective in higher concentration, the regulation by QS guarantees that surfactants are only produced at a high cell density (Ochsner and Reiser, 1995). Briefly, A RhlR-C4-HSL complex is created when RhlR and N-butanoyl-L-homoserine lactone (C4-HSL), which is made by RhlI, bond together. The rhlA promoter interacts with the RhlR-C4-HSL complex to start the transcription of the rhlAB genes, which results in the production of rhamnolipids.

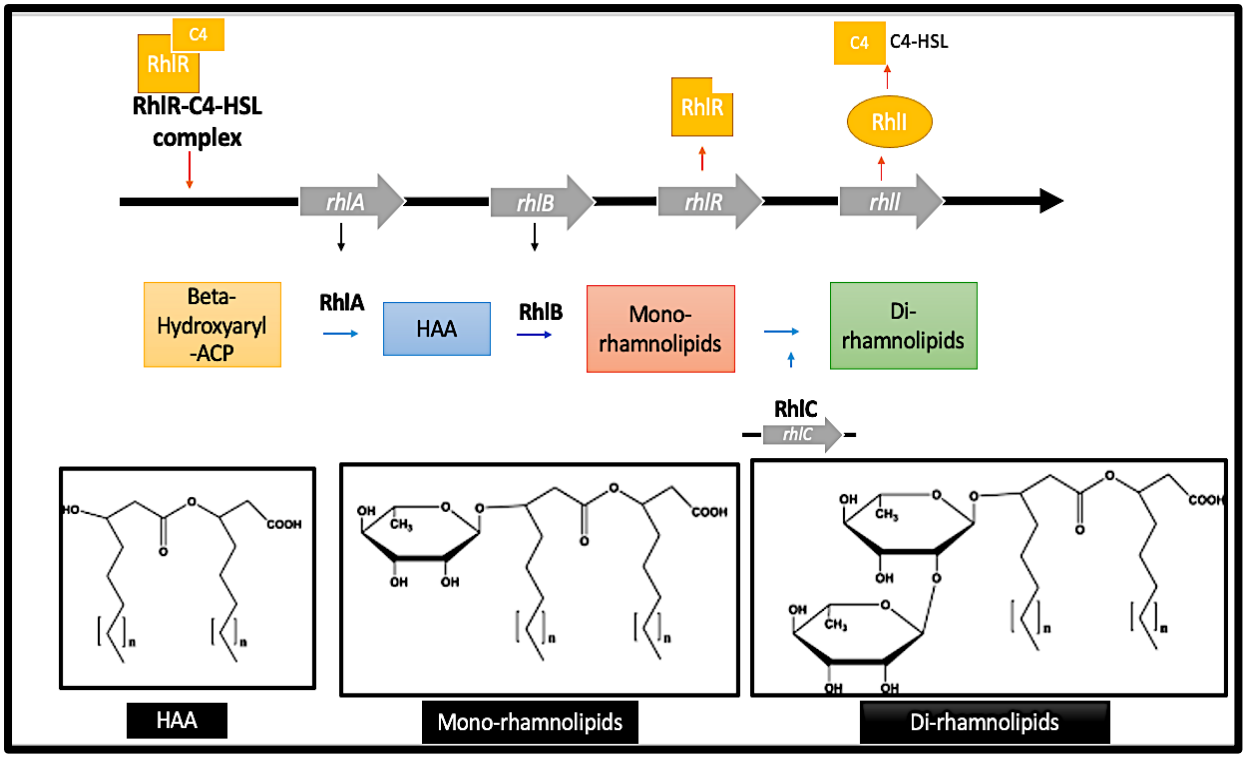

Figure 9: schematic illustration of the pathway for rhamnolipid production in *P. aeruginosa.* A RhlR-C4-HSL complex is created when RhlR and N-butanoyl-L-homoserine lactone (C4-HSL), which is made by RhlI, bond together. The rhlA promoter interacts with the RhlR-C4-HSL complex to start the transcription of the rhlAB genes, which results in the production of rhamnolipids. 3-(hydroxyalkanoyloxy) alkanoic acid is known as HAA. Rhamnolipids produced by *P. aeruginosa* frequently contain fatty acids with chain lengths between C8 and C1. Image was adopted from an original by (Wood *et al*., 2018) , which is licenced under CC BY-ND 4.0, that allows sharing and customisation.

Furthermore, rhamnolipids are thought to have a role in the ubiquity and success of *P.aeruginosa* in colonisation of different environments due to two reasons. The first is the antagonistic activity of rhamnolipids on a diverse panel of microorganisms, giving *P.aeruginosa* a competitive advantage in polymicrobial environments (Soberón-Chávez *et al*., 2005). The second is the involvement of rhamnolipids in the active detachment of the bacteria from the biofilm to return it to its free-living states (Boles *et al*., 2005).

3. Quorum Sensing and Host Immune Response

It was established from previous sections the important role QS in the bacterial community plays in unifying the bacterial response to enhance survivability. Recently, the interaction between bacterial QS molecules and host immunity gathered much attention. It was believed

that bacteria use the QS signalling molecules to promote survivability inside the host by activating and repressing the innate immune system (Kariminik *et al*., 2017). The bacteria benefit when the immune system is unduly activated by triggering the production of the pro-inflammatory response, resulting in tissue destruction and thus easily accessible nutrients (Jarosz *et al*., 2011). Also, bacteria QS signals, specifically 3-oxo-C12-AHL12HSL of *P. aeruginosa*, as secreted in large amounts in the initial growth stages, can downregulate NF-κB and reduce TLR4-dependent innate immune responses, promoting bacterial persistence (Kravchenko *et al*., 2008). The production of 3-oxo-C12-AHL12HSL also suppresses the activation of immune cells and induces apoptosis in macrophages by supressing IL12 (Zhu *et al*., 2008), thereby compromising host immune defences. On the other hand, 3-oxo-C12-AHL12HSL activates IL8 in respiratory epithelial cells (Hu *et al*., 2021).

Moura-Alves *et al*. (2019) used human cells, zebrafish, and mice to evaluate the role of the aryl hydrocarbon receptor (AhR), a highly conserved receptor in human cells that regulates the immune system response during bacterial infection. They concluded that in a *P. aeruginosa* infection, the AhR receptor "eavesdrops" on the QS molecules produced by *P.aeruginosa* during different disease stages to customise the immune response during bacterial infection properly. Moreover, it was revealed from both *in vitro* and *in vivo* that the AhR qualitatively identifies *P. aeruginosa* QS molecules and measures their relative quantities. This fine-tuning of immune response is believed to minimise the collateral damage resulting from activating the immune cells and also for efficient host defence and clearing with reasonable energy cost. Other mammalian receptors that detect Gram-positive bacterial QS signals, such as Mrgprb2 and the human homologue MRGPRX2 in mast cells found in the connective tissues, were identified. When the QS signals bind to the receptor Mrgprb2 or MRGPRX2, mast cell degranulation is activated, resulting in an antimicrobial immunity response that prohibits bacterial growth and prevents biofilm formation (Pundir *et al*.,

2019). As it is clear from the previous, the bacterial QS and host immunity interaction is best described as an arms race; wherein bacteria and host continuously reacts to each other's evolving strategies.

4. Cutaneous *P.aeruginosa* Infection

Both immunocompromised and healthy people can develop superficial to deep skin *P. aeruginosa* infections. *P.aeruginosa* skin infection can vary from a primary condition with a unique presentation such as 'green nail syndrome', to severe skin and soft tissue infection resulting from the rapid progression of the bacteria to skin failure and death. Examples of such serious skin infections include severe cellulitis and necrotizing fasciitis. *P.aeruginosa* remains the most common bacteria in burn patient populations, as it thrive*s* in a burn wound setting (Schlager *et al*., 1994, Lari *et al*., 1998).

A study by Gonzalez *et al*. (2016) investigated the survivability of *Pseudomonas aeruginosa, Staphylococcus aureus* and *Acinetobacter baumannii* in a human burn infection. The study showed that *P. aeruginosa* was the only pathogen that could grow within human fluids found at the burn site. The expression of typical virulence factors such as pyocyanin and pyoverdine was even increased compared to levels measured after culturing bacteria in a standard laboratory medium (LB). *P. aeruginosa* grew well under these conditions, showing that human burn exudates provide all the nutrients necessary for *P. aeruginosa* development, which may explain why this organism is a predominant pathogen in burn victims. Whereas the increased expression of VFs by *P. aeruginosa* can lead to delays in healing or a fatal outcome (Ruffin and Brochiero, 2019).

Epithelial tissue is the first line of defence against various pathogens. Therefore, an effective repair mechanism after injury is essential to maintain this line of defence. Four phases are involved in cellular repair after injury: (1) cell spreading, (2) cell migration, (3) cell proliferation, and (4) cell differentiation. When infected with *P.aeruginosa*, the bacteria have

been found to disrupt the epithelial cell repair process and increase the incidence of chronic infection (**Figure 10**).

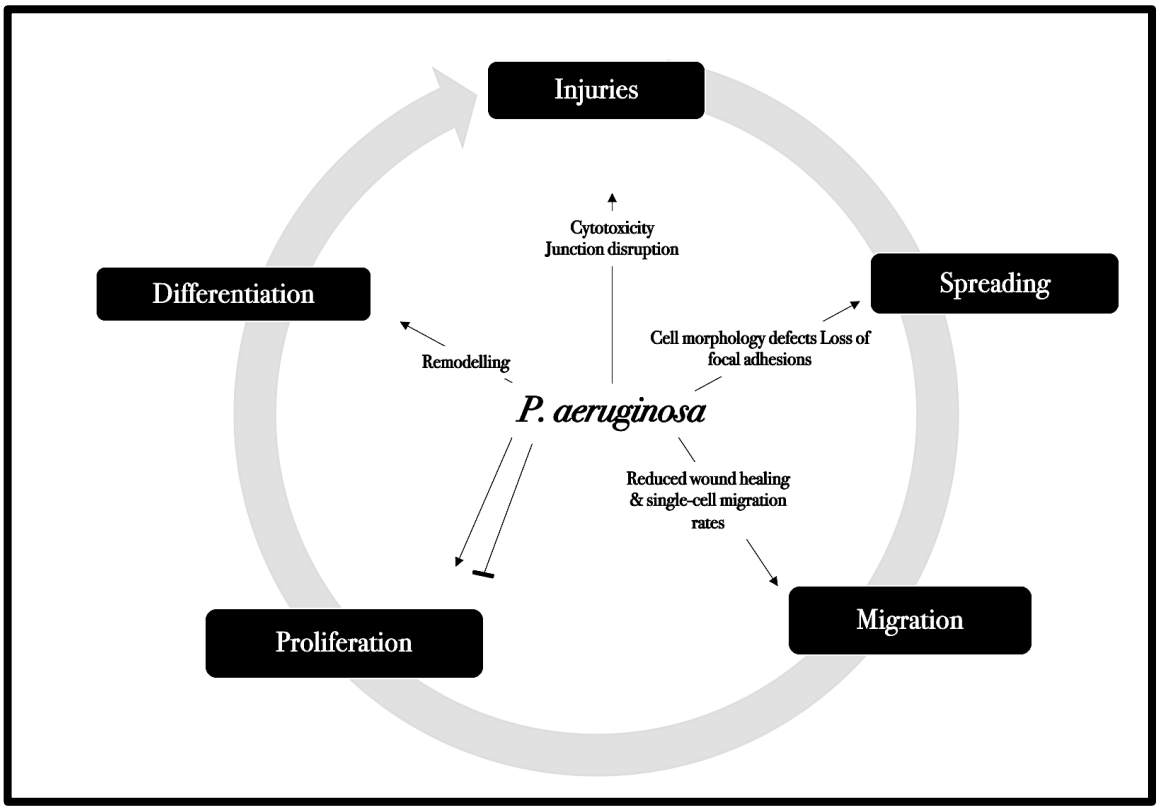

Figure 10: schematic diagram illustrating the Overview of *P. aeruginosa* negative effects on epithelial integrity and healing.

P.aeruginosa can interfere with wound healing by disrupting various stages of cellular repair processes. First, *P.aeruginosa* can exacerbate injury by promoting cytotoxicity and disruption of junctions (Nagano *et al*., 2001). Second, *P.aeruginosa* can reduce cell spreading by altering cell shape through destruction of the actin cytoskeleton, reduced stress fibres, focal adhesions and lamellipodial structures (de Bentzmann *et al*., 2000). Thirdly, *P.aeruginosa* can inhibit cell migration by decreasing the rate of cell migration and proliferation (Muller *et al*., 2009). And finally, *P.aeruginosa* can promote cell remodelling in its favour by inhibiting cell differentiation prolonging injury. Image was recreates from an original by (Ruffin and Brochiero, 2019), licenced under CC BY-ND 4.0, which allows sharing and customisation

Numerous studies have reported that *P.aeruginosa* activate epithelial cell death. In (Shepherd *et al*., 2009) it was reported that a three-dimensional tissue engineering model of human skin wounds infected with *P. aeruginosa* results in epidermal loss, de-keratinisation and basement membrane loss. Other documented effects of *P.aeruginosa* and its VF on cells include alteration of cell shape due to destruction of the actin cytoskeleton, decreased stress fibre, focal adhesions, and lamellipodial structures (de Bentzmann *et al*., 2000). Lipopolysaccharide (LPS) and rhamnolipids of *P.aeruginosa* can alter cell morphology and destroy tight cell junctions by

targeting proteins ZO -1 and ZO -2 (Cabrera-Benítez *et al*., 2016, Yi *et al*., 2000). LasB elastase produced by *P. aeruginosa* can affect epithelial cells in two ways: 1) it targets type I and type IV collagen proteins and can thereby directly damage epithelial cells (Nagano *et al*., 2001), it induces the turnover of MMP into active enzymes that promote collagen degradation (de Bentzmann *et al*., 2000). Exotoxins can be injected into epithelial cells through the T3SS system and induce cell death (Hauser, 2009). Muller *et al*. (2009) demonstrated that exposure to pyocyanin causes growth arrest, apoptosis and senescence of cells, and inhibition of wound healing through the generation of reactive oxygen species. It is worth noting that all these VFs are regulated by quorum sensing systems. A study by Jacobsen *et al*. (2012) has shown that the use of a mutant lacking *lasR* and *rhlR* genes prevents the inhibitory effect of *P.aeruginosa* on the repair mechanism of epithelial cells, proving that QS plays a key role in delaying wound healing. **Figure 11** contains a summary of the effects of VF on epithelial cells, ranging from activation of apoptosis to alteration of cell morphology, leading to a delay in healing.

The importance of QS in infections has been questioned by the emergence of QS mutant phenotypes, such as *lasR* mutants, during the progression of chronic infections (D'Argenio *et al*., 2007). Cabrol *et al*. (2003) reported that 50% of all clinical isolates lack the QS gene *lasR*, which regulates the tissue-destroying enzymes LasA and LasB. Such phenotypes could indicate the decreasing effect of QS in chronic infections, where a fitness advantage arises from the loss of the QS system (Heurlier *et al*., 2006). However, this view is challenged by evidence of persistent QS activity isolated directly in the sputum of CF patients. Recent experimental reports have shown that a *lasR* mutant still contains a functioning rhl system, suggesting that QS continues to play a role in infection (Winstanley and Fothergill, 2009), Furthermore, the loss of the QS system, as in the lasR mutant, could influence the switch in the course of P.aeruginosa infection between the acute and chronic states, as lasR mutant phenotypes are common in chronic infections (Jiricny *et al*., 2014).

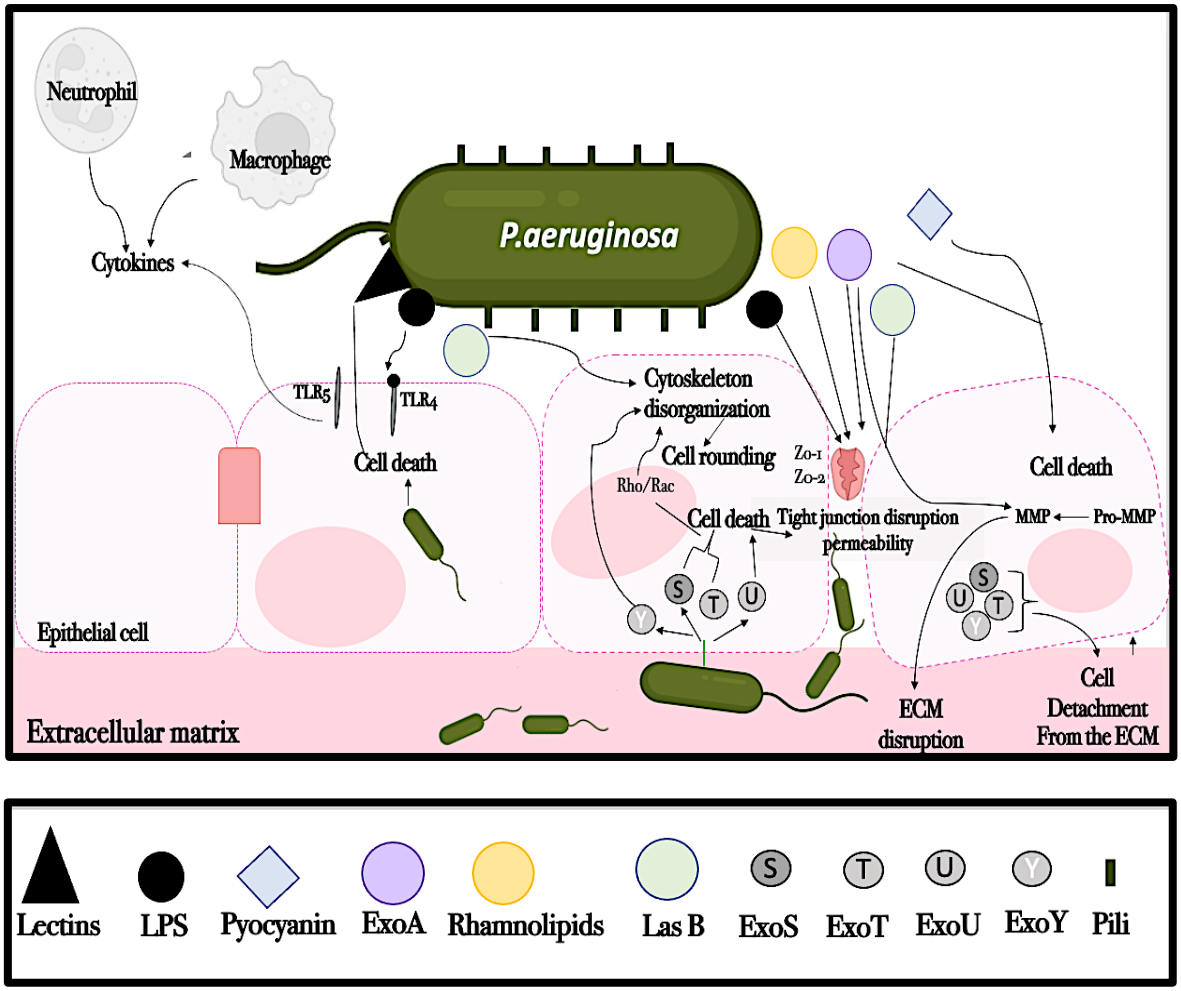

Figure 11: schematic model of the effects of *P. aeruginosa* VFs on epithelial integrity.
P.aeruginosa contribute to cell death, cytoskeleton disorganization and/or tight junction disruption. Image was recreated from an original by (Ruffin and Brochiero, 2019), licenced under CC BY-ND 4.0, which allows sharing and customisation.

5. QS Biosensors: *Chromobacterium Violaceum* CV026

QS biosensors for the detection of AHLs production are strains of bacteria that have a functional LuxR promoter but lack the AHLs synthase enzyme, allowing for only externally provided AHLs to be detected. QS biosensors can be divided broadly into two types: Biosensors that detect acyl-homoserine lactones with a small 4C to 8C such as *Chromobacterium violaceum* CV026 , and biosensors that can detect long chains of AHLs with 10C to 14C such as *Agrobacterium tumefacient* KYC55 (pJZ410,pJZ384, and pJZ372) (Zhu *et al*., 2003). In this project we used *Chromobacterium violaceum* CV026, common QS detector. *C. violaceum* CV026 is a mutant of the Gram-negative bacteria *C.violaceum* ATCC 31532

*(*re-classified recently *to C. subtsugae)* that unlike the mutant CV026 can produce a purple pigment (violacein) encoded by the *vio* operon that is directly controlled by the LuxI/luxR homologue, CviI/CviR, and C6-AHL AHLs (McClean *et al*., 1997a). The *C.violaceum* CV026 biosensor is a mini-Tn5 mutant constructed by McClean (1997), as it does not produce AHLs; the colonies remain white due to lack of violacein production. Production of the violacein pigment is restored when the bacteria are incubated with either the supernatant of bacteria that release AHLs, or synthetic exogenous AHLs, which are commercially available. The simple colour change allows for a straightforward assay for both the presence of AHL and for putative blockers of AHLs (**Figure 12)**.

C.violaceum CV026 was chosen because it is an easily quantifiable QS marker through the production of observable pigment, making *C.violaceum* CV026 a model organism for QS research. In addition, CV026 responds best to short-chain AHLs in natural and synthetic forms (Steindler and Venturi, 2007). For this reason and due to the fact that the HB-PNIPAM is a functionalised polymer with a butyrolactone (C4), *Chromobacterium violaceum* CV026 was selected for this project (see **Chapter 2, section 2.1.1**).

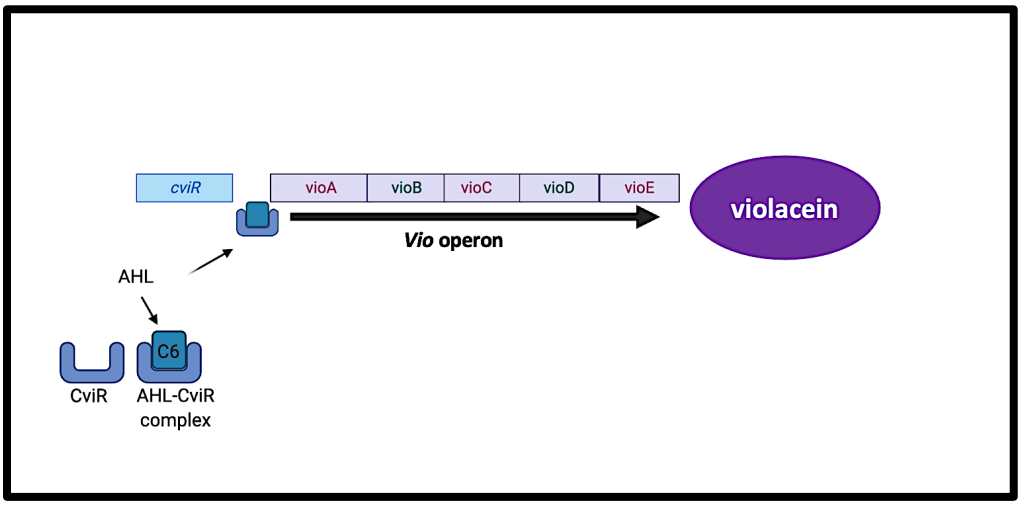

Figure 12: *C.violaceum* CV026 as a biosensor of QS in Gram-negative bacteria. Exogenous AHLs bind to the receptor cviR in *C.violaceum* that promotes the expression of genes within the vio operon encoding for violacein.

6. The Poly(NIPAM) Polymer

Poly(N-isopropylacrylamide) (PNIPAM) was synthesised in 1956 and started out as an effective rodent repellent (Malcolm and Rowlinson, 1957, Schild, 1992). The PNIPAM polymer is part of a large class of synthetic polymers, called stimuli-responsive polymers or "intelligent polymers." These polymers are macromolecules that express swift reversible changes in response to different external environmental factors and return to their previous states after removing the stimulants (Bae *et al*., 1991). Such environmental factors can be pH (Dalmont *et al*., 2008) , light (Schumers *et al*., 2010), electric field (Yan, Q., 2010) or temperature (Zhang *et al*., 2004). The PNIPAM polymer is the most studied stimuli-responsive polymer in biomedical research (Ashraf *et al*., 2016). This is because its lower critical solution temperature (LCST) is close to the physiological temperature of living tissue and it is very flexible to adapt to different medical applications such as drug delivery, cardiovascular repair and medical imaging (He *et al*., 2020). The first report of the ability of these polymers to respond to different stimuli was in 1988 (Kungwatchakun and Irie, 1988). Using the search term "PNIPAM" in PubMed provides more than 3,600 results, where 70% of the results were conducted in the last ten years.

PNIPAM has both hydrophobic and hydrophilic moieties. The polymer's amide group is hydrophilic, whereas the isopropyl moiety and the carbon backbone are both hydrophobic (Gorelov *et al*., 1997). PNIPAM is a thermosensitive polymer that enters a temperature-dependent phase of separation from a coil to a globule, as the elevated temperature initiates an imbalance between the hydrophobic and hydrophilic moieties of the polymer **(Figure 13).** In low-temperature aqueous solutions, PNIPAM remains soluble, while in elevated temperatures the polymer forms insoluble globules. This was explained by Wu and Zhou (1995), as being connected with the strength of bonding between hydrogen bonds and water molecules in low-temperature water (hydrophilic). However, in raised temperatures, the hydrogen bonds are

weakened and disturbed, while the polymer-polymer bonds get stronger, leading to the formation of insoluble precipitates (hydrophobic). PNIPAM undergoes transition from a hydrophilic to a hydrophobic phase when the temperature is above the lower critical solution temperature (LCST) or cloud point (CP), which has been shown empirically to be between 30 and 35°C making it ideal for biological applications. In addition to LCST, some polymers can also have an upper critical solution temperature (UCST). The LCST can change if an ending is attached as it is recorded in Teratanatorn *et al*. (2017) with the polymer Highly branched poly(N-isopropylacrylamide) modified with vancomycin (HB-PNIPAM-van) that shows an LCST to be 18°C before the ending is added and an LCST of 35°C after.

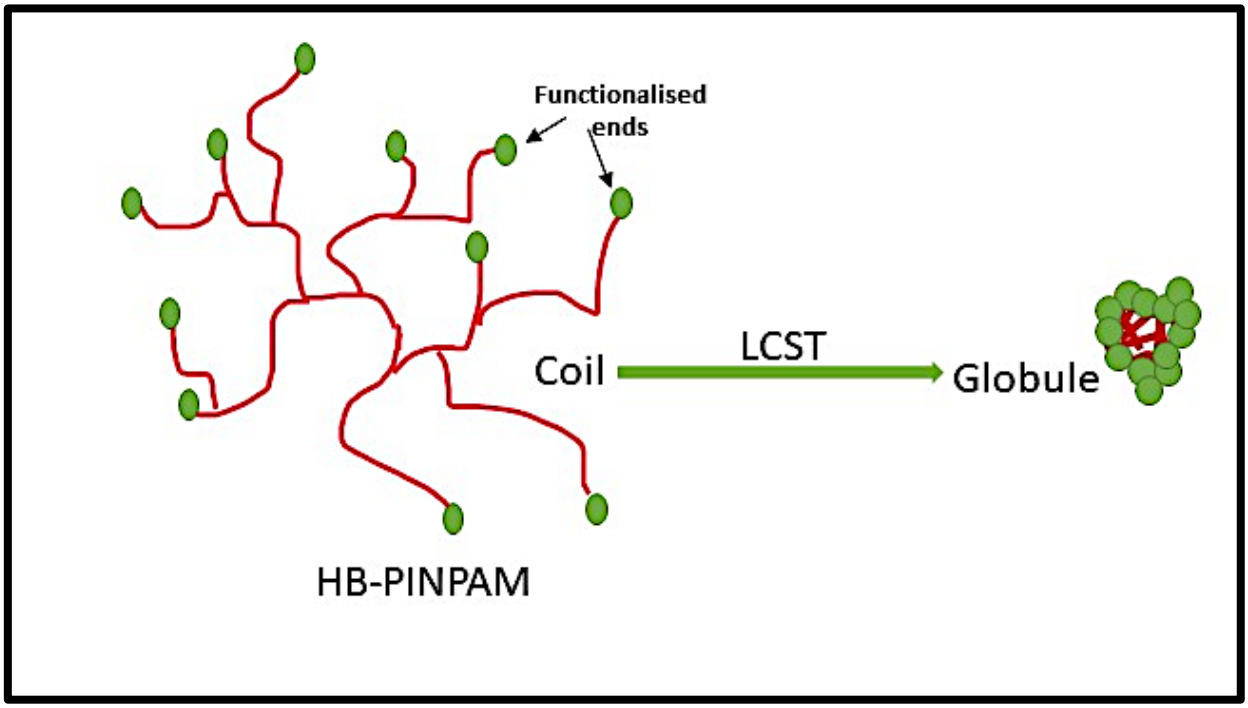

Figure 13: schematic diagram for PNIPAM a thermosensitive polymer when it enters a temperature-dependent phase of separation from a coil to a globule.

6.1 Application

The PNIPAM polymer has gathered much interest in recent years as a valuable material that can be used in different scientific domains, such as immunoassays, drug delivery, and prosthesis. PNIPAM has been produced in many forms, such as microgels, membranes, coatings, and films. Moreover, LCST PNIPAM responses to stimuli can be altered by the

addition of either hydrophobic or hydrophilic monomers. **Table 6** summarises some of the recent biomedical applications of PNIPAM.

Table 6: an overview of some biomedical PNIPAM applications.

Authors	Bio application	Scientific innovation	Improvement in the biomedical field
Lu *et al*. (2022)	Tissue generation	PNIPAM-grafted-chitosan (PNIPAM–Chi) promoting tissue generation through the thermally controlled release of growth factor	Understanding these modified biogenic PNIPAM characteristics can lead to applications as stimuli-responsive coatings that control the adsorption and release of ECM proteins and growth factors to promote the growth and differentiation of stem and other cells on supports for cell culture as well as implants and scaffolds for tissue engineering.
(Ji *et al*., 2022)	Preventing cancer cells from forming through removing H_2O_2 from the environment.	Au@PNIPAm can decompose the intracellular H_2O_2 in living cells, delaying the senescence cells and thus preventing cancer cell formation.	They are removing H_2O_2 from the environment, a key player in transforming cells into senescence cells, which are known to change the cellular microenvironment by a senescence-associated secretory phenotype (SASP).
Wang *et al*. (2022)	Antimicrobial effect against Gram negative and positive bacteria	CuS-PNIPAm NPs can capture bacterial cells and kill them by releasing copper sulfide ions.	The ability of the polymer to capture bacterial cells and expose the bacteria to copper sulfide ions can present a novel approach for treating skin infection.
Pattem *et al*. (2021)	Decrease the count of the biofilm forming bacteria *S.aureus* by physically removing the bacteria .	HB-PNIPAM-Van binds to *S.aureus* to physically remove the bacteria from the cornea surface.	This physical removal of the bacteria can reduce a load of bacteria on the cornea surfaces, thus reducing the infection and cutting the work done by the practitioners. This offers a non-microbial approach to controlling infections.

Overstre *et al*., (2019)	Antimicrobials delivery system	A poly (N-isopropylacrylamide-co-dimethylbutyrolactone acrylate-co-Jeffamine M-1000 acrylamide) (PNDJ) hydrogel that releases antimicrobials at a sustainable concentration in deep surgical wounds, for bacterial eradications and decreasing the chance for surgical site infections.	Application of self-dissolving PNDJ hydrogel (within 4-6 weeks), for multiple dosage to release drugs at a sufficient concentration, that resulted in biofilm eradication from wounds.
Tan *et al*., (2019)	Thermoresponsive polymer functionalised with graphene oxide disrupting bacterial membrane	Poly(ethylene glycol) and poly-N-isopropylacrylamide (PEG-PNIPAM) was designed for investigating bacteria-graphene interfaces for the study of graphene antimicrobial activity	Promising antimicrobial coatings
Alenezi *et al*., (2019)	A gold nanoparticle with a thin layer of PNIPAM coating	The PNIPAM coating allowed for a controlled release of vancomycin on demand.	The incorporation of a gold nanoparticle can convert the light absorbed from the near infra-red, which is then converted into heat. Providing a heat source for the release of drugs from the PNIPAM coating.
Zhan *et al*., (2018)	A dual modified PNIAM and antimicrobial peptide (AMP) bone implant	Improving the biocompatibility of antimicrobial peptides infused bone implants by the conjugation with PNIPAM polymer	The use of PNIPAM with AMP can increase their antimicrobial ability at a room temperature and decrease the AMP cytotoxicity inside the human body.
Lu *et al*., (2018)	A drug delivery that allows for the local release of tobramycin (antibiotic) on the swarming colonies.	A polymer loaded with the antibiotic tobramycin that has a high affinity for the lipopolysaccharide in Gram-negative can strip part of the polymer when adhered to the surface, causing an immediate release on the swarming colonies.	The PNIPAM polymer is conjugated with the peptide ligands YVLWKRKRKFCFI-NH2, to increase the affinity to Gram-negative lipopolysaccharide.
Spagnol,	An antimicrobial	A film made from	Can be employed in different

et al., (2018)	film that has a good antimicrobial activity against candid albicans, and different Gram-negative and -positive bacteria	PNIPAM, and silver nanoparticles impeded on cellulose nanowiskers produced by electrospinning.	antimicrobial film application such as wound dressing.
Doroshenko *et al*., (2018)	A highly branched PNIPAM polymer with vancomycin end group (HB-PNIPAM-van)	The HB-PNIPAM-van was shown to reduce bacterial attachment on the cornea and thus decrease the chance of biofilm formation.	The HB- PNIPAM-van polymer can be employed in combined therapy with different antibiotic to increase their efficacy in resolving a bacterial infection.
Shepherd *et al*., (2011)	A highly branched PNIPAM polymer with a Vancomycin (van) and Polymyxin-B (PMX)	The HB-PNIPAM polymer with antibiotic functionalised ending (van and Pmx) binds to *Staphylococcus aureus* and *P.aeruginosa* respectively, forming a bacteria-polymer complex. The formation of the polymer-bacteria complex made it easy to physically remove the bounded bacteria from the skin model when washed with PBS, decreasing the load of bacteria in the tissue.	Provides a non-bactericidal infection control, which can be employ in topical medical application, such as, wound dressing.
Pasparakis *et al*., (2007)	Reusable bacterial sensing material	A PNIPAM polymer with a multiple sugar residues, which did not attach to the bacteria at temperature above 37°C (LCST).	Providing a control polymer to bacterial interactions can offer the opportunity for innovative diagnostic tools.

7. Quorum Sensing as a Target for Infection Control

Quorum Sensing Inhibition (QSI), also known as Quorum Quenching (QQ), is thought to be a natural mechanism that evolved from bacteria producing AHLs. Examples of QSI include enzymes that degrade AHLs (Uroz *et al*., 2009), or other bacteria and organisms that attempt to compete with these AHL-producing organisms (Grandclément *et al*., 2016). Research on controlling and exploiting QS has also been extended into applied areas to develop antibacterial

and disease control strategies targeting pathogens and invasive populations in medicine. The development of treatments based on QS interferences is largely driven by the need for alternative or complementary approaches to phytochemicals and antibiotics. Quorum sensing is an attractive target for bacterial control for many reasons. First, successful control of bacterial QS can simultaneously target many QS -regulated virulence factors. The advantage of inhibiting QS is that it can attenuate pathogens by interrupting the production of many VFs; thus, it could give the immune system time to eradicate the pathogen (Kong *et al*., 2006).

A large body of literature supports the notion that targeting QS can decrease bacterial pathogenicity (Adonizio *et al*., 2006, Piletska *et al*., 2010, Brackman and Coenye, 2015). Bjarnsholt *et al*., (2005) showed that blocking QS in *P. aeruginosa* can significantly affect the susceptibility of the biofilm to antibiotics and the clearance of immune system cells, namely polymorphonuclear neutrophils. QS intervention targets can be roughly divided into the following areas: (i) autoinducer synthesis, (ii) cell-to-cell autoinducer exchange, and (iii) autoinducer signal perception and transduction through their interaction with sensing/transcription factors.

Several applications for anti-quorum sensing have been proposed, ranging from the use of enzymes that target signalling molecules, such lactonases and acylases (Kalia *et al*., 2011), to QS synthase inhibitors, such as anthranilic acid, which block the synthesis of quinolone signals (pqs) (Lesic *et al*., 2007). Moreover, the discovery of compounds that can competitively bind to the receptors of QS has been proposed (Welsh and Blackwell, 2016) Other examples is the development of vaccines targeting the components of QS (Park *et al*., 2007). However, this application has several shortcomings that explain why no vaccine has yet been developed. First, production costs are high, as in the case of the (AI) antibodies developed by (Park *et al*., 2007). Second, is the unknown risk of immune induction following reinfection. Third, it is difficult to develop a universal QS based vaccine that can broadly target different bacteria, as the

identification and further confirmation of virulence factors secreted by different bacteria is considered an expensive and time-consuming method (Fleitas Martínez *et al*., 2019). Another application is using QS antagonists such as halogens. Borchardt *et al*. (2001) showed that oxidised halogen compounds could react with the signalling molecules 3-oxo-acyl AHL found in *P.aeruginosa.* They are, however, too toxic to mammalian cells to even be considered for medical applications. Most proposed applications would be useful in industrial rather than health-related settings.

Recently, polymers have emerged as promising quorum inhibitors. Linear methacrylate polymers developed by Cavaleiro *et al*. (2015) absorb AHLs and thus reduce biofilm formed by *Aeromonas hydrophila.* Broderick *et al*. (2014) designed a polymer-coated surface that releases macrocyclic peptides 1 and 2, quorum sensing inhibitors, that inhibit the group-III QS system in *S. aureus* is responsible for toxic shock syndrome (TSS) regulation.

7.1 Resistance to anti-QS

It has been argued that resistance pressure is low when using anti- QS because anti- QS agents do not target survivability and resistance pressure is therefore low. However, it is possible for bacteria to develop resistance to some anti- QS agents both in the laboratory and in the clinic, especially in the case of cross-resistance. An example of such resistance is the possibility of mutation in the efflux pump when bacteria are exposed to antibiotics (Maeda *et al*., 2012).

A study by Fozard *et al*. (2012) showcased that the timing of the administration of the anti- QS agent plays a key role in the development of bacterial resistance to the anti- QS agent. It further found that in order to limit the risk of resistance, the early administration of the anti-QS treatment is crucial for the success of biofilm control. Another possibility for resistance is permeability of the biofilm, which proves difficult when the biofilm is mature (Anguige *et al*., 2005, Fozard *et al*., 2012). This illustrates that the state and timing of infection is a limitation for some anti- QS agents to eliminate the bacterial biofilm. Moreover, (Koch *et al*., 2005)

suggested that although there is no immediate selection pressure from the use of quorum-sensing inhibitors, there may be sufficient pressure "in the long term" to develop resistance by promoting bacteria with QS mutations. From this we can deduce that resistance to QS is possible and that treatment with anti-quorum sensing is not a panacea as previously thought. However, the current state of antibiotic resistance makes the search for alternative treatments urgent. The limitations of anti QS treatments to date do not negate their potential impact in fighting infections, but rather regulate their use. For example, anti QS can be a first option to treat an infection, i.e., when a wound first occurs, to stop the progression of the infection. This allows preservation with antibiotics and gives the immune system the opportunity to gain control over the attenuated bacteria. For more details on the interaction between bacteria and the host immune system (see **Chapter 1, section 3**).

7.2 Highly branched PNIPAM polymer with a Homoserine Lactone end group (HB-PNIPAM-HL)

This project explores a promising solution that could have biomedical applications. Here we present a polymer, Highly Branched PNIPAM polymer with a Homoserine Lactone end group (HB-PNIPAM-HL), that can target QS, the polymer could be mass-produced with readily available techniques, unlike, for example, antibodies. In Pasparakis *et al*. (2007) a PNIPAM polymer with functionalised multiple sugar residues was created for inciting a controlled bacterial aggregation when the multiple glucose ends bind to bacteria. However, the sugar binding site was only available for binding when the polymer had transitioned to its globule state. For improving PNIPAM's ability to bind to biological surfaces, whether the polymer is in its coil or globule state, a highly branched PNIPAM (HB-PNIPAM) was developed by (Rimmer *et al*., 2007). Teratanatorn *et al*. (2017) compared the highly branched PNIPAM with a functionalised ending and a linear analogue and showed that highly branched polymers with functionalised ligands have improved polymer binding to the cellular target.

HB-PNIPAM with different functionalised endings were produced by the same group, Rimmer and Teratanatorn, that had the same goal of infection control (**Figure 14**). Shepherd *et al*. (2010) developed a highly branched PINIPAM with modified antibiotics at the chain ends, Vancomycin (van) (Shepherd *et al*., 2010) and Polymyxin-B (PMX) (Shepherd *et al*., 2011), binding selectively to Gram positive (*S. aureus)* and Gram negative (*P.aeruginosa)* bacteria respectively. This binding induced the transition of the polymer from the coil-to globule form, forming visible insoluble aggregates of polymer and bacteria complex which made it easy to physically remove the bound bacteria from a tissue engineered infected human skin model when washed with PBS, decreasing the bacteria load in the tissue. Doroshenko *et al*. (2018) used the highly branched PNIPAM polymer with a vancomycin end group (HB-PNIPAM-van) to reduce bacterial attachment on corneas and thus decrease the chance of biofilm formation.

In this project, the Highly Branched PNIPAM polymer (HB-PNIPAM) was synthesised using self-condensing reversible addition fragmentation transfer polymerization (SCVP-RAFT) (Carter, S. *et al*., 2005). In summary, the process uses a 4-vinylbenzyl pyrrole carbodithioate, a branching monomer that can also act as a transfer agent that has a dithionate ester and a polymerizable vinyl group for RAFT process mediation. HB-PNIPAM was then functionalised with homo-serine lactone (HL), which is readily used by Gram-negative bacteria for QS **(Figure 14).**

The main intention for the development of HB-PNIPAM-HL is to create a polymer that can interact with bacteria and obstruct the QS regulatory process. In previous work by Shepherd *et al*. (2019), the HB-PNIPAM-HL was shown to inhibit the production of the violacein pigment in *C. violaceum* CV026. The work suggested that the effect was due to disturbing QS by inhibiting the formation of the CviR/AHL complex, resulting in prevention of the expression of the *vio* operon (*vio ABCDE*). This project is an extension of this work, as we

will further investigate the polymer, HB-PNIPAM-HL, and its effects on other, more pathogenically relevant Gram-negative bacteria, using *P.aeruginosa* as an exemplar organism.

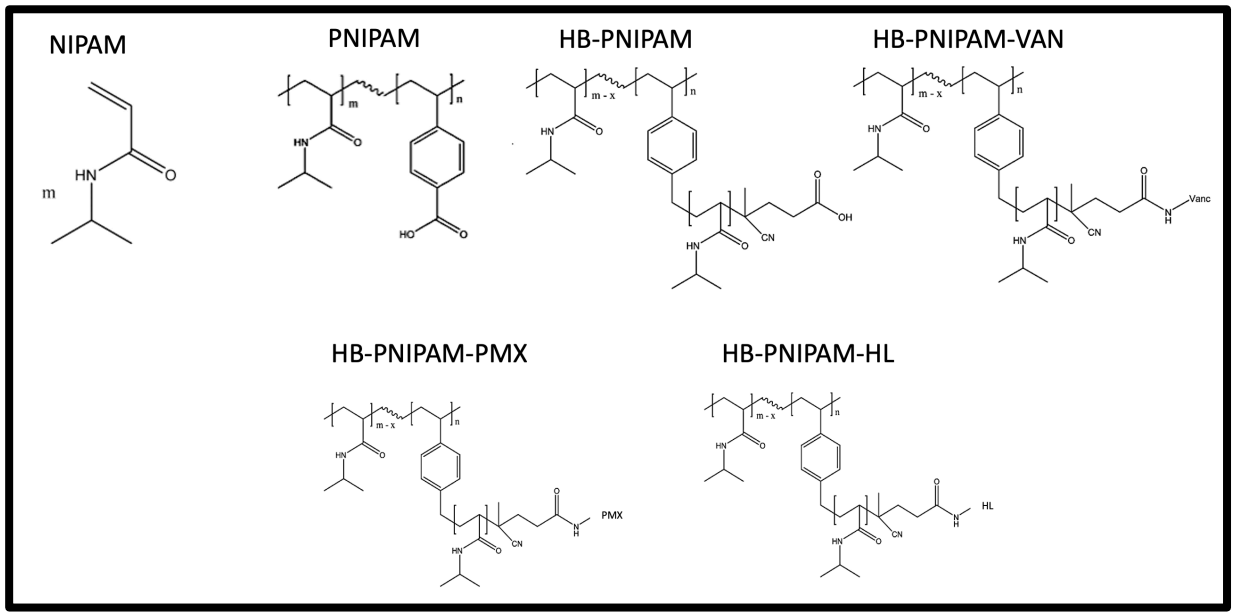

Figure 14: 2D chemical structure of NIPAM, PNIPAM, HB-PNIPAM-van, HB-PNIPAM-PMX, and HB-PNIPAM-HL.

8. Aims and Objectives

Based on the previous section exploring the possibilities of controlling QS, this study aims to investigate the ability of the polymer HB-PNIPAM-HL to disrupt quorum sensing (QS) in Gram-negative bacteria by measuring its effects on various virulence factors regulated by QS, and thus investigate its potential as an alternative approach to infection control. To achieve this goal, the project has the following objectives:

1- *Chromobacterium violaceum* CV026, a QS biosensor, will be used to indicate the concentrations of the polymer HB-PNIPAM-HL necessary to block the production of violacein.

2- Production and expression of *P.aeruginosa* secreted virulence factors LasA and LasB, pyocyanin, rhamnolipids and biofilm will be measured to investigate the extent of HB-PNIPAM-HL disruption of QS-regulated VF production in *P.aeruginosa.*

3- Gene expression levels of QS genes in HB-PNIPAM-HL treated samples compared to untreated samples will be measured using RT -QPCR to investigate potential molecular mechanisms of the action of HB-PNIPAM-HL.

4- Cytotoxicity of HB-PNIPAM-HL will be evaluated using two human cell types, human dermal fibroblasts (HDF) and a keratinocyte cell line HaCat.

5- The effect of the polymer HB-PNIPAM-HL on cell migration of two types of cell lines: HDF and HaCat, to evaluate its potential for wound healing.

6- The effect of the polymer HB-PNIPAM-HL is further investigated in vitro using a 3D skin burn model infected with *P. aeruginosa.* The polymer is administered at two different time points. The first time point is 2 hours after infection, which is an early treatment. The other time point is after 24 hours, which is a late treatment. This helps to determine the optimal time to administer the polymer.

Chapter 2: Evaluating HB-PNIPAM-HL on *Chromobacterium Violacein* CV026 (a quorum sensing (QS) biosensor)

1 Introduction

The main objective of this chapter was to assess the anti-Quorum sensing (QS) potential of the polymer HB-PNIPAM-HL on the bacteria *Chromobacterium violaceum* CV026, an indicator strain ('biosensor') for bacterial QS activities (see **Chapter 1, section 5**). This chapter aims to use our polymer, HB-PNIPAM-HL, with *Chromobacterium violaceum* CV026 to decide the optimum concentration of polymer for inhibition of the violacein pigment. Whilst our polymer has been tested previously on these bacteria (Shepherd *et al*., 2019), here we have investigated a two-fold serial dilution of the polymer on *C.violaceum* and also evaluated the receptor CviR (*cviR*) gene expression as well in the presence of HB-PNIPAM-HL.

1.1 Aims and Experimental Approaches

This chapter aims to investigate the anti-quorum sensing ability of HB-PNIPAM-HL on *Chromobacterium violaceum* CV026,by:

1- Confirming that HB-PNIPAM-HL can inhibit production of the QS regulated pigment, violacein in *C.violaceum* CV026.

2- Measuring gene expression of the CV026 QS system's receptor, *cviR;* and the genes coding for the purple pigments; *vioA, vioC, and vioD* in the presence of HB-PNIPAM-H, using RT-qPCR.

3- Measuring effect of HB-PNIPAM-HL on *C.violaceum* CV026 growth and viability.

2. Materials

2.1 List of materials, instruments, and software used in Chapter 2

2.1.1 Polymer HB-PNIPAM-HL

Dr Tom Swift and Dr Richard Hoskins (polymer chemists at the University of Bradford) synthesised the HB-PNIPAM-HL. The polymer was synthesised using the previously published methodology in (Teratanatorn *et al*., 2017) and (Plenderleith *et al*., 2014) and summarised in

Figure 15. Briefly, the polymer was synthesised by constructing the HB-PINAPM by dissolving NIPAM and ACVA in 140 ml of 1,4 Dioxane. The solution was degassed with nitrogen for 10 min; then, polymerisation was done with a nitrogen blanket for 48h at 60°C. After this, the polymer was purified and precipitated twice in diethyl ether, followed by vacuum filtration, resulting in a dry, unformed powder. 22 g from the resulted HB-PNIAPAM was dissolved in 150 ml of DMV in a nitrogen atmosphere at 65C. A 19g of ACVA was added three times at 24h intervals.

The polymer was again precipitated into diethyl ether. The solid was dissolved in ethanol, then concentrated by ultra-filtration then evaporated to remove any trace of ethanol. This process transformed the ending of the HB-PNIAPM into carboxylic acid (-COOH). The carboxylic ends were then converted into succinimide. The conversion was done by dissolving 17.7g of the HB-PNIPAM-COOH in 150ml DMF. Then 3.03g of N-hydroxy succinimide and 5.5 g of Di cyclohexyl carbodiimide were added to the solution and stirred for 15h at room temperature. Again, the solution was ultra-filtered and precipitated into diethyl ether. The solid was dissolved in ethanol, concentrated by ultrafiltration, and evaporated until dry. A 0.20 g from the resulted HB-PINAPM-succ was dissolved in PBS at room temperature. Then 23 mg of -α-Amino-γ-butyrolactone hydrobromide was added, and the pH was made to pH 9.5 by adding NaOH. The reaction was cooled at 4°C for 16h and then stirred at room temperature for another 32h. The resulting solution was ultra-filtrated and washed four times with ultrapure water. The remaining water droplets were removed by freeze-drying. This results in HB-PNIAPAM-HL. See **Appendix 1** for an image of the polymer in the freeze dry form.

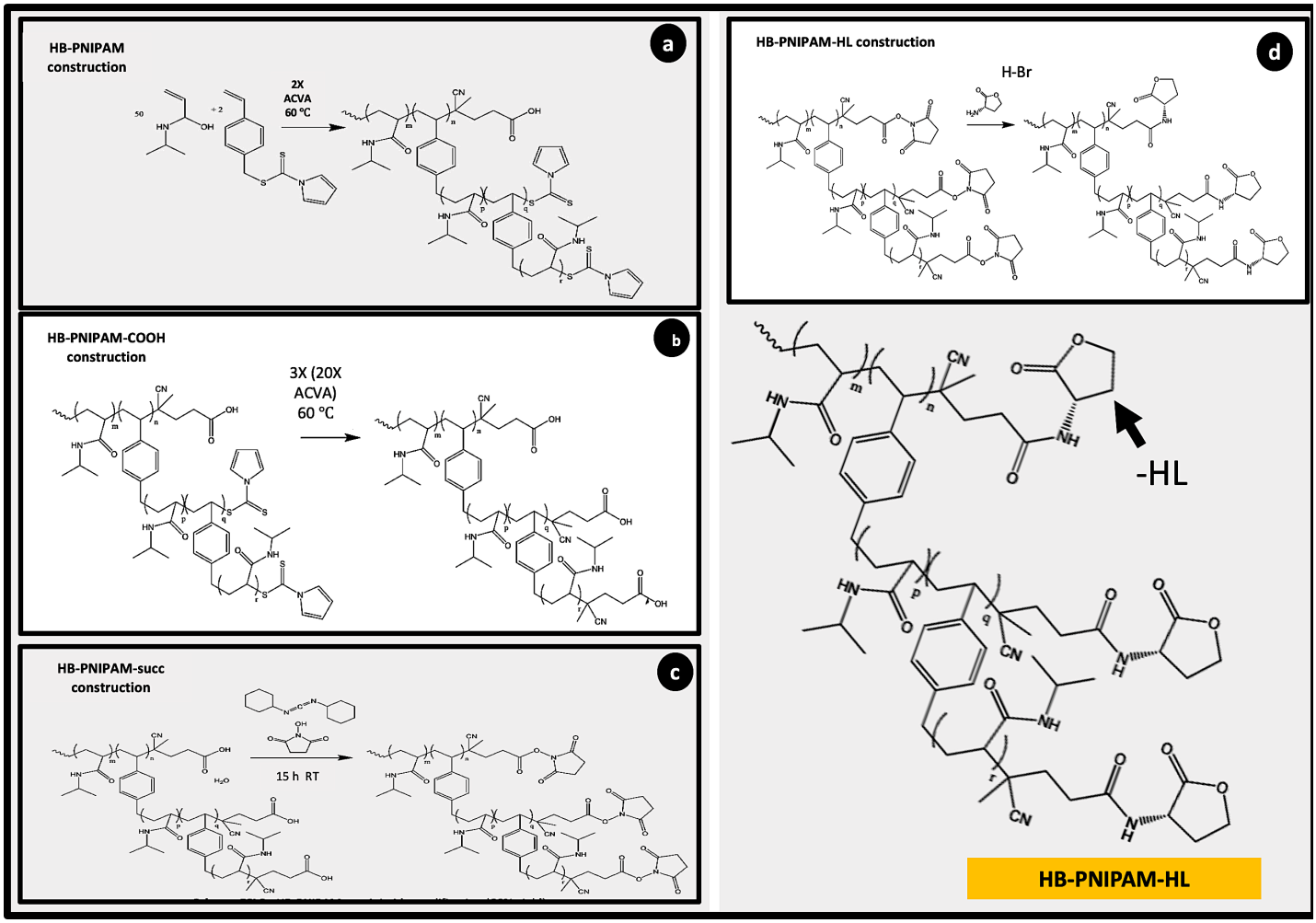

Figure 15: schematic diagram illustrating the process of HB-PINAPM-HL synthesis.
Started by constructing **(a)**HB-PNIPAM, then **(b)** HB-PNIPAM-COOH. After that the COOH ends were then converted to **(c)**HB-PINAPM-succ, and finally the succ ends were converted to **(d)** HB-PINAPM-HL.

2.1.2 Bacterial strains and culture conditions

Table 7: Bacterial strains used in Chapter 2.

Bacteria	Strain	Media	Source
Chromobacterium violaceum	CV026 - mini-Tn5 mutant ATCC 31532	Luria-Bertani (LB) broth and agar (Miller) at 28°C.	Dr Jonathan Shaw , Department of Infection, Immunity & Cardiovascular Disease, University of Sheffield.

2.1.3 Media and Culture

Table 8: List of media used for bacterial culture.

Media	Form	Description	Purpose	Supplier
Luria-Bertani (LB)	Solid	Luria-Bertani agar (powder) and distilled water (DW) 40 g in 1 L	Storage and reactivation of the bacteria	Fisher Scientific

Luria-Bertani (LB)	Broth	Luria-Bertani (LB) broth (powder) and distilled water 25g in 1 L	Overnight growths, and biosensor assay.	Sigma- Aldrich

2.1.4 Reagents

Table 9: Reagents used in Chapter 2.

Reagent	Description	Cat#; Manufacturer details
N-hexanoyl-L-Homoserine lactone(C6-AHL)	**N-hexanoyl-L-Homoserine lactone(C6-AHL)**	**Cat# 10007896; Cayman Chemical, USA**
Thermo Scientific ™ 1kb DNA ladder	-	Cat #11833963; Thermo Scientific ™ GeneRuler™, USA
PCRBIOSYSTEMS 100pb DNA ladder	-	Cat##PB10.14; PCRBIOSYSTEMS,
RNA loading dye	-	Cat# B0363S; BioLabs®
DNA loading dye	-	Cat # B7025S; BioLabs®
Dimethyl sulfoxide	-	Cat# 10213810; Fisher Chemical, Loughborough, UK
Nuclease-free water	-	Cat# AM9920; Invitrogen™, Inchinnan, UK
2x qPCRBIO SyGreen Blue Mix Hi-ROX	-	Cat# PB20.12-05; PCRBIOSSTEMS, London, UK

2.1.5 Kits

Table 10: Kits used in Chapter 2.

Kit name	Cat#; manufacturer info
High-Capacity cDNA Reverse Transcription Kit	Cat# 4368814; Life Technologies Ltd, Paisley, UK
RNA isolation Kit: RNeasy Mini Kit	Cat# 74104; QIAGEN, Manchester, UK
qPCRBIO SyGreen Mix Lo-ROX	Cat# PB20.11-05;PCRBIOSYSTEMS, London, UK

2.1.6 Instruments

Table 11: Instruments used in Chapter 2.

Instrument	Purpose	Manufacturer information
Infinite® M200 Pro Series	Plate reader	Tecan UK Ltd, Reading, UK
QIAGEN' Rotor-Gene Q	RT-qPCR	QIAGEN, Manchester, UK
NanoDrop™	Spectrophotometer	ThermoFisher, USA

2.1.7 Software

Table 12: Software used in Chapter 3 for result analysis.

Software	Distributor
GraphPad Prism	GraphPad Software, CA, USA
Magellan ^{TM} Data Analysis Software	Tecan UK Ltd, Reading, UK

2.1.8 Miscellaneous

Table 13: list of miscellaneous chemicals and tools used in Chapter 2.

Miscellaneous	#Catalogue ;Manufacturer info
96-well flat Bottom microplates	Cat#M0687; Greiner CELLSTAR®, Sigma-Aldrich, UK
PCR strip tubes, 0.1 ml	Cat# I1402-0400; Rotor-Gene®, UK
Agarose	#17850; Fisher Chemical, Loughborough, UK

3. Methodology

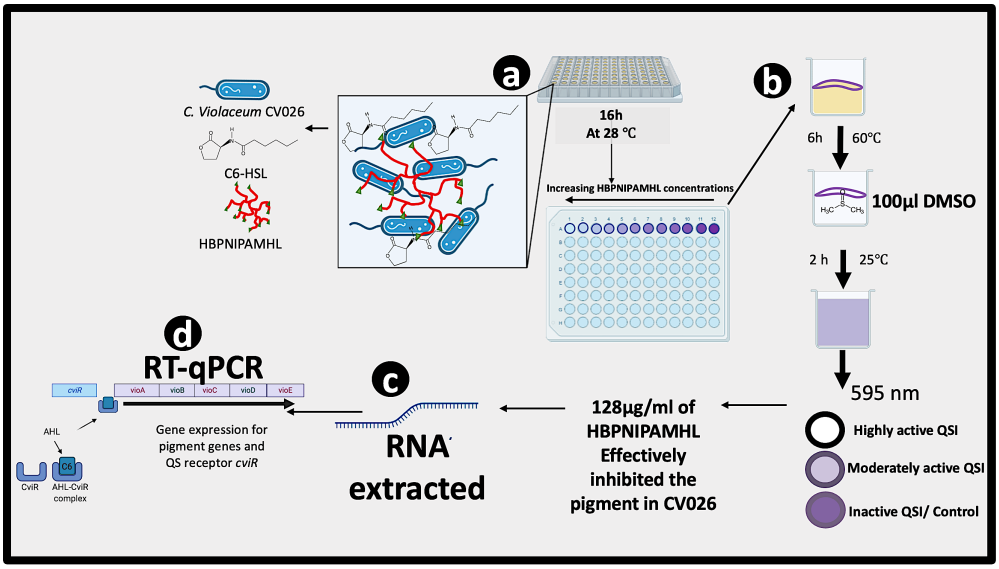

Figure 16 Illustration summarises the experimental methodology used in Chapter 2.
(a) *Chromobacterium violacein* CV026 was added to 96 well plates at OD of 0.3 at 600nm incubated with a constant concentration of C6-AHL (0.15 mg/ml) and increasing concentration of HB-PNIPAM-HL (0-512µg/ml) **(b)** After a static incubation of 16 hours at 28°C, a violet pigment forms in the wells, which is shown as a violet ring/shadow colour in the illustration above. The wells were dried at 60°C for 6 hours. Then the residues were dissolved by adding 100 ml of DMSO and shaking for 2 hours at room temperature. The absorbance was measured at 595nm using a spectrophotometer (The infinite 200 PRO, Tecan). Since the concentration 128µg/ml of HB-PNIPAM-HL showed the most significant pigment inhibition, it was chosen, were **(c)** RNA was extracted from samples treated with 128µg/ml . Then **(d)** gene expression of pigment genes (*vioA, vioC and vioD*) and QS receptor (*cviR)* was measured in the samples treated with 128µg/ml using RT-qPCR.

3.1 Bacteria and culture conditions

Chromobacterium violaceum CV026 (mutant from *C. violaceum* ATCC31532) was cultured in Luria-Bertani (LB) broth medium at 28 °C for 24 h. When required, the medium for *C. violaceum* CV026 was supplemented with the autoinducer, C6-AHL (Caymanchem, Cat#10007896) with a final concentration of 0.15 mg/ml per well. The overnight culture was prepared for the biosensor assay by growing the bacteria in 4 mL LB broth at 28 °C for 24 h in a shaking incubator (130 r/min). For the biosensor assay, the inoculum was diluted to OD of 0.3 at 600nm and added to a 96-well plate (Greiner); please check (**section 3.2 in Chapter 2**) for more Biosensor assay details.

3.2 *Chromobacterium violacein* CV026 bioassay

Principle:

Quorum sensing (QS) is dependent on the interaction between (AI) molecules and their receptors, transcriptional activators. *C. violaceum* produces a violet pigment, violacein, where the encoding *vio* operon is under the control of the QS system. *C. violaceum* CV026 cannot produce its own N-acyl homoserine lactones (AHLs) but can react to exogenous AHLs added. The principle of this assay is that when exogenous AHL is added to the media, the pigment production in CV026 is restored. Otherwise, no pigment is produced in the absence of AHLs. The pigment production is dose-dependent, which means the more AHLs, the more pigment is produced. Pigment production can be quantified by reading absorbance at 595nm using a spectrometer. Putative QS blockers can be added to the *C.violaceum* CV026 alongside exogenous AHLs; no pigment will be produced if the blockers are functional.

Procedure:

The *C. violaceum* CV026 bioassay was carried out according to (McClean *et al*., 1997a). A 10 mg/ml stock of HB-PNIPAM-HL was made in PBS. Then, two-fold serial dilutions of HB-PNIPAM-HL in LB broth medium were prepared, where the concentrations ranged from 512

µg/ml to 0.5 µg/ml **(Figure 15).** In a 96-well plate, overnight culture of CV026 was diluted to (O.D 0.3)[1] in 100 µl of the LB broth (Sigma Aldrich, UK) and HB-PNIPAM-HL mixture. Then, 3 µl of synthetic exogenous C6-AHL (with a final concentration of 0.15 mg/ml)[2] was added, in each well. The plate was incubated statically at 28°C for 16h. After incubation, the 96-well plate was dried for 6 h at 60 °C, and pigment dissolved using Dimethyl sulfoxide (DMSO) and absorbance measured at 590nm using a spectrophotometer (The infinite 200 PRO, Tecan) **(Figure 16).**

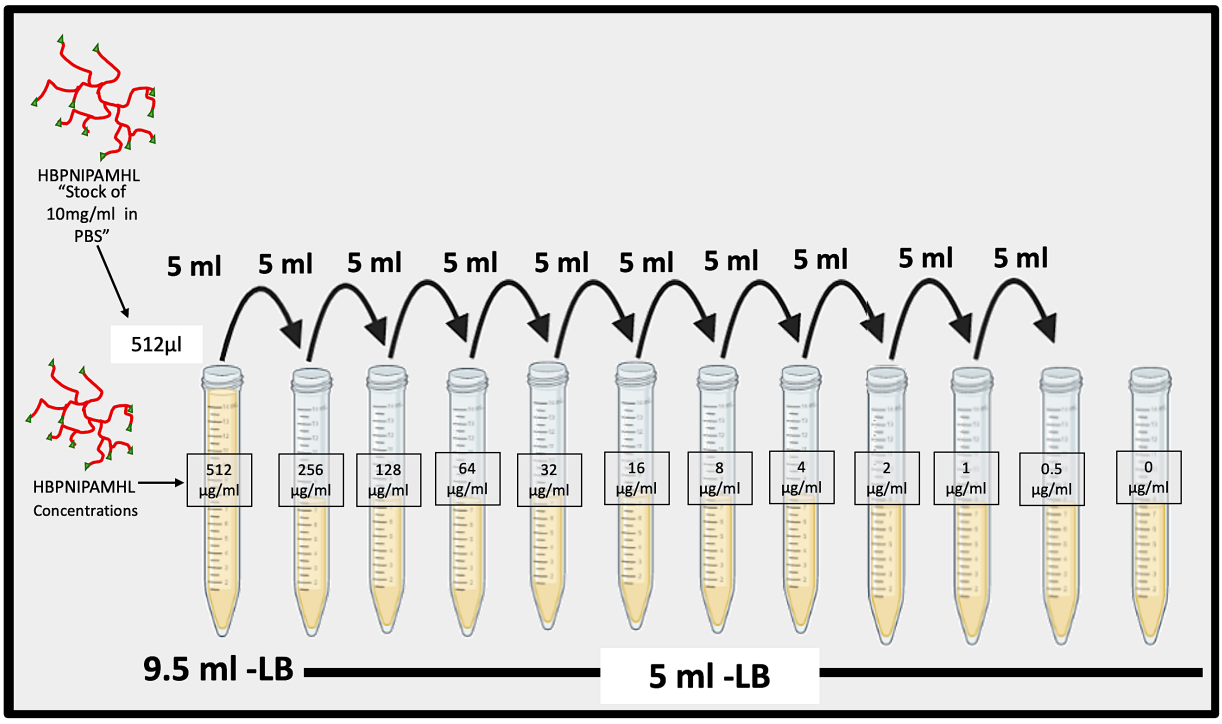

Figure 17: dilutions preparations from HB-PNIPAM-HL 10 mg/ml stock.
The purpose of the following dilutions is to create a two-fold concentrations of HB-PNIPAM-HL that ranged from 0 to 512µg/ml.

3.3 mRNA expression analysis of *C. violaceum* CV026 using RT-PCR

3.3.1 Total RNA extraction and purification

Total RNA was extracted from 300 µl culture of *C. violaceum* CV026 treated with 128 µg/ml for 16 hours using Rneasy Mini Kit, QIAGEN Cat#74106. DNA was removed by the treatment with QIAGEN Rnase-Free DNase1 (Rnase-Free DNase11 Set QIAGEN Cat#79254).

[1] The following OD:0.1,0.2,0.3,0.4,and 0.5. was tested before choosing the OD 0.3.
[2] Different concentrations of C6-AHL before choosing the following: 0.05, 0.1, 0.15, 0.2, and 0.25 mg/ml.

The kit and the DNase treatment manufacturer's instructions were followed (protocol four and protocol seven from RNAprotect Bacteria Reagent Handbook 01/2015). However, some optimisations were attempted for the best results. Such modifications were: (i) isolating the total RNA from the samples after centrifugation for 10 min at 8000 g. (ii)After discarding the supernatant, the pellets were stored at -80C for 1 hour before extraction. (iii) DNase treatment was left for longer than 15 min and sometimes was repeated twice for effective removal of DNA from the samples. (iv) It was found that the samples performed better without the addition of β-mercaptoethanol, as evidenced by less contamination and better quality when measured with Nanodrop (260/280 and 230/260 ratio) (see **section 3.3.1.2**), so it was eliminated from the protocol. (v) The last step of RNA extraction, the same flow-through was run twice through the spin membrane, as it was found that it does increase the expected RNA yield.

RNA isolations start with centrifuging the samples for 10 min at max speed (10000 g). The supernatant was discarded, and the pellet was used. Each samples' pellets were dissolved by 500 µl of RNA Protect solution (RNAprotect Bacteria Reagent, QIAGEN Cat# 76506) and left to incubate at room temperature (25°C) for 5 min. After incubation, samples were centrifuged for 10 min at 5000 g. The supernatant was decanted, and tubes were gently dabbing the inverted onto a paper towel. Pellets were dissolved with 10 µl QIAGEN Proteinase K with 100 µl TE buffer containing lysozyme(Lysozyme from chicken egg white, Sigma-Aldrich Cat#L3790) Samples were vortexed for 10s, then incubated at a room temperature on a shaker. Then, the samples were homogenised by adding 350 µl of the RNA lysis buffer (RLT) per sample and vortexed vigorously. 250 µl of 100% ethanol was added to samples and mixed by pipetting. The lysate was filtered by loading into a 2 mL Mini spin column and centrifuged (15s ≥ at 8000×g).

The flow-through was discarded, and 700 µl Buffer RW1 was added and centrifuged for 15s at 8000 X g to wash the spin column membrane. After discarding flow-through, 350 µl of Buffer RW1 was added to the column and centrifuged for 15s at 8000 g then flow-through was again discarded. The stock solution was made by adding 70 µl of RNase free DNase digestion buffer (RDD) to 20µl from DNase-I stock solution for each sample (no vortex, just gentile inverting of the tube was used to mix as DNase is sensitive to physical denaturation). 80 µl of the DNase solution was used to treat each sample by adding it directly to the membrane of the column (O-ring) and left to incubate for more than 15 minutes. Again, samples were treated with 350 µl RNA wash buffer 1 (RW1) to the spin column and left to incubate for 5 min then centrifuged for 15s ≥ at 8000 g. Here both the collection tube and flow-through was discarded. In a new 2 ml collection tube, the spin column was placed, and 500 µl of the second RNA wash buffer with ethanol (RPE) was added, then centrifuged for 2 min at 8000 g. This step was repeated but in a new 2 ml collection tube. The spin column was placed on a new 1.5 collection tube, and elution with 50 µl of Rnase-free water was added and centrifuged for 1 min at 8000 g. This step was repeated but by rerunning the flow-through through the spin column**.** A volume of 100 ng/ml of RNA was reverse transcribed into cDNA. A High-Capacity cDNA Reverse Transcription kit ™ (Applied Biosystems, Cat#4368814) was used to generate cDNA, followed by the manufacturer's recommendations.

3.3.1.1 Quantification of RNA concentration and purity

RNA isolation is an essential step in determining gene expression levels in samples. Making sure of the purity of the RNA sample is of utmost importance. To achieve such goals, here we have established multiple-step system. First, all RNA samples were cleaned using the kit (RNA Clean-up Kit, Monarch Cat# T2030L). Second, the quality and concentration of the RNA samples were checked at A260/280 ratio and made sure to be ~2.0 using Nano drop (NanoDrop™ Lite, Thermo Fisher). Lastly, the integrity of RNA was investigated through 1%

agarose gel as was recommended by (Sambrook, 1989). Samples were mixed with RNA buffer dye 1:2 (RNA Gel Loading Dye, Thermo Fisher Cat# R041) and heated at 70°C for 10 min then left to cool at room temp for 15-20 min, before running on agarose gel.

3.3.2 Reverse Transcription (RT) of RNA to complementary DNA (cDNA)

The RNA concentration was diluted in all samples to 100 ng/ ml for cDNA synthesis. The calculation was done using the equation below: The dilution of the RNA concentration is necessary because the undiluted concentration could be too high for RT-qPCR.

A volume of 100 ng/ml of Total RNA=100/total RNA concentration X10 (µl)

A High-Capacity cDNA Reverse Transcription kit ™ (Applied Biosystems, Cat#4368814) was used to generate cDNA, followed by the manufacturer's recommendations (**Table 14**).

Table 14: Reverse Transcriptase master mix.

Component	20 µl Volume (per 1 reaction)
10X RT Buffer	2 µl
25X dNTP mix (100mM),	0.8 µl
10X RT Random Primers	2 µl
MultiScribe Reverse Transcriptase	1 µl
Nuclease- free WATER	4.2 µl
RNA sample	10 µl (con. 100 ng/ ml)
TOTAL per each sample	**20µl**

A master mix of a total 10 µl per reaction was prepared on ice by mixing: 2 µl 10X RT Buffer, 0.8 µl 25X dNTP mix (100mM), 2 µl 10X RT Random Primers, 1 µl MultiScribe

Reverse Transcriptase, and 4.2 µl Nuclease- free WATER. Then 10 µl of RNA at a concentration of 100 ng/ml was added for each sample. The cycling condition was set as follows:

	1st step	2nd step	3rd step	4th step
Temperature	25°C	37 °C	85°C	4°C
Time	10 min	120 min	30 min	∞

3.3.3 Quantitative Real-Time Polymerase Chain Reaction (RT-qPCR)

3.3.3.1 RT-qPCR

RT-qPCR is the standard technique for quantifying gene expression, even if the expression level of the target genes is low (Holland, 2002). Here SYBR green qPCR was chosen for measuring the gene expression of QS genes in *C.violaceum* CV026. Before choosing the appropriate endogenous gene, 3 genes were chosen, (*16S rRNA*, *rpoD,* or *gyrB*), to test their stability with and without the treatment. The stabilization step is vital to eliminate any non-specific variation in the cDNA and RNA extraction contamination (Rocha *et al*., 2016). SYBR green is a fluorescent dye that is only released when bound to the double-strain DNA measured after each cycle. There are three considerations for RT-qPCR; (i) primers designed must be specific to the target genes, (ii) the RNA must be purified and free from any protein or phenols contamination and include a DNase digestion step on extraction, and (iii) the stability of the chosen reference target genes. A further step of investigating the integrity of the RNA through a 1% agarose gel is recommended (Sambrook, 1989).

3.3.3.2 Primer design

Wherever available or found in the literature **(Table 15),** primers for QS genes were designed and ordered from Sigma-Aldrich, USA. When designing the following article was taken as a guide (Bustin and Huggett, 2017). The primer quest tool (available at:

https://www.idtdna.com/Primerquest/Home/Index) was used for primer design. Each gene's forward and reverse primer was tested against the genomic DNA first. The absence of a band, wrong size or having more than one band was an indication of the unsuitability of the primers, where either a change in the annealing temperature or a redesign of the primers was performed.

Table 15: Primers used in Chapter 2.

Reference genes				
Gene	**Primer sequence**	**Length (bp)**	**Reference/ Designed**	**Supplier**
16s rRNA	**Fwd** 5′-TAACGCATCGGAATGTACCG-′3 **Rev** 5′- TAATCAGACATCGGCTGCTC-′3	129	Designed	Sigma-Aldrich, UK
rpoD	**Fwd** 5′-GAATTCGGAGTCCACCGAGG -′3 **Rev** 5'-GCATCCAGGTATGCGAGGAA –'3	128	Designed	
gyrB	**Fwd** 5′- CAGCCAGACCAAAGATAA -′3 **Rev** 5′- TTTCCAGCAGATAGGTTT -′3	92	(Shepherd *et al*., 2019)	
The evaluation result to choose the most stable reference gene can be found in **Appendix 3**				
Target genes				
Gene	**Primer sequence**	**Length (bp)**	**Reference/ Designed**	**Supplier**
cviR	**Fwd** 5′-ATCCTGGACATCAGCGAAAG-′3 **Rev** 5′- GCACAATGGCGTGAGTACGAT-′3	91	Designed	Sigma-Aldrich, UK
vioA	**Fwd** 5′-GACTACAAGCTGGAAGAT-′3 **Rev** 5′- GTCGGTATAGAAGAACAC-′3	93	(Shepherd *et al*., 2019)	
vioC	**Fwd** 5′-CTACATGCACGGCAAGTTTC-′3 **Rev** 5′- TACGGCTCGGAAGTGAAATAC-′3	75	Designed	
vioD	**Fwd** 5′-TAATCCGCTGTCCTATCT-′3 **Rev** 5′- CTCGTTATGGTGGATCAG-′3	82	(Shepherd *et al*., 2019)	

3.3.3.3 Evaluating the reference genes

RT-qPCR is a technology to measure a gene's expression (the amount of mRNA produced) and how they change in different conditions, i.e., when treated vs untreated samples. The mRNA produced has many factors that might affect the production levels, such as gene activity and the

initial amount of cDNA between different samples tested. A second gene, termed housekeeping, or reference gene was used for a normalisation step to mitigate these factors. One important characteristic of this reference gene is that this reference gene is not affected by the treatments tested. Here, we tested several reference genes (*16sRNA, rpoD, and gyrB*) under different conditions (untreated and treated). Then we assessed the variability in measured Ct values for each reference gene by measuring the standard deviations (SD) (**Appendix 3**).

3.3.3.4 RT-qPCR protocol

A master mix of 10 µl for each sample using 2 X qPCRBIO SyGreen Blue Mix Hi-ROX (PCR BIOSYSTEMS, Cat#PB20.15-05) was prepared following the manufacturer's instructions **(Table 16).** Briefly, 5 µl of qPCRBIO SyGreen Blue Mix, 0.5 µl from both forward and reverse primers **(Table 15),** 3.5 µl of nuclease-free water, and 0.5 µl of cDNA were pipetted in qPCR 0.1 ml tube strips (T319-4N RotoCycler™).

The cycle temperature was set as follow: initial incubation of 95°C for 10 minutes, followed by 40 cycles of 95°C (10 sec), 62°C (30 sec),72°C (20 sec). The melt curve was set by increasing 1ºC increments from 72°C to 95°C. The analysis was done by relative quantifying of the expression level for reference genes and target genes after and before polymer exposure. The calculation was performed using the $2^{-\Delta\Delta Ct}$ method (Schmittgen, 2008). The formula (2-ΔΔCt for control / 2-ΔΔCt for treated) was used to calculate the fold change. For example, the control 2-ΔΔCt always gets a value of 1. If the treated samples get a value above 1, it means that the gene is upregulated in the treated samples, and if it is below 1, it is downregulated. If the treated samples get a 2-ΔΔCt value of 0.5, we divide 1 by 0.5, which means down-regulation by 2-fold.

Table 16: SYBR™ Green Master Mix.

Component	10 µl Volume (per 1 reaction)
2X qPCRBIO SyGreen Blue Mix	5 µl

Forward primer (10 mM)	0.5 µl
Reverse primer (10 mM)	0.5 µl
Nuclease-free water	3.5 µl
Template DNA	0.5 µl
TOTAL per each sample	**9.5 µl**

3.4 Determination of *C. violaceum* CV026 viability (Miles and Misra surface drop method)

A viable colony count of *C. violaceum* CV026 in the presence of 128 µg/ml of HB-PNIPAMHL was carried out using (Miles *et al*., 1938) surface drop method. The surface drop method provides an estimation for the number of viable bacteria cells. Serial dilutions in PBS (10^{-1} – 10^{-12}) of *C. violaceum* CV026 cultured overnight with or without polymer (HB-PNIPAM-HL) in PBS were performed in a 96 well plate. Then, 5 µl drops from the dilutions 10^{-1} – 10^{-12} were spotted on LB agar plates. Plates were allowed to dry for 15 minutes then incubated overnight at 28°C. The following day the numbers of colonies were counted, and the number of colonies forming units per ml of media (CFU/ml) was calculated using the following formula:

CFU per ml = Average number of colonies for a dilution x 200 x dilution factor.

3.5 Statistical analyses

The University of Sheffield Statistics Department (301) was consulted throughout the project. All data were first checked for normality before statistical analysis began. Normality was checked mainly with the D'Agostino-Pearson Omnibus test, as the Shapiro-Wilk test does not work well when there are ties, which is recommended on the official GraphPad Prism website. When the data are normally distributed, ANOVA was used with Tukey's, Dunnett, or

Bonferroni tests post-tests was used to determine significance between groups ($p < 0.05$). If the data are not normally distributed, a Mann-Whitney test analysis was used to determine statistical significance ($p < 0.05$). All values are presented as mean ±SD. The graphs and normality of distribution for the data were tested and created with the software GraphPad Prism (version 9.3.1; GraphPad Software, Inc., La Jolla, CA, USA).

4 Results

4.1 *C.violaceum* CV026 pigment production is inhibited as the concentration of the polymer HB-PNIPAM-HL is increased.

The current study investigated the anti-Quorum sensing (QS) activity of the polymer HB-PNIPAM-HL by using the QS biosensor bacteria *C.violaceum* CV026. The production of violacein (purple pigment) in *C.violaceum* CV026 is controlled by the addition of the AHLs (C6-AHL) **(Figure 18, A).** The investigation was done using LB media supplemented with fixed concentrations of the synthetic AHL C6-AHL which represents the endogenous AHLs produced by wild type *C.violaceum*. Effects on violacein production in CV026 after incubation with twofold serial dilutions of HB-PNIPAM-HL were measured. Results showed significant reductions in violacein at the polymer concentrations of 8,16,32,64,128,256, and 512 μg/ml, as shown in **Figure 18, B** with a pigment production from treated samples of 58,35,21,16.7,14.8, 15.9,and 19% respectively **(Table 17).** The percentage of reduction can be calculated from **Table 17** for samples treated with HB-PNIPAM-HL at the concentrations from 8-512 μg/ml to be 42,65,79,83,85,84,and81%. There is a clear trend of decreasing pigment production in CV026, as the HB-PNIPAM-HL concentrations increased (**Figure 18, B).** The result indicates that the effect of HB-PNIPAM-HL is dose-dependent, as the higher the concentration of the polymer, the more efficient the reduction of pigment production. These results mirror those observed in an earlier study by (Shepherd *et al*., 2019) using the same polymer, although it was at different concentrations.

Interestingly, when observing the data in **(Table 17),** we can see that using a 128 µg/ml concentration of HB-PNIPAM-HL results in the lowest amount of violacein produced by *C.violaceum* CV026, slightly lower than the higher concentrations of 256 and 512 µg/ml, although the differences are not statistically significant.

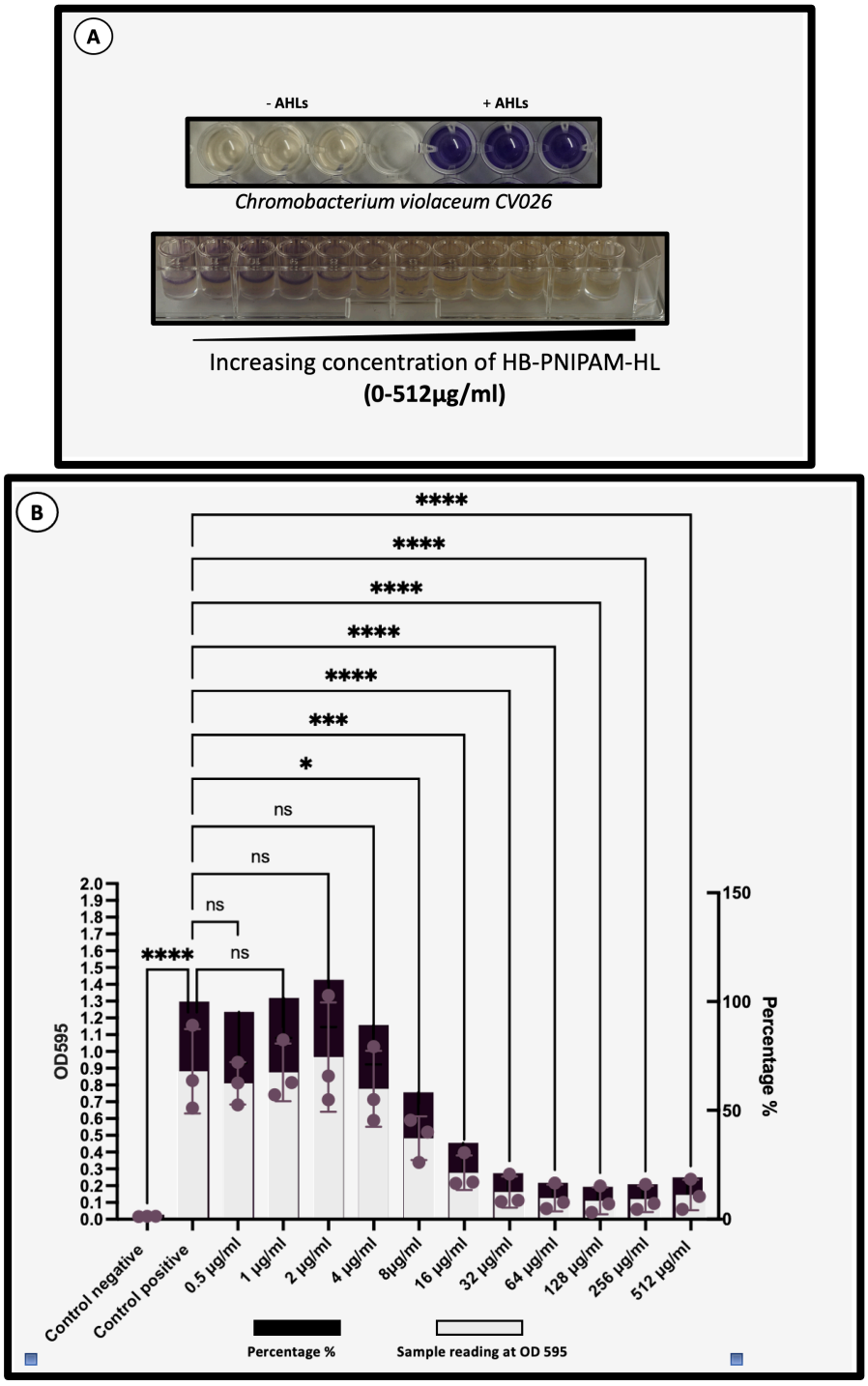

Figure 18: effect of increasing concentration of HB-PNIPAM-HL on violacein production

in *C.violaceum CV026*.

(A) shows that *C.violaceum* CV026, without supplementation with AHLs (here is C6-AHL used), the bacteria cannot produce violacein. The image below shows how pigment decreased in production as the concentration of HB-PNIPAM-HL increased. An overnight culture of *C.violaceum* CV026 (OD 0.3) and increasing concentration of HB-PNIPAM-HL (two-fold dilution; from 0-512µg/ml was incubated in 96-well plates with supplemented LB media with C6-AHL (0.15 mg/ml). Incubation conditions were static at 28°C for 16h. **(B)** shows the data obtained from measuring the pigment produced in the 96-well plates after drying at 60°C for 6 h and dissolving in 100µl DMSO, then measuring at 595nm. The black graphs represent these data after converting them into a percentage with the sample positive control (no polymer) fixed as 100%. Control negative represent only *C.violaceum* CV026 in LB without the supplementation with C6-AHL; Control Positive is *C.violaceum* CV026 growing in LB with C6-AHL added to the media and no polymer treatment. (n=3). Experimental data are expressed as mean ± standard deviation. Significance was determined using one-way ANOVA analysis of variance with Dunnett's test (version 9.3.1) *, *P*= 0.04, ***,*P*=.0008, ****, *P*> .0001. Error bars= SD. (Full ANOVA Results can be found in **Appendix 4**).

Table 17: Mean (±SD, Range) percentage of violacein pigment produced from *C.violaceum* CV026 after treatment with a twofold dilution (0-512 µg/ml) of HB-PNIPAM-HL compared to control.

Sample	% Mean of produced violacein (±SD, Range)
Control Positive (0 polymer , no AHLs)	1.336% (±0.6760,1.332-2.668)
Control Negative (0 µg/ml HB-PNIPAM-HL 0.15 mg/ml of AHLs)	100% (±0.000. 100-100)
0.5 µg/ml HB-PNIPAM-HL, with 0.15 mg/ml of AHLs	95.30% (±23.56, 80.87-122.5)
1 µg/ml HB-PNIPAM-HL, with 0.15 mg/ml of AHLs	101% (±18.39,89.73-122.9)
2 µg/ml HB-PNIPAM-HL , with 0.15 mg/ml of AHLs	110% (±21.76, 86.11- 128.7)
4 µg/ml HB-PNIPAM-HL, with 0.15 mg/ml of AHLs	89.28% (±18.16, 71.28-107.6)
8 µg/ml HB-PNIPAM-HL, , with 0.15 mg/ml of AHLs	58.33% (±26.67, 41.02-89.04)
16 µg/ml HB-PNIPAM-HL , with 0.15 mg/ml of AHLs	35% (±21.79, 18.51-59.71)
32 µg/ml HB-PNIPAM-HL, with 0.15 mg/ml of AHLs	21.08% (±17.07, 9.054-40.62)
64 µg/ml HB-PNIPAM-HL, with 0.15 mg/ml of AHLs	16.74% (±14.05, 5.494-32.48)
128 µg/ml HB-PNIPAM-HL, with 0.15 mg/ml of	14.85 (±13.56, 3.560-29.89)

AHLs	
256 µg/ml HB-PNIPAM-HL, with 0.15 mg/ml of AHLs	15.97 (±13.67, 5.160-31.34)
512 µg/ml HB-PNIPAM-HL, with 0.15 mg/ml of AHLs	19.21 (±15.66, 5.085-36.06)

4.2 Pigment genes expression and *cviR* with the addition of HB-PNIPAM-HL at a concentration of 128µg/ml

A further molecular investigation was carried out after observing the reduction in violacein pigment in *C. violaceum* CV026 assay upon treatment with HB-PNIPAM-HL **(section 4.1).** The violacein pigment produced by CV026 is controlled by the QS system in *C. violaceum*, as violacein is synthesised through tryptophan, a product of the *vioABCD* operon (August *et al*., 2000b), where *vioA* is regulated directly by CviR, the QS receptor in *C. violaceum* (Swem *et al*., 2009). This control starts with the receptor CviR binding to the AHLs (C6-AHL), forming a complex that binds to DNA at the promoter driving violacein genes to be regulated (**see Figure 12 in Chapter 1, section 7**).

The analysis of gene expression undertaken here, is aimed to understand the effect of our polymer on violacein production at the gene level. Gene expression analysis using RT-qPCR was performed for different genes coding for violacein pigment (*vioA, vioC, and vioD*) and quorum-sensing regulated receptor gene (*cviR*) in *C. violaceum* CV026 after treatment with 128µg/ml of HB-PNIPAM-HL and incubated for 16h at 28°C. The results obtained from RT-qPCR (**Figure 19, A)** show that HB-PNIPAM-HL significantly (P=0.05, P= 0.002, and P=.0076) downregulated the vio genes responsible for the production of violacein (*vioA*, *vioC*, and *vioD*), calculating a reduction of 2.5, 2.9 and 2.3-fold, respectively .This effect can be traced to the observed significant (P=.0002) downregulation of *cviR* 8 folds. The gene *cviR* that codes for the receptor CviR in CV026 acts as the primary activator of the *vio* operon for

violacien production. This finding corroborates the ideas of Shepherd *et al*. (2019), who suggested that the reduction effect of HB-PNIPAM-HL on violacein might be due to the polymer's antagonist effect on *cviR.* However the nature of this antagonism between *cviR* and HB-PNIPAM-HL, passive or active, is yet to be explored.

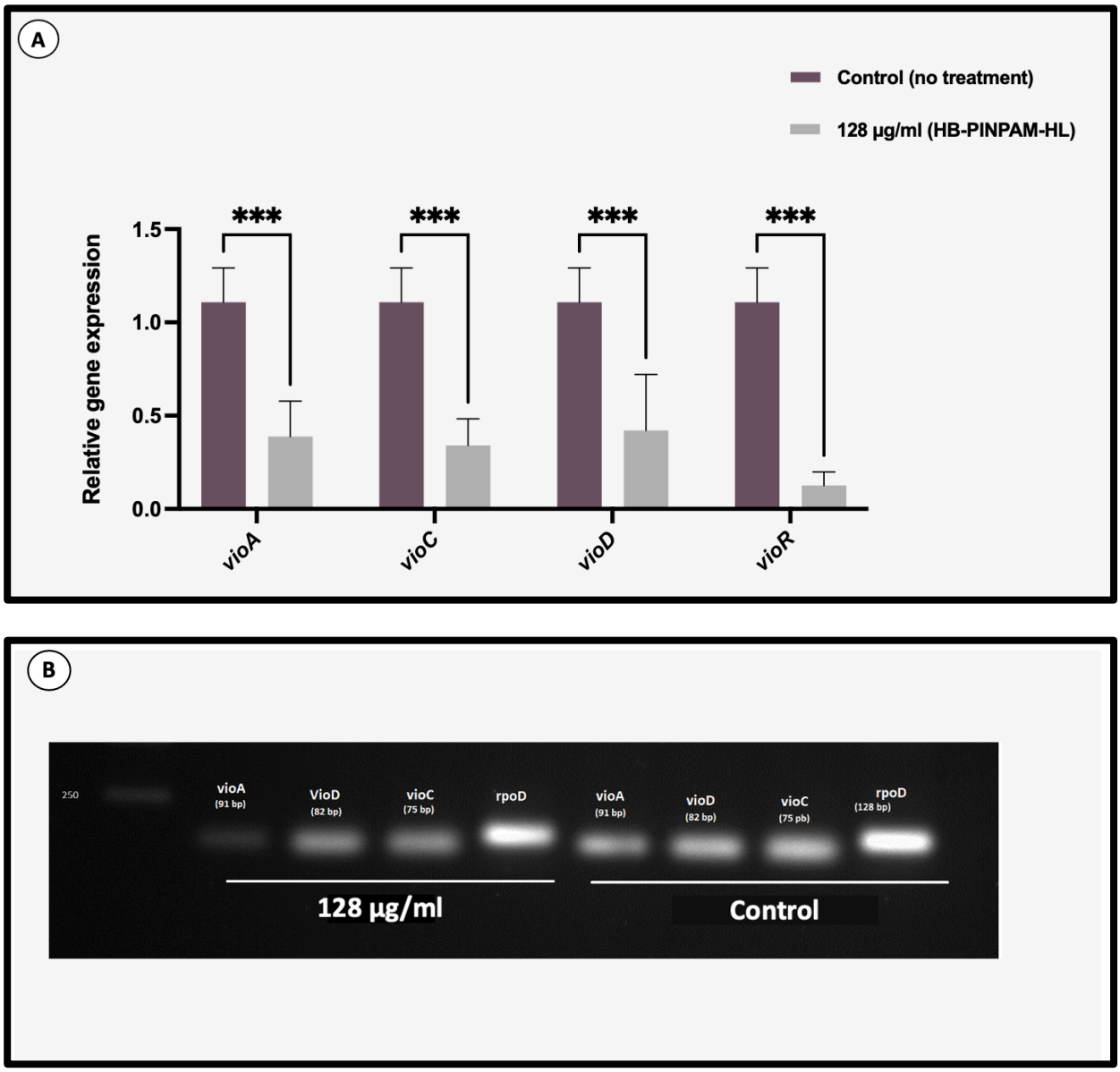

Figure 19: gene expression levels changes in *C. violaceum* CV026 treated with 128ug/ml of HB-PNIPAM-HL quantified by RT-qPCR and normalised with the reference gene *rpoD*

Here, the violacein genes of CV026 (*vioA, vioC, and vioD)* and the luxR homologue, *cviR*, were investigated**. (A) T**he graph shows the effect of 128 µg/ml of HB-PNIPAM-HL on the expression of violacein regulated genes and the QS receptor CviR (*cviR*). The untreated sample was used as a negative control. The relative expression was considered as 1 . **(B)** shows a gel run on an agarose gel (1%) of the RT-qPCR products after a run to examine product size in (bp) here, *rpoD* was

used as a reference gene. (n=3). Experimental data are expressed as mean ± standard deviation. Significance was determined using two-way ANOVA analysis of variance with Bonferroni test (version 9.3.1) ***,*P*>0.0001. Error bars= SD. (Full ANOVA Results can be found in **Appendix 4**).

4.3 Viability of *C.violaceum* CV026 in the presence of 128µg/ml concentration of HB PNIPAM-HL

The numbers of colonies were counted and number of colony forming units per ml of media (cfu/ml) calculated for *C.violaceum* CV026 after treatment with 128µg/ ml HB-PNIPAM-HL. The colony showed a non-significant reduction between treated and untreated **(Figure 20, A&B)**. However, the number of bacterial cells/ ml is very high, which could indicate a technical error.

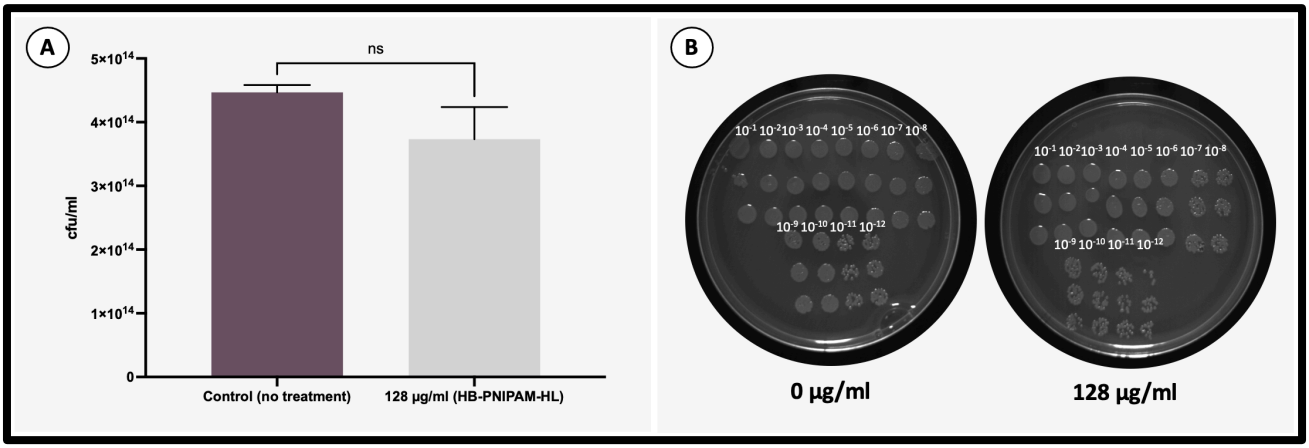

Figure 20: viability of *C.violaceum* CV026 was measured after treatment with 128µg/ml of HB-PNIPAM-HL, using the Miles and Misra drop surface method.

(A) shows no decrease in colony forming units (CFU) in the sample treated with 128µg/ml of HB-PNIPAM-HL. **(B)** shows the serial dilution of the Colony on LB agar plates. (n=3). Experimental data are expressed as mean ± standard deviation. Significance was determined using a Mann-Whitney test analysis in prism (version 9.3.1). ns= not significant Error bars= SD.

5 Discussion

The use of the polymer HB-PNIPAM-HL aims to reduce bacterial QS regulated virulence without significantly affecting viability. Targeting virulence factors results in weaker bacteria that cause less harm to the host, as immune cells can quickly eliminate the bacteria (Choo *et al*., 2006). *Chromobacterium violaceum* (*C. violaceum* was recently renamed *C. subtsugae*), a

Gram-negative bacterium, produces the pigment violacein in response to QS regulated gene expression. A biosensor strain, *C. violaceum* CV026 (mini-Tn5 mutant of the wild-type strain), which lacks (AI) synthase (*cviI*) and requires exogenous addition of AHL to produce violacein, was developed to provide a practical tool for biological assays to screen QS inhibitors and investigate the QS mechanism. Inhibition of the violacein pigment in *C. violaceum* CV026 is commonly used for screening anti- QS compounds (see **Chapter 1, section 7**).

The experiments in this chapter were conducted to investigate the anti-quorum sensing (QS) potential of the HB-PNIPAM-HL polymer by assessing its effect on the QS regulated production of the purple pigment (violacein) in *C.violaceum* CV026 in the presence of C6-AHL. The CviR-dependent quorum sensing pathway regulates the production of the violacein pigment in CV026 (Swem *et al*., 2009). Therefore, inhibition of the pigment suggests disruption of the AHL-regulated QS process (Husain *et al*., 2019). The result sections **4.1, 4.2 and 4.3** of this chapter show that HB-PNIPAM-HL inhibits the production of the pigment violacein in *C.violaceum* CV026 in a dose-dependent manner without significantly affecting growth.

The main objective of the initial investigation on *C.violaceum* CV026 was to find out which polymer concentrations can stop or significantly inhibit violacein production without killing the bacteria. Increased concentrations of HB-PNIPAM-HL, specifically the following concentrations: 8,16,32,64,128,256 and 512 μg/ml, resulted in significant inhibition of violacein production calculated as 42,65,79,83,85,84,and 81%. respectively **(Figure 18, A&B).** A concentration of 128 μg/ml of HB-PNIPAM-HL was selected as it was most effective in reducing violacein production (85%).

Violacein production is promoted by the binding of the signalling molecule C6-HSL to the QS receptor CviR to form the complex (cviR-C6-HSL). The complex is stabilised into a dimer that binds to the DNA binding site and interacts to allow gene expression of violacein

(August *et al*., 2000a). Violacein is synthesised from tryptophan by the products of the vioABCD operon, with the vioA promoter regulated by the QS receptor CviR (Swem *et al*., 2009). Gene expression of the pigment genes (*vioA, vioC, and vioD*,) and the QS receptor c*viR* in *C.violaceum* CV026 was examined at RT-qPCR in section **4.2, Chapter 2** after treatment with 128 µg/ml. All genes examined (*vioA, vioC, vioD* and *cviR*) showed a significant reduction in expression in the samples treated with 128 µg/ml HB-PNIPAM-HL (**Figure 18**). The reduction of *cviR* after treatment with HB-PNIPAM-HL compared to control was 8- fold reduction and for the *vio* genes, *vioA*, *vioC* and *vioD* was 2.5- fold, 2.9 and 2.3-fold reduction respectively. This suggests that the inhibition of violacein observed in **Figure 19** might be due to HB-PNIPAM-HL preventing AHLs from binding to the receptor cviR (Mcclean *et al*., 1997b). Bacterial viability, measured by counting CFU/ml of *C.violaceum* CV026 after treatment with 128 µg/ml HB-PNIPAM-HL, was calculated using the method of Miles and Misra (Miles *et al*., 1938). There was no significant difference in CFU/ml of *C.violaceum* CV026 between the untreated samples and the samples treated with 128 µg/ml HB-PNIPAM-HL (**Figure 19**). In summary, the data shown in this chapter suggest that HB-PNIPAM-HL has an anti- QS effect on *C.violaceum* CV026, leading to the to the downregulation of pigment genes (*vioA, vioC* and *vioD*) and a QS receptor (*cviR*). The mechanism of this ability has not yet been explored for HB-PNIPAM-HL. However, there are several theories on the possible explanations for the QS quenching abilities of HB-PNIPAM-HL. One is that HB-PNIPAM-HL sequesters the added AHLs in the media, making it difficult for bacteria to sense and interact with the AHLs to form the CviR /AHLs complex that can trigger violacein production. Recently, several functionalised polymers have been shown to potentially disrupt QS by sequestering signalling molecules. Cavaleiro PhD *et al*. (2015) reported the use of linear polymers to sequester AHLs through covalent and non-covalent interactions. In addition,

Piletska *et al*. (2010) developed molecularly imprinted polymers (MIPs) for passive sequestration of AHL molecules.

A second theory was proposed in (Shepherd *et al*., 2019), namely active binding to the QS receptor CviR. Although the hydrodynamic radius of the polymer was measured to be (≈17 nm), which is too large for channel-mediated transport. The end of the polymer functionalised by homoserine lactone (-HL) could actively interact with CviR. Further studies are needed as interaction with a cytoplasmic CviR seems to be difficult, especially in Gram-negative bacteria, as their cell wall provides a natural resistance to the size of the polymer (Osborn *et al*., 1964), making it difficult for HB-PNIPAM-HL to penetrate the outer membrane barrier to actively bind to CviR. However, it cannot be excluded that part of the polymer (-HL ends) interacts with the cytoplasmic receptor in CV026 without further investigation **(see Future Work, Chapter 5).**

6 Summary of Chapter 2 Findings

6.1 HBPNIPAM-HL can stop violacein production significantly at a concentration of 128 μg/ml.

6.2 We can trace the anti-Quorum sensing effect of the polymer HB-PNIPAM-HL at a concentration of 128 μg/ml to a molecular level, as it downregulated the expression for the QS receptor *cviR* in *C.violaceum* CV026. Consequently, downregulating the expression of the violacein pigment genes (*vioA, vioC, and vioD*).

6.3 The concentration of 128 μg/ml of the HB-PNIPAM-HL did not significantly affect the CFU number of *C.violaceum* CV026.

From the above, we can confidently choose the concentration of **128** μg/ml **of HB-PNIPAM-HL** as a baseline when moving to the opportunistic pathogen *Pseudomonas aeruginosa* PAO1 in **Chapter 3.**

Chapter 3: Evaluating HB-PNIPAM-HL Inhibiting Virulence Factors Controlled by the QS Systems in *Pseudomonas aeruginosa* PAO1.

1. Introduction

The previous chapter concluded that the polymer HB-PNIPAM-HL could disrupt the quorum sensing (QS) in *Chromobacterium violaceum* CV026 as evidenced by significantly inhibiting production of the violacein pigment. This chapter aims to move the investigation of our polymer from an QS indicator bacterial strain to the Gram-negative opportunistic pathogen *Pseudomonas aeruginosa*. *P. aeruginosa* was selected for the following reasons: 1) *P.aeruginosa* has been the model pathogen for studying QS, where the QS regulated pathways for virulence factors in *P.aeruginosa* have been studied extensively. 2) HB-PNIPAM-HL will be tested on a burnt 3D skin model, and where *P. aeruginosa* is a prevalent pathogen in chronic burn wounds (Church *et al*., 2006).

As discussed in **section 2.1**, **Chapter 1**; *P.aeruginosa* is an important opportunistic bacterial species that causes many chronic infections in humans. *P. aeruginosa* is notorious for possessing multiple and, in some cases, all known resistance mechanisms **(Chapter1, Table 2).** These factors make *P.aeruginosa* one of modern medicine's greatest challenges, and the development of alternative treatments is a matter of urgency.

P. aeruginosa has an arsenal of virulence factors (VFs) that the bacteria employ to establish the infections niche (Barr *et al*., 2015). Two examples of these VFs are tissue destructing enzymes, and biofilm formation (Nadal Jimenez *et al*., 2012). VFs enable *P.aeruginosa* to fight/evade immune cells (Kharazmi, 1991) and destroy tissues (Saint-Criq *et al*., 2018) that can cause deaths or promote chronicity that demands lifelong treatments (Barr *et al*., 2015). Most of these VFs are under Quorum sensing (QS) regulations. The vast arsenal that *Pseudomonas aeruginosa* has demanded more than one QS regulator, as was discovered in (Toder *et al*., 1994, Pearson *et al*., 1995, Pesci *et al*., 1999), *Pseudomonas*

aeruginosa possesses three QS systems that regulate different VFs: *las* system, *rhl* system, and *pqs* system. Each of the three QS systems regulates different VFs or shares the production, as seen in lasB elastase and rhamnolipids expression (Pearson *et al*., 1997). The QS *las* system regulates several VFs, including the expression of the genes that encode lasA protease, lasB elastase, alkaline protease, and exotoxin A (Winson *et al*., 1995). The *rhl* system controls the regulation of lasB elastase, alkaline protease, pyocyanin, and rhamnolipid (Brint and Ohman, 1995). lastly, the *pqs* system regulates the following VFs: pyocyanin, lasB elastase, and rhamnolipid (Lee and Zhang, 2015).

1.1 **Aims and experimental approaches.**

This chapter aims to investigate the anti-quorum sensing ability of HB-PNIPAM-HL on *Pseudomonas aeruginosa* PAO1, by:

1- Testing whether the HB-PNIPAM-HL can inhibit some QS regulated important virulence factors, such as lasA protease, lasB elastase, pyocyanin, rhamnolipids, and biofilm formation.

2- Testing the gene expression of the QS systems; *las* system (*lasl, lasR*), *rhl* system (*rhlI, rhlR*) after treatment of HB-PNIPAM-HL and compare it with the two polymer controls HB-PNIPAM-succ and HB-PNIPAM-COOH.

3- Analysing the RNA-seq of samples treated with HB-PNIPAM-HL and HB-PNIPAM-succ.

3- Evaluating the growth of *Pseudomonas aeruginosa* PAO1 treated with HB-PNIPAM-HL.

2. Material

2.1 List of materials, equipment, and softwires used in Chapter 3

2.1.1 Bacterial strains and culture conditions

Table 18: Bacterial strains used in Chapter 3

Bacteria	Strain	Media	Source
Pseudomonas aeruginosa	PAO1	Luria-Bertani (LB) broth and agar (Miller) at 37°C	Dr Katie Muddiman ,Department of Animal and Plant Sciences ,University of Sheffield

2.1.2 Media and Culture

Table 19: List of media used for bacterial culture.

Media	Form	Description	Purpose	Supplier
Leria-Bartani (LB)	Solid	Luria-Bertani agar (powder) and distilled water (DW) 25 g in 1 L	Storage and reactivation of the bacteria	Fisher Scientific
Leria-Bartani (LB)	Broth	Luria-Bertani (LB) broth (powder) and distilled water 40g in 1 L	Overnight growths, and biosensor assay.	Sigma- Aldrich

2.1.3 Reagents

Table 20: Reagents used in Chapter3

Reagent	Description	Cat#; Manufacturer details
0.2% azocasein in 50mM Tris-HCL	2 mg of azocasein (Sigma) was dissolved in 1 ml of 50mM Tris-HCL (pH 7.2)	Azocasein (Cat#A2765; Sigma-Aldrich, Dorset, UK)
10% trichloroacetic acid (TCA)	A stock of 5 ml was made by adding 500 µl trichloroacetic acid solution (Sigma) in 4500 µl of distilled water	Trichloroacetic acid solution (Cat#T0699;Sigma-Aldrich, Dorset, UK)
Elastin –Congo red (ECR) buffer	100mM of Tris (Fisher scientific), 1mM $CACl_2$ (Merck chemicals), 600 mg of tris base and 44.4 mg in 400 ml of DW. The pH was adjusted to 7.5	Tris Base (Cat# 178204;Fisher scientific) $CACl_2$ (Cat# 1.02382 ;Merck chemicals)
19% Orcinol reagent	47.5 mg of Orcinol (Sigma-Aldrich)was dissolved in 2.5 ml 53% H_2SO_4 the sample was then diluted further to reach 0.19% to be used in the assay.	Orcinol (Cat#447420;Sigma-Aldrich, Dorset, UK)
Thermo Scientific ™ 1kb DNA ladder	-	Cat #11833963; Thermo Scientific ™ GeneRuler™, USA
PCRBIOSYSTEMS 100pb DNA ladder	-	Cat##PB10.14; PCRBIOSYSTEMS,
RNA loading dye	-	Cat# B0363S; BioLabs®
DNA loading dye	-	Cat # B7025S; BioLabs®
Dimethyl sulfoxide	-	Cat# 10213810; Fisher Chemical,

		Loughborough, UK
Nuclease-free water	-	Cat# AM9920; Invitrogen™, Inchinnan, UK
2x qPCRBIO SyGreen Blue Mix Hi-ROX	-	Cat# PB20.12-05; PCRBIOSSTEMS, London, UK

2.1.4 Kits

Table 21: Kits used in Chapter 3

Kit name	Cat#; manufacturer info
High-Capacity cDNA Reverse Transcription Kit	Cat# 4368814; Life Technologies Ltd, Paisley, UK
RNA isolation Kit: RNeasy Mini Kit	Cat# 74104; QIAGEN, Manchester, UK
qPCRBIO SyGreen Mix Lo-ROX	Cat# PB20.11-05;PCRBIOSYSTEMS, London, UK

2.1.5 Instruments

Table 22: Instruments used in Chapter 3

Instrument	Purpose	Manufacturer information
Infinite® M200 Pro Series	Plate reader	Tecan UK Ltd, Reading, UK
QIAGEN' Rotor-Gene Q	RT-qPCR	QIAGEN, Manchester, UK
NanoDrop™	Spectrophotometer	ThermoFisher, USA
Sunrise ™	Plate reader	Tecan UK Ltd, Reading, UK

2.1.6 Software

Table 23: Software used in Chapter 3 for result analysis

Software	Distributor
GraphPad Prism	GraphPad Software, CA, USA
Magellan ^{TM} Data Analysis Software	Tecan UK Ltd, Reading, UK

2.1.7 Miscellaneous

Table 24: List of miscellaneous chemicals and tools used in Chapter 3

Miscellaneous	#Catalogue ;Manufacturer info
0.22 µm syringe filter	Cat#SLGSM33SS; Millipore™, Watford, UK
96-well flat Bottom microplates	Cat#M0687; Greiner CELLSTAR®, Sigma-Aldrich, UK
PCR strip tubes, 0.1 ml	Cat# I1402-0400; Rotor-Gene®, UK
Agarose	#17850; Fisher Chemical,

	Loughborough, UK
Chloroform	Cat# 10102190; Fisher Chemical, Loughborough, UK
Elastin-Congo red	#MKCD7537; Sigma-Aldrich, Dorset, UK
Ethanol	Cat#: A4094; Fisher Chemical, Loughborough, UK
Ethyl acetate	#270989; Sigma-Aldrich, Dorset, UK
Ethidium bromide	Cat# 15585011; Invitrogen™, Inchinnan, UK
Isopropanol	#10674732; Fisher Chemical, Loughborough, UK
L-Rhamnosemonohydrate	Cat#R3875; Sigma-Aldrich Dorset, UK
Methanol	Cat#: A412-500; Fisher Chemical, Loughborough, UK
Phenol-chloroform	#77617; Sigma-Aldrich, Dorset, UK

3. Methodology

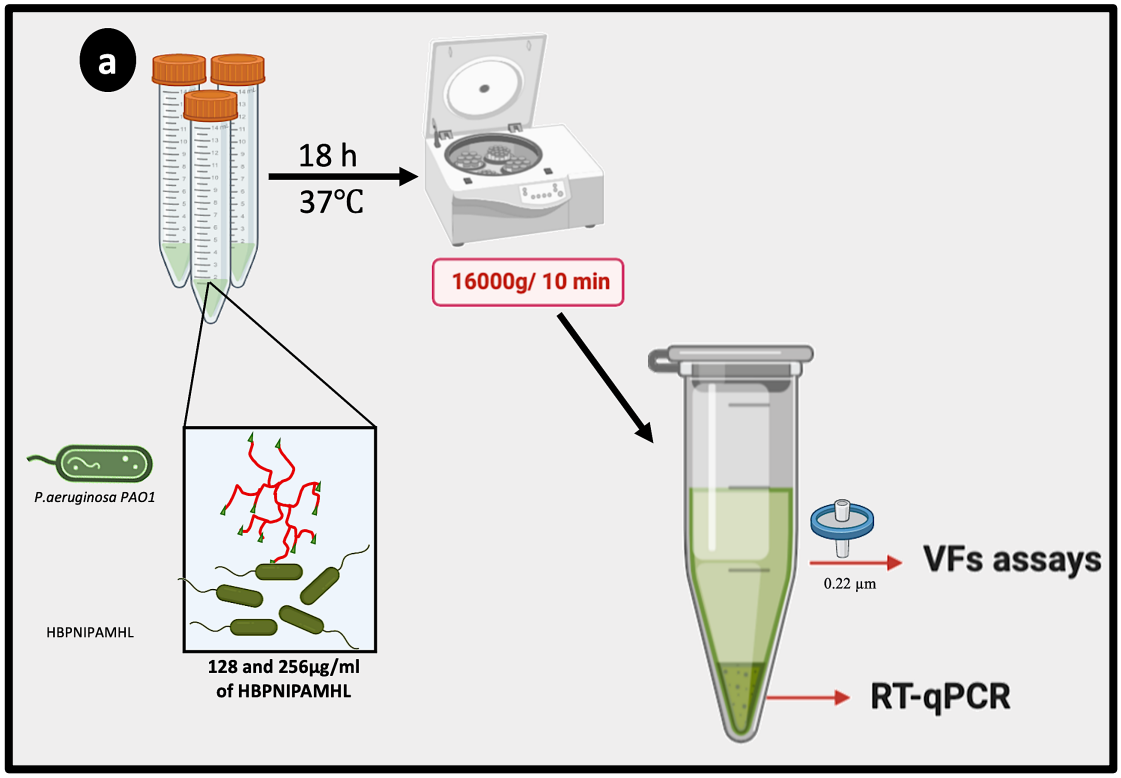

Figure 21: schematic illustration of *Pseudomonas aeruginosa* supernatant preparations.
(a)*P.aeruginosa* PAO1 was diluted from an overnight culture to an OD600 of 0.1 in LB media with various concentrations of HB-PNIPAM-HL and then incubated for 18 hours at 37°C. After incubation, samples were centrifuged at 16000g for 10 minutes.

3.1 Bacteria and culture conditions

Pseudomonas aeruginosa PAO1 was cultured in Luria-Bertani (LB) medium at 37 °C for 24 h. The overnight culture was prepared for investigation of various assays by growing the bacteria in 4 ml LB broth at 37 °C for 24 h in a shaking incubator (130 r/min). For testing the effects of HB-PNIPAM-HL on *Pseudomonas aeruginosa* PAO1, the inoculum was diluted to OD of 0.1 at 600nm see (**Figure 21).**

3.2 Growth curve

A growth curve was measured to examine the growth patterns of *P. aeruginosa* PAO1 over 20h in the presence of 256 μg/ml of HB-PNIPAM-HL and HB-PNIPAM-succ (control polymer). For the growth curve, an overnight culture of *P. aeruginosa* PAO1 was diluted to OD600 of 0.05 in LB media then 100 μl incubated with 100 μl of different concentrations of HB-PNIPAM-HL and HB-PNIPAM-succ in 96 well plates (Greiner, UK Cat# 655101). The plates were incubated at 37°C for 20 h in a plate reader (Sunrise plate reader, Tecan) with orbital shaking for 2s every 30 min before reading absorbance at 600nm. The bacterial growth rate show in **(Figure 31,B**) was calculated using the following formula:

$$\mu = (\log N_t - \log N_0) * 2.303/(t-t_0)$$

μ= growth rate at the log phase
N_t= bacteria OD reading at the end time (hour),t
N_0= bacteria OD reading at the start time (hour), t_0
t= Time of the calculation of the growth (end of the log phase)
t_0= Time of the beginning of the bacterial growth (start of the log phase)

The small diagram on the left of (**Figure 30, A)** was calculated with the same formula as above, but without focusing on the log phase, but on the time of the set point and afterwards, as seen in the table here:

hours	Control average reading	HB-PNIPAM-HL Average readings	HB-PNIPAM-succ Average readings	percentage growth for control	percentage growth for samples treated with HB-PNIPAM-HL	percentage growth for treated with HB-

						PNIPAM -succ
1	0.1715	0.11	0.102			
2	0.19075	0.12175	0.10125	104% Example =LOG(0.19075)-LOG(0.1715)*2.303/(2 h-1h)	123%	143%
3	0.2245	0.1345	0.139	101%	119%	131%
4	0.21825	0.15375	0.21875	83%	126%	113%
5	0.25875	0.2425	0.40675	94%	122%	64%
6	0.331	0.635	0.55	87%	41%	44%
7	0.6185	0.89625	0.694	90%	14%	30%
8	0.92775	1.0655	0.85975	45%	-4%	12%
9	1.05225	1.0505	0.9225	10%	-2%	7%
10	1.115	1.0615	0.9685	0%	-4%	4%
11	1.1615	1.043	1.00875	-4%	-4%	0%
12	1.1035	1.00275	1.03175	-11%	-2%	-1%
13	1.047	0.964	1.04075	-8%	1%	-2%
14	1.03025	0.947	1.03625	-3%	2%	-2%
15	1.04775	0.93225	1.02525	-1%	3%	-2%
16	1.03625	0.9115	1.01	-3%	4%	-1%
17	1.011	0.88675	1.0055	-3%	6%	0%
18	1.008	0.8775	1.00525	-1%	6%	-1%
19	1.0125	0.85525	0.9995	0%	8%	0%

3.3 Supernatant preparation

P.aeruginosa PAO1 was grown in LB broth for 24 h at 37°C. The overnight suspension was diluted to an OD600 of 0.1, then 5 µl of the diluted overnight growth was transferred into new 15 ml centrifuge tubes (15 ml polypropylene centrifuge tubes, Greiner, UK Cat#339650) with 1 ml fresh LB broth containing 128 or 256 µg/ml HB-PNIPAM-HL, and incubated for 18h at 37°C. The lid was loosened for optimal extraction of pyocyanin for more oxygen circulation, which is essential for its production. The tubes were shaken with the lowest rpm setting (<90 rpm) for effective rhamnolipids extraction. After 18h of incubation, bacteria were transferred into new 1.5ml Eppendorf tubes (1.5 ml Eppendorf tubes, Greiner, UK Cat#616201). The cells were harvested by centrifugation at 16000g for 10 minutes. The supernatant was filtered using

a 0.22 µm syringe filter (Syringe filter, Millipore™, UK Cat# GSWP04700). The pellets were stored immediately at -80 °C for further molecular investigations.

The methodology used for *P.aeruginosa* virulence factor investigation in the presence and absence of HB-PNIPAM-HL is summarised in (**Figure 22).**

3.4 Evaluating HB-PNIPAM-HL on *Pseudomonas aeruginosa* PAO1 QS controlled virulence factors (VFs)

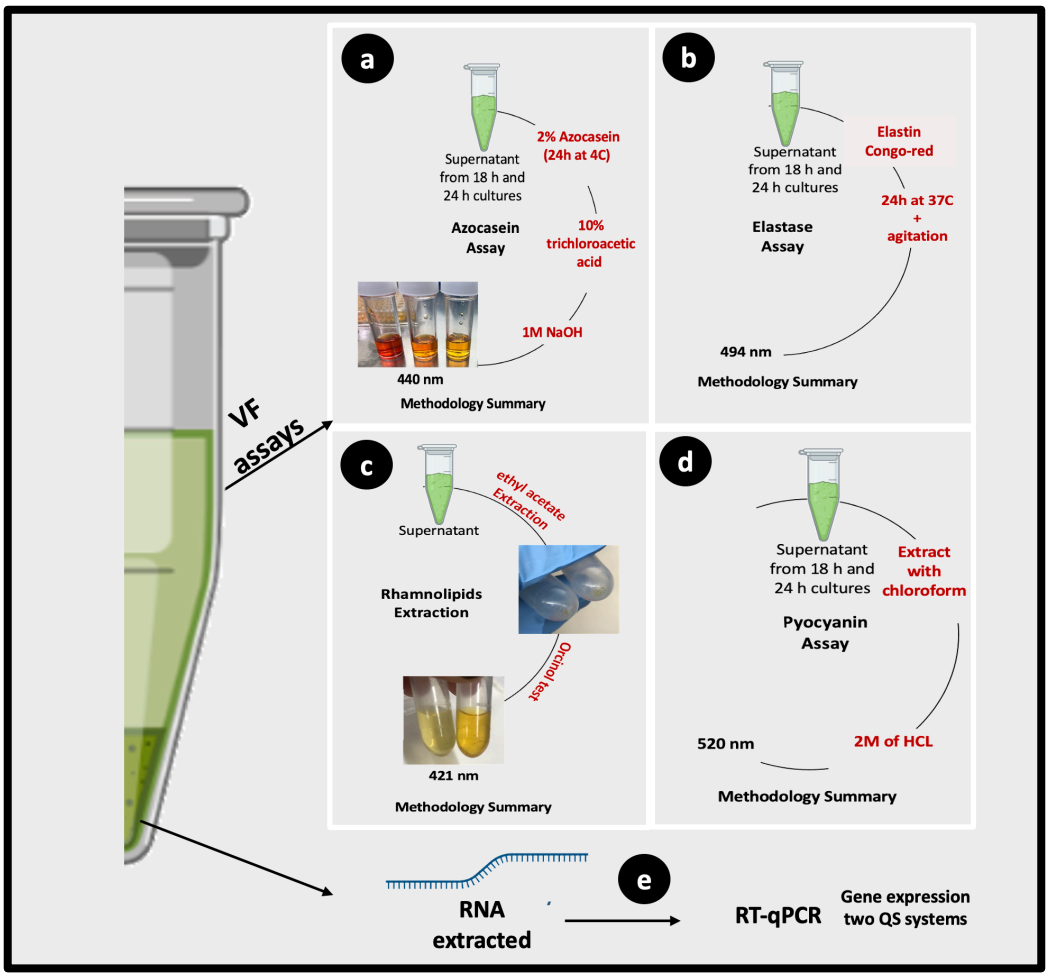

Figure 22: schematic illustration summarising the different assays used to evaluate QS controlled VFs

(a) Azocasein Protease (lasA) assay. **(b)** Elastase (lasB) assay. **(c)** Rhamnolipid extractions. **(d)** Pyocyanin extractions. **(e)** RNA was extracted from the sample treated with 256 µg/ml HB-PNIPAM-HL, which showed the most significant of VFs reduction, and compared with two control polymers HB-PNIPAM -succ and HB-PNIPAM -COOH at the same concentration of 256 µg/ml. Then gene expression was measured with RT-qPCR of QS systems in *P.aeruginosa* genes (*lasI, lasR, rhlI,* and *rhlR,*).

3.4.1 Protease (lasA) extraction

Principle:

The substrate azocasein was used to determine the LasA protease in the supernatant. Azocasein is a chromogenic derivative of casein. As the protease in the supernatant hydrolyses, the azo dye (yellow) casein is released, which can be detected by measuring absorbance at 440 nm The intensity of the colour released positively correlates with the amount of protease present in the supernatant. Azocasein has been widely used for the estimations of protease produced by bacteria (Coêlho *et al*., 2016).

Procedure:

The estimation of amount of the protease LasA was made as described in (Hentzer *et al*., 2002). In short, 2% azocasein (Azocasein, Sigma Aldrich Cat# A2765) in 50mM Tris-HCl was prepared, then 250 µl of 2% azocasein was added to 150 µl of the supernatant. Then, the solution was incubated at 4°C for 4 hours. Azocasein was precipitated by adding 1.2 ml 10% trichloroacetic acid (TCA) (Trichloroacetic acid ,Sigma-Aldrich Cat# 8.22342) for 15 minutes and centrifugation at 10000 g for 10 minutes. Finally, 1.4 ml of 1M NaOH was added, then the absorbances were read at 440nm in a spectrophotometer (**Figure 22, a**).

3.4.2 Elastase (lasB) Extraction

Principle:

The Elastin-Congo red assay was performed as described by (Ohman *et al*., 1980) to determine the elastase enzymes present in a supernatant. The principle of the assay is that the amount of elastase present in the media will free the Congo red dye from the elastin/dye complex, resulting in a change in colour that a spectrophotometer can measure at a wavelength of 495nm (Rust *et al*., 1994).

Procedure:

100 µl of each sample was added to 20 mg Elastin- Congo red (Elastin- Congo red, Sigma-Aldrich Cat# E0502) with 900 µl of elastin- Congo red buffer. The buffer was prepared by mixing 100mM tris-HCL[7.5 pH]with 1mM CaCl2. The solution was then incubated at 37°C

for 3 hours in a shaking incubator. After incubation, the absorbance was read at 495nm (**Figure 22, b**).

3.4.3 Rhamnolipids Extraction

Principle:

The orcinol test was performed to investigate the concentration of rhamnolipids in *P.aeruginosa* supernatant with or without the HB-PNIPAM-HL. The orcinol test is a colorimetric test, where the orcinol reagent reacts with the pentose group in the rhamnolipids. The intensity of the colour emitted correlates with the amount of rhamnolipids present in the sample (Marchant and Banat, 2017).

Procedure:

Three tubes with 1 ml of culture with/without the HB-PNIPAM-HL were adjusted to pH 8. Then the cells were harvested by centrifugation at 16000g for 10 minutes. The supernatant was adjusted after centrifugation to a pH 2 (to allow the separation of rhamnolipids). Next, rhamnolipids were extracted twice using 3 ml of ethyl acetate (Ethyl acetate, Sigma Aldrich Cat# 270989) (Çakmak, 2017). The organic phase was then pooled and air-dried for 12 h, and 500 µl of distilled water (DW) was added. 0.19% orcinol (Orcinol, Sigma Aldrich Cat# 447420) was prepared in 53% (v/v) of H_2SO_4 (orcinol reagent). 900 µl of the orcinol reagent was added to each 100 µl of the samples, were then heated at 80°C for 30 minutes. After heating the samples, they were left to cool at room temperature for 15 minutes. Then, the colour change was quantified by reading absorbance at 421nm in a spectrophotometer (**Figure 22, c**).

3.4.4 Pyocyanin extraction

Principle:

The basis of this assay is to extract pyocyanin pigment in an acidic solution, then quantify the pigment spectrophotometrically. Firstly, the pigment is extracted using chloroform, and then 2

M of HCL is added, resulting in a pink solution, the absorbance of which is read in a spectrophotometer at 520nm (Essar *et al*., 1990).

Procedure:

Pyocyanin was extracted and measured as described in (Essar *et al*., 1990). Briefly, 0.6 ml of chloroform was added to 1 ml of supernatant (see **section 3.3).** The tubes were first vortexed for 20 seconds to ensure that the chloroform was well mixed with the supernatant. Then the solution was centrifuged at 8000 g. for 10 minutes. This process was repeated twice. After centrifugation, the greenish-blue layer was transferred to clean tubes, where 1ml of 0.2M of HCL was added and then vortexed for 20 seconds. The samples were centrifuged again for 2 minutes at 8000 g. The resultant pink layer was removed, and absorbance read at OD 520, with 2 M HCL as a blank. In order to obtain the amount of pyocyanin in µl/ml, the value obtained from the 520 nm read was multiplied by 17.072 (molar extinction coefficient) (**Figure 22, d**).

2.4.5 Biofilm formation

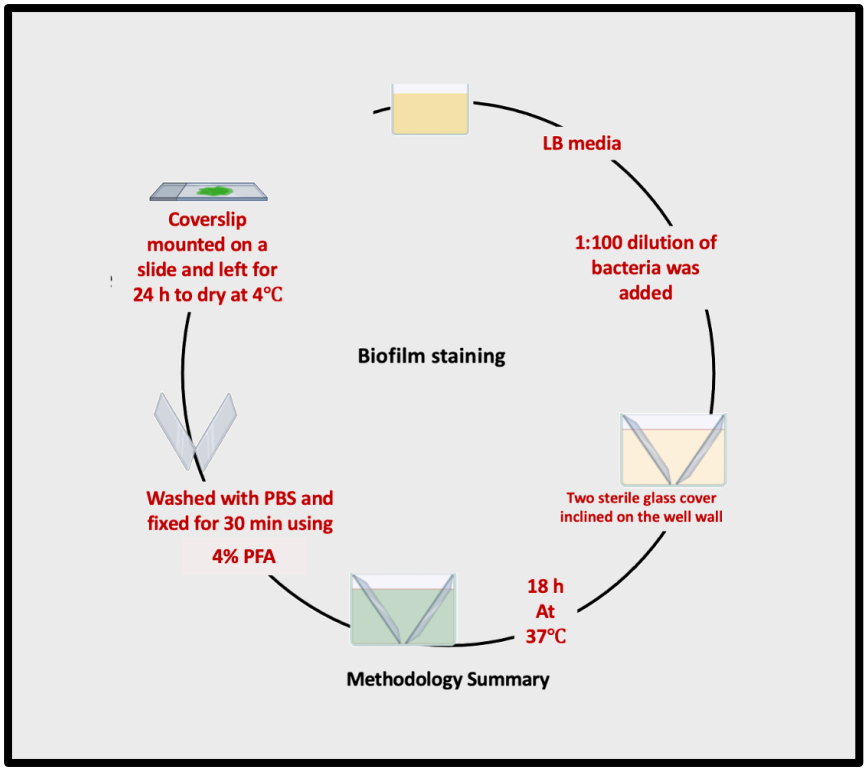

Figure 23: illustration of the biofilm protocol used to assess *Pseudomonas aeruginosa* PAO1 biofilm in the presence of increasing concentrations of HB-PNIPAM-HL.
PFA= paraformaldehyde

3.4.5.1 Biofilm preparation

In a 6-well plate, two sterile glass cover slips with 70% ethanol were placed opposite each other and angled towards the well walls (**Figure 23**). Into each well containing the glass coverslips were pipetted 50 µl of *P.aeruginosa* overnight and 5ml of LB containing various concentrations of fluorescent HB-PNIPAM-HL. The HB-PNIPAM-HL labelled with fluorescein isothiocyanate (FITC) provided by R. Hoskins, Bradford. The plate was covered with an adhesive seal and incubated statically at 37°C for 18 hours.

3.4.5.2 DAPI staining

Principle:

4′,6-diamidino-2-phenylindole (DAPI) is a commonly used staining method for DNA. DAPI can pass through the cell membrane and bind to the AT region in dsDNA (Huschka *et al*., 2010). Here it was used to visualise *P.aeruginosa* PAO1 in the presence of fluorescein labelled HB-PNIPAM-HL. Under the fluorescence microscope, DAPI will stain the bacterial DNA blue, and our polymer will be green.

Procedure:

After incubation period of 24h coverslips removed from wells and washed three times with PBS and let dry for 15 min. After coverslips were dry , each coverslip was fixed using 4% PFA (4 % paraformaldehyde, Thermo Fisher Cat# J19943.K2) for 30 minutes and mounted with DAPI mounting media (DAPI, Thermo Fisher Cat# P36962) on a microscope glass slide. Nail varnish was used to seal and immobilize coverslips. Slides were covered with aluminium foil, to minimise photo-bleaching, and left for 24 h, at 4°C. Samples were visualised using fluorescence microscopy, under blue light (excitation 350 nm and emission 465 nm)**.**

3.5 Gene expression of QS system genes in *P.aeruginosa PAO1*

Total RNA extraction was performed using a kit (RNeasy Mini Kit, QIAGEN Cat#74106) with the same methodology and optimisation steps applied to *Chromobacterium violaceum* in **Chapter 2, section 3.3**. The different gene expression of QS systems and VFs for *P.aeruginosa* samples treated with 256 µg/ml HB-PNIPAM-HL and other mediated polymers HB-PNIPAM-succ and HB-PNIPAM-COOH (see **Chapter 2, section 2.1.1**).

The concentration and purity were estimated using Nano drop (NanoDrop™ Lite, Thermo Fisher) and by running the isolated RNA on a 1% agarose gel. Before running on the agarose gel samples were mixed with RNA buffer dye 1:2 (RNA Gel Loading Dye, Thermo Fisher Cat# R041) and heated at 70°C for 10 min and left to cool at room temp for 15-20 min. The first-strand cDNA was generated from the purified RNA using the High-Capacity cDNA Reverse Transcription kit ™ (Applied Biosystems, Cat#4368814). RT-qPCR using 2 X qPCRBIO SyGreen Blue Mix Hi-ROX (PCR BIOSYSTEMSCat#PB20.15-05) was prepared following the manufacturer's instructions **(**see **Chapter 2, section 3.3.3).**

Table 25: Primers used in Chapter 3

Reference genes				
Gene	**Primer sequence**	**Length (bp)**	**Reference/ Designed**	**Supplier**
16s rRNA	**Fwd** 5′- AGATGAGCCTAGGTCGGATTA -′3 **Rev** 5′- AGTCTGGACCGTGTCTCA -′3	115	Designed	Sigma-Aldrich, UK
ProC	**Fwd** 5′- CAGGCCGGGCAGTTGCTGTC -′3 **Rev** 5'- GGTCAGGCGCGAGGCTGTCT -'3	188	(Dumas *et al*., 2006)	
rpoD	**Fwd** 5′- GGGCGAAGAAGGAAATGGTC -′3 **Rev** 5′- CAGGTGGCGTAGGTGGAGAA -′3	178	(Shepherd *et al*., 2019)	
rpsL	**Fwd** 5′- GCAAGCGCATGGTCGACAAGA -′3 **Rev** 5′- CGCTGTGCTCTTGCAGGTTGTGA -′3	201	(Dumas *et al*., 2006)	
The graph for choosing the most stable reference gene can be found in **Appendix 6**				
Target genes				
Gene	**Primer sequence**	**Length (bp)**	**Reference/ Designed**	**Supplier**

lasI	**Fwd** 5′- AGGCGTGGAGAAGATGATG -′3 **Rev** 5′- ATCTGGGTCTTGGCATTGAG -′3	120	(Luo *et al*., 2017)	Sigma-Aldrich, UK
lasR	**Fwd** 5′- GATGCTCAAGGACTACGC -′3 **Rev** 5′- CGATATCTCCCAACTGGTCTTG -′3	139	Designed	
rhlI	**Fwd** 5′- TGCAGCCATTCCGGGTGGTA -′3 **Rev** 5′- TCGTTCGCAACGGCGTGAT -′3	139	(Luo *et al*., 2017)	
rhlR	**Fwd** 5′- TCGTTCGCAACGGCGTGAT -′3 **Rev** 5′- TTGCTCAGCGTGCTTTCCGT -′3	146	(Luo *et al*., 2017)	
The gel run for the annealing temperature testing can be found in **Figure 29** and **Appendix 5**				

Reference genes				
Gene	**Primer sequence**	Length (bp)	Reference/ Designed	**Supplier**
rpsL	**Fwd** 5′- GCAAGCGCATGGTCGACAAGA -′3 **Rev** 5′- CGCTGTGCTCTTGCAGGTTGTGA -′3	201	(Dumas *et al*., 2006)	Sigma-Aldrich, UK
Target genes				
Gene	**Primer sequence**	**Length (bp)**	**Reference /Designed**	**Supplier**
rhlA	**Fwd** 5′- AAGCCAGCAACCATAGC -′3 **Rev** 5′- GCACCTGGTCGATGTTGAAA -′3	78	Designed	Sigma-Aldrich, UK
PhzH	**Fwd** 5′- GCTCATCGACAATGCCGAACT -′3 **Rev** 5′- GCGGATCTCGCCGAACATCAG -′3	124	Designed	
lasA	**Fwd** 5′- GCGCGACAAGAGCGAATAC -′3 **Rev** 5′- CGGCCCGGATTGCAT -′3	94	(Li *et al*., 2015)	
lasB	**Fwd** 5′- AGACCGAGAATGACAAAGTGGAA -′3 **Rev** 5′- GGTAGGAGACGTTGTAGACCAGTTG -′3	81	(Li *et al*., 2015)	

3.5.1 Reference primers evaluations

RT-qPCR is a technology that allows measurement of a gene's expression (the amount of mRNA produced) and how this changes under different conditions, i.e., when treated vs untreated samples. The mRNA produced has many factors that might affect the production

levels, such as gene activity and the initial amount of cDNA between different samples tested. A second gene, termed housekeeping, or reference gene was used for a normalisation step to mitigate these factors. One important characteristic of this reference gene is that this reference gene is not affected by the treatments tested. Here, we tested several reference genes (*16sRNA, rpoD, proC,and rpsL*) under different conditions (untreated and treated). Then we assessed the variability in measured Ct values for each reference gene by measuring the standard deviations (SD) (see **Appendix 6).** In this project, we made sure to check the stability of the reference gene before attempting RT-qPCR, which was recommended by the Minimum information for publication of Quantitate Real-Time PCR Experiments (MIQE) published in 2009 (Bustin *et al*., 2009). Four different reference genes were selected for evaluation based on their use in QS studies. The reference gene *16s rRNA* was commonly used in the QS studies on *P.aeruginosa* such as (Zhao *et al*., 2018), (Malgaonkar and Nair, 2019), and (Coelho *et al*., 2021). The reference gene *rpsL* was used in (Köhler *et al*., 2010) where they tested the QS dependent VFs of *P.aeruginosa.* The two reference genes *rpoD* and *proC* were recommended as reference genes by (Savli *et al*., 2003), where 6 reference genes were tested in 7 strains of *P.aeruginosa* at RT-qPCR. These four reference genes were tested under different treatments and stability was derived from their standard deviations (SD). The results in **Appendix 6** show that *rpsL* was more stable compared to the other three genes tested.

3.6 RNA seq

Three samples were treated with 256 μg/ml HB-PNIPAM-HL, HB-PNIPAM-succ , or untreated were prepared as described in previous **Chapter 2, section 3.3**; and RNA was extracted with a RNeasy Mini Kit (QIAGEN Cat#74106) with the same optimisation steps shown in **Chapter 2, section 3.3.1.2**. The resulting RNA was measured using Nano drop (NanoDrop™ Lite, Thermo Fisher) and run on 1% gel to measure the quality of the samples **(Figure 25).** RNA samples were sent to Genewiz (Germany GmbH, Bahnhofstrasse 86, 04158

Leipzig), where library construction and RNA sequencing of the samples. Bioinformatics was also carried out by the company. **(Figure 26)** shows a summary of the bioinformatics that the company performed on the samples. The samples were then re-illustrated using Prism (version 9.3.1) and Venn diagrams (http://bioinformatics.psb.ugent.be/webtools/Venn/).

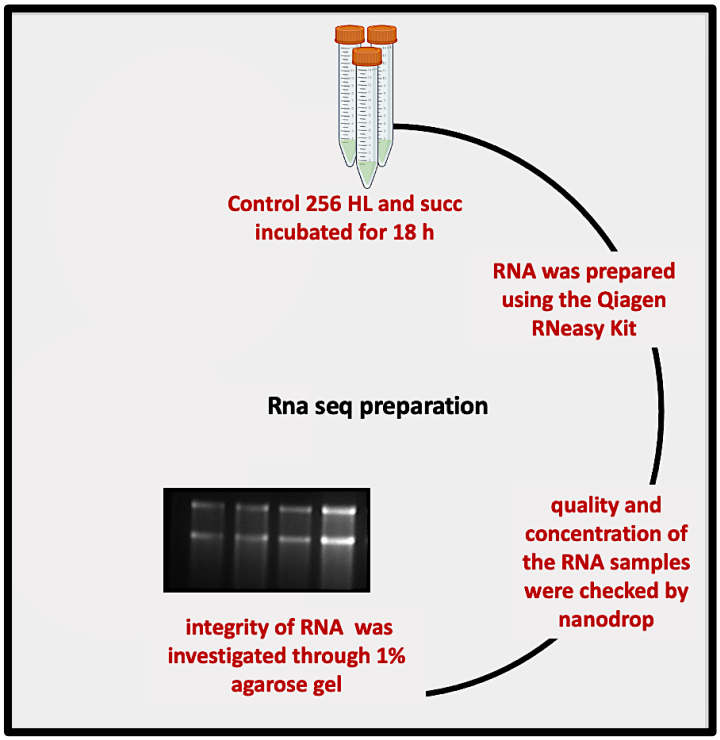

Figure 24: illustration of samples preparation before sending to RNA sequences

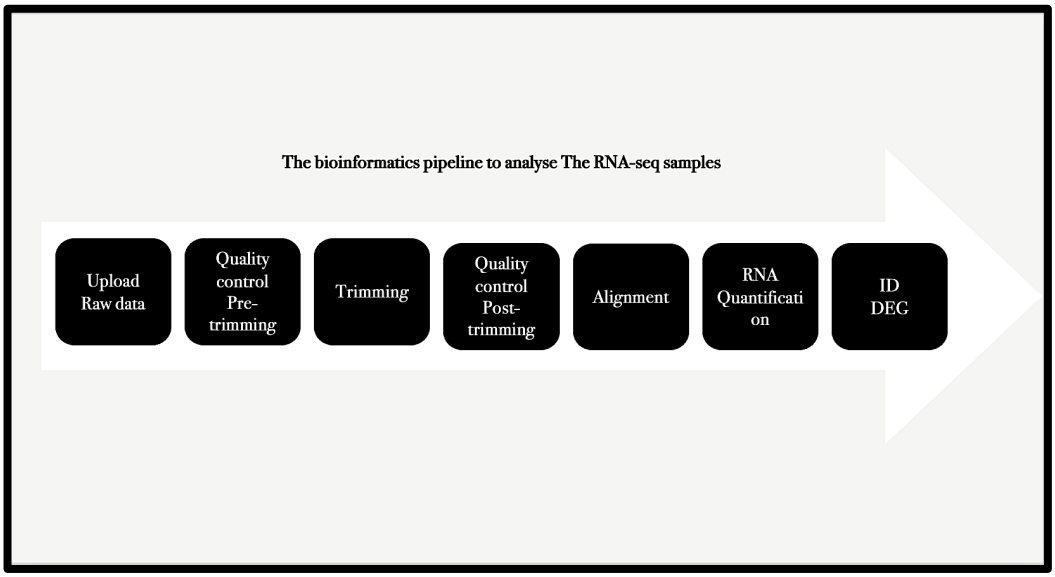

Figure 25: the bioinformatics pipeline to analyse the RNA seq samples by Genewiz.

3.7 Statistical analyses

All data generated in this chapter were initially tested to assess their distribution before attempting any statistical analysis. All values are presented as mean ±SD. Graphs and normality of distribution for data were tested and created using GraphPad Prism software (version 9.3.1; GraphPad Software, Inc., La Jolla, CA, USA). *P*-values >0.05 were considered significant.

4. Results

4.1 HB-PNIPAM-HL reduces the production of several important virulence factors in *P.aeruginosa* PAO1

Incubation of HB-PNIPAM-HL at concentrations of 128 and 256 μg/ml for 18h at 37°C resulted in attenuation of secreted virulence factors of *P.aeruginosa* PAO1, though no complete inhibition was observed. The effect of the HB-PNIPAM-HL on the secreted VFs can be seen in **(Figure 27, A-H)**. The description data of all VFs evaluated compared to the untreated control can be found in (**Table 27-31).** HB-PNIPAM-HL at the concentrations of 128 and 256 μg/ml can reduce the production of LasA proteases by an average of ~31% and 52% respectively **(Figure 27, A&B).** For the LasB elastase the reducing effect was only significant for the concentration of 256 μg/ml for at 71% inhibition **(Figure 287, C&D).** For the surfactant rhamnolipids, a prerequisite of biofilm formation, a significant reduction was observed for all concentrations of HB-PNIPAM-HL used with 69% reduction when treated with 128μg/ml, and 76% reduction when treated with 256 μg/ml (**Figure 27, E&F).** The pyocyanin production was monitored for 12h from the start of the stationary growth phase, as was shown when the QS activity began (Castric *et al*., 1979). For *P.aeruginosa* PAO1 used in this study, the start of the stationary phase was inferred from the growth curve in **section 4.4, Chapter 3** to be at 12h of growth. The difference in production of pyocyanin was more apparent between treated and untreated samples after 24h incubation, as shown in **(Figure 27,**

G&H). After 24h growth, the reduction for the HB-PNIPAM-HL concentrations, 128 and 256 µg/ml, is on average ~60% and 70%respectively **(Figure 27 G&H).**

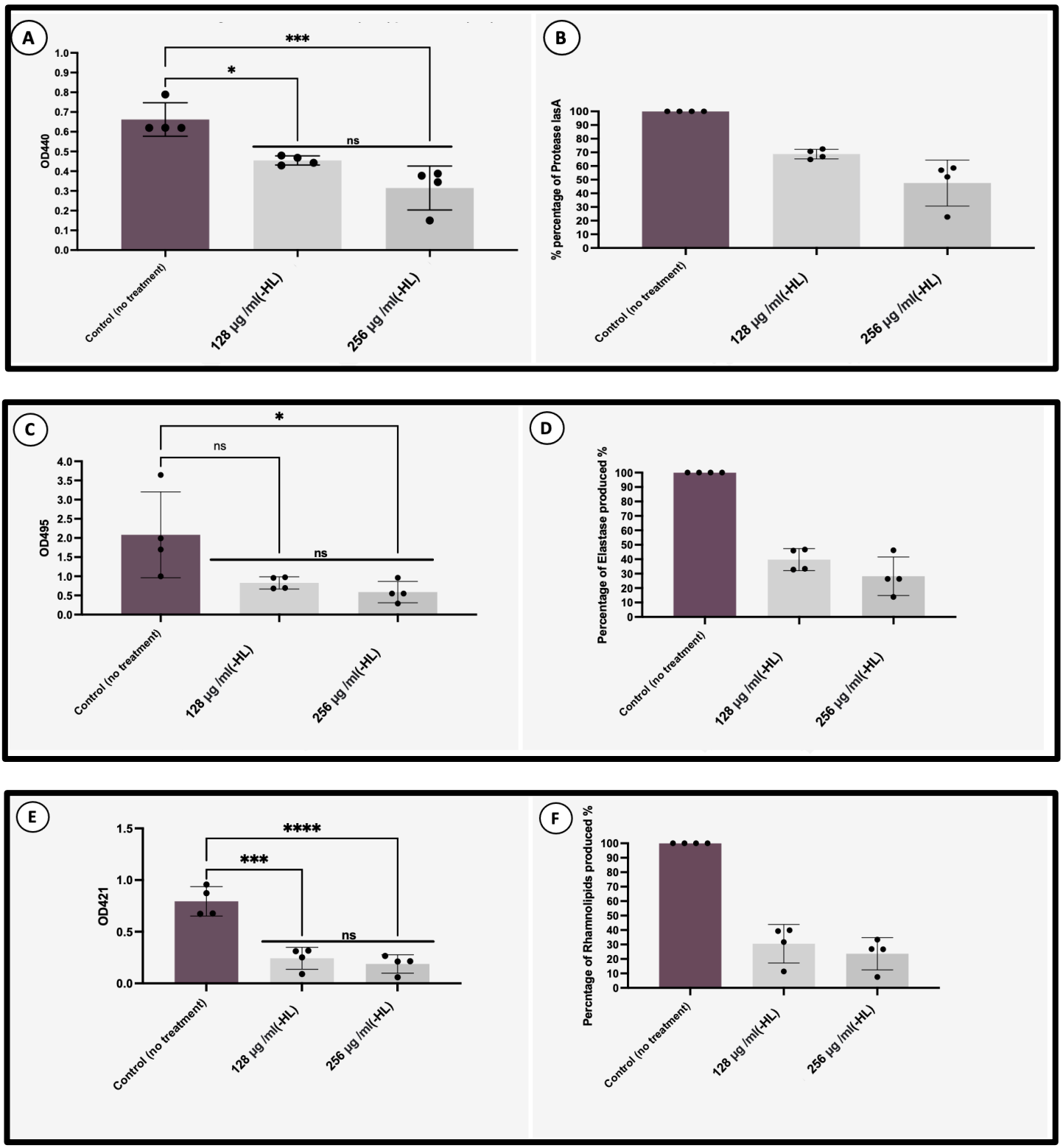

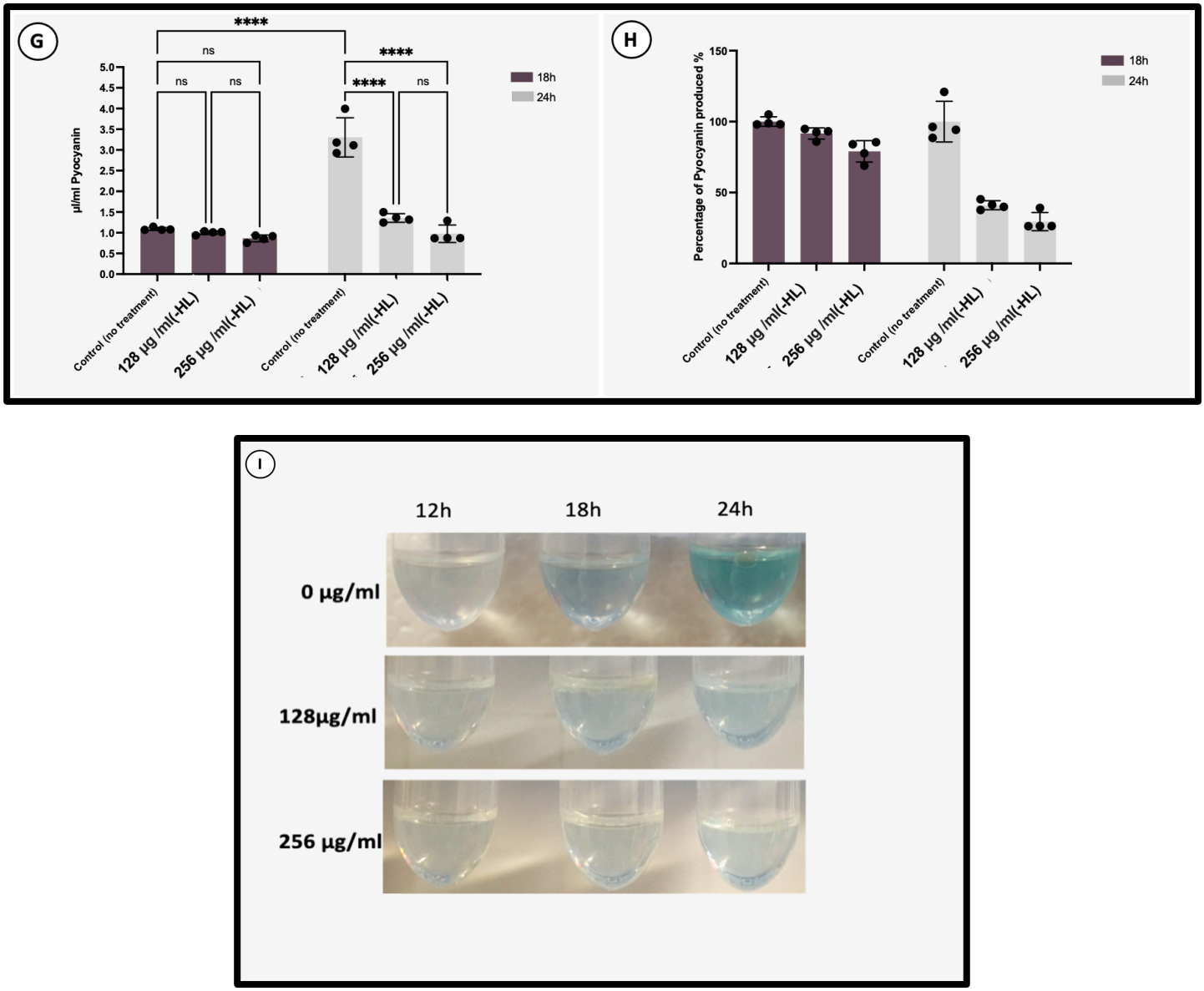

Figure 26: *P.aeruginosa* PAO1 cell – free culture supernatant extracellular virulence factors levels treated with 128 and 256µg/ml of HB-PNIPAM-HL.

(A-B) production of protease**,(C-D)**– production of elastase, **(E-F)** – production of Rhamnolipids, **(G-H)** production of pyocyanin at 18h and 24h. **(A,C,E, and G) g**raphs represent the actual readings, while **(B,D,F and H)** graphs represent the percentage of production with control made as 100%. **(I)** Images of pyocyanin extraction for samples after different time points (12h, 18h , and 24h) (n=4). Experimental data are expressed as mean ± standard deviation. Significance **(A,C, and E)** was determined using one-way ANOVA analysis of variance with Tukey test in prism (version 9.3.1). While Significance in (G) was determined using two-way ANOVA analysis of variance with Tukey test. *,$P < 0.01$, **,$P < 0.001$, ****,$P < 0.0001$. Error bars= SD. (Full ANOVA Results can be found in **Appendix 9**).

Table 26: Statistical description of protease (lasA) readings at OD440.

Sample	Reading mean (±SD, Range)	Percentage mean (Range)	P value for raw data (compared to control negative)
Control negative (no treatment)	0.6620 (±0.08464, 0.6194-0.7890)	100%	Not applicable

128 µg/ml (HB-PNIPAM-HL)	0.4547 (±0.02319, 0.4288-0.4796)	67% (65-72%)	0.0108
256 µg/ml (HB-PNIPAM-HL)	0.3148 (± 0.1113, 0.1502-0.3876)	47.5% (23-58.5%)	0.0004

Table 27: Statistical description of Elastase (lasB) readings at OD495.

Sample	Reading mean (±SD, Range)	Percentage mean (Range)	P value for raw data (compared to control negative)
Control negative (no treatment)	2.83 (±1.120, 0.9998-3.643)	100%	Not applicable
128 µg/ml (HB-PNIPAM-HL)	0.8273 (±0.0.1595, 0.6837-0.9733)	40% (33-47%)	0.06
256 µg/ml (HB-PNIPAM-HL)	00.5880 (± 0.2779, 0.2897-0.9619)	28% (14-46%)	0.0289

Table 28: Statistical description of rhamnolipids readings at OD 421.

Sample	Reading mean (±SD, Range)	Percentage mean (Range)	P value (compared to control negative)
Control negative (no treatment)	0.7947(± 0.1426, 0.6734-0.9567)	100%	Not applicable
128 µg/ml (HB-PNIPAM-HL)	0.2430 (±0.1060, 0.0.09020-0.3170)	30.5% (11-40%)	0.0002
256 µg/ml (HB-PNIPAM-HL)	0.1878 (± 0.08885, 0.05983-0.2655)	24% (7.5-33%)	<0.0001

Table 29: Statistical description of Pyocyanin readings at OD 520for 18h

Sample	Reading mean (±SD, Range)	Percentage mean (Range)	P value for raw data (compared to control negative)
Control negative (no treatment)	0.06398 (±0.002143, 0.06270-0.06717)	100%	Not applicable
128 µg/ml (HB-PNIPAM-HL)	0.05862 (±0.002506, 0.05497-0.06063)	~92% (86-95%)	0.9906
256 µg/ml (HB-PNIPAM-HL)	0.05056 (± 0.004817, 0.04410-0.05467)	79% (69-85%)	0.6844

Table 30: Statistical description of Pyocyanin readings at OD 520 nm for 24h

Sample	Reading mean (±SD, Range)	Percentage mean (Range)	P value for raw data (compared to control negative)

Control negative (no treatment)	0.1935 (±0.02776, 0.1713-0.2340)	100%	Not applicable
128 µg/ml (HB-PNIPAM-HL)	0.07948 (±0.006158, 0.07303-0.01460)	41% (38-45%)	<0.0001
256 µg/ml (HB-PNIPAM-HL)	0.05715 (± 0.01236, 0.05085-0.07570)	29% (26-39%)	<0.0001

4.2 HB-PNIPAM-HL effect on *P.aeruginosa* PAO1 biofilm

As described in **Chapter 1, section 2.3.1.2**; biofilm formation is one of the virulence factors controlled by QS. The *P.aeruginosa* biofilm formation in the presence of our polymer, HB-PNIPAM-HL, was tested at two concentrations (128 or 256 µg/ml) using coverslip method. HB-PNIPAM-HL was added to each well with biofilm grown on glass coverslips at 128 or 256 µg/ml (**Figure 28**). The biofilm was visualised using a fluorescence microscope (Zeiss, Germany). The biofilm formed on the coverslips with HB-PNIPAM-HL in comparison with the control was less, when it was visualised with fluorescence microscope (**Figure 28)** .

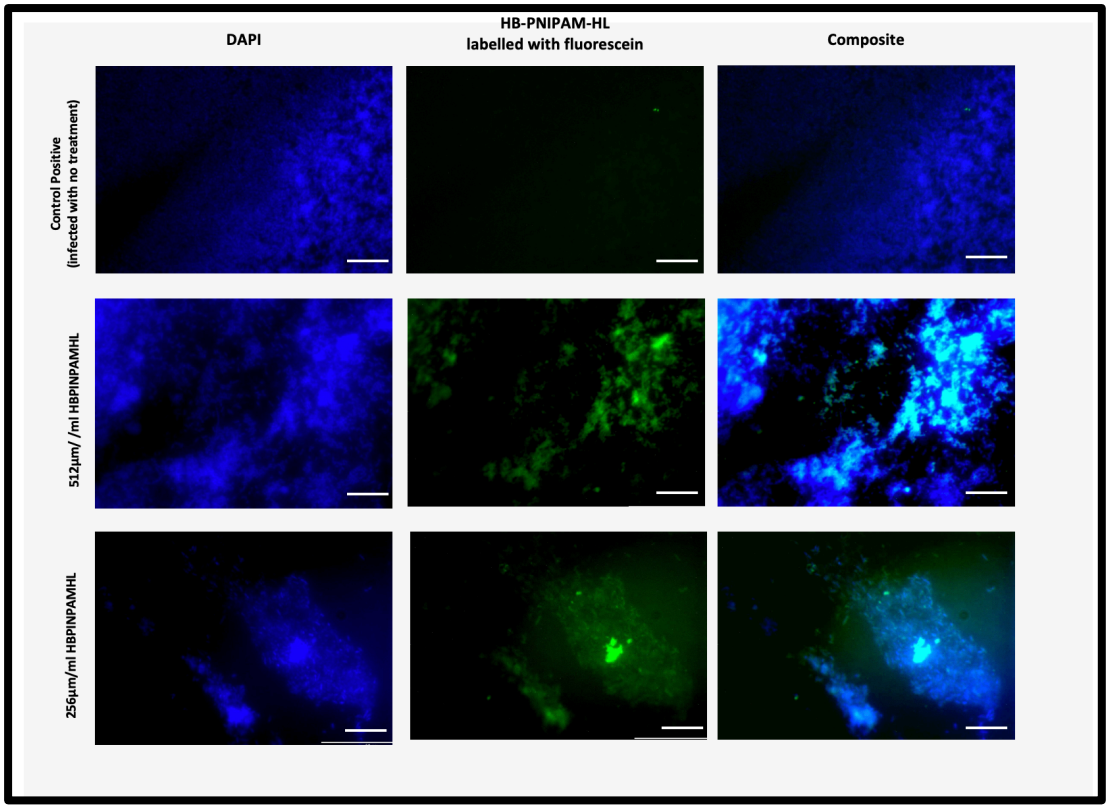

Figure 27: *P.aeruginosa* PAO1biofilm visualised by fluorescence microscope.
Biofilm was grown for 18 h on glass coverslips with different concentrations of fluorescence labelled HB-PNIPAM-HL. Scale = 100µm. More replicates can be found in **(Appendix 7*).***

4.3 Effect of HB-PNIPAM-HL on Transcription of QS -controlled virulence genes and virulence factors genes

As shown in **section 4.1** of this chapter, HB-PNIPAM-HL inhibited the production of several VFs regulated by QS in *P.aeruginosa* PAO1. Here, the four genes encoding the *las* and *rhl* QS systems in *P.aeruginosa* were examined after treatment: the synthase of the las system, *lasI*, the transcriptional regulator *lasR*, the synthase of the *rhl* system, *rhlI*, and the transcriptional regulator *rhlR.* The concentration of 256 µg/ml HB-PNIPAM-HL was chosen to measure gene expression because it had the greatest inhibitory effect on the production of VFs in **section 4.1.** In addition to HB-PNIPAM-HL, two other mediating polymers from the production process of HB-PNIPAM-HL (see **Chapter 2, section 2.1.1**) were also tested: HB-PNIPAM -succ (polymers with succinamide and without homoserine lactone) and HB-PNIPAM-COOH (with acidic end without homoserine lactone), to determine whether the effect of HB-PNIPAM-HL

was solely due to the homoserine lactone end. Treatment with 256 μg/ml HB-PNIPAM-HL significantly (p> 0.01) reduced the expression of the QS transcriptional regulatory gene *lasR* by 2-fold. Also, HB-PNIPAM-HL caused a significant (P< 0.0001) 3-fold reduction in the *rhlI* synthase gene after treatment. The sample treated with HB-PNIPAM-succ caused a significant reduction of (*lasR*, *rhlI* and *rhlR*), with an overall higher reduction than the samples treated with - HL. The polymer with -succ end caused a significant (P > .0001) reduction of *lasR* by 3-fold and of *rhlI* (P > .0001) by 14-fold. HB-PNIPAM -succ was able to significantly (P > .0001) reduce the transcriptional regulator of the *rhl* system, *rhlR*, by 6-fold **(Figure 29, A).**

In the sample treated with HB-PNIPAM-COOH, neither a significant increase nor a decrease in expression was observed with the QS genes (*lasI, lasR, rhlI* and *rhlR*). The result suggests that the anti-QS effect of HB-PNIPAM-HL may not be limited to the functionalised end, as the -succ ending polymer downregulates the QS gene *lasR* and the genes encoding the *rhl* system.

Considering the four VFs we evaluated in **Chapter 3, section 4.1**; and the result of RT-qPCR of HB-PNIPAM-succ, LasA protease, LasB elastin, rhamnolipids and pyocyanin genes were investigated after treatment with the polymer HB-PNIPAM-HL and HB-PNIPAM-succ. Four genes encoding these four VFs were selected, namely *lasA* and *lasB* (Toder *et al*., 1994), *rhlA* (Van Gennip *et al*., 2009) and *phzH* (Thees *et al*., 2021). In **(Figure 29, C),** the rhamnolipid-encoding gene *rhlA* was significantly (P=.02) downregulated by 3-fold in - HL and (P >.01) by 6-fold in -succ. The *phzH* gene were also downregulated in both samples, significantly (P >.01) by (5) fold in the treated sample - HL and (P>.001) by 10-fold in the sample treated with -succ. *lasA* treated with the polymer ending in - HL and with -succ was significantly (P=.04) downregulated by 3-fold and significantly (P >.001) by 6-fold. The gene encoding for LasB (*lasB*) was not significantly downregulated by the polymers - HL or -succ.

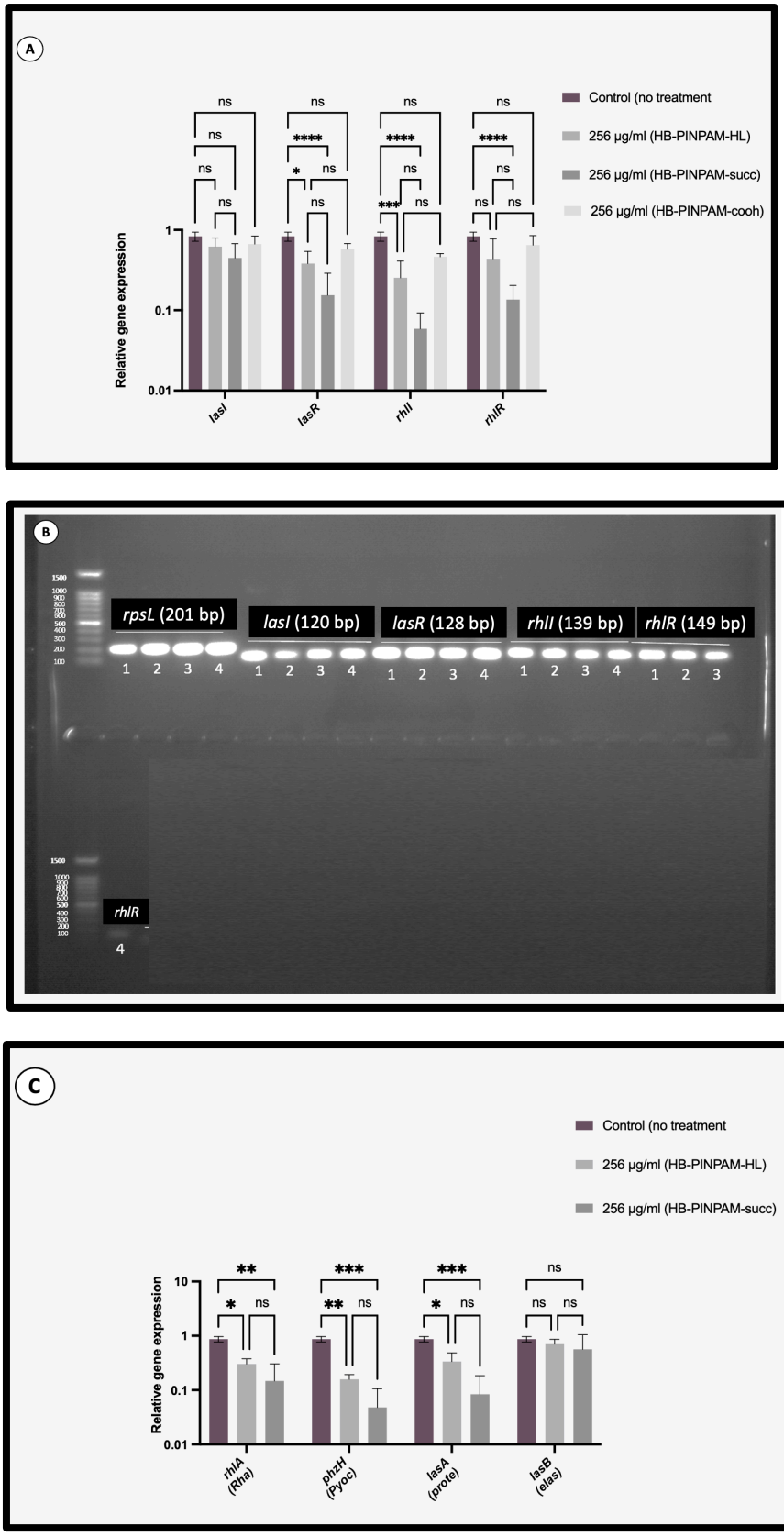

Figure 28: gene expression levels changes in *P.aeruginosa* PAO1 treated with 256µg/ml of HB-PNIPAM-HL, -succ, and -COOH (acid) quantified by RT-qPCR and normalised with reference gene *rpsL*

Here, the QS genes of *P.aeruginosa* (*lasI, lasR, rhlI,* and *rhlR*) were investigated**.** (**A)** The

graph shows the effect of 256 μg/ml of HB-PNIPAM-HL/succ/COOH on the expression of genes coding for the QS systems ;*las, and rhl* systems. The untreated sample was used as a negative control. The relative expression was considered as 1 . **(B)** shows a gel run on an agarose gel (1%) of the RT-qPCR products after a run to examine product size in (bp). 1= Control, 2= HB-PNIPAM-HL, 3= HB-PNIPAM-succ, and 4= HB-PNIPAM-COOH.(n=3). **(C)** VFs genes of *P.aeruginosa* (*rhlA, PhzH, lasA, and lasB*)) of the RT-qPCR. Gel run on agarose gel (1%) shown in Appendix 8 (n=3).Experimental data are expressed as mean ± standard deviation. Significance was determined using two-way ANOVA analysis of variance with Tukey Test in prism (version 9.3.1) *,P<0.05 ,**,P<.01 and ***,P < 0.001 ****,P <0.0001.Error bars= SD. (Full ANOVA Results can be found in **Appendix 9**).

4.4 Growth curve of *P. aeruginosa* PAO1 with 256μg/ml HB-PNIPAM-HL and HB-PNIPAM-succ

Treatment with HB-PNIPAM-succ (-succ) resulted in increased down-regulation of QS genes for the *lasR* and the *rhl* system for this we evaluated the growth of *Pseudomonas aeruginosa* in the presence of HB-PNIPAM-H and HB-PNIPAM-succ. As shown in **(Figure 30, A)**, all samples grew equally well with and without treatment with HB-PNIPAM-HL and HB-PNIPAM-succ. However, a more detailed analysis was attempted by calculating the growth rate (small box) for each sample using the growth curve in (**Figure 30, A**). Overall, the samples treated with polymers, HB-PNIPAM-HL or HB-PNIPAM -succ, had a significantly lower growth rate in the log phase than the control group. As seen in **(Figure 30, B),** the polymer with HB-PNIPAM-succ had a lower growth rate than HB-PNIPAM-HL; this delay could be related to the observed anti-QS effect observed with RT-qPCR.

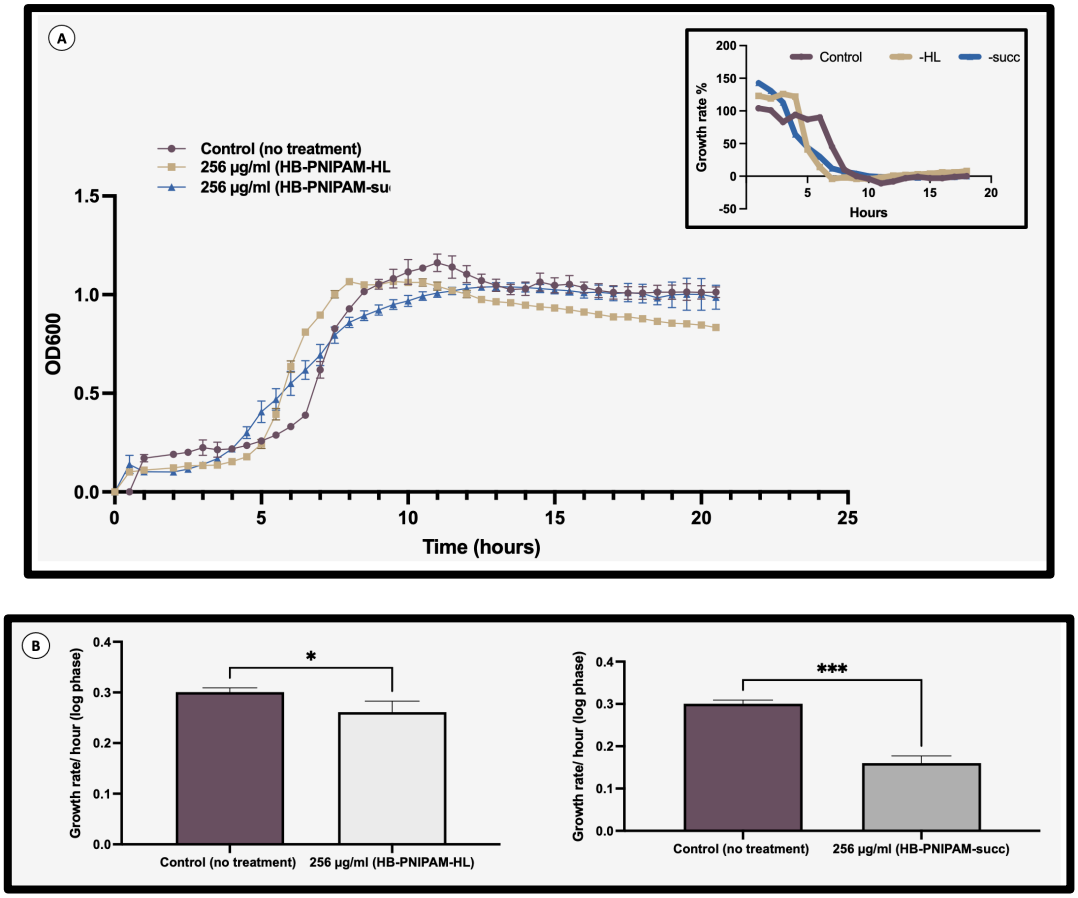

Figure 29: growth curve of *Pseudomonas aeruginosa* PAO1 after treatment of HB-PNIPAM-HL and HB-PNIPAM-succ for 20h.

(A) shows the growth curve of *P.aeruginosa* PAO1 treated with HB-PNIPAM-HL and HB-PNIPAM-succ at the concentration of 256 µg/ml. **(B)** shows the mean growth rate of *P.aeruginosa* PAO1 at the log phase treated with HB-PNIPAM-HL and HB-PNIPAM-succ at the concentration of 256 µg/ml (n=4). Significance was determined using student T-test analysis of prism (version 9.3.1). *,*P*<0.01; ***, *P*<.0001. Error bars= SD.

4.5 Exploratory RNA-seq between HB-PNIPAM-HL and HB-PNIPAM-succ

Having established in **Chapter 3, section 4.3**; that the "control" HB-PNIPAM-succ down-regulated the QS transcriptional regulator and the *rhl* system genes *rhlI* and *rhlR* in *P.aeruginosa*. Three samples were sent for RNA sequencing: an untreated sample, a sample treated with 256 µg/ml HB-PNIPAM-HL and a sample treated with 256 µg/ml HB-PNIPAM-succ. The data were treated on a preliminary basis as (n=1) were sent. The classification of up- and down-regulated genes in the samples treated with HB- PNIPAM-HL or HB-PNIPAM -succ based on the Kyoto Encyclopaedia of Genes and Genomes Pathway Prediction can be found in

(**Appendix 11**). QS-regulated pathways were analysed using bioinformatic tools, including pseudo Cyc, iDEP.96, and the Pseudomonas Genomes Database (www.pseudomonas.com).

The results in **Chapter 3, Figure 31 A-D** generally show that HB-PNIPAM-succ has a similar effect to HB-PNIPAM-HL. Both polymers show the same trends with the lowering of some VF genes under the regulation of QS. Several genes encoding different signalling pathways were obtained from Pseudo-Cyc **(Figure 31, A&C),** including Biofilm, pathogenesis, quorum sensing, flagella and pilus . As this experiment was conducted on an exploratory basis, the general result in (**Figure 31**) is treated as preliminary data, that needs more investigations.

Venn diagrams in **(Figure 31, G)** showed similarity in the differential gene expression (DGE) with sharing the expression profile of 5022 genes, and that more than 300 genes are upregulated in HB-PNIPAM-HL that are downregulated in samples treated with HB-PNIPAM-succ. This might have a relation to the different growth rate calculated in **Chapter 3, section 4.5**. However, this can only be deduced after further biological replicates.

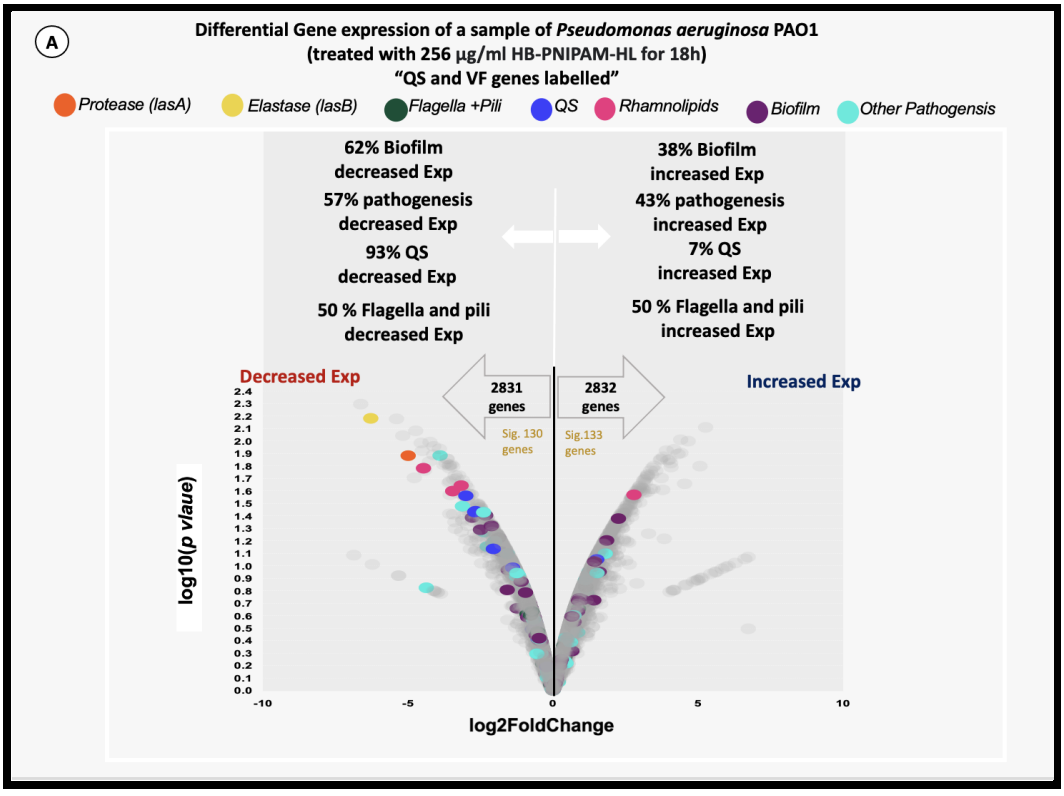

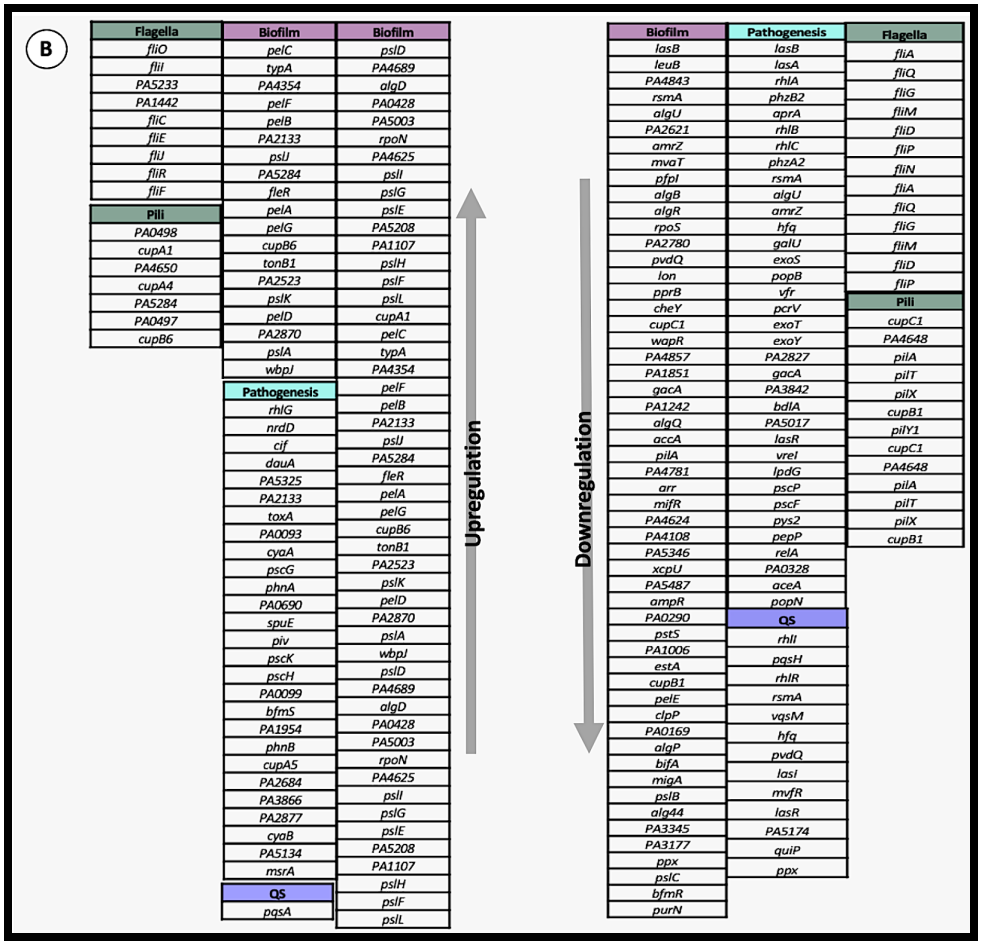
B
Flagella
fliO
fliI
PA5233
PA1442
fliC
fliE
fliJ
fliR
fliF
Pili
PA0498
cupA1
PA4650
cupA4
PA5284
PA0497
cupB6
Biofilm
pelC
typA
PA4354
pelF
pelB
PA2133
pslJ
PA5284
fleR
pelA
pelG
cupB6
tonB1
PA2523
pslK
pelD
PA2870
pslA
wbpJ
Pathogenesis
rhlG
nrdD
cif
dauA
PA5325
PA2133
toxA
PA0093
cyaA
pscG
phnA
PA0690
spuE
piv
pscK
pscH
PA0099
bfmS
PA1954
phnB
cupA5
PA2684
PA3866
PA2877
cyaB
PA5134
msrA
QS
pqsA
Biofilm
pslD
PA4689
algD
PA0428
PA5003
rpoN
PA4625
pslI
pslG
pslE
PA5208
PA1107
pslH
pslF
pslL
cupA1
pelC
typA
PA4354
pelF
pelB
PA2133
pslJ
PA5284
fleR
pelA
pelG
cupB6
tonB1
PA2523
pslK
pelD
PA2870
pslA
wbpJ
pslD
PA4689
algD
PA0428
PA5003
rpoN
PA4625
pslI
pslG
pslE
PA5208
PA1107
pslH
pslF
pslL
Upregulation
Downregulation
Biofilm
lasB
leuB
PA4843
rsmA
algU
PA2621
amrZ
mvaT
pfpI
algB
algR
rpoS
PA2780
pvdQ
lon
pprB
cheY
cupC1
wapR
PA4857
PA1851
gacA
PA1242
algQ
accA
pilA
PA4781
arr
mifR
PA4624
PA4108
PA5346
xcpU
PA5487
ampR
PA0290
pstS
PA1006
estA
cupB1
pelE
clpP
PA0169
algP
bifA
migA
pslB
alg44
PA3345
PA3177
ppx
pslC
bfmR
purN
Pathogenesis
lasB
lasA
rhlA
phzB2
aprA
rhlB
rhlC
phzA2
rsmA
algU
amrZ
hfq
galU
exoS
popB
vfr
pcrV
exoT
exoY
PA2827
gacA
PA3842
bdlA
PA5017
lasR
vreI
lpdG
pscP
pscF
pys2
pepP
relA
PA0328
aceA
popN
QS
rhlI
pqsH
rhlR
rsmA
vqsM
hfq
pvdQ
lasI
mvfR
lasR
PA5174
quiP
ppx
Flagella
fliA
fliQ
fliG
fliM
fliD
fliP
fliN
fliA
fliQ
fliG
fliM
fliD
fliP
Pili
cupC1
PA4648
pilA
pilT
pilX
cupB1
pilY1
cupC1
PA4648
pilA
pilT
pilX
cupB1

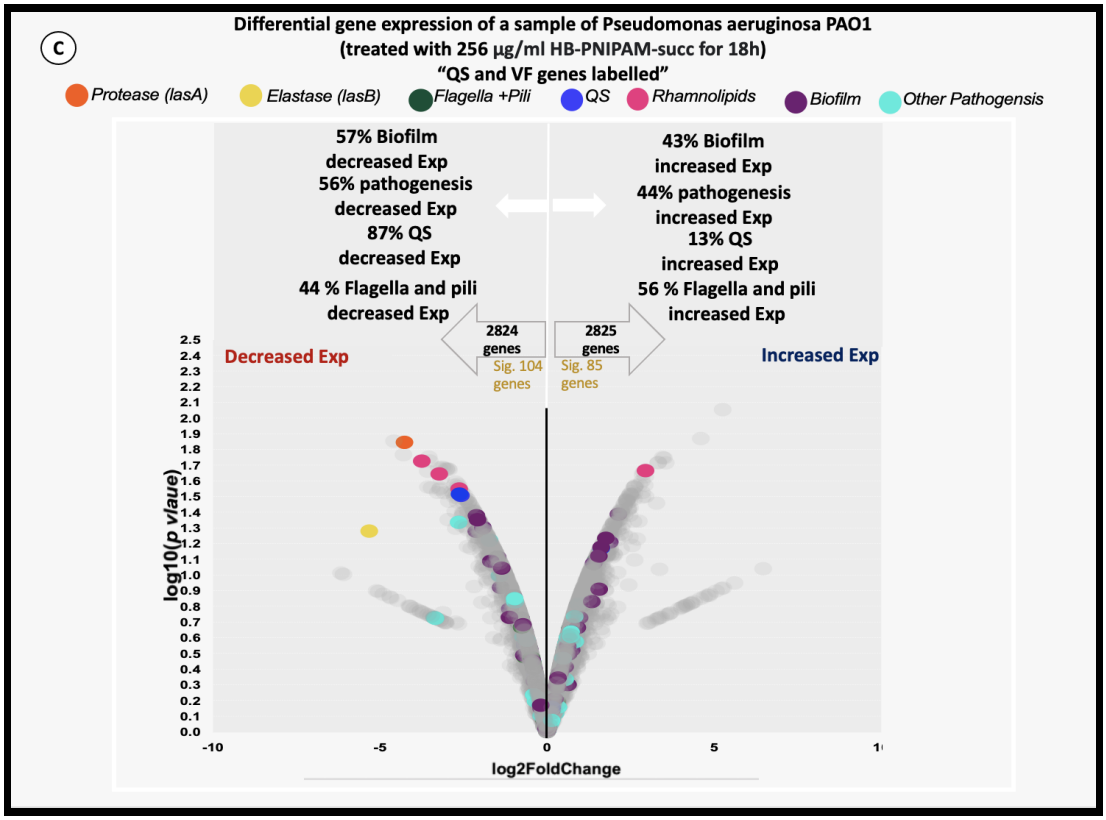
C
Differential gene expression of a sample of Pseudomonas aeruginosa PAO1
(treated with 256 µg/ml HB-PNIPAM-succ for 18h)
"QS and VF genes labelled"
Protease (lasA)
Elastase (lasB)
Flagella +Pili
QS
Rhamnolipids
Biofilm
Other Pathogensis
57% Biofilm decreased Exp
56% pathogenesis decreased Exp
87% QS decreased Exp
44 % Flagella and pili decreased Exp
43% Biofilm increased Exp
44% pathogenesis increased Exp
13% QS increased Exp
56 % Flagella and pili increased Exp
2824 genes
Sig. 104 genes
2825 genes
Sig. 85 genes
Decreased Exp
Increased Exp
log10(p value)
log2FoldChange

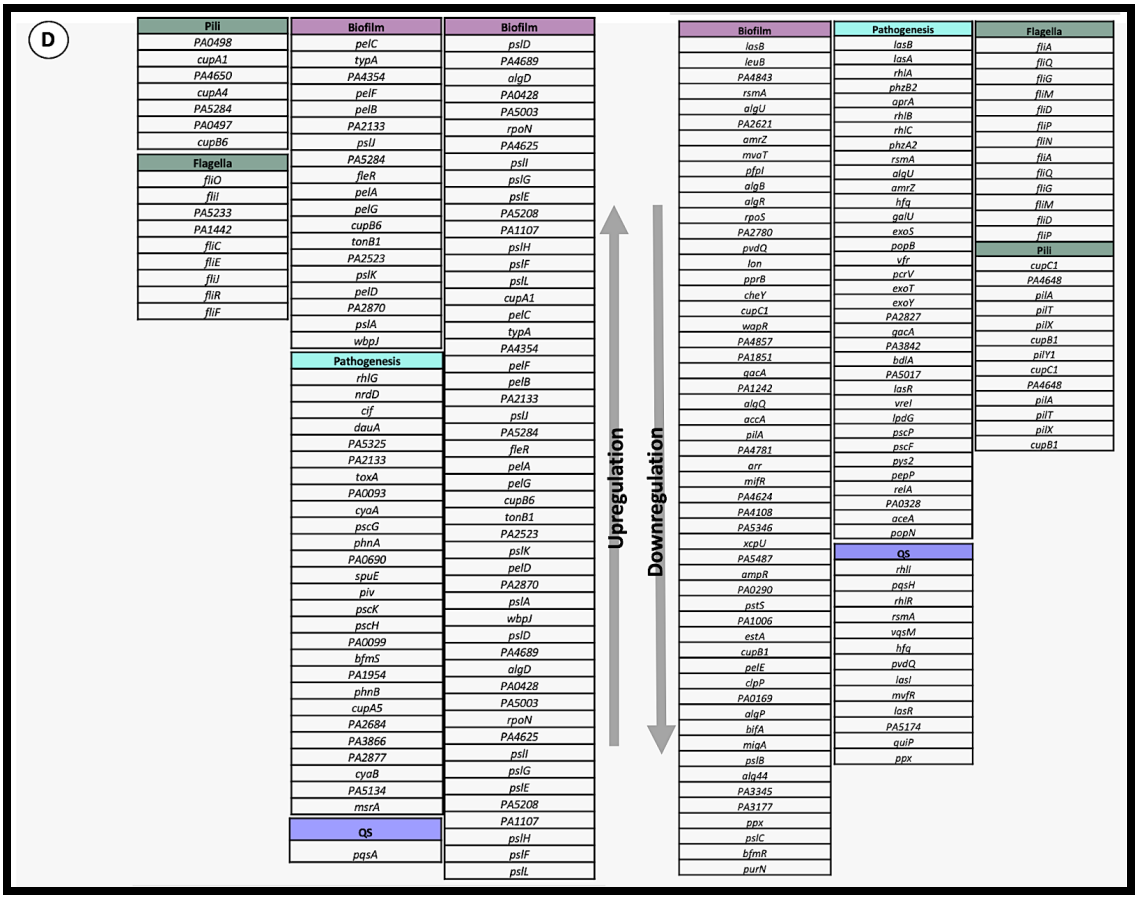

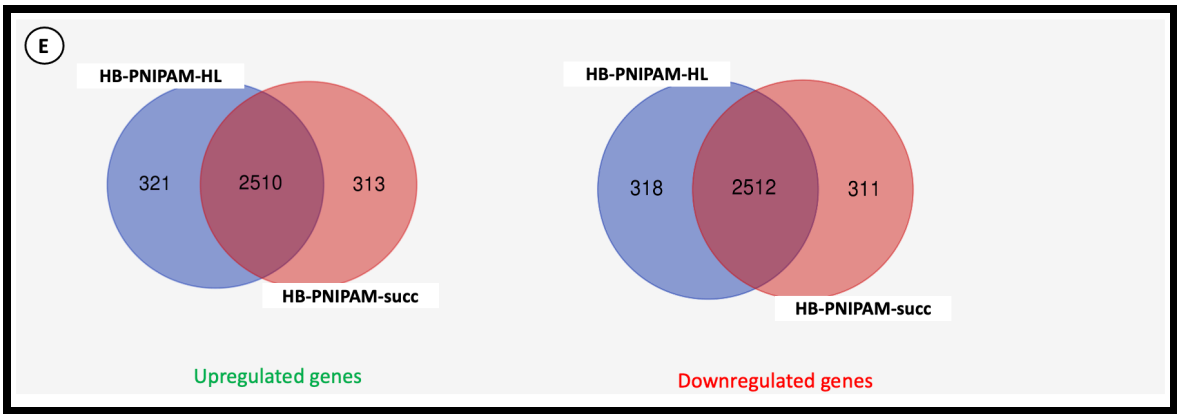

Figure 30: gene expression detected by RNA seq in samples treated with HB-PNIPAM-HL and HB-PNIPAM-succ

(A-D) show a summary results of the different QS and VF genes expression in samples treated with 256 µg/ml of HB-PINPA-HL and HB-PNIPAM-succ **(E)** Venn diagram displaying the relationship of DEGs between the two comparisons HB-PNIPAM-HL and HB-PNIPAM-succ.

5. Discussion

This chapter has focused on *Pseudomonas aeruginosa* PAO1, a pathogen with well-defined QS pathways. *P. aeruginosa* has several QS systems, two of which are mediated by acyl homoserine lactone (AHL) (3O-C_{12}-HSL,and C4-HSL), one by 2-heptyl-3-hydroxy-4-quinolone (Latifi *et al*.,

1996). According to a global gene expression analysis, the AHL-mediated QS system (*las* and *rhl*) regulates 6 to 10% of the *P. aeruginosa* genome (Schuster *et al*., 2003). QS plays a role in *P.aeruginosa* chronic wound infections by promoting several QS-regulated virulence factors (VFs) such as tissue-destroying enzymes, pyocyanin (Harrison *et al*., 2014) biofilm and rhamnolipids (Bjarnsholt, 2013). *Pseudomonas aeruginosa* PAO1 was treated with the polymer HB-PNIPAM-HL to investigate the anti-QS effect on the QS systems in *P.aeruginosa* PAO1, from the QS phenotypes to the molecular level.

The anti-QS effect of the polymer was indirectly assessed by measuring VFs production levels known to be regulated by QS systems in *P. aeruginosa*. Then, the anti-QS effect of HB-PNIAPM-HL Anti-QS was directly assessed by monitoring the gene expression of the QS systems to determine whether the VFs production and the QS systems that regulate these VFs, were similarly affected by the polymer. Several VFs were chosen to evaluate our polymer's effect on their production. We observed that HB-PNIPAM-HL treated *P.aeruginosa* showed a dose-dependent reduction in the production of the VFs studied after being incubated for 18 hours. First, we examined the protease LasA, which is interactively mediated by the *las* system, and the elastin LasB, which is mediated by both the *las* and *rhl* systems QS. The VFs enzymes studied were chosen for their clinical importance in wound infections, including promoting tissue destruction (Sun *et al*., 2020) and the ability to evade immune cells (Park *et al*., 2000). A review by Lindsay *et al*. (2017) highlighted the effects of extracellular enzymes produced by *P. aeruginosa*, such as LasA and LasB, which include tissue penetration and endothelial damage. In (Wang *et al*., 2016), elastin was found to induce degradation of human skin proteins, including fibroblast proteins, during skin infection with *P.aeruginosa,* leading to inhibition of their growth. Overall, these studies highlight the central role these enzymes play in the development of wound infections and contribute to a delay in wound healing. In this study, HB-PNIPAM-HL at a concentration of 256μg/ml was able to reduce both enzymes, LasA and LasB, by (52%) and

(71%) respectively (**Figure 27).** Similar reductions in LasB and LasA have been observed with other known compounds targeting the QS system in *P. aeruginosa*, including treatment with trans-cinnamaldehyde and salicylic acid, which resulted in effective reductions of 80% for LasA and 46% for LasB (Ahmed *et al*., 2019).

Another VF evaluated in this project is rhamnolipids, a surfactant produced by *P. aeruginosa* that is regulated by the *rhl* and *pqs* systems QS systems, promotes biofilm maturation (Nickzad and Déziel, 2014) and supports bacterial penetration into host cells during the initial phase of infection (Zulianello *et al*., 2006). In addition, a study by (Dössel *et al*., 2012) found that rhamnolipids can manipulate the host immune system by preventing the pathogen-induced hBD-2 response in keratinocytes and promoting *P. aeruginosa* resistance during wound infection. Our polymer HB-PNIPAM-HL (256 μg/ml) was able to reduce the secretion of rhamnolipids by 70% (**Figure 27**) The reduction of rhamnolipids by HB-PNIPAM-HL was comparable to the reduction of rhamnolipids using the anti-QS phenol (Coelho *et al*., 2021), which was able to reduce rhamnolipids by ~66% at a concentration of 512g/ml phenol. Pyocyanin, a pigment produced by *P.aeruginosa* and regulated by *rhl* and *pqs* systems, promotes a cytotoxic effect mediated by free radical production (Hall *et al*., 2016). Pyocyanin was found by (Muller *et al*., 2009) to prematurely inhibit wound healing by inducing cellular senescence. The HB-PNIPAM-HL reduced pyocyanin by 70% after 24 hours, not after 18 hours, like other VFs tested (**Figure 27**). This late expression might be related to the fact that the main regulator of pyocyanin is the rhl system, which is expressed in a growth-dependent manner, with the activation of each gene occurring in the last half of the log phase (Pesci *et al*., 1997). The use of these VFs assay to assess the anti-QS ability of our polymer HB-PNIPAM-HL is well documented in the literature (Luo *et al*., 2016). The rational is based that these VFs is under direct regulation of the QS systems in *P.aeruginosa* (Wagner *et al*., 2004, Girard and Bloemberg, 2008).

Another important virulence and characteristic features of *P. aeruginosa* is biofilm formation. Biofilm is of clinical importance as it plays a key role in the ability of organisms to resist antibiotics and persist in long-term infections such as burn wounds (Corehtash *et al*., 2015). Many compounds with QS inhibitory activity have the ability to interfere with biofilm formation (Brackman and Coenye, 2015). As already mentioned in **section 2.3.1, chapter 1**, QS controls the formation of biofilms through the two systems QS *las* and *rhl* (Hentzer *et al*., 2002). In this study, biofilm formation was assess using a coverslip method in samples treated with 128 and 256 μg/ml HB-PNIPAM-HL (**Figure 28 and Appendix 7**). After visualisation under the fluorescence microscope, the samples treated with HB-PNIPAM-HL showed less biofilm formation on the coverslip compared to the untreated samples. Other functionalised polymer have been shown to reduce the biofilm such as the highly branched poly(*N*-isopropyl acrylamide) with vancomycin end groups (HB-PNIPAM-van) in (Doroshenko *et al*., 2018).

Various polymers from different stages of HB-PNIPAM-HL production **(Figure 15)** were investigated for their effect against QS on different QS system genes. These polymers are the HB-PNIPAM-COOH, a polymer formed after the formation of HB-PNIPAM, HB-PNIPAM-succinimide, a polymer in which the COOH is converted to (-succ) ends, and our polymer HB-PNIPAM-HL. All polymers at 256 μg/ml were investigated for expression of genes encoding the QS systems (*las* and *rhl*) using RT-qPCR. Four QS genes and four VFs genes were examined. These were (*lasI*, *lasR*, *rhlI* and *rhlR*) QS genes, and (*rhlA*, *PhzH lasA*, and *lasB) VFs* genes in the presence of both polymers HB-PNIPAM-HL and HB-PNIPAM-succ to assess the extent of the anti-QS effect on both polymers.

The RT-qPCR results showed that the treatment with HB-PNIPAM-HL reduced the expression of *lasR* and *rhlI* significantly. *lasR* activates *rhlI and rhlR* when its encoded receptor (LasR) binds to 3O-C12-HSL (Kostylev *et al*., 2019), however only *rhlI* was significantly downregulated in samples treated with HB-PNIPAM-HL. HB-PNIPAM-succ

significantly downregulated genes encoding for *lasR* and the *rhl* system (*rhl* and *rhlR*). No significant effects on the expression of QS genes were found in the samples treated with HB-PNIPAM-COOH. The results in **Figure 29** shows also that both polymers are significantly downregulated in all three genes (*rhlA, phzH, and lasA*). This down-regulation in the VFs genes can be correlated with the down-regulation in the QS genes (Lee and Zhang, 2015b) seen in **Figure 29.**

For the QS genes tested, HB-PNIPAM-succ has a greater effect on the *rhl* system **(Figure 20).** The *rhl* regulated in the middle of the stationary phase (Lee and Zhang, 2015a), and both are activated by *lasR* (*las* system), which is activated in the early stationary phase. From the growth curve in **Figure 30** and the calculated growth rate, we can suggest that the anti-QS effect in both HB-PNIPAM-HL (VFs assay) and -succ (effect on *rhl* system) might be due to a subinhibitory effect, which was more pronounced in the polymer HB-PNIPAM-succ. The growth rate for both polymers was closely observed in **section 4.5** showing that bacteria treated with -HL and -succ decreased the growth rate during the log phase. A similar effect on growth was observed with the anti- QS compound (OligoG CF -5/20) at a concentration of 0.2%, which showed a significant reduction in VFs, such as pyocyanin and rhamnolipids and QS genes expression. It was suggested that the OligoG CF -5/20 does not act as a "true" QS inhibitor, but as an antagonist that indirectly influences the QS signalling pathways in *P. aeruginosa* through its dose-dependent effect on growth (Jack *et al*., 2018). It can be therefore assume that the effect of the polymers be the same as suggested by (Jack *et al*., 2018). Similar results are reported in (Dai *et al*., 2019) where a sub-inhibition effect in *P.aeruginosa* by ibuprofen resulted in reduction in several VFs and QS genes.

An exploratory RNA-seq study focusing on QS -regulated virulence factor genes between samples treated with 256 g/ml HB-PNIPAM-HL and HB-PNIPAM-succ compared to an untreated sample was summarised in **Figure 29.** It was found that both polymers had a

similar effect on the analysis of the QS genes. The QS gene for the *pqs* system, *pqsA*, was upregulated in RNA-seq. We suspect that this is due to the downregulation of the rhl system (McGrath *et al*., 2004). It is recommended that the RNA-seq investigation be repeated in the future as there is much scope for further investigation. As the Venn diagram in **Figure 31** shows, there are more than 300 different genes expressed in different directions in the samples treated with HB-PNIPAM-HL and -succ. However, without biological replicates, we cannot obtain conclusive results. In Conesa *et al*. (2016), it was pointed out that biological replicates are crucial for minimising bias, especially in library preparation. In Schurch *et al*. (2016) 6 replicates per condition were suggested to minimise false positives. It is suggested here that RNA sequencing be repeated in the future and the results analysed in more detail.

6. Summary of Chapter 3 Findings

6.1 Higher concentrations of HB-PNIPAM-HL have a reducing effect on the production of several important virulence factors in *P. aeruginosa* PAO1. The reduction of these VFs correlated with the significant down-regulation of the genes encoding them

6.2 HB-PNIPAM-HL have a reducing effect on *P. aeruginosa* PAO1 biofilm grown in a glass cover slip.

6.3 Bacterial growth with 256 μg /ml of HB-PNIPAM-HL and HB-PNIPAM-succ, show a delay in growth rate that might imply for a subinhibitory effect.

6.4 The effect of HB-PNIPAM-HL on the transcription of QS -controlled and virulence genes shows that HB-PNIPAM-HL significantly downregulates lasR and rhlI, while HB-PNIPAM -succ downregulates *lasR*, *rhlI* and *rhlR*. In all VFs genes assessed (*rhlA, PhzH*, *lasA* and *lasB*), both polymers showed significant downregulation in *rhlA*, *PhzH*, and *lasA* but not *lasB.*

Chapter 4: Assessing the Anti-QS Effect of the Polymers HB-PNIPAM-HL and HB-PNIPAM-succ on 2D Cell Monolayers and 3D Skin Tissue Engineered Models

1. Introduction

Previous chapters show that the polymer, HB-PNIPAM-HL, affects bacterial Quorum sensing, resulting in decreased virulence factors (VFs), such as the production of destructive tissue enzymes, biofilms, and pyocyanin in *P.aeruginosa* PAO1. Also, the polymer functionalised with succinimide ending; HB-PNIPAM-succ expressed anti-QS abilities by lowering the expression of the genes coding for the QS systems and VFs coding genes in *P.aeruginosa*. This chapter expands the investigation of the anti-QS effect of the two polymers, HB-PNIPAM-HL and HB-PNIPAM-succ , in a more complex multi-layered in-vitro 3D tissue-engineered infected skin model. However, before investigating the effects of the polymers on the bacteria in the 3D tissue engineered skin model, it was necessary to establish whether there were any cytotoxic effects of the polymers on mammalian cells. Effects on the metabolism of monolayers of adult human dermal fibroblasts (HDF, Thermo Fisher, UK Cat#C0135C) and HaCat (Promega) of HB-PNIPAM-HL and HB-PNIPAM-succ were measured using Presto Blue™ (Thermo Fisher, UK Cat#A13261). Presto Blue™ is a resazurin based dye that can detect healthy cells after 30 minutes of incubation (Manlong Xu *et al*., 2014). HB-PNIPAM-HL and -succ were also investigated for any potential wound healing properties or delay using a wound healing assay (also referred to as the migration assay).

The 3D skin model, in comparison to a 2D culture, provides a better model of investigation that can better predict the clinical outcomes of our polymers, as the 2D culture lacks the oxygen/nutrient gradient and the physiological cell functions that a 3D skin model provides (Randall *et al*., 2018). The 3D tissue engineered model can offer an excellent in vitro investigative tool for disease progression, treatments, and diagnostic technologies. Here, the main aim was to test the QS quenching effect of the polymers, HB-PNIPAM-HL and HB-

PNIPAM-succ , in a 3D model infected with *P.aeruginosa* that reflects the physiology and microenvironment of skin *in vivo*. The focus was on how the decreased virulence factors (VFs) such as protease and elastase (destructive tissue enzymes) translate in such models and to compare them to models treated with HB-PNIPAM-HL and -succ. Both polymers ending in -HL and -succ were investigated in a 3D skin model at two periods of treatment, the first after 2 hours of infection with *P.aeruginosa* to represent very early stages of infection, and the other after a more established 24h of infection. The objective was to provide data that might infer the optimal dosage/time for applying treatment to infected wounds with the polymers.

1.1 Aims and experimental approach:

1- To investigate whether the polymers HB-PNIPAM-HL and -succ are cytotoxic against two dermal cell lines, HDF (fibroblasts) and HaCat (keratinocytes), which are used in creation of the 3D skin model.

2- To investigate potential wound healing properties of HB-PNIPAM-HL and HB-PNIPAM-succ on two different cell lines, HDF and HaCat, using the wound healing assay.

3- To investigate the interaction of our polymers with the bacterium *P.aeruginosa* PAO1 in a more challenging environment resembling an *in vivo* environment using a 3D tissue-engineered skin model. The challenge was divided into two treatment periods to determine the optimal dosage/time for treating infected wounds with the polymers.

2. Materials

2.1 List of materials, instruments, and software used in Chapter 4

2.1.1 Bacterial strains and culture conditions

Table 31: Human cells used in Chapter 4.

Bacteria	Supplier
Human dermal Fibroblast (HDF)	Thermo fisher , UK Cat# C0135C
Immortalized Keratinocytes (HaCat)	Promega Cat# (discontinued)

2.1.2 Media and Culture

Table 32: Culture condition and media recipe.

Cell line	Media Recipe	Storage	Culture Condition
Human dermal Fibroblast	• 450 ml DMEM (High glucose) • 50 ml serum = 10% • 5ml Pen/Strep. • 5ml L-Glutamine. • 5. Antifungal (Amphotericin) 1.250 ml	4°C and heated to 37°C when used	37°C 5% CO_2
HaCat	• 335ml DMEM (High glucose). • 115ml F12 (for weaker growing cells ad 1:1, DMEM:F12) • 50ml Serum.=10% • 5ml Pen/Strep. • 5ml L-Glutamine. (When media lack it) • 5ml Adenine.= 1.8X10 -4 • 2mls Hydrocortisone.= 0.5ug/ml if 10X stock found then dilute the stock to 1X (1ml 10X+9ml media)…. To reach the wanted concentration (0.5ug/ml) add 2ml to 500ml of media • 250 µl Insulin. =0.5ng/ml • 500 µl EGF (10µg/ml) or 50 µl (100 µg/ml). =10 ng/ml • Antifungal (Amphotericin) 1.250 ml • 100ulTGF-alpha for 100 ml media =1 ng/ml	4°C and heated to 37°C when used	37°C 5% CO_2

2.1.3 Reagents

Table 33: Reagents used in Chapter 4.

Material	Manufacturer and Recipe
Dulbecco's modified Eagle's Medium (DMEM)	Gibco, Paisley, UK and came supplemented with 4500mg/l glucose GlutaMAX™ I and sodium pyruvate.
Nutrient Mixture F12 (Ham's F12)	Biosera, East Sussex, UK, supplemented with L-glutamine and sodium bicarbonate. Fetal Calf Serum (FCS)
FCS (heat inactivated)	Biosera, East Sussex, UK was stored frozen
Penicillin/Streptomycin	Sigma Aldrich, Dorset, UK.
Amphotericin B	Sigma Aldrich, Dorset, UK.
Adenine	5g Adenine powder (Sigma Aldrich, Dorset, UK) was mixed

	with 70 ml distilled water. 1M Hydrochloric acid (HCl) was added to the mixture until the powder dissolved completely. The solution was filter sterilised and made up to 80 ml with distilled water to give a final concentration of 6.25µg/ml.
Hydrocortisone	25 mg of hydrocortisone powder (Sigma Aldrich, Dorset, UK) was added to 1ml distilled water. The volume was then made up to 10 ml with PBS.
EGF (Epidermal Growth Factor)	0.2 mg Vial add 10ml DMEM containing 10% FBS aliquot into 0.5ml (10 µg/ml) and store at -20 o C. Final Concentration 10ng/ml
Insulin	10ml sterile water add 100 µl glacial acetic acid add to vial of insulin (100 mg) resulting in 10 mg/ml conc. Aliquot into 250 µl and store at 4C
Adenine	Weigh out 330 mg add 100mls 0.1M HCL, agitate to mix well, filter and aliquot into 5 mls store at -20 o C. (1.8x10 -2 M stock).Final Concentration 1.8x10 -4
Recombinant Human TGF-alpha or TGF-α (Animal-free)	Dissolved in at a concentration of 100µg/ml and aliquoted in 100µl aliquots Biolegen, San Diego, USA. Cat #NM_003236
Presto Blue™	In the cytotoxicity assay a 10% of the Presto Blue™ reagent was use where it was diluted using a high glucose DMEM media.

2.1.4 Kits

Table 34: Kits used in Chapter 4.

Kit name	Cat#; manufacturer info
EZ-PCR™ Mycoplasma Detection Kit	Cat# 20-700-20; Biological Industries, USA

2.1.5 Instruments

Table 35: Instruments used in Chapter 4.

Instrument	Purpose	Manufacturer information
Infinite® M200 Pro Series	Plate reader	Tecan UK Ltd, Reading, UK
Nikon Eclipse TS 100Phase contrast inverted Tissue culture Microscope	Visualising mammalian cells	-
Leica TP1020 benchtop ,tissue processor	Processing skin tissues	Leica microsystems Milton Keynes, UK
Leica EG1160 embedding centre, dispenser +hot plate	Embodying models in wax	Leica microsystems Milton Keynes, UK
Leica RM2235 ,microtome	Cutting tissues for processing	Leica microsystems Milton Keynes, UK

Oven	Drying the slides before staining	Preston LTD, Sheffield, UK
Shandon Linear Stainer	Staining tissues	USA
widefield light microscope	Visualising stained skin tissues	Olympus, UK

2.1.6 Software

Table 36: Software used in Chapter 4 for result analysis.

Software	Distributor
GraphPad Prism	GraphPad Software, CA, USA
Magellan ^{TM} Data Analysis Software	Tecan UK Ltd, Reading, UK
Fiji Image J	Rasband, W.S., ImageJ, U. S. National Institutes of Health, Bethesda, Maryland, USA, https://imagej.nih.gov/ij/, 1997-2018.
Spot 5.1 Basic and advanced Modular Imaging software for microbiology	Spot imaging, USA
Cellsens Entry	Imaging acquisition software, Olympus, UK

2.1.7 Miscellaneous

Table 37: List of miscellaneous chemicals and tools used in Chapter 4.

Miscellaneous	#Catalogue; Manufacturerinfo
T-75 flask	Cat# GN658175; Greiner CELLSTAR®, Sigma-Aldrich, UK
96-well flat Bottom microplates	Cat#M0687; Greiner CELLSTAR®, Sigma-Aldrich, UK
12 well flat Bottom microplates	Cat# I1402-0400; Rotor-Gene®, UK
12-well cell culture inserts (0.4µm pore diameter, translucent, sterile)	Cat#665640; Greiner, UK
Phosphate-Buffered Saline (PBS)	Cat# AM9624; Thermo Fisher, UK
Disposable scalpel, no 10	Cat# INS4761;Swann-Morton, Scientific laboratory supplies, UK
Superfrost^{TM} slides	Cat# J1800AMINZ; Fisher, UK
Microtome blades, S35 type	Cat# 207500003;Feather, Japan
Paraformaldehyde Solution, 4% in PBS	Cat# 15670799; Fischer, UK

3. Methodology

3.1 General cell culture maintenance

3.1.1 Cell lines and culture condition

Human dermal fibroblasts were purchased from (Thermofisher, UK, Cat# C-013-5C)and HaCat cells (Promega). Cell culturing and maintenance was performed under sterile conditions in a Class II biohazard laminar flow cabinet. Good cell culture practises (GCCP) guidelines were exercised during the whole process. For media recipes and other reagents see (**Table 32-34).**

3.1.2 Passaging the cells

Passaging, or subculturing, of cells is a typical method that involves dividing, or "splitting," cells from the initial culture into new cultures and feeding them with a fresh medium to allow further expansion. All cells used in this study were cultured in T75 cell culture flasks with filter caps (Greiner Bio-One Ltd, UK Cat# GN658170). Media was removed and replaced with fresh media every two days until ~80% confluency. When the desired confluency was reached, cells were split into new flasks. The splitting process starts with removing old media from flasks and washing cells twice using 5 ml of phosphate-buffered saline (PBS) (Sigma-Aldrich, Dorset, UK Cat#P4417). For cell detachment from flasks surface, 2-3 mL of Trypsin-EDTA solution (Sigma-Aldrich, UK Cat# 59430C) was introduced for ~15 minutes at 37°C. Further dislodging was encouraged with a gentle agitating and shaking of the flasks. The Trypsin was neutralised with addition of 6 ml of serum-containing medium to the flask. The cell suspension was then placed in a 15 ml Falcon tube (Scientific laboratory supplies, UK Cat#352096) and centrifuged for 5 minutes at 1000g. After decanting supernatant, the cell pellet was resuspended in fresh media and added to two new T75 flasks.

3.1.3 Mycoplasma testing for cell lines

Mycoplasma is a bacteria that lack a cell wall. Infection with mycoplasma is one of the main problems faced when culturing cells, as it can affect cells' physiology and metabolism, resulting

in erroneous experiments outcomes or even the loss of unique cell lines. Mycoplasma sources can vary as it may include but not be limited to; laboratory personnel as it can be found naturally in human oropharyngeal, fetal bovine serum, and trypsin solutions provided by swine. Infection with mycoplasma is invisible to the naked eye as it adheres to the surfaces of cells using unique organelles loaded with a high concentration of adhesin. For this reason, routine checks such as checking media turbidity for contamination might not be efficient. However, one effective way to detect mycoplasma contamination is by polymerase chain reaction (PCR).

Principle:

The PCR test detects the 16S rRNA gene of the most common mycoplasma species contaminating cell cultures. The primers should have a specific level of breadth and sensitivity to recognize *Mycoplasma* spp variants and prevent the amplification of common bacteria in the PCR reagents (i.e., DNA polymerase).

Procedure:

The detection assay was performed routinely (monthly). The kit for detection is EZ-PCR™ Mycoplasma Detection Kit (Biological Industries, USA. Cat# 20-700-20). The procedure was done per manufacturer instructions. Briefly, 1 ml of cell culture media was centrifuged (250 g for 30 seconds) to remove cell debris, and the supernatant was transferred in a new 1.5 ml sterile tube. Then again, the supernatant was centrifuged (15,000 to 20,000 x g for 10 minutes) to sediment mycoplasma at the bottom of the tube. The supernatant was removed carefully, and the pellet was kept intact. The pellet was resuspended with 50 µl buffer and vortexed for ~20 seconds. The solution was then heated for 3 minutes at 95°C. Three tubes were set for: Sample test, positive control, and negative control. PCR reagents were added to samples, as it is shown in (**Table 39).**

Table 38: mycoplasma detection PCR reaction table

Component	Test sample	Negative control	Positive control
Sterile water	29 µl	29 µl	33 µl
PCR reaction mix	10 µl	10 µl	10 µl

Internal control primer mix	5 µl	5 µl	5 µl
Internal control DNA template	1 µl	1 µl	1 µl
Buffer sample	--	5 µl	--
Test sample	5 µl	--	--
Positive template control	--	--	1 µl

3.1.4 Cell Storage in Liquid Nitrogen

Media was removed from the flasks. Cells were washed twice with 3 ml of PBS. Then,3 ml of Trypsin was added and incubated for ~15 mins at 37°C. Trypsin was inactivated with 6 ml of serum-containing media. The suspension was transferred in a 15 ml falcon tube then centrifuged for 5 minutes at 1000g. Cells were counted using Trypan Blue (See **Chapter 4, section 3.1.6**), where only 90% viability of cells are frozen. Cells were centrifuged again for 5 minutes at 1000g. the supernatant was removed; the pellet was dissolved in freezing media (10%DMSO+ serum). 1 ml of the media is transferred into a cryovial, placed inside Mr frosty's container, and stored overnight at -80C. Then cells were ready to be stored in liquid N_2.

3.1.5 Thawing Cells from liquid Nitrogen's

Cryovials were removed from the N_2 and placed in a water bath, 37°C, for less than a minute. (cells should not be thawed completely). The vial was then transferred to and opened in a laminar hood. Then all the content of the cryovial was added to a falcon tube that contained 9 ml of complete growth media. The falcon tube was centrifuged for 5min at 5000g to wash the DMSO from the cells. The supernatant was discarded, and the pellet was dissolved in complete media. Then it was transferred to a T75 flask and incubated at 37°C.

3.1.6 Quantification of cell number

Cells were counted using a haemocytometer with Trypan blue (Sigma Aldrich, UK Cat#T8154). The process starts after cell collection, as in **Chapter4, section 3.1.4**. The pellet was resuspended in 1 ml of PBS or serum-free complete medium, as the proteins in serum can

be stained with trypan blue and thus might produce misleading results. An equal amount of trypan blue and the cell suspension was transferred in Eppendorf tubes then left to incubate for 2 minutes. Then 10ul of the suspension was transferred to a haemocytometer with a glass coverslip. The slide was visualised using (Nikon Eclipse TS 100) phase contrast inverted microscope.

It is worth mentioning that counting cells must not exceed 5 minutes from mixing cells with Trypan blue as more extended incubation periods will lead to cell death, and reduced viability counts. Cells were counted from 4 squares in the haemocytometer slide. The following formula was used to estimate the total number of viable cells:

Total number of viable cells= n/4 X dilution factor X10^4

N= # of cells counted

3.2 Presto Blue™ Cell cytotoxicity assay

Principle:

To investigate whether our polymers have any cytotoxic effect against two the types of skin cells, Fibroblasts and HaCat, used in construction of the 3D model, Presto Blue™ cell -viability reagent was used. The Presto Blue™ is a resazurin-based reagent that uses the live cells' natural reducing ability to quantify viability. *Resazurin* is a phenoxazine dye that can enter cells and is irreversibly reduced to fluorescent resorufin by the NAD coenzyme on metabolically active cells. Resazurin is blue with weak fluorescence, while resorufin is fluorescent pink.

Procedure:

Human dermal fibroblasts (HDF) and human immortalised keratinocytes (HaCat) were seeded each at a density of 100,000 cells per well in two different 12 well sterile tissue culture plates in 1 ml of Dulbecco's minimal essential medium (DMEM) high glucose (4500 mg/L glucose) and incubated overnight at 37°C/5% CO_2 to form a monolayer. Then different concentrations of

HB-PNIPAM-HL and HB-PNIPAM-succ were dissolved in 1 ml of DMEM and added to the monolayers.

500 µl of absolute Dimethyl sulphide (DMSO, Sigma Aldrich, UK Cat# D2650) was used as positive toxicity control. For negative toxicity controls, cells without any treatment were used; plates were incubated for 24h at 37°C/5% CO_2. The analysis was done using the metabolic assay PrestoBlue™. Where 500µl of 10% (v/v) Presto Blue™ in complete media was added to each well, Presto Blue™ alone was used as a blank. After two hours, 300 µl in triplicate were removed from the 12well plates and added to a 96 well plate for reading. Fluorescence was then read with excitation/emission wavelengths of 560 nm/590 nm using a Tecan spectrophotometer **(Figure 32).** Images of the cells before treatment with polymers and after was taken using (microscope, software).

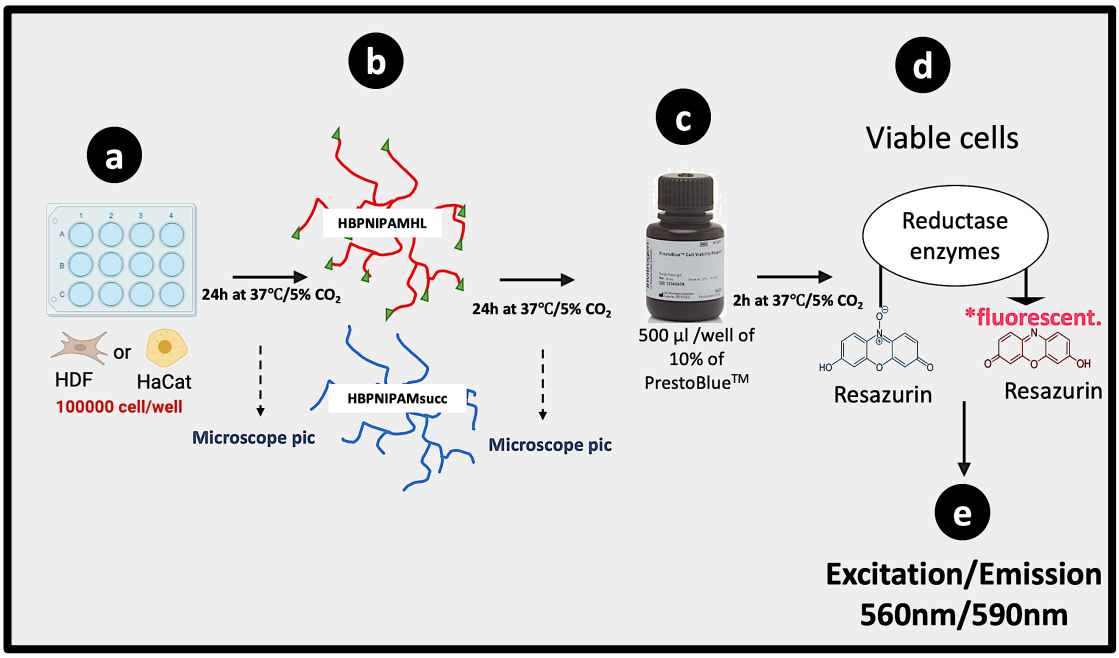

Figure 31: schematic illustration shows the overview of the cytotoxicity assay.
(a) Both HaCat and fibroblasts were seeded at 100000 cells per well in separate 12-well plates**. (b)** After incubation for 24h at 37°C, an image of the cells was taken at a10X magnification before treatment with the polymers. The polymers ended with HL, and succ were added at different concentrations (256 and 512 µg/ml), and the positive control was treated with 500 µl of DMSO, then incubated for a further 24h. **(c)** After incubation, another images were taken, then media was removed, and 500µl of 10%f Presto Blue™ reagent was added and incubated for 2 h**.(d)** The resazurin dye can reduced to the fluorescence resazurin by metabolically active cells, the more fluorescence the more active cells **(e)** Fluorescence was then read with excitation/emission wavelengths of 560 nm/590 nm using a Tecan spectrophotometer.

3.3 Wound healing assay

Principle:

Cell migration is an essential step in the process of wound healing. The wound-healing assay, also known as a migration assay, starts with scratching a confluent cell monolayer to create a cell free gap. This gap very basically mimics a wound, and the closing of the gap "healing " as cells migrate over the area is monitored over several hours.

Procedure:

$2X10^5$ cells per well of HDF and HaCat were seeded in separate 12 well plates (Greiner). The plates were incubated at 37°C/5% CO_2 until a confluence of 100 % was reached. When the full confluence was reached, cells were treated with 10 mg/ml of Mitomycin for HaCat and 2 mg/ml for HDF for 2 hours. Mitomycin C reduces the risk of proliferation, and thus reduces the chances of confounding results (Wang *et al*., 2012). After two hours of treatment with Mitomycin C, the treatment was removed and using pipette tips, a scratch in the HaCat wells was created. After the scratch, wells were washed with 1 ml PBS to remove all detached cells. Different concentrations of -HL and -succ were dissolved in complete DMEM, and 2 ml was added to each designative well. The plates were imaged for 0 h (baseline) images. The migration was monitored, and images after 21 h and for the slower growing HDF were imaged again at 42 h **(Figure 33).**

.

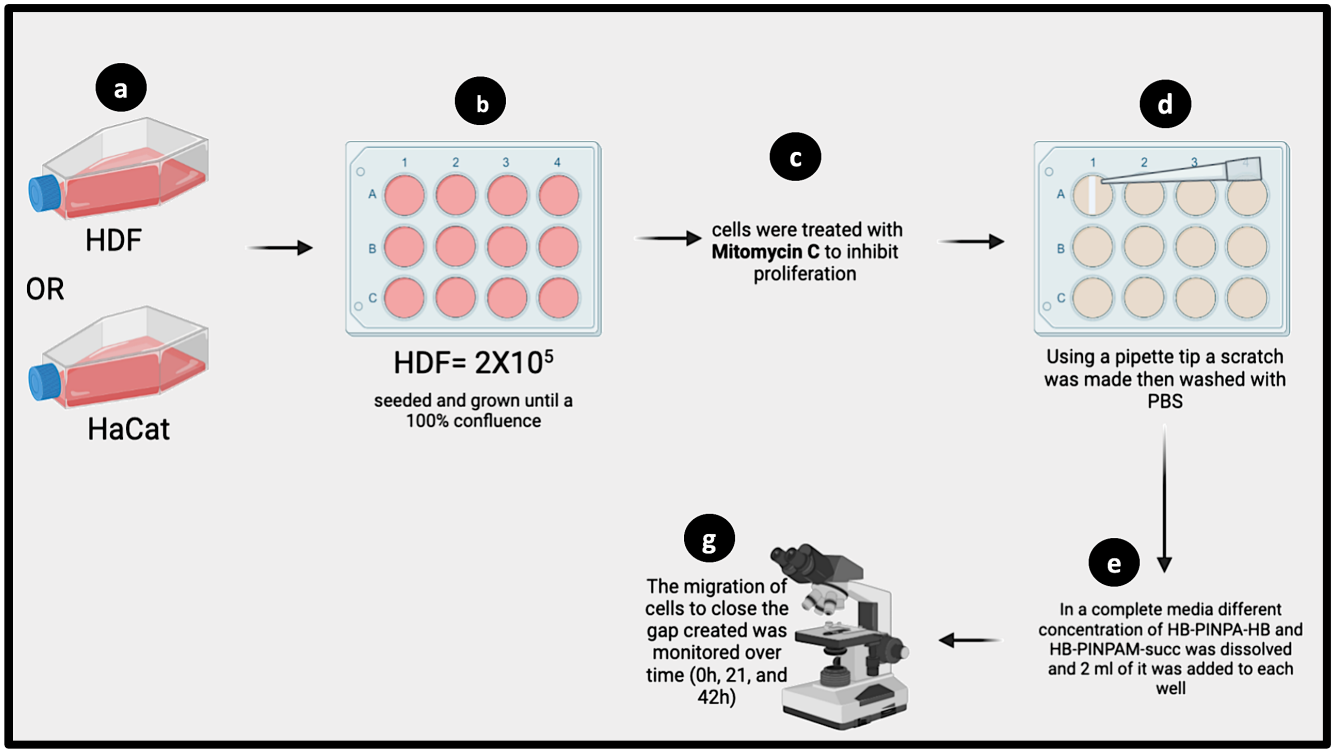

Figure 32 schematic illustration the methodology of the wound healing assay used in this project. **(a-b)** HDF or HaCat were seeded in 12 well plates and left to grow until a confluence of 100%. **(c)** To eliminate any confounding effect of cell prefoliation in the healing wound, Mitomycin C was applied for 2h at 37°C/5% CO_2**. (d)** A scratch was made with a 1000P tip in the HaCat monolayer and a 10P tip for the HDF cells. **(e)** different concentrations of HB-PNIPAM-HL and HB-PNIPAM-succ (256 and 512 µg/ml) were dissolved in a complete media then 2 ml was put in designative wells. **(g)** The monitoring of the cells' emigration after treatment was done during the following period: 0h, 21h and 42h, where an image was taken for analysis using Image J software.

3.3.1 Analysing images using Fiji, Image J for migration assay

Analysis of migrated cells was performed using Fiji, Image J (bundled with Jave1.8.0_172). The analysis was used to measure the percentage of cells that migrated to close the scratch control (Gab). First change the unit of measurement from pixels to µm by selecting the Straight tool and selecting the scale bar present in the image. Then change the "known distance" to the value of the selected scale bar (i.e., 100 um) via Analysis > Set Scale . the measurement was taken for the scratch. The scratch area is converted to a percentage. For example, the scratch size at 0h is 25um=100%. After 21 hours, the measured value of the scratch is now 10um. Then the migrated cells between 0 and 21 hours have migrated by 40% **(** see **Appendix 12)**.

3.4 Establishing 3D construct.

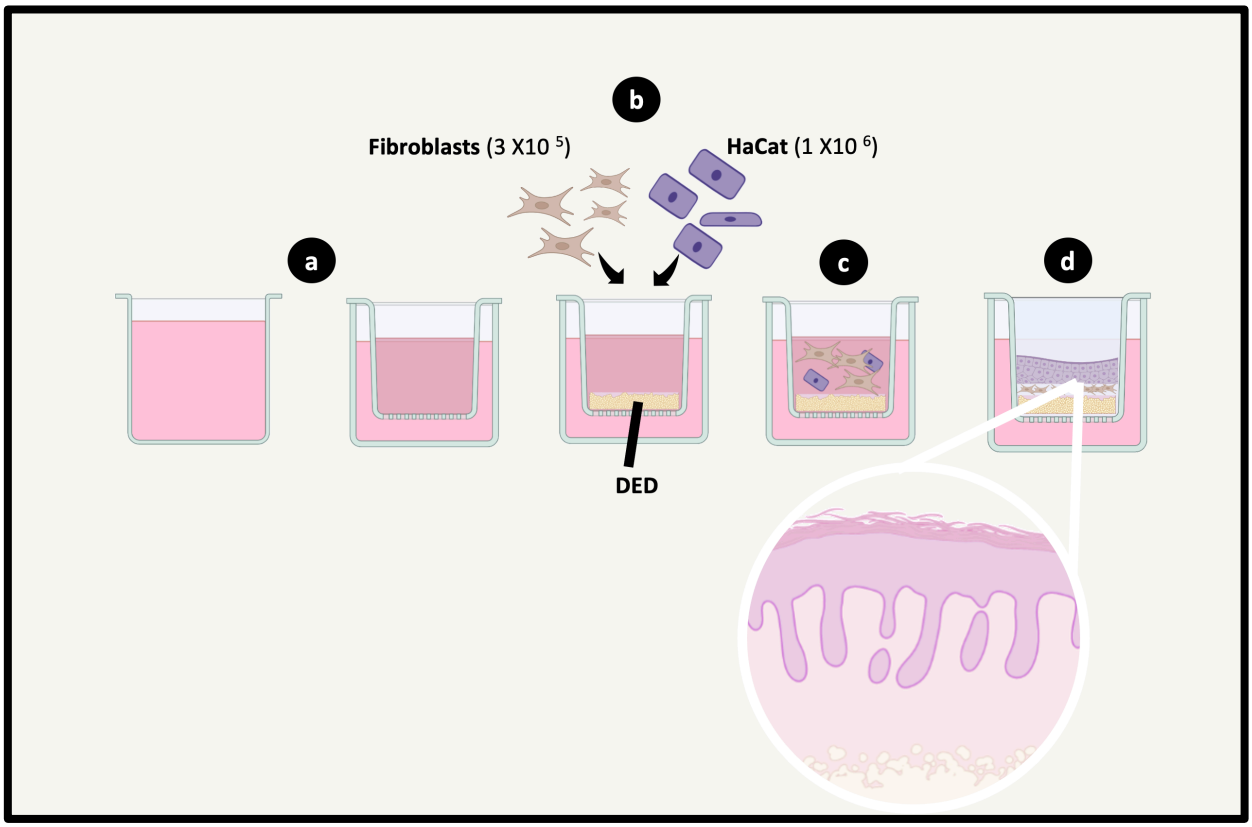

Figure 33: schematic illustration shows the overview process of constructing the 3D skin model. (a&b) The DED scaffolds were cut to fit the inserts of 12-well plates. Each insert was seeded with 250µl $3X10^5$ fibroblasts and $1X10^6$ skin keratinocytes (total volume 500µl). 1-2 ml DMEM containing 10% serum) supplemented with 2ng/ml TGFa was added to the wells around the inserts**.(c)** After 24 hours, the media inside and outside the insert was removed and replaced with fresh media. After a further 24 hours, the media around the inserts was replaced with 800 µl of fresh KGM media. **(d)** The media inside the inserts was removed to form the air-liquid interface. The medium was replenished every 2-3 days, for 14-21 days.

3.4.1 Preparation of Decellularized dermis (DED) from donor skin

DED was prepared by Dr Joey Shepherd according to MacNeil *et al*., (2011). In brief, donor skin (Euro Skin, ETB Biolife, the Netherlands, ethical approval for research not required by user) preserved in glycerol was washed with 40 ml sterile PBS by placing the skin in 50 ml Falcon tube and left on a shaker for 5-7 days at 37°C with changing the PBS daily. After the washing, the skin was placed on a petri dish and covered entirely with a sterile 1 M NaCl and left overnight at 37°C or until the epidermis was visibly separated from the dermis (the pale-yellow colour of the dermis peaks through the brown epidermis). Separation was aided by gently scraping using a scalpel and was continued until all epidermis was removed, resulting in

an acellular DED (pale yellow). The now acellular dermis was flooded with DMEM and incubated at 37°C for 48h to check for sterility. After 48h DMEM was replaced with fresh DMEM supplemented with (Pen. strep & fungizone) and stored at 4°C until use.

3.4.2 Culturing Tissue-engineered skin

The 3D tissue engineered skin model used was constructed as in (Paterson *et al*., 2020) with the number of keratinocytes (HaCat) increased from $5X10^5$ to $1X10^6$ and the number of HDF increased from $1X10^5$ to $3X10^5$. Both cell lines, the human dermal fibroblasts (HDF) and the immortalised keratinocytes (HaCat), were cultured for at least one week before construction of the 3D tissue engineered skin model. The DED scaffolds were cut to fit into 12-well plate inserts. Care was taken to ensure that the edges were tight (i.e., no gaps at the edges) and the epidermal side was facing up (the smoother side facing up). Each insert was seeded with 250µl 3×10^5 fibroblasts and $1X10^6$ skin keratinocytes (total volume 500µl). 1-2 ml DMEM containing 10% serum (see Table 46) supplemented with 2ng/ml TGFa was added to the wells around the inserts. After 24 hours, the media inside and outside the insert was removed and replaced with fresh media. After a further 24 hours, the media around the inserts was replaced with 800µl of fresh KGM media. The media inside the inserts was removed to form the air-liquid interface. The medium was replenished every 2-3 days, for 14-21 days, using 800µl fresh KGM medium for the first 7 days , after which the amount was reduced to 500µl for the rest of the experiment. This was found to lead to better differentiations. Antibiotic-free media was used for 72 hours prior to the experiment to allow for infection[3] **(Figure 34).**

[3] The antibiotic-free media was filtered using a 0.22 µm syringe filter (Millipore™) before using to minimise the risk of cross infecting the models.

3.4.3 Infecting the 3D skin model with *Pseudomonas aeruginosa* PAO1 and treatment with HB-PNIPAM-HL

3D skin models were washed with antibiotic-free media for three days (72h) before infection with *P.aeruginosa* PAO1. Each 3D skin model was burned using an electric heat pen (World precision instruments, USA Cat# 500389) for ~6 seconds, then 1X10^6 of *P. aeruginosa* PAO1 in 20µl of LB media was pipetted on the 3D construct surfaces. The infection was incubated at 37°C for 2 or 24 h before treating with HB-PNIPAM-HL and HB-PNIPAM-succ at different concentrations. After incubation the skin constructs were cut in half with sterile scalpels. Half of the construct was placed in 10% formalin for > 24 hours and then processed and paraffin embedded for histological analysis (see **Chapter 4, sections 3.4**). The other half was weighed and then the tissue was homogenised in 1 ml PBS (Shepherd *et al*., 2009). The resulting homogenates were serially diluted and used to count the viable bacteria in the samples using the same method as in **Chapter 2, section 3.4; and Chapter 3, section3.2**. The process is summarised in **(Figure 35).**

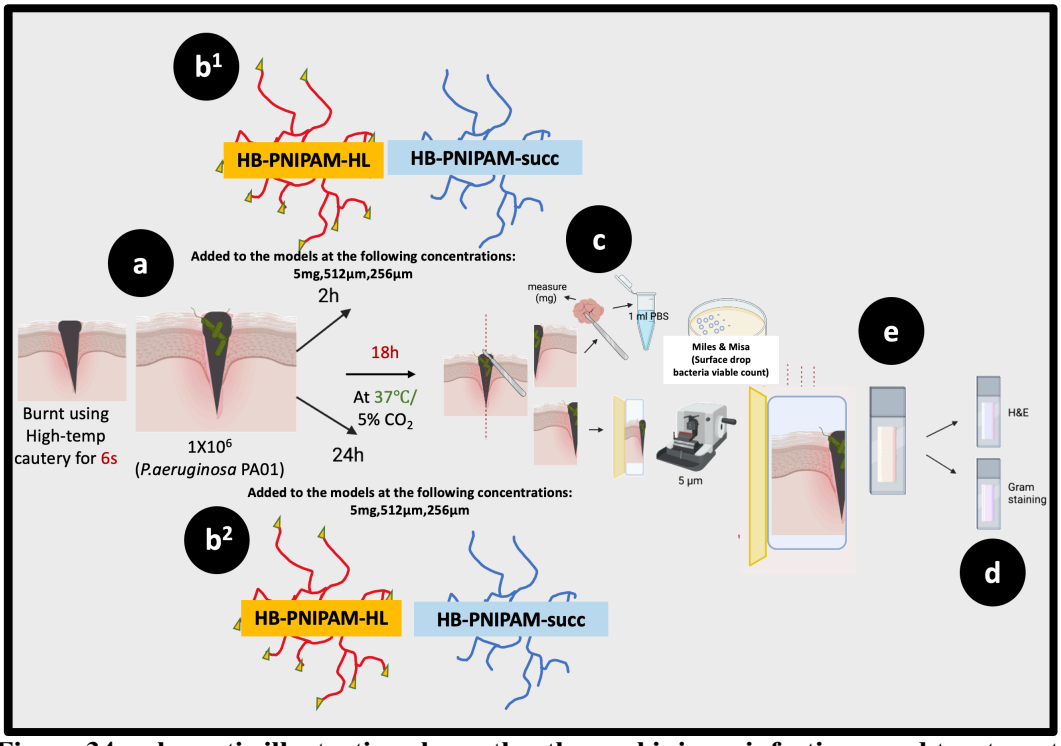

Figure 34: schematic illustration shows the thermal injury, infections, and treatment.

(a) The ready-to-infect 3D skin model was burned for ~6 s using a high-temperature cautery tip, and then a $1X10^6$ of *P.aeruginosa* PAO1 in 20 µl of LB was added on top of the burned skin. **(b1)** After 2 h of incubation of the models with the bacteria only at 37°C, different concentrations of the polymers ended with HL and succ in 100 µl PBS were added, and the control was treated with only PBS**. (b2)** A treatment with different concentrations of the polymers ended with HL, and succ was added after 24h of infection instead of 2h for comparison. **(c)** After incubating 24h after treatment, models were cut into two halves using a scalpel. One half was minced using the scalpel, weight, and vortexed for ~ 20 s in 1 ml of PBS, then Miles and Misra (M&M) were done to determine the CFU/mg. **(d)** The other half was processed and then embedded in wax, where they were sectioned to a ~5µm thickness and **(e)** Stained with H&E or Gram staining.

3.5 Histological analysis of 3D skin model

3.5.1 Fixing and processing 3D model

For histology the samples were preserved in 4% PFA (paraformaldehyde) until samples were processed using a Leica TP1020 benchtop tissue processor (Leica microsystems, Milton Keynes, UK) overnight. The following solutions were used to process the samples: (**Table 40**).

Table 39: Histological processing steps.

Solution	Exposer time (min)
Neutral buffered formalin (10%)	60 min
Alcohol (70%)	60 min
Alcohol (70%)	60 min
Alcohol (90%)	60 min
Alcohol (90%)	60 min
Absolute alcohol	60 min
Absolute alcohol	60 min
Absolute alcohol	60 min
Xylene	90 min
Xylene	90 min
Paraffin wax	120 min
Paraffin wax	120 min

After processing the samples and before embedding them in molten paraffin wax, the rough edges were trimmed using a heated blade to have clean tissue edges. Using the Leica EG1160 embedding centre, dispenser, and hot plate (Leica microsystems, Milton Keynes, UK), each sample was placed perpendicular in the metal mould to have a section of the proper orientation and wax was dispensed to make the wax block.

3.5.2 Sectioning blocks of the 3D tissue engineered models

The wax blocks were cooled overnight and placed at -20°C for one h before using the Leica RM2235 microtome (Leica microsystems, Milton Keynes, UK) with microtome blades, S35 type (Feather, Japan). The initial cut was 7µm in thickness to allow the tissue to be exposed from the wax mould; then, the thickness was adjusted to 5µm. The slices were immediately transferred to a water bath (40°C) to allow the resulting ribbon to flatten out before mounting them onto SuperFrost® Plus slides (VWR International, Lutterworth, UK Cat# 630-0951). The slides then were dried in a (65°C) oven for 45-60 min or overnight on a bench. For an overview of the infection progression in the models, different samples were taken at different depths of the wax block **(Figure 35).**

3.5.3 Haematoxylin and Eosin (H&E) Staining

Principle:

Haematoxylin and eosin, or the H&E stain, is a combination of two stains that differentiate different tissue structures. Haematoxylin (purplish-blue dye) and eosin (red or pink dye) are standard stains that have been used widely used stains for the study of histochemical tissue pathology. For example, Haematoxylin is a basic dye that can stain the acidic structures inside the cells blue or light blue; this includes DNA in the nucleus and the RNA found in both ribosomes and the rough endoplasmic reticulum. On the other hand, eosin is acidic with a negative charge that stains acidophilic cell structures pink, such as the cytoplasm and the extracellular structure (Gurina and Simms, 2020).

Procedure:

Formalin-fixed paraffin-embedded (FFPE) samples were stained with haematoxylin and eosin using a Shandon linear staining machine (Department of Pathology, School of Clinical Dentistry, Sheffield, UK) . The procedure briefly was as follows: after cutting the section , it was dried either in the oven on (65°C) for 45min or on a bench for 24-48h, then slides were

put on the machine to be stained in each solution for ~45 seconds as in (**Table 41**) . After staining, the slides were quickly mounted using DPX mountant (Sigma-Aldrich, Dorset, UK Cat# 44581) then covered with glass coverslips. Slides then were observed using a widefield light microscope with a camera, and images were obtained using Cellsens entry software (Olympus, Essex, UK).

Table 40: H &E staining procedure.

Solution	Purpose
Xylene (X3)	Removal of the wax from the section, leaving only the tissue section adhered to the slide.
Absolute alcohol	Gradually rehydrate the section
Absolute alcohol	
70% alcohol	
Running tap water	
Harris's Haematoxylin (Shandon) (X5)	Staining basophilic parts of the section (cell nuclei)
Running tap water (X2)	Washing off excess Haematoxylin
0.1% HCl in 70 % alcohol	For stain differentiation of the sample (helping the sample to take up the red eosin stain)
Running tap water	Washing off acidic alcohol
Scott's tap water substitute	Helping with making haematoxylin bluer
Running tap water	Washing salt from Scott's water substitutes off
Eosin Y-aqueous stain (Shandon)	Staining eosinophilic parts of the section (inc. cytoplasmic proteins, collagen, and keratin)
Eosin Y-aqueous stain (Shandon)	
Running tap water	Washing off excess eosin stain
95 % alcohol	Gradually dehydrate the sample
Absolute alcohol (X4)	
50:50 absolute alcohol: xylene	
Xylene (X2)	

3.5.4 Gram staining

Principal:

Gram staining is a widely used bacteriology staining. It consists of primary and counter stains, with a mordant to increase the affinity of the primary stain and alcohol for decolourising. Gram staining divides bacteria into two branches according to cell wall type. Gram positive bacteria retain the crystal violet staining due to their thick cell wall with high peptidoglycan (protein -

sugar) and low lipid content and appear purple. Also, the decolourising step with alcohol can result in drying or the wall shrinking the pores, making it hard for the stain to seep outside. On the other hand, Gram negative bacteria cannot retain the CV due to their low peptidoglycan and high lipid content. The alcohol washes off the lipids removing the CV and iodine complex formed with it. Gram stains are usually pink after staining because of the pink counter stain used, safranine (Tripathi and Sapra, 2020).

Procedure:

Briefly, the paraffin wax was removed using the last five steps in the linear Stainer then moved to be Gram stained manually. The first step was applying the purple stain crystal violet (CV) for one minute, then adding Gram's iodine, a mordant (to attach to the CV, making it insoluble and thus resisting the decolourising step). Next, apply alcohol acetone for 30 seconds was applied. After rinsing, the counterstain safranin (Pink) is applied (**Table 41**).

Table 41: Gram's staining process.

Reagent	Function
Crystal Violet	Primary staining -stains bacteria with thick wall with purplish stain
Gram's iodine	A mordant that binds to the crystal violet staining making a complex that cannot be soluble with alcohol
Acetone	Decolorising steps to remove any retained stain
Saffranine	A counter stain

4. Results

4.1 HB-PNIPAM-HL was not toxic to mammalian cells tested.

The aim was to evaluate whether the - HL and -succ ending polymers have a cytotoxic effect on the two cell lines HDF and HaCat. The reason for using these concentrations was to test the cytotoxicity for the concentration that significantly affected the VFs in *P.aeruginosa*, namely 256 μg/ml , as shown in **Chapter 3**. In addition, a higher (2-fold) concentration of both polymers was also tested (512μg/ml).Cells were incubated with the polymers at 37°C/5% CO_2. After 24 hours, the cell viability of HDF and HaCat was tested with 10% Presto Blue™.

(**Figure 36)** shows the quantitative data on cell viability in the presence of different concentrations of the polymers (256-512 μg/ml). From (**Figure 36, A&B**) it can be seen that for HaCat **(A)** and HDF **(B)** and there was no significant cytotoxicity for either HB-PNIPAM-HL or HB-PNIPAM-succ at all concentrations used. In contrast, viability increased with HaCat at 256 and 512 g/ml of HB-PNIPAM-succ and 512μg/ml of HB-PNIPAM-HL (**Figure 36, A**). The descriptive statistical data of the assay for both cell lines are shown in **(Table 43 &44).**

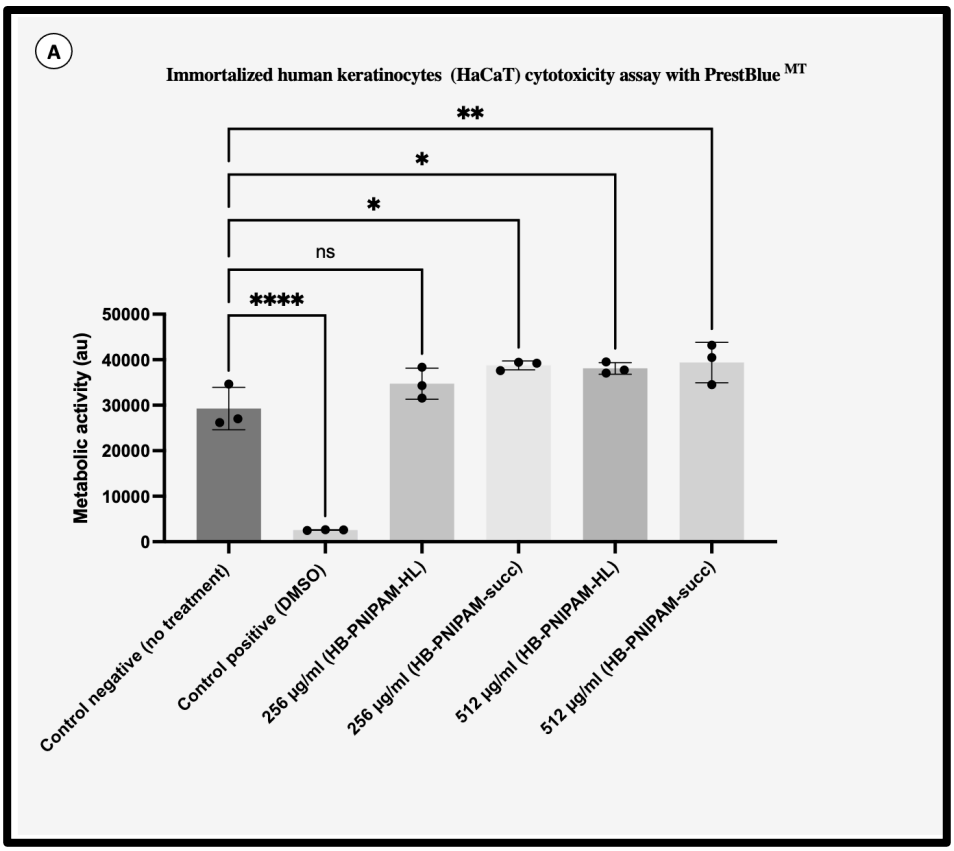

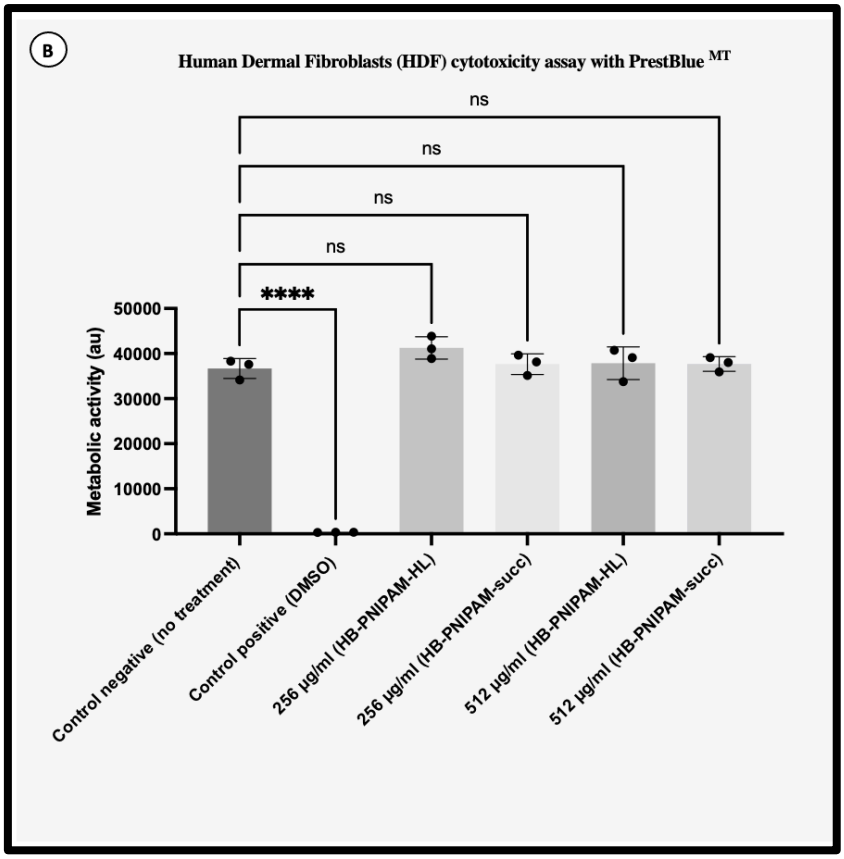

Figure 35: toxicity of HB-PNIPAM-HL and HB-PNIPAM-succ tested against mammalian cells. Toxicity of three different concentrations HB-PNIPAM-HL against a monolayer of **(A)** immortalized human keratinocytes (HaCat) and **(B)** Human Dermal cells (HDF) over 24h exposure assessed by metabolic activity measured using a Presto Blue™ assay.(n=3). Experimental data are expressed as mean ± standard deviation. Significance was determined using one-way ANOVA analysis of variance with Dunnett test in prism (version 9.3.1) *,P<0.01;**,P<0.001; ****, P<0.0001, and ns-not significant. Error bars= SD. (Full ANOVA Results can be found in **Appendix 13**).

Table 42 Descriptive data of HaCat cytotoxicity reading using PrestoBlue™

Sample	Mean (±SD, Range)	P value (compare to control negative)
Control negative (no treatment)	29275 (± 4669, 8470)	Not applicable
Control positive (DMSO)	2574 (±71.44, 135)	<0.0001
256 µg/ml (HB-PNIPAM-HL)	34743 (±3423, 6807)	0.1655
256 µg/ml (HB-PNIPAM-succ)	38756 (±991.9, 1809)	0.0100
512 µg/ml (HB-PNIPAM-HL)	38098(± 1274, 2462)	0.0160
512 µg/ml (HB-PNIPAM-succ)	39383(± 4434, 8662)	0.0065

Table 43 Descriptive data of HDF cytotoxicity reading using PrestoBlue™

Sample	Mean (±SD, Range)	P value (compare to control negative)
Control negative (no treatment)	36696 (± 2220, 4143)	Not applicable
Control positive (DMSO)	348.3 (±18.18, 35)	<0.0001

256 µg/ml (HB-PNIPAM-HL)	41259 (±24801, 4947)	0.1156
256 µg/ml (HB-PNIPAM-succ)	37643 (± 2293, 4507)	0.9802
512 µg/ml (HB-PNIPAM-HL)	37855 (± 3635, 6947)	0.9553
512 µg/ml (HB-PNIPAM-succ)	37683 (± 1611, 3168)	0.9764

4.2 Wound healing assay

As shown in **section 4.1,** treatment with 512 and 256 µg/ml of the two polymers showed no cytotoxicity for the two cell lines HDF and HaCat. Here, the functional effect of the two polymers at the same concentrations on cell migration was investigated using a wound healing assay, also known as a "scratch assay". This was to investigate whether the polymers at the above concentrations would assist or delay the healing process in the two cell lines, HDF and HaCat.

No significant delay in migration was observed in HDF, except for HB-PNIPAM-succ at a concentration of 512 µg/ml, where an overall delay of 57% was measured compared to the control (~88% after 42h) **(Figure 37, A-G) .** For healing of HaCat cells, the control showed slightly faster healing (gap closure) with an overall average of (10.8%) than the samples treated with HB-PINPA-HL or -succ (**Table 45**). However, all samples were able to close the gap without significant differences compared to the untreated samples **(Figure 38, A-G).**

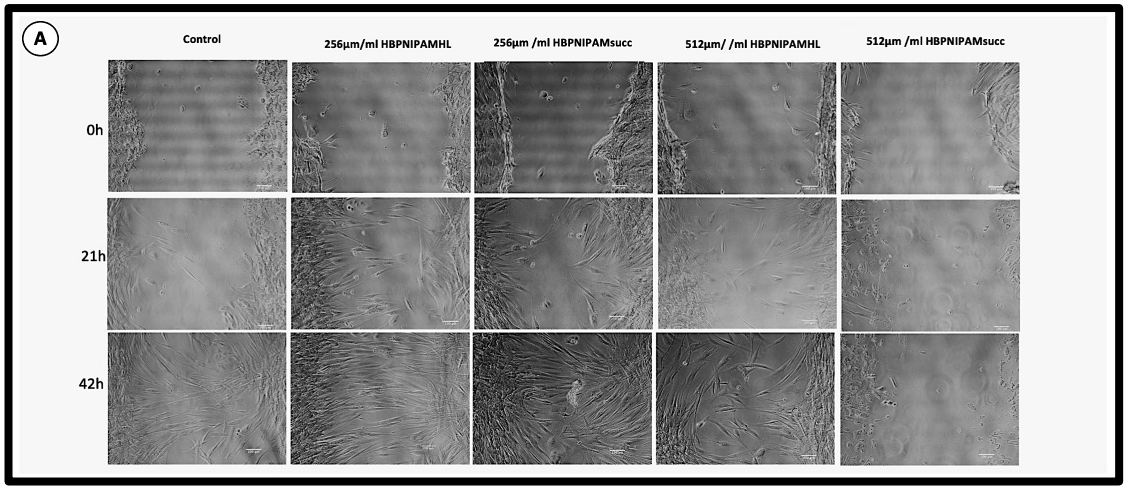
A
Control
256µm/ml HBPNIPAMHL
256µm /ml HBPNIPAMsucc
512µm/ /ml HBPNIPAMHL
512µm /ml HBPNIPAMsucc
0h
21h
42h

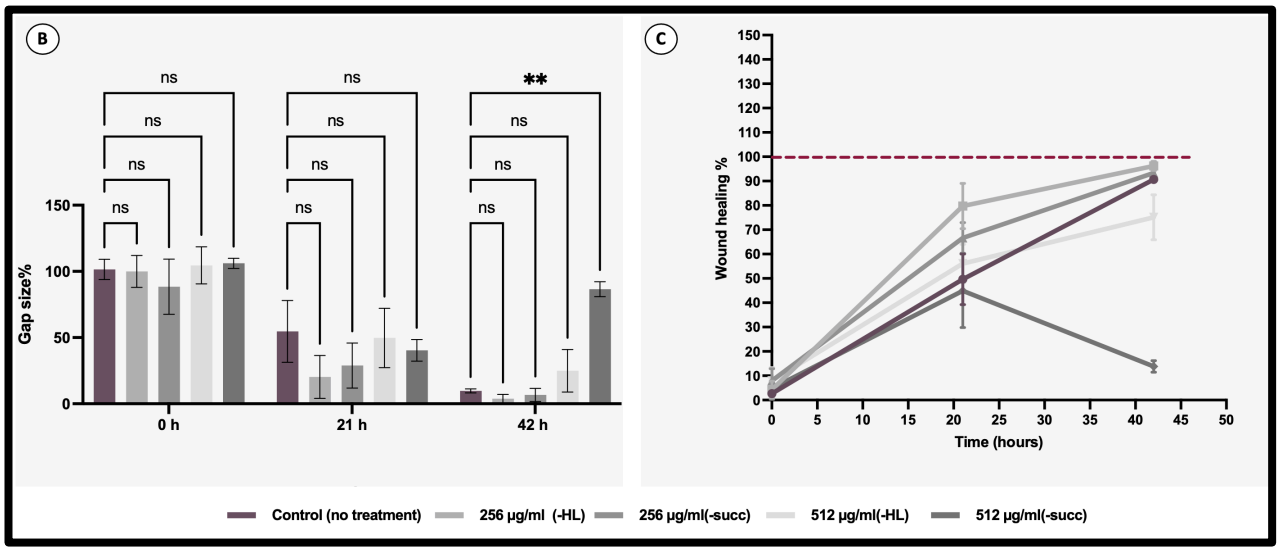
B
Gap size%
ns
**
0 h
21 h
42 h
C
Wound healing %
Time (hours)
Control (no treatment)
256 µg/ml (-HL)
256 µg/ml(-succ)
512 µg/ml(-HL)
512 µg/ml(-succ)

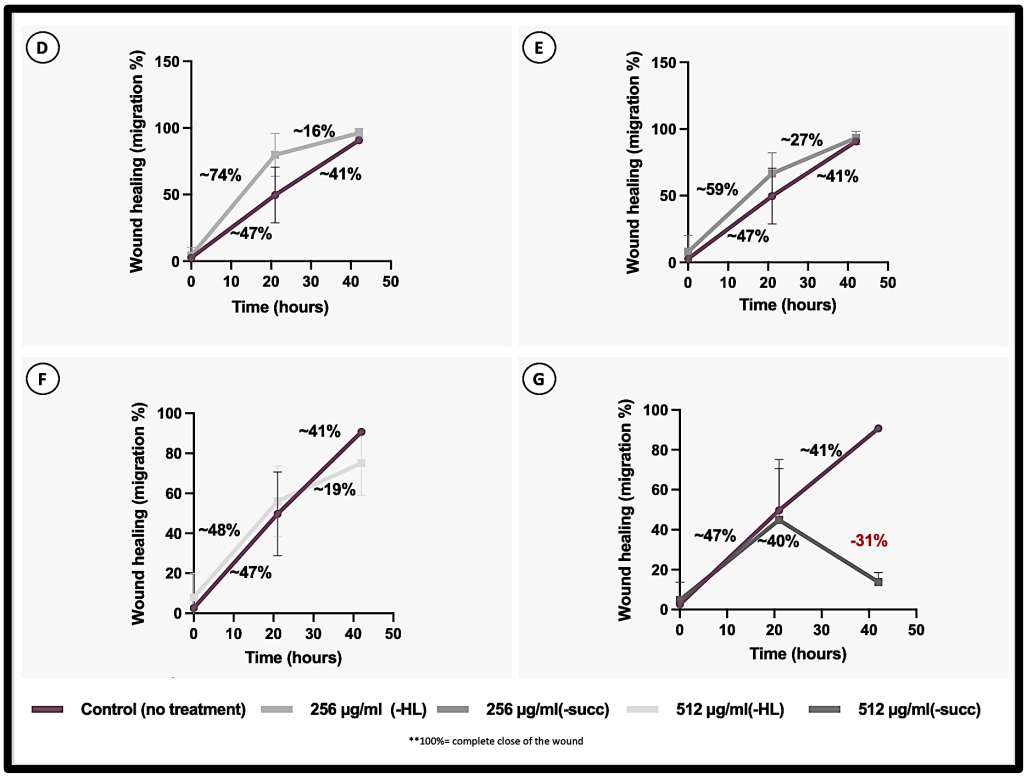
D
Wound healing (migration %)
~74%
~16%
~47%
~41%
Time (hours)
E
~59%
~27%
~47%
~41%
F
~48%
~47%
~19%
~41%
G
~47%
~40%
-31%
~41%
Control (no treatment)
256 µg/ml (-HL)
256 µg/ml(-succ)
512 µg/ml(-HL)
512 µg/ml(-succ)
**100%= complete close of the wound

Figure 36: wound healing assay for HDF after treatments with different concentrations of HB-PINPMA-HL and HB-PNIPAM-succ

(A) progression of wound healing for the human dermal fibroblasts (HDF) after treatments with different concentrations of HB-PNIPAM-HL and HB-PNIPAM-succ . **(B&C)** The quantitively analysis of the migrated cells from 0h until 42h treated and untreated with HB-PNIPAM-HL or HB-PNIPAM-succ using image J **(Appendix 12).** Red dotted line indicates a complete (100%) closing of the gap. Separate graphs were created for HDF cells treated with **(D)** 256 µg/ml of HB-PNIPAM-HL **(E)**256 µg/ml of HB-PNIPAM-succ **(F)** 512µg/ml of HB-PNIPAM-HL, and **(G)**512 µg/ml HB-PNIPAM-succ . Their migrations were monitored after 21h and 42h. The percentages show the gap's closing, where 100% means a complete closing of the wound. The scale bar size=100µm. (n=3).Experimental data are expressed as mean ± standard deviation. Error bars= SD. Significance was determined using two-way ANOVA analysis of variance with Dunnett test in prism (version 9.3.1) ns-not significant, and**,P<0.001. Error bars= SD. (Full ANOVA Results can be found in **Appendix 13**).

Table 44: Percentage of the amount HDF cells migrated to close the wound after treatment with HB-PINPA-HL or HB-PINAPM-succ.

HDF cells treated with	Percentage of closing the gap from 0 until 21h	Percentage of closing the gap from 21 until 42h
Control negative (no treatment)	47.0	40.9
256 µg/ml (HB-PNIPAM-HL)	75.4	16.4
256 µg/ml (HB-PNIPAM-succ)	58.7	26.6
512 µg/ml (HB-PNIPAM-HL)	48.1	19.0
512 µg/ml (HB-PNIPAM-succ)	40.1	-31.0

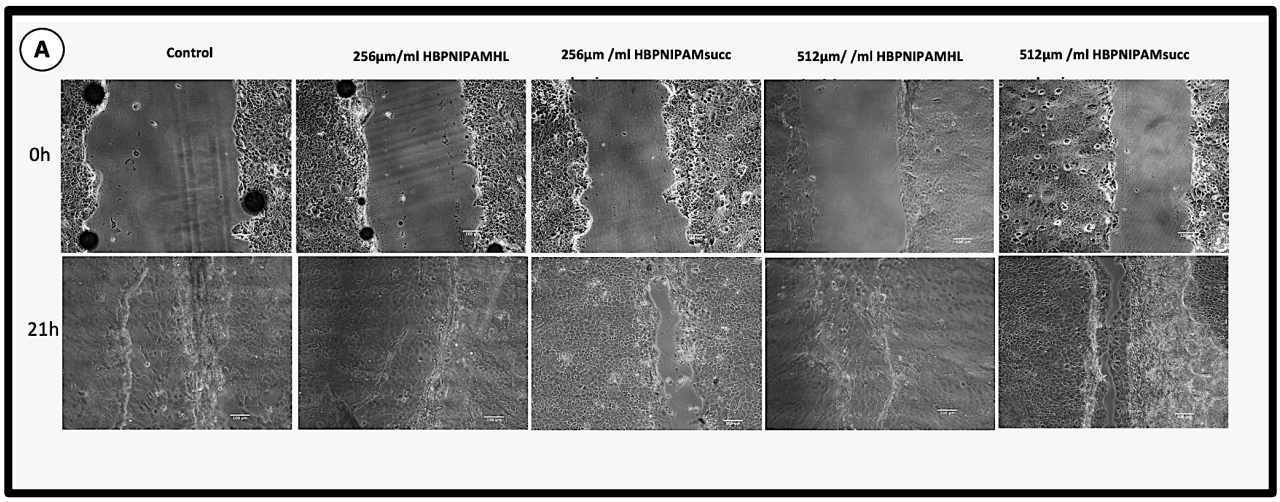

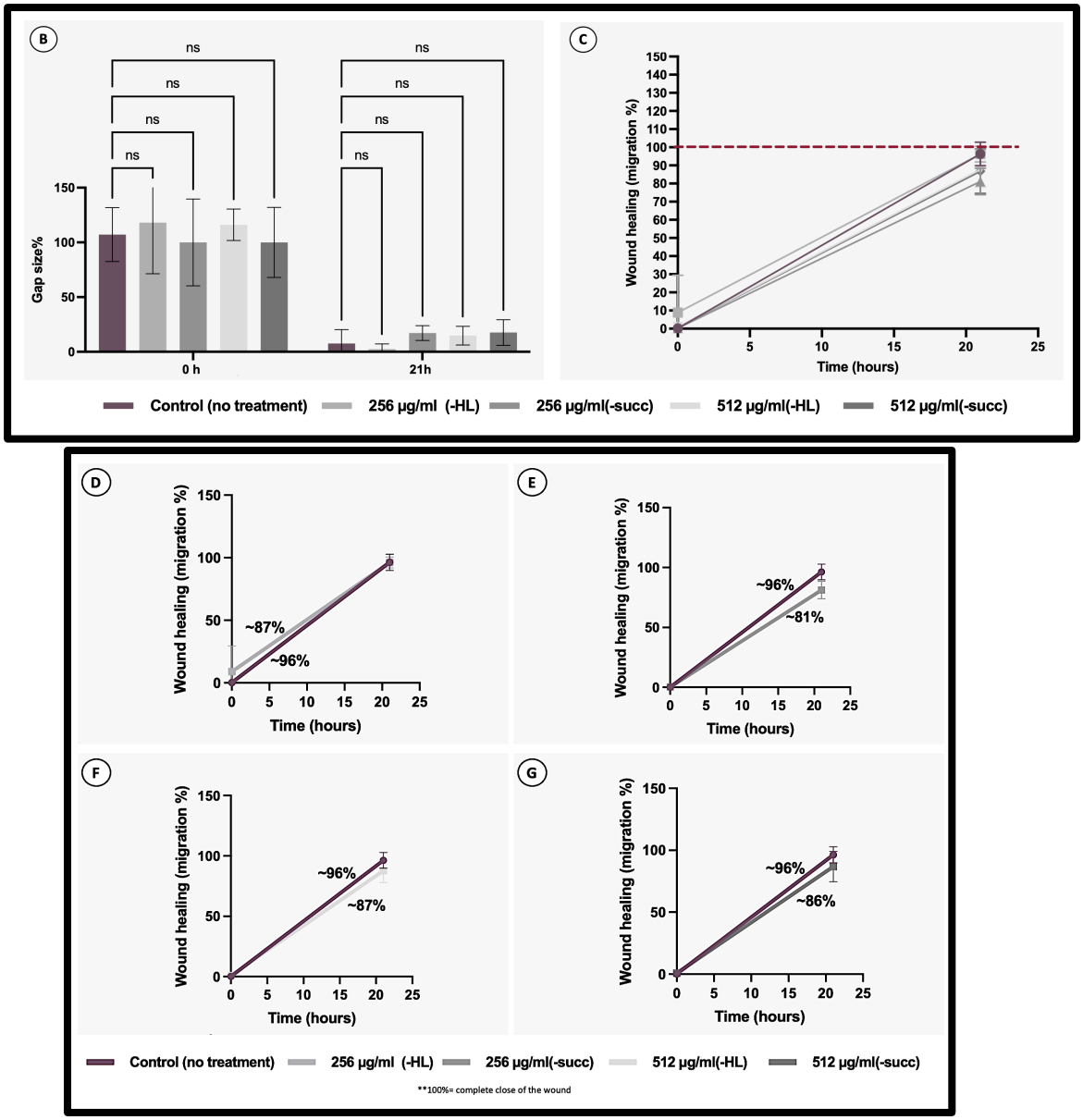

Figure 37: wound healing assay for HaCat cells after treatments with different concentrations of HB-PINPMA-HL and HB-PNIPAM-succ .

(A) Progression of wound healing for the immortalised keratinocytes (HaCat) after treatments with different concentrations of HB-PNIPAM-HL and HB-PNIPAM-succ . **(B&C)** The quantitively analysis of the migrated cells from 0h until 21h treated and untreated with HB-PNIPAM-HL or HB-PNIPAM-succ using image J. Red dotted line indicates a complete (100%) closing of the gap. Separate graphs were created for HaCat cells treated with **(D)** 256 µg/ml of HB-PNIPAM-HL **(E)**256 µg/ml of HB-PNIPAM-succ **(F)** 512µg/ml of HB-PNIPAM-HL, and (G) 512 µg/ml HB-PNIPAM-succ Their migrations were observed after 21h. The percentages show the gap's closing, where 100% means a complete closing of the wound. The scale bar size=100µm. (n=3) Experimental data are expressed as mean ± standard deviation. ns-not significant .Error bars= SD. Error bars= SD. Significance was determined using two-way ANOVA analysis of variance Dunnett test in prism (version 9.3.1) ns-not significant. Error bars= SD. (Full ANOVA Results can be found in **Appendix 13**).

Table 45: Percentage of the amount HaCat cells migrated to close the wound after treatment with HB-PINPA-HL or HB-PINAPM-succ.

HDF cells treated with	Percentage of closing the gap from 0 until 21h
Control negative (no treatment)	96.1
256 µg/ml (HB-PNIPAM-HL)	87.3
256 µg/ml (HB-PNIPAM-succ)	80.8
512 µg/ml (HB-PNIPAM-HL)	86.7
512 µg/ml (HB-PNIPAM-succ)	86.0

4.3 Evaluation of the effects of HB-PNIPAM-HL and HB-PNIPAM-succ on a 3D tissued engineered skin infected with *P.aeruginosa* PAO1

Figure 39 shows an untreated 3D skin model resembling native human skin, with differentiated epidermal layers and a collagenous dermis. The 3D skin models were used to investigate two treatment periods post infection with *Pseudomonas aeruginosa* PAO1. The first treatment was applied after 2h of infection and the second period after 24h of infection. Both were treated for 18h with HB-PNIPAM-HL and HB-PINAPAM-succ at different concentration.

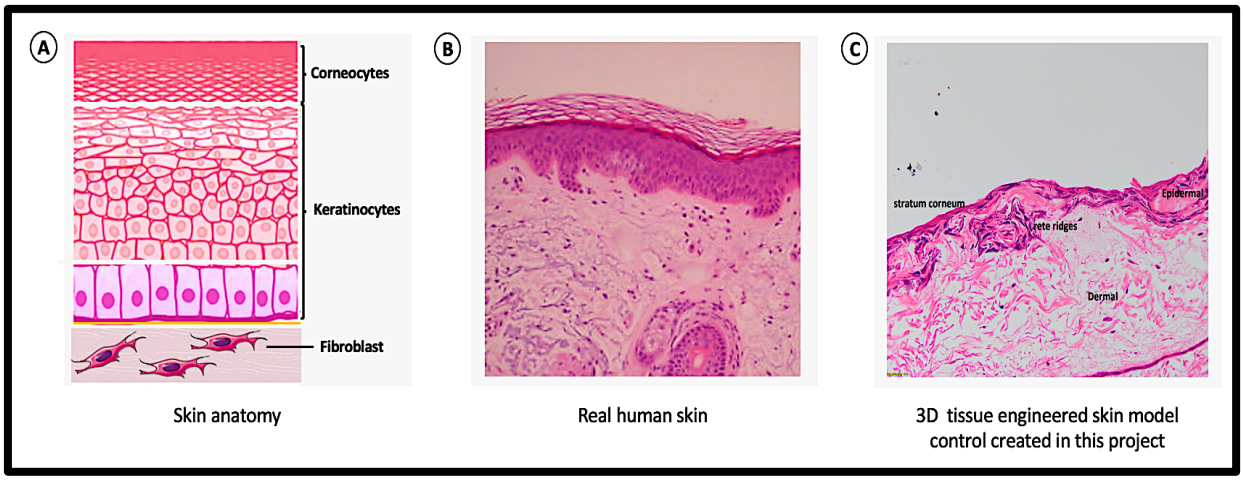

Figure 38: a comparison between a 3D tissue engineered skin model and a human skin. **(A)** An illustration of skin anatomy in human. **(B)** H&E of human skin. Source:(https://dermnetnz.org/cme/dermatopathology/special-stains-and-tests). Copyright **Licences under** (CC BY-NC-ND 3.0 NZ). **(C)** H&E staining of untreated 3D tissue engineered skin model produced in this project**.**

4.2.1 Treatment with both HB-PNIPAM-HL and HB-PNIPAM-succ after 2h of infection

The effect of the two polymers ending in -HL and -succ was investigated using haematoxylin and eosin staining (H and E) of an infected 3D tissue-engineered skin model after infection with *P.aeruginosa* ($1X10^6$) for a total incubation time of 20 hours. In **(Figure 40 A),** a cross-section of the uninfected 3D skin model stained with (H and E) shows an intact epidermis with well-differentiated epidermal layers. In **(Figure 40 B),** a positive control, an infected 3D skin model infected with *P.aeruginosa* ($1X10^6$) for 2 hours and then treated with 100 µl PBS and incubated for 18 hours shows destruction of the epidermis (black arrows) and dermis. In **(Figure 40 C and D),** the two 3D skin constructs were infected for 2 hours and then treated with 100 µl of 512 µg/ml HB-PNIPAM-HL or -succ and incubated for 18 hours. In **(Figure C)** we see that the destruction of the epidermis is less in the samples treated with 512 µg/ml HB-PNIPAM-HL than in the positive control in **(B).** The destruction of the dermis is moderate, there are epidermis shedding (orange markings). (**Figure 40 D)** shows the sample treated with HB-PNIPAM-succ 512 µg/ml with slightly less destruction than the positive control in **(B)** but more than the sample treated with HB-PNIPAM-HL in **(C).** It can also be seen that the destruction extends into the dermal layer. (**Figure 40 G)** shows that the treatment with lower concentrations (256 µg/ml) of HB-PNIPAM-HL has similar destruction effect (black arrow) to the higher concentration of (512 µg/ml) HB-PNIPAM-HL but less than positive control in **(B)**. **Figure H** shows that treatment with HB-PNIPAM-succ at 256 µg/ml results in less destruction than the positive control in **(Figure 40 B),** however epidermal shedding can be observed. However, compared to HB-PNIPAM-succ at the same concentration, HB-PNIPAM-HL appears to destroy less. Post-infection bacterial CFU was not significantly reduced in all treated samples compared to the positive control. **(Figure 40 I).**

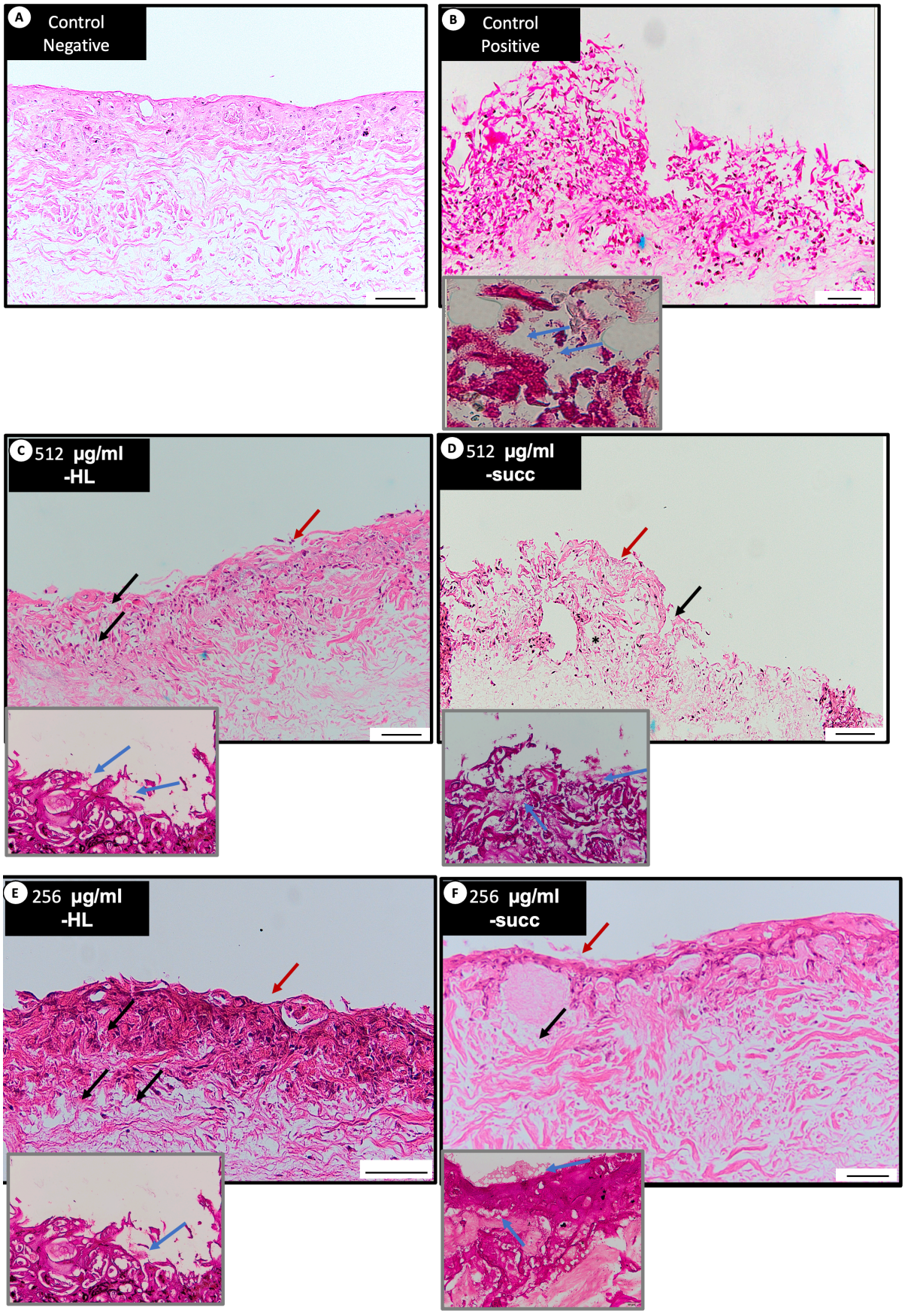
A
Control
Negative
B
Control
Positive
C
512 µg/ml
-HL
D
512 µg/ml
-succ
E
256 µg/ml
-HL
F
256 µg/ml
-succ

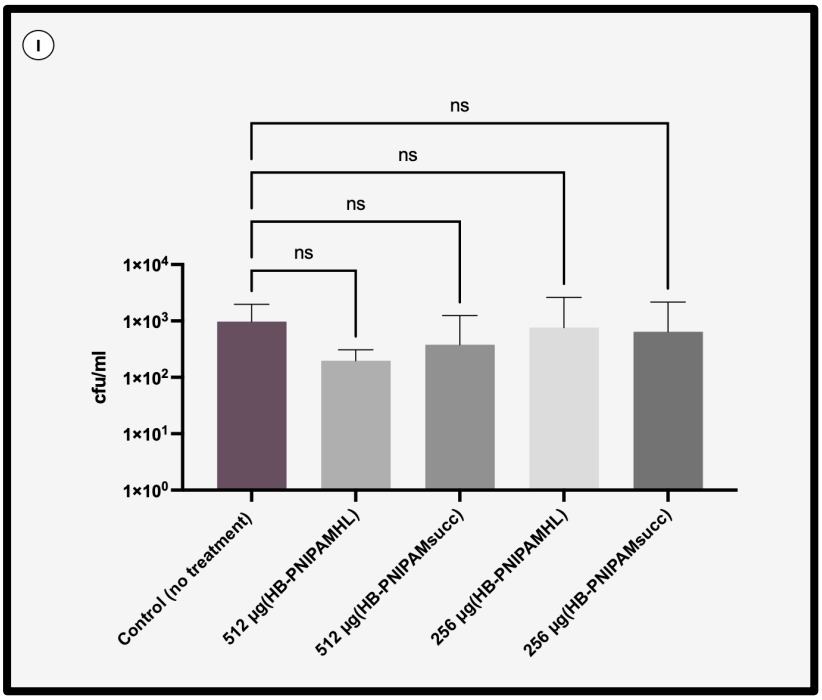

Figure 39: *3D* tissues engineered skin infected with *P.aeruginosa* for 2h and treated with different concentration of HB-PINPA-HL and HB-PNIPAM-succ for 18h

.**(A-H)** shows the histological examination for tissues after processing and stained with H&E and Gram staining for **(A)** The untreated and not infected (control negative) **(B)** The untreated infected with *P.aeruginosa* (positive control) **(C)** Infected and treated with 512 µg/ml HB-PNIPAM-HL.**(D)** Infected and treated with 512 µg/ml HB-PNIPAM-succ. **(E)** Infected and treated with 256 µg/ml HB-PNIPAM-HL **(F)** Infected and treated with 256 µg/ml HB-PNIPAM-succ. (Black arrow) shows destruction within the epidermis, (orange arrows) show destruction on the surface of the epidermis, (blue arrows) indicate to *P.aeruginosa* within models after Gram staining **(I)** The graph showed the quantitively data from the Miles and Misra (M&M) showing the CFU number in each samples. The magnification power= X10 and the scale bar = 100µm. (n=3) Experimental data are expressed as mean ± standard deviation. Significance was determined using one-way ANOVA analysis of variance with Dunnett test in prism (version 9.3.1) ns-not significant. Error bars= SD. (Full ANOVA Results can be found in **Appendix 13**).

4.2.2 Treatment with both HB-PNIPAM-HL and HB-PNIPAM-succ after 24h of infection resulted in no significant effect with a complete loss of epidermal keratinocytes.

After applying 100 µl of HB-PNIPAM-HL or -succ and PBS for the control after 24h of infection, measured differences in destruction between samples were insignificant, with a complete loss of the epidermal keratinocytes in all samples and severe destruction of the dermal (**Figure 41, A**). The destruction is still severed even with treatment with higher concentration (5 mg) of the polymers HB-PNIPA-HL and HB-PNIPAM-succ. Viable bacteria (CFU) were

decreased signifyingly in the samples treated with 5 mg, 512 and 256 μg/ml of HB-PNIPAM-HL and 512 μg/ml of HB-PNIPAM-succ . However, this decreased CFU count did not result in less destruction, which leads to speculation that the lost CFU in the previous samples is due to technical limitation due to the severity of the tissue destruction when processing them (42h total infection period) (**Figure 41, A&C**).

Gram Staining
H &E Staining
X40
X20
X10
Control negative (no infection no treatment)
Control Positive (infected with no treatment)
5mg/ml HBPINPAMHL
5mg/ml HBPINPAMsucc
512µm/ml HBPINPAMHL
512µm/ml HBPINPAMsucc
256µm/ml HBPINPAMHL
256µm/ml HBPINPAmsucc

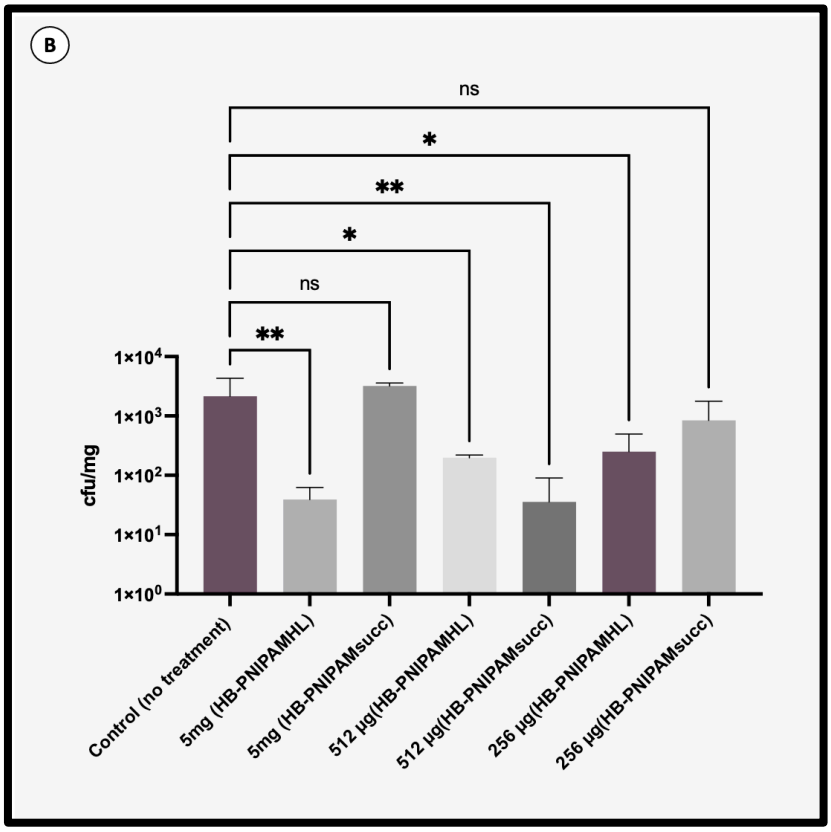

Figure 40: 3D tissues engineered skin infected with *P.aeruginosa* for 24h and treated with different concentration of HB-PINPA-HL and HB-PNIPAM-succ for another 24h.
(A) Tissues after processing and stained with H&E and Gram staining. **(B)** The graph showed the quantitively data from the Miles and Misra (M&M) showing the CFU number in each samples. The magnification power and the scale bar = 100µm. (n=2) Experimental data are expressed as mean ± standard deviation. Significance was determined using one-way ANOVA analysis of variance with Dunnett test in prism (version 9.3.1) *,*P*=0.05 **,*P*= 0.005,and ns-not significant. Error bars= SD. (Full ANOVA Results can be found in **Appendix 13**).

5. Discussion

In this chapter, the effect of the polymer HB-PNIPAM-HL on two types of human skin cells, HDF and HaCat, was first investigated to evaluate the cytotoxicity of the polymer. This cytotoxicity test is used to test the presence of cytotoxic effects of the polymers to evaluate their safety for topical application. The test was performed using the Presto Blue™ Cell Viability Reagent, a ready-to-use reagent that can be used to rapidly assess the viability and proliferation of various cell types. The Presto Blue™ reagent is rapidly consumed by

metabolically active cells and allows quantifiable assessment of viability and cytotoxicity. As shown in **(Figure 36),** we investigate the cytotoxicity of HB-PNIPAM-HL and HB-PNIPAM -succ on HaCat and HDF using Presto Blue^{TM} at different concentrations (256 and 512 μg/ml). Our results in (**Figure 36, A &B**) showed that HB-PNIPAM-HL and HB-PNIPAM-succ had no significant cytotoxic effects on both types of cells, HDF and HaCat after treatment for 24h.

Another investigation carried out in this chapter is the wound healing test. This involves the two questions of whether or not the polymer has healing properties. And whether the polymer can interfere with the wound healing process. To this end, we used a migration assay that mimics the *in vivo* healing process (Liang *et al*., 2007). Two concentrations were tested, 256 and 512 μg/ml of the two polymers HB-PNIPAM-HL and HB-PNIPAM-succ. In (**Figure 37**) it can be seen that only after treatment with HB-PNIPAM-succ at the concentration of 512 μg/ml, the migration of fibroblasts was impaired when observed after 42 hours. One possible explanation could be that higher concentrations of the polymer is slightly cytotoxic to fibroblasts. In (Cooperstein and Canavan, 2013) it was found that PNIPAM polymers, unlike NIPAM monomers, are not cytotoxic. However, in (Yogev *et al*., 2019) the cytotoxicity of four Thermoresponsive polymers was compared, including PNIPAM, which was found to have a cytotoxic effect on fibroblasts. It has been suggested that this cytotoxicity may be due to the monomer NIPAM, which is left over from the production of PNIPAM (Wadajkar *et al*., 2009). Here we propose that the impaired migration of fibroblasts treated with 512 μg/ml observed could be influenced by the presence of traces of toxic impurities in our HB-PNIPAM-succ influencing this delay. It is worth noting that the wound healing process is more complex and involves several steps (Velnar *et al*., 2009).

The results in **Figure 36** show that the healing rate for both polymers on keratinocytes was not significantly increased or decreased compared to the untreated control. The same result

can be observed with fibroblasts, except in the case of the sample treated with HB-PNIPAM-succ.

Our current migration test dealt with the migration behaviour only in keratinocytes or fibroblasts. In future research, it may be possible to use different wound healing tests where more complex healing processes can take place, such as the 3D wound healing model mentioned in (Macneil *et al*., 2011b). Briefly, two stainless steel rings of different sizes are placed on a DED with the smaller ring inserted into the larger ring. Both keratinocytes and fibroblasts are seeded into the gap between the two rings to form a donut shape. The migration of the cells into the centre of the construct is monitored, for example, by staining the construct with MTT, and observed until the wound has closed. This assay allows for the joint migration of keratinocytes and fibroblasts, which should be closer to the healing process *in vivo*. Another area for further investigation is to study the supernatant of treated and untreated *P.aeruginosa* with the polymers on cell migration rates such as the one proposed in (Jacobsen *et al*., 2012). Burns are a very common health problem, and burns are prone to infection with *P. aeruginosa* (Elmassry *et al*., 2020). Therefore, the study was moved to a more complex and challenging setting, namely an infected 3D tissue-engineered skin model. The similarity between the 3D skin model and the structural features of human skin, including the similarity of the barriers and the layered epidermis (Shepherd *et al*., 2009). A 3D skin model, compared to a 2D culture, provides a better investigative model to predict clinical outcomes of treatment more accurately with the polymers tested. 2D culture lacks the oxygen/nutrient gradient and physiological cellular functions that a 3D skin model offers (Randall *et al*., 2018). The 3D skin model can be an excellent in vitro research tool for disease processes, treatments, and diagnostic technologies (Teimouri *et al*., 2018).

Both polymers - HL and -succ - were studied in a 3D skin model in two treatment periods; the first was after 2 hours of infection with *P.aeruginosa,* the other after 24 hours of

infection. The rationale behind the two time periods was to obtain data that would indicate the optimal dosage/time for treatment with the polymers. Treatment with the HB-PNIPAM-HL resulted in reduced destruction after 2 hours of infection compared to the control positive. This positive effect of HB-PNIPAM-HL can be suggested to be connected with the reduced production of tissue-destroying enzymes (LasA and LasB) **(Chapter 3, section 4.1**). Jeffery Marano *et al*. (2015) compared the effects of secreted enzymes such as LasA and LasB in the supernatant between a wild-type *P.aeruginosa* strain and a double mutant lacking the *lasR* and *rhlR* genes. They found that strains lacking the quorum sensing genes prevent the inhibitory effect of extra secreted *P.aeruginosa* on keratinocyte cells. A review by Lee and Zhang (2015a) highlighted the key role of LasA and LasB in the pathogenesis of *P. aeruginosa.* In our late infection model (***section 4.3.2***), no positive results were observed after 24 hours of treatment even with increase concentration (X10) of both HB-PNIPAM-HL and HB-PNIPAM-succ (5 mg). This may indicate that the polymers have a preventive rather than a curative and treatment effect. In contrast to HB-PNIPAM-HL, HB-PNIPAM -succ did not perform as well at higher concentrations in terms of lower destruction. This could be due to the negative effect of the polymer shown in (**section 4.2**).

Furthermore, the number of CFU/mg did not correlate with less tissue destruction in the model treated after 24 hours. This shows that the skin model used here is might not be able to contain a *P.aeruginosa* PAO1 at the initial CFU inoculated for ~42h. This is also confirmed by the condition of the skin model before the histological processes were performed.

In Shepherd *et al*. (2009), using a similar model to the one used in (**section 4.3.2**), showed that *P.aeruginosa* could infect the model at least for 72h. However, a different *P.aeruginosa* strain (som-1) was used, which could explain the result in **(Figure 41),** which did not last up to 72 hours.

7. Summary of Chapter 4 Findings

6.1 256 and 512 μg/ml concentrations of the polymers HB-PNIPAM-HL and HB-PNIPAM-succ were not toxic to mammalian cells tested (Fibroblasts and HaCat).

6.2 Wound healing assay in the presence of different concentration of polymers (256 and 512 μg/ml), HB-PNIPAM-HL and HB-PNIPAM-succ showed that the polymer did not affect the migration of either cell line, HDF and HaCat, except for HB-PNIPAM -succ at the concentration of 512 μg/ml concentration of HB-PNIPAM -succ.

6.3 Treatment with 256 and 512 μg/ml HB-PNIPAM-HL and 256 μg/ml HB-PNIPAM-succ after 2 hours of infection in a 3 D tissue engineered model infected with *P.aeruginosa* PAO1 resulted in less tissue destruction of the 3D tissue engineered model.

6.4 Treatment with HB-PNIPAM-HL and HB-PNIPAM -succ at doses of 5 mg, 256 and 512 g/ml after 24 hours of infection in a 3D tissue culture model infected with P.aeruginosa PAO1 did not improve infection outcomes (i.e., reduced destruction of skin and dermis) compared to the control group in which the model construct was completely destroyed.

Chapter 5: General Discussion and Future Work

5.1 Thesis overview

QS-mediated infectious diseases and the potential of using anti-QS compounds have been the focus of many biomedical studies in recent decades (see **Chapter 1, section 8.1 and 9**). This has been especially for the treatment of Gram-negative infections . Therefore, the search for alternative strategies to combat bacterial infections is necessary. Bacterial quorum sensing (QS) has become a promising target for infection control in recent years (Whiteley *et al*., 2017). Control of the QS regulon offers the possibility of controlling multiple VFs simultaneously, which, when QS is disrupted, inhibit the regulated VFs (K Bhardwaj *et al*., 2013). Allowing the host's defence mechanism to eliminate attenuated bacteria or significantly enhance the effect of antibiotics administered simultaneously (Santhakumari and Ravi, 2019).

This project aims to add to the existing anti- QS compounds developed that target the Gram-negative QS systems with our polymer HB-PNIPAM-HL and -succ that showed great anti-QS ability against *P.aeruginosa.* Unlike other well-known anti- QS such as costly antibodies (Kaufmann *et al*., 2008) that target QS components and cytotoxic halogens (Borchardt *et al*., 2001), our polymer offers a great tool to fight infection.

This project is an extension of the work (Shepherd *et al*., 2019) describing the highly branched polymer poly(N-isopropylacrylamide) (HB-PNIPAM) functionalised with a homoserine lactone ring (- HL) (see **Chapter 2, section 2.1.1**) as a novel QS inhibitor and its anti- QS activity in a *Chromobacterium violaceum* QS biosensor assay. The first goal in this project was to confirm and extend the results of this work. Therefore, the same reporter was used, the Gram-negative bacterium *Chromobacterium violaceum* CV026. *C. violaceum* produces violacein, a purple pigment, when QS is activated, making it an excellent reporter for screening compounds against QS (Manner and Fallarero, 2018). The CviR-dependent quorum sensing pathway regulates the production of the violacein pigment in CV026 (Mcclean *et al*., 1997).

Therefore, inhibition of pigment production suggests disruption of the AHL-driven QS process (Husain *et al*., 2019). In various screenings of anti- QS substances, the CV026 biosensor is used as the first step to test the anti QS activity. The biosensor not only provides a binary determination of the anti- QS, but also indicates the intensity, i.e. how strongly the violet pigment is inhibited (McClean *et al*., 1997a).

In this project we tested the effects of different concentrations of HB-PNIPAM-HL on the QS of *C. violaceum* CV026 were measured. This approach led to the identification of an effective concentration of HB-PNIPAM-HL that can inhibit the activation of QS in *C. violaceum* CV026 with minimal effect on viability . Since violacein production is encoded by the operon *vioABCDE*, which is regulated by the QS system (*cviI* and *cviR*) in *C.violaceum* (Antônio and Creczynski-Pasa, 2004) gene expression for the pigment genes and the luxR homologue, *cviR*, in *C.violaceum* CV026 was studied using RT-qPCR. All genes examined (*vioA, vioC, vioD* and *cviR)* showed a significant reduction in expression in the samples treated with 128 μg/ml HB-PNIPAM-HL

Chapter 3 moves onto *Pseudomonas aeruginosa* PAO1, a pathogen with well-defined QS pathways. As mentioned in the introduction, infection with *Pseudomonas aeruginosa* would greatly benefit from alternative treatment with a novel mode of action, as *P. aeruginosa* is reported to have increasing rates of resistance worldwide (Pang *et al*., 2019). The step of testing anti- QS compounds on *P. aeruginosa* after screening on *C. violaceum* is well documented in the literature, which encouraged us to test our polymer on *P. aeruginosa*, starting with the concentration that showed the most significant inhibition of violacein in *C. violaceum*. Moreover, many QSI have been discovered that inhibit the activity of QS in both bacteria, such as Forsythia suspense (Zhang and Chu, 2017), Psidium guajava (Vasavi *et al*., 2014), flavonoid (Liu *et al*., 2017), Melaleuca bracteata (Wang *et al*., 2019) and terpinen-4-ol found in tea tree plants (Noumi *et al*., 2018). Starting at the effective concentration of HB-

PNIPAM-HL on *C. violaceum* CV026 for the suppression of certain aspects of QS in the opportunistic pathogen *Pseudomonas aeruginosa* was measured (**Chapter3**), demonstrating that HB-PNIPAM-HL was able to supress several important VFs. VFs studied include protease LasA and elastase LasB, which are secreted by *P. aeruginosa* and promote tissue destruction (Sun *et al*., 2020) and the ability to evade immune cells (Park *et al*., 2000). Rhamnolipids, a surfactant produced by *P. aeruginosa* known to promote bacterial penetration into host cells during the initial phase of infection (Zulianello *et al*., 2006). Pyocyanin, a pigment produced by *P.aeruginosa* in the host that promotes a cytotoxic effect through the production of free radicals (Hall *et al*., 2016) (**Chapter3, Figure 27, A-J)**. In addition to the secreted VFs, the effect of HB-PNIPAM-HL on biofilm formation was also investigated. The result in **Chapter3, Figure 28** shows a reduced biofilm attachment onto the coverslips at a polymer concentration of128 and 256 μg/ml. The effect of treatment with HB-PNIPAM-HL at 256 μg/ml was studied on the gene expression of the genes of the QS systems and compared with the untreated samples and the "control" HB-PNIPAM -succ, which lacked the HL endings. Gene expression for the genes *lasR* and *rhlI* of the QS systems, in *P.aeruginosa* was significantly down-regulated in the presence of HB-PNIPAM-HL. The expression of QS genes, *lasR, rhlI*, and *rhlR*, and VFs genes *rhlA, PhzH*, *lasA* was also downregulated in samples treated with HB-PNIPAM-succ **(Chapter3, Figure 29).** For the QS genes, it was observed that the HB-PNIPAM-HL and HB-PNIPAM-succ effectively target the *rhl* system genes. This is also reflected in the effective down-regulation of the pyocyanin gene (*PhzH*) and rhamnolipids (*rhlA*), which are under the down-regulation of the *rhl* system (Lee and Zhang, 2015a). Many anti-QS genes were found to target the *rhl* system. These QS include meta-bromothiolactone (O'Loughlin *et al*., 2013) and tannic acid. (Naik and Mahajan, 2013). The expression of four important VFs were examined in *P. aeruginosa* encoding rhamnolipids (*rhlA*), pyocyanin (*PhzH*), protease LasA (*lasA*) and elastin LasB (*lasB*). Although *lasI* was not significantly downregulated in the samples treated

with HB-PNPAM-HL, *lasA* expression was downregulated and correlates with the downregulation of *lasR*, which is its transcriptional activator (Storey *et al*., 1998). *lasA* was downregulated by HB-PNIPAM-HL and -succ by 3-fold and 6-fold of reduction respectively. *rhlA* was downregulated by 3-fold reduction , for samples treated with HB-PNIPAM-HL and by 6-fold reduction in samples treated with HB-PNIPAM-succ. The pyocyanin gene *PhzH* the reduction in samples treated with -HL and -succ was 5 and 10. This highlights the fact that the anti- QS effect of the polymer may not be due to the ending alone, but rather to HB-PNIPAM with -succ. There is little literature on succinimide as an anti-QS. Recently, however, succinimide derivatives developed by (Konstantinović *et al*., 2020) were tested for their anti-virulence activity on *P. aeruginosa* and showed activity against secreted elastase LasB, which is regulated by QS. Furthermore, comparison via an exploratory RNA-seq study (n=1) between HB-PNIPAM-HL and HB-PNIPAM-succ has a similar anti-QS effect as observed with HB-PNIPAM-HL.

In **Chapter 4,** the cytotoxic effect of HB-PNIPAM-HL and HB-PNIPAM-succ at doses of 256 and 512 μg/ml on a monolayer of HDF and HaCat was investigated, showing no cytotoxic effect in either cell line. This is important to investigate because a similar highly branches polymer developed by (Hopkins *et al*., 2007) can cross the membrane of eukaryotic cells, so investigating the polymers for cytotoxic effect is important. Another study conducted in this chapter is the wound healing assay. Epithelial wound closure is required for skin tissue repair and physical barrier restoration (Werner *et al*., 2007). The migration assay was an attempt to obtain more information on whether or not the polymer can interfere with this natural healing process (Li *et al*., 2013). To this end, we investigated the rate of cell migration using a scratch assay (Liang *et al*., 2007) on monolayers of two cell types (HaCat), an immortalised keratinocyte representing keratinocytes in the epidermis of the skin (Liang *et al*., 2007), which have an important function as innate immunity against injury and bacterial

infection (Piipponen *et al*., 2020), and human dermal fibroblasts (HDF), which are naturally occurring in the skin and are responsible for the formation of connective tissue that promotes healing of injuries (Nilforoushzadeh *et al*., 2017). In this wound healing assay, 256 and 512 µg/ml of the two polymers were tested against both cell types to assess any adverse effects on wound healing. There was no significant delay with 256 µg/ml and 512 µg/ml HB-PNIPAM-HL, and 256 µg/ml HB-PNIPAM -succ. However, the 512 µg/ml HB-PNIPAM -succ resulted in a significant delay in wound closure in this assay. As explained in **Chapter 4, Section 5**; migration is an aspect of cell physiology and an important step in healing (Liang *et al*., 2007). The polymer HB-PNIPAM-HL showed that it did not affect this important step, nor did HB-PNIPAM-succ at 256 µg/ml. The investigation was then moved to a more complex and challenging setting, a 3D tissue-engineered skin model. The main objective in **Chapter 4** was to test the anti-QS effect of the polymers HB-PNIPAM-HL and HB-PNIPAM-succ in a 3D model infected with *P.aeruginosa* that can somewhat reflect the physiology and microenvironment of the skin *in vivo*. The heterogeneous cells and extracellular matrix of a 3D model can give a better picture of the action of the polymer in an application, i.e., treating a human skin infection *in vivo.* The effects of treatment with both polymers ending in HL and succ on early (2h) and late (24h) *P.aeruginosa* infection were investigated in a three-dimensional tissue-based wound infection model. These data suggesting a potential positive effect of both polymers ending in HL and succ on early infections, 2h, (reducing tissue destruction) when compared to control after treatment with either 256 or 512 µg/ml for HB-PNIPAM-HL. The observed reduced tissue destruction in tissues treated with the polymer HB-PNIPAM-HL and lower concentration of HB-PNIPAM-succ (256µg/ml) may be associated with the control of VFs production, including elastases, in *Pseudomonas aeruginosa* PAO1 in a 3D skin infection model. Further research should be conducted to investigate the previous

suggestion, such as using *lasA* and *lasB* as well as QS (*lasR*: *rhlR*) mutants of *P. aeruginosa* to compare their effect with that of wild-type *P. aeruginosa* treated with the polymer.

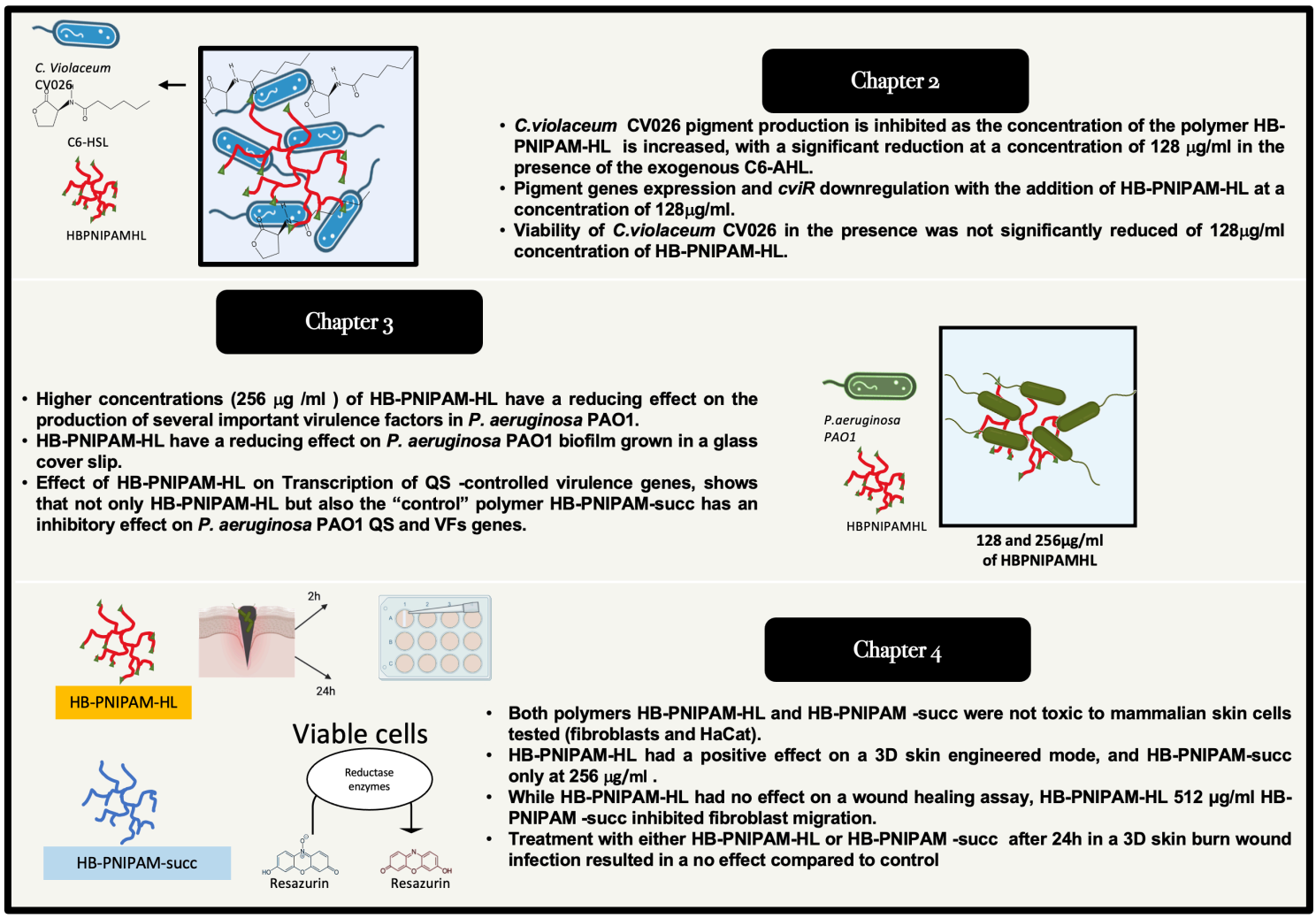

Figure 41: summary of results by Chapter.

Here we have summarised the three chapters of results, starting with Chapter 2 and ending with Chapter 4.

5.2 Potential mechanism of action of HB-PNIPAM-HL and HB-PNIPAM-succ

The results presented here answered several research questions on the evaluation of HB PNIPAM-HL as an inhibitor against QS for Gram-negative bacteria, namely *C. violaceum* and *P. aeruginosa.* In addition, the evaluation of HB-PNIPAM-HL as a treatment for *P. aeruginosa* infections was conducted in a more complex setting, i.e., in a 3D tissue-engineered skin model. Future studies should deepen our understanding of HB-PNIPAM-HL as an anti- QS tool and its mechanism. At this point, there is not sufficient data to pinpoint the exact method of QS

inhibition, however a partial mechanistic picture can be drafted . Several theories can be proposed for the anti- QS ability of the polymers HB-PNIPAM-HL and -succ. The first theory was mentioned in **Section 5, Chapter 3** and summarised in **Figure 43**. Here, it is theorised that the anti QS effect is due to the subinhibitory effect of the polymer, which lowers the quorum of the bacteria and delays the expression of the products of the VFs regulated by HB-PNIPAM-HL. Growth curve calculated as a percentage from the growth curve of *P.aeruginosa* in **Chapter 3, Figure 30**, shows that there was a significant growth delay in samples treated with HB-PNIPAM-HL, HB-PNIPAM -succ. Many compounds have been shown to exert an anti-QS effect on P.aeruginosa, to name but a few cinnamaldehyde (Topa *et al*., 2020), vanillin (Mok *et al*., 2020) ,ibuprofen (Dai *et al*., 2019), curcumin (Bahari *et al*., 2017). However, this could enhance an accompanying anti QS mechanism, such as sequestration of signalling molecules or interaction with the luxR receptor (Theory 2 and 3).

The second theory is based on the that HB-PNIAM-HL is sequestering signal molecules, 'confusing' the bacteria by inferring that a quorum is not reached because there are not enough AHLs in the environment. Polymers sequestering AHLs has been mentioned in the work of Piletska *et al*. (2011) , where the polymer was described as a "passive" control of quorum sensing in *Pseudomonas aeruginosa*. This theory was investigated further by nuclear magnetic resonance (NMR) analysis (see future work in **Chapter 5**). NMR analysis is used to determine the molecular structure, phase changes and configuration changes of the polymer (Krishnan, 2019). The data from NMR analysis could help us confirm or reject the theory that our polymer sequesters AHLs. The last theory also deserves further investigation, although there are some reservations about its feasibility. The theory is that the homoserine lactone (HL) ending actively binds to the receptor inside the bacteria (both bacteria tested have cytoplasmic QS receptors). It is assumed that the improbability of this theory results from the natural resistance of the Gram-negative cell wall to the large size of the polymer.

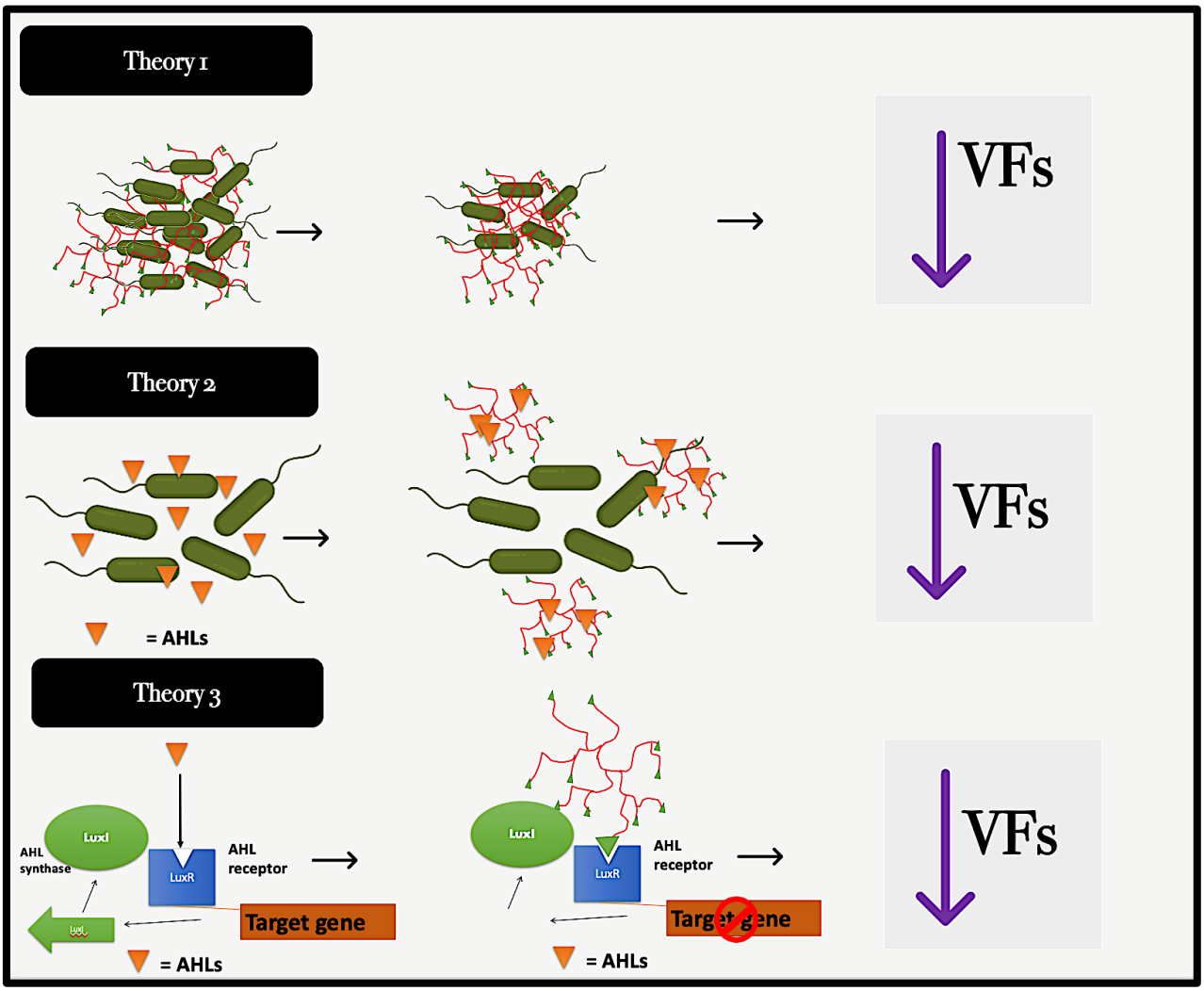

Figure 42: schematic diagram for the possible mechanism of the polymer HB-PNIPAM-HL. We have only discussed three theories here, others could exist, such as influencing the plasma membrane of bacteria, a theory investigated by (Yap *et al*., 2014).

5.4 Future applications of HB-PNIPAM-HL and -succ

In this project, we evaluated the polymers HB-PNIPAM-HL and -succ as a control agent for *P.aeruginosa* (see **Chapter 1, section 6**). All the applications proposed here are derived from **Chapter 4** of this thesis. As shown in **Chapter 4,** the polymers HB-PNIPAM-HL and -succ (256 µg/ml) can only have a positive effect on early infection (2 h). This positive effect can be described as less tissue destruction by *P. aeruginosa.* However, no effect was observed when the infection was well established (treatment after 24 hours) even with higher concentration (5

mg). Considering the continuum of bacterial infection in wound, which characterises the course of infection of a wound proposed by the International Wound Infection Institute in (2016) (Swanson *et al*., 2016) and found in **Figure 44**, this polymer fits perfectly into the early stages of bacterial infection where no intervention is yet prescribed. The hope is that this early intervention with the polymers will not allow progression of the infection and may lead to not needing to use antibiotics or improve their efficacy.

The basic idea of anti QS, as described in (LaSarre and Federle, 2013, Jiang *et al*., 2019), is to give the host immune response a 'head start' by reducing bacterial VFs production . However, this approach excludes patients with a weakened immune system. Combining an antibiotic with an anti- QS could be an effective approach for patients with a weakened immune system. In addition, the anti- QS can be used to indirectly make bacteria more sensitive to antibiotics by reducing biofilm formation. If antibiotics are used in tandem with anti-QS treatments, it should be possible to lower the amount of antibiotic used , an aim in good antimicrobial stewardship. This is supported by published data indicating the synergistic effect of antibiotics and anti- QS agents. Vadekeetil *et al*. (2016) reported the synergistic interaction between the active fraction of proanthocyanidin, an anti- QS and ciprofloxacin against *P. aeruginosa*. Their study showed that ciprofloxacin in combination with the active proanthocyanidin fraction had higher control over *P. aeruginosa* . Chanda *et al*. (2017) showed that linolenic acid and tobramycin significantly inhibited pathogenic secretion and biofilm production in control of *P. aeruginosa* compared with linolenic acid or tobramycin alone. Roudashti *et al*. (2017) also investigated the synergistic efficacy of curcumin with ceftazidime and ciprofloxacin on the *P. aeruginosa* PAO1 signalling system. Their results showed that curcumin, ceftazidime, and ciprofloxacin in combination, can drastically reduce biofilm production. Therefore, we also propose to combine different antibiotics with our polymer,

which was discussed in more detail in the Future Work section, to see what impact this might have, especially in the case of polymicrobial infection.

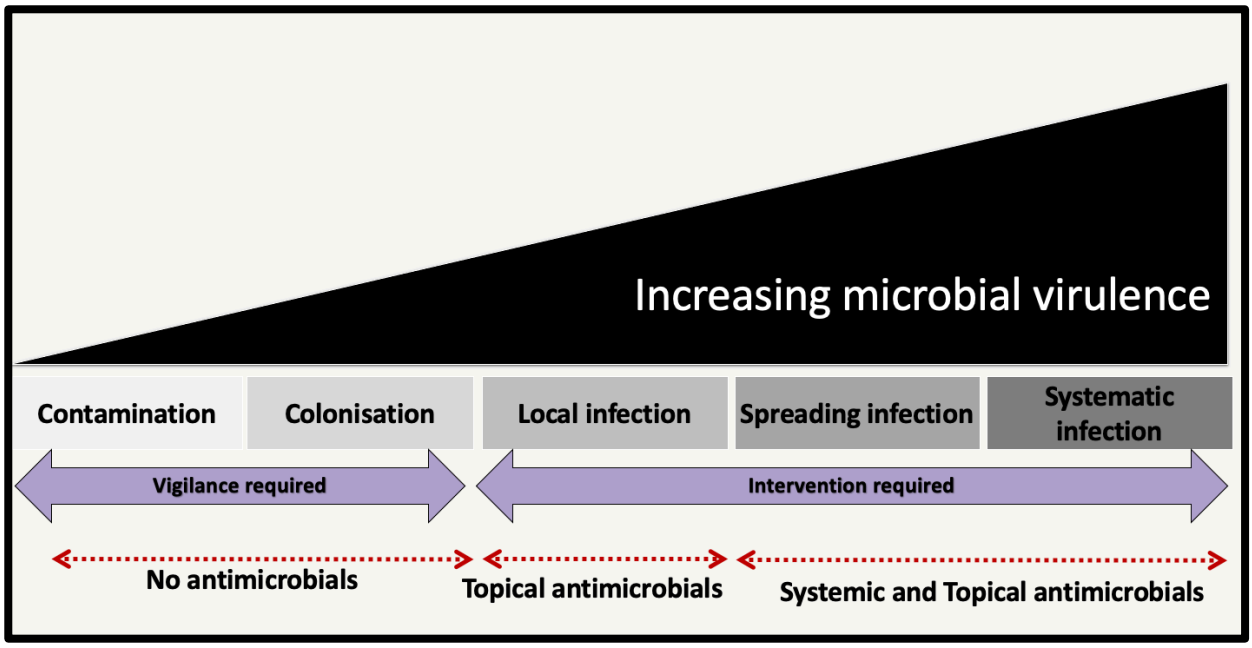

Figure 43: wound Infection Continuum.
It was proposed by The International Wound Infection Institute, which characterises the course of infection of a wound proposed by the International Wound Infection Institute. The image has been adopted and redesigns from (Swanson *et al*., 2016).

5.5 Limitations and challenges of treatments against quorum sensing

As mentioned in **Chapter1, section 7,** anti-QS therapy could be a promising alternative for infection control. However, as with any strategy, there are some limitations and challenges.

5.5.1 QS does not only regulate VFs- (QS is not specific).

Although the role of QS has been highlighted, other processes of microorganisms are also subject to the regulation and action of QS; these include metabolism (DeLisa *et al*., 2001), DNA repair (Yadav *et al*., 2018). The universal signalling molecules (AI2) can be used by commensal microbiomes such as Bifidobacterium (Sun *et al*., 2014) and Lactobacillus (Lebeer *et al*., 2007). Therefore, applying a general anti-QS targeting fatty acid-based signalling molecules could inadvertently negatively affect other beneficial microbiomes by distributing AI2 used by commensal microbiomes (Christiaen *et al*., 2014). Anti-QS distribution to commensal microbiomes prevents them from establishing their niche and producing beneficial

metabolites. This could affect their establishment and cause microbiome imbalance, such as gut dysbiosis (Gagnière *et al*., 2016).

5.5.2 Less QS systems does not mean less virulent.

The loss of a QS system does not mean the bacteria are less contagious. In the case of the *lasR* mutant, the loss of lasR genes did not result in less virulent bacteria. Many reports show that a mutant lasR *P.aeruginosa* exerts more pyocyanin (Cabeen, 2014), motility (Robitaille *et al*., 2020) and production of beta-lactamases (D'Argenio *et al*., 2007) used for antibiotic resistance. Also, attenuation of VFs, such as the use of anti-QS to disrupt a biofilm, could trigger the release of planktonic bacteria, allowing these planktonic bacteria to enter the bloodstream, which could be fatal.

5.5.3 Anti-QS resistance

The notion that anti-QS cannot induce anti-QS formed prior to 2012 when a report of the first case of resistance of the anti-QS compounds in brominated furanones to *P.aeruginosa* by mutation of efflux pumps that exert the anti-QS outside the cell before causing any damage (Maeda *et al*., 2012). This resistance mechanism is similar to antibiotic resistance (Nikaido, 1998).

5.5.3 Immunodeficiency

As mentioned in the future application of the polymer, anti-QS excludes people with weak immune systems. Removal of bacteria and not just attenuation is important to avoid promoting chronic infections in an immunocompromised host.

5.5.5 Mechanistic ambiguity

Many anti-QS do not yet have defined mechanisms to combat QS or phenotypes of QS, such as biofilm.

5.5.6 Many anti-QS are cytotoxic.

An example of these are furans ((Martinelli *et al*., 2004)) and cytotoxic halogens (Borchardt *et al*., 2001).

5.6 Conclusions

1- HB-PNIPAM- HL can significantly reduce the production of violacein at a concentration of 128μg/ml in *C.violaceum* CV026.

2- The same concentration (128 μg/ml) of HB-PNIPAM-HL had no significant effect on the viability of *C.violaceum* CV026.

3- The anti-quorum-sensing effect of HB-PNIPAM-HL can be traced to the molecular level, as it down-regulated the expression of the QS receptor gene *cviR* in *C.violaceum* CV026. Consequently, the expression of the violacein pigment genes (*vioA, vioC* and *vioD*) is downregulated.

4- Higher concentrations (256 μg/ml) of HB-PNIPAM-HL reduce the production of several important virulence factors in *P. aeruginosa* PAO1.

5- HB- PNIPAM-HL reduces biofilm formation of *P. aeruginosa* PAO1.

6- The effect of HB-PNIPAM-HL on the transcription of QS -controlled virulence genes shows that not only HB-PNIPAM-HL, but also the "control polymer" HB-PNIPAM-succ has an inhibitory effect on *P. aeruginosa* PAO1 QS and VFs genes.

7- Concentrations (128 and 256 μg/ml) of the polymers HB-PNIPAM-HL and HB-PNIPAM-succ were not toxic to mammalian skin cells tested (fibroblasts and HaCat).

8- While HB-PNIPAM-HL had no effect on a wound healing assay, 512 μg/ml of HB-PNIPAM -succ inhibited fibroblast migration.

10- Treatment with either 256 and 512 μg/ml HB-PNIPAM-HL or 256 μg/ml HB-PNIPAM -succ , after 2h of infection in a 3D skin burn wound infection resulted in less tissue destruction.

11- Treatment with either HB-PNIPAM-HL or HB-PNIPAM -succ after 24h in a 3D skin burn wound infection resulted in a no effect compared to control.

5.7 Future work

Future research should consider the potential effects of the two polymers HB-PNIPAM-HL and -succ more carefully, for example:

5.7.1 Polymicrobial infection HB-PNIPAM-HL

In this project, the focus was on monocultures (*C.violaceum* CV026 and *P.aeruginosa* PAO1). However, in a natural infection environment, i.e., within the host, a monoculture is unnatural, and the infection environment is often polymicrobial, as mentioned in (**Chapter 1, Section 4**) *S. aureus* and *P. aeruginosa* coexist in polymicrobial biofilms at the same infection site. A burn wound infection, for example, is polymicrobial and contains many microorganisms, including *S. aureus* with a predominance of *P. aeruginosa* (see **Chapter 1, section 6**). For this reason, the effect of the polymer on *P. aeruginosa* should be investigated in coculture with *S. aureus* bacteria. In **Appendix 14**, we conducted a pilot study in which we treated a 3D burn wound model infected with *S.aureus* with a supernatant of from *P.aeruginosa* PAO1 untreated or treated with 256 and 512 µg/ml HB-PINAP-HL for 24 hours. The supernatant was used instead of co-culturing *S.aureus* with *P.aeruginosa* because of the challenge of creating polymicrobial models that replicate the natural niches in which the different bacterial species can generally self-organise and compete within this polymicrobial consortium. The result of the pilot study showed a reduced inhibition of *S.aureus* when incubated with supernatant from *P.aeruginosa* PAO1 treated with polymer compared to the untreated *P.aeruginosa*. This can be explained by the documented effect of the polymer on *P.aeruginosa* on LasA protease expression. LasA protease, a protease produced by *P.aeruginosa* to lyse *S.aureus.* (see **Chapter 1, section 2.3.2**). Future studies are needed to validate these results and to investigate the effect of the polymer on *S.aureus*

5.7.2 Mechanistic studies

As mentioned in **Chapter 5**, a more mechanistic study of the polymer should be undertaken. An understanding of the mechanism of the polymer would be beneficial to better understand the possibility of resistance development. The importance of this knowledge is discussed in more detail in the next point. In **Chapter 5, section 5.3**, three theories were discussed. Samples incubated with different concentrations of the polymer were sent along with external AHLs to measure whether the polymer absorbs the AHL signal (awaiting result data).

5.7.3 HB-PNIPAM-HL and -succ and development of resistance

Investigating the possibility of resistance to the polymer may provide a more comprehensive approach to infection control through HB-PINAPM-HL and - succ. Although the QS system has been extensively studied, particularly its role in various bacterial phenotypes, the QS system and the development of resistance is still not fully understood. A review paper by García-Contreras *et al*. (2013) found that there are many pathways through which a bacterium can develop resistance to an anti QS compound. However, to find out how or if bacteria could develop resistance to HB-PNIPAM-HL, the mechanism of the polymer should first be confirmed to better assess the possible pathways of resistance.

5.7.4 Combined therapy with antibiotics

In **Chapter 5, section 5.4;** combination therapy between HB-PNIPAM-HL and different classes of antibiotics was suggested as a future application. In a paper by Murray *et al*. (2022) it was found that *S. aureus* in a mixed biofilm is protected from tobramycin by *P. aeruginosa.* However, the anti QS quinazolinones (QZN), which are only directed against *P. aeruginosa,* in combination with the aminoglycoside tobramycin can also positively influence the elimination of *S. aureus* in mixed biofilms. For this reason, and because a polymicrobial environment has been proposed to further challenge the polymer, a future direction would be to combine HB-

PNIPAM-HL with tobramycin as in the previous study and measure responses to different concentrations of both therapeutics in a dose-response matrix.

5.7.5 The administration of multiple dosage of the polymer

As shown in **Chapter 4**, **section 4.2.2**; the polymers HB-PNIPAM-HL and HB-PNIPAM-succ had no obvious effects on attenuating tissue destruction in late infection. One explanation for this is that the concentration of the polymers used is below the threshold level, as the bacteria are free to develop their virulence, which is in line with (Kalia *et al*., 2014). Resistance to, or inactivation of an anti QS treatment is possible. Here we propose to counteract this by introducing the polymer into the infection in multiple doses and ensuring that the concentration of the polymer is high enough to maintain its effect until the infection is overcome. However, this could be challenging in a 3D skin model, as it would be difficult to maintain the model beyond 48 hours due to tissue destruction which occurs rapidly since there is no vasculature or immune cells in this model. Furthermore, an experimental expansion of the migration assay (Scratch assay) could be attempted using the ring wound healing described in (MacNeil *et al*., 2011a) which proved superior to the Scratch assay.

5.8 Concluding Statement

HB-PNIPAM-HL and HB-PINPAM-succ show promising anti- QS properties by reducing the virulence and pathogenicity of *P.aeruginosa,* resulting in less tissue destruction in a human skin infection model. The polymer could be considered as an alternative to conventional antibiotics as a promising non-antibiotic therapy for wound infections. However, studies are still needed to determine the mechanism of action and further clinical investigations are required to validate the use of HB-PNIPAM-HL in humans.

5.9 Covid Impact

Due to the SARS-CoV-2 outbreak, I, like many of my fellow students, had difficulty getting into the labs when the University of Sheffield closed for teaching and research at the end of

March 2020 and reopened in September 2020 with limited capacity of only about 50% and time restrictions on bookings. The restrictions on laboratories were not fully lifted until September 2021. Several aspects of the work were affected by this restriction, especially the time restrictions (end of year 3 when the restriction was lifted).

References

ADONIZIO, A. L., DOWNUM, K., BENNETT, B. C. & MATHEE, K. 2006. Anti-quorum sensing activity of medicinal plants in southern Florida. *Journal of ethnopharmacology,* 105**,** 427-435.

AHMED, S. A., RUDDEN, M., SMYTH, T. J., DOOLEY, J. S., MARCHANT, R. & BANAT, I. M. 2019. Natural quorum sensing inhibitors effectively downregulate gene expression of Pseudomonas aeruginosa virulence factors. *Applied microbiology and biotechnology,* 103**,** 3521-3535.

ALLESEN-HOLM, M., BARKEN, K. B., YANG, L., KLAUSEN, M., WEBB, J. S., KJELLEBERG, S., MOLIN, S., GIVSKOV, M. & TOLKER-NIELSEN, T. 2006. A characterization of DNA release in Pseudomonas aeruginosa cultures and biofilms. *Molecular microbiology,* 59**,** 1114-1128.

ALMEIDA, F. A. D., CARNEIRO, D. G., DE OLIVEIRA MENDES, T. A., BARROS, E., PINTO, U. M., DE OLIVEIRA, L. L. & VANETTI, M. C. D. 2018. N-dodecanoyl-homoserine lactone influences the levels of thiol and proteins related to oxidation-reduction process in Salmonella. *PLOS ONE,* 13**,** e0204673.

ANDERL, J. N., FRANKLIN, M. J. & STEWART, P. S. 2000. Role of antibiotic penetration limitation in Klebsiella pneumoniae biofilm resistance to ampicillin and ciprofloxacin. *Antimicrobial agents and chemotherapy,* 44**,** 1818-1824.

ANGUIGE, K., KING, J. & WARD, J. 2005. Modelling antibiotic-and anti-quorum sensing treatment of a spatially-structured Pseudomonas aeruginosa population. *Journal of mathematical biology,* 51**,** 557-594.

ANGUS, B. L., CAREY, A. M., CARON, D. A., KROPINSKI, A. & HANCOCK, R. 1982. Outer membrane permeability in Pseudomonas aeruginosa: comparison of a wild-type with an antibiotic-supersusceptible mutant. *Antimicrobial agents and Chemotherapy,* 21**,** 299-309.

ANTÔNIO, R. V. & CRECZYNSKI-PASA, T. B. 2004. Genetic analysis of violacein biosynthesis by Chromobacterium violaceum. *Genet Mol Res,* 3**,** 85-91.

ARTHUR, M., BRISSON-NOËL, A. & COURVALIN, P. 1987. Origin and evolution of genes specifying resistance to macrolide, lincosamide and streptogramin antibiotics: data and hypotheses. *Journal of antimicrobial chemotherapy,* 20**,** 783-802.

ASFAHL, K. L. & SCHUSTER, M. 2018. Additive effects of quorum sensing anti-activators on Pseudomonas aeruginosa virulence traits and transcriptome. *Frontiers in microbiology,* 8**,** 2654.

ASHRAF, S., PARK, H.-K., PARK, H. & LEE, S.-H. 2016. Snapshot of phase transition in thermoresponsive hydrogel PNIPAM: Role in drug delivery and tissue engineering. *Macromolecular Research,* 24**,** 297-304.

AUGUST, P. R., GROSSMAN, T. H., MINOR, C., DRAPER, M., MACNEIL, I. A., PEMBERTON, J. M., CALL, K., HOLT, D. & OSBURNE, M. S. 2000a. Sequence analysis and functional characterization of the violacein biosynthetic pathway from Chromobacterium violaceum. *Journal of molecular microbiology and biotechnology,* 2**,** 513-519.

AUGUST, P. R., GROSSMAN, T. H., MINOR, C., DRAPER, M. P., MACNEIL, I. A., PEMBERTON, J. M., CALL, K. M., HOLT, D. & OSBURNE, M. S. 2000b. Sequence analysis and functional characterization of the violacein biosynthetic pathway from Chromobacterium violaceum. . *Journal of molecular microbiology and biotechnology***,** pp.513-519.

BAE, J., OH, E. & JEON, B. 2014. Enhanced transmission of antibiotic resistance in Campylobacter jejuni biofilms by natural transformation. *Antimicrobial agents and chemotherapy,* 58**,** 7573-7575.

BAE, Y. H., OKANO, T. & KIM, S. W. 1991. "On–Off" thermocontrol of solute transport. I. Temperature dependence of swelling of N-isopropylacrylamide networks modified with hydrophobic components in water. *Pharmaceutical research,* 8**,** 531-537.

BAHARI, S., ZEIGHAMI, H., MIRSHAHABI, H., ROUDASHTI, S. & HAGHI, F. 2017. Inhibition of Pseudomonas aeruginosa quorum sensing by subinhibitory concentrations of curcumin with gentamicin and azithromycin. *Journal of global antimicrobial resistance,* 10**,** 21-28.

BALES, P. M., RENKE, E. M., MAY, S. L., SHEN, Y. & NELSON, D. C. 2013. Purification and characterization of biofilm-associated EPS exopolysaccharides from ESKAPE organisms and other pathogens. *PloS one,* 8**,** e67950.

BARR, H. L., HALLIDAY, N., CÁMARA, M., BARRETT, D. A., WILLIAMS, P., FORRESTER, D. L., SIMMS, R., SMYTH, A. R., HONEYBOURNE, D. & WHITEHOUSE, J. L. 2015. Pseudomonas aeruginosa quorum sensing molecules correlate with clinical status in cystic fibrosis. *European Respiratory Journal,* 46**,** 1046-1054.

BASSLER, B. L. 2002. Small talk: cell-to-cell communication in bacteria. *Cell,* 109**,** 421-424.

BASSLER, B. L., WRIGHT, M., SHOWALTER, R. E. & SILVERMAN, M. R. 1993. Intercellular signalling in Vibrio harveyi: sequence and function of genes regulating expression of luminescence. *Molecular microbiology,* 9**,** 773-786.

BJARNSHOLT, T. 2013. The role of bacterial biofilms in chronic infections. *Apmis,* 121**,** 1-58.

BOLES, B. R., THOENDEL, M. & SINGH, P. K. 2005. Rhamnolipids mediate detachment of Pseudomonas aeruginosa from biofilms. *Molecular microbiology,* 57**,** 1210-1223.

BONOMO, R. A. & SZABO, D. 2006. Mechanisms of multidrug resistance in Acinetobacter species and Pseudomonas aeruginosa. *Clinical infectious diseases,* 43**,** S49-S56.

BORCHARDT, S., ALLAIN, E., MICHELS, J., STEARNS, G., KELLY, R. & MCCOY, W. 2001. Reaction of acylated homoserine lactone bacterial signaling molecules with oxidized halogen antimicrobials. *Appl. Environ. Microbiol.,* 67**,** 3174-3179.

BRACKMAN, G. & COENYE, T. 2015. Quorum sensing inhibitors as anti-biofilm agents. *Current pharmaceutical design,* 21**,** 5-11.

BRINKLOV, S., KALKO, E. K. V. & SURLYKKE, A. 2009. Intense echolocation calls from two 'whispering' bats, *Artibeus jamaicensis* and *Macrophyllum macrophyllum* (*Phyllostomidae*). *Journal of Experimental Biology,* 212**,** 11-20.

BRINT, J. M. & OHMAN, D. E. 1995. Synthesis of multiple exoproducts in Pseudomonas aeruginosa is under the control of RhlR-RhlI, another set of regulators in strain PAO1 with homology to the autoinducer-responsive LuxR-LuxI family. *Journal of bacteriology,* 177**,** 7155-7163.

BRITO, N., FALCON, M., CARNICERO, A., GUTIERREZ-NAVARRO, A. & MANSITO, T. 1989. Purification and peptidase activity of a bacteriolytic extracellular enzyme from Pseudomonas aeruginosa. *Research in microbiology,* 140**,** 125-137.

BRODERICK, A. H., STACY, D. M., TAL-GAN, Y., KRATOCHVIL, M. J., BLACKWELL, H. E. & LYNN, D. M. 2014. Surface Coatings that Promote Rapid Release of Peptide-Based AgrC Inhibitors for Attenuation of Quorum Sensing in Staphylococcus aureus. *Advanced healthcare materials,* 3**,** 97-105.

BUSTIN, S. & HUGGETT, J. 2017. qPCR primer design revisited. *Biomolecular detection and quantification,* 14**,** 19-28.

BUSTIN, S. A., BENES, V., GARSON, J. A., HELLEMANS, J., HUGGETT, J., KUBISTA, M., MUELLER, R., NOLAN, T., PFAFFL, M. W. & SHIPLEY, G. L. 2009. The MIQE Guidelines: M inimum I nformation for Publication of Q uantitative Real-Time PCR E xperiments. Oxford University Press.

CABEEN, M. T. 2014. Stationary phase-specific virulence factor overproduction by a lasR mutant of Pseudomonas aeruginosa. *PLoS One,* 9**,** e88743.

CABRERA-BENÍTEZ, N. E., PÉREZ-ROTH, E., RAMOS-NUEZ, Á., SOLOGUREN, I., PADRÓN, J. M., SLUTSKY, A. S. & VILLAR, J. 2016. Inhibition of endotoxin-induced airway epithelial cell injury by a novel family of pyrrol derivates. *Laboratory Investigation,* 96**,** 632-640.

CABROL, S. G. N., OLLIVER, A., PIER, G. B., ANDREMONT, A. & RUIMY, R. 2003. Transcription of Quorum-Sensing System Genes inClinical and Environmental Isolates of Pseudomonasaeruginosa. *Journal of bacteriology,* 185**,** 7222-7230.

CAO, J.-G. & MEIGHEN, E. 1989. Purification and structural identification of an autoinducer for the luminescence system of Vibrio harveyi. *Journal of Biological Chemistry,* 264**,** 21670-21676.

CASE, R. J., LABBATE, M. & KJELLEBERG, S. 2008. AHL-driven quorum-sensing circuits: their frequency and function among the Proteobacteria. *The ISME Journal,* 2**,** 345.

CASILAG, F., LORENZ, A., KRUEGER, J., KLAWONN, F., WEISS, S. & HÄUSSLER, S. 2016. The LasB elastase of Pseudomonas aeruginosa acts in concert with alkaline protease AprA to prevent flagellin-mediated immune recognition. *Infection and immunity,* 84**,** 162-171.

CASTRIC, P. A., EBERT, R. F. & CASTRIC, K. F. 1979. The relationship between growth phase and cyanogenesis inPseudomonas aeruginosa. *Current Microbiology,* 2**,** 287-292.
CAVALEIRO PHD, E., DUARTE PHD, A. S., ESTEVES PHD, A. C., CORREIA PHD, A., WHITCOMBEPHD, M. J., PILETSKA PHD, E. V., PILETSKY PHD, S. A. & CHIANELLA PHD, I. 2015. Novel linear polymers able to inhibit bacterial quorum sensing. *Macromolecular bioscience,* 15**,** 647-656.
CHANDA, W., JOSEPH, T. P., PADHIAR, A. A., GUO, X., MIN, L., WANG, W., LOLOKOTE, S., NING, A., CAO, J. & HUANG, M. 2017. Combined effect of linolenic acid and tobramycin on Pseudomonas aeruginosa biofilm formation and quorum sensing. *Experimental and Therapeutic Medicine,* 14**,** 4328-4338.
CHEN, F., GAO, Y., CHEN, X., YU, Z. & LI, X. 2013. Quorum quenching enzymes and their application in degrading signal molecules to block quorum sensing-dependent infection. *International journal of molecular sciences,* 14**,** 17477-17500.
CHOO, J., RUKAYADI, Y. & HWANG, J. K. 2006. Inhibition of bacterial quorum sensing by vanilla extract. *Letters in applied microbiology,* 42**,** 637-641.
CHRISTENSEN, D. G. & VISICK, K. L. 2020. Vibrio fischeri: laboratory cultivation, storage, and common phenotypic assays. *Current protocols in microbiology,* 57**,** e103.
CHRISTIAEN, S. E., O'CONNELL MOTHERWAY, M., BOTTACINI, F., LANIGAN, N., CASEY, P. G., HUYS, G., NELIS, H. J., VAN SINDEREN, D. & COENYE, T. 2014. Autoinducer-2 plays a crucial role in gut colonization and probiotic functionality of Bifidobacterium breve UCC2003. *PLoS One,* 9**,** e98111.
CHRZANOWSKI, Ł., ŁAWNICZAK, Ł. & CZACZYK, K. 2012. Why do microorganisms produce rhamnolipids? *World Journal of Microbiology and Biotechnology,* 28**,** 401-419.
CHUGANI, S. & GREENBERG, E. P. 2014. An evolving perspective on the Pseudomonas aeruginosa orphan quorum sensing regulator QscR. *Frontiers in Cellular and Infection Microbiology,* 4**,** 152.
CHURCH, D., ELSAYED, S., REID, O., WINSTON, B. & LINDSAY, R. 2006. Burn wound infections. *Clinical microbiology reviews,* 19**,** 403-434.
CHURCHILL, M. E. & HERMAN, J. P. 2008. Acyl-Homoserine Lactone Biosynthesis: Structure and Mechanism. *Chemical communication among bacteria***,** 273-289.
CHURCHILL, M. E., SIBHATU, H. M. & UHLSON, C. L. 2011. Defining the structure and function of acyl-homoserine lactone autoinducers. *Quorum Sensing.* Springer.
COCHRAN, W. L., MCFETERS, G. A. & STEWART, P. S. 2000. Reduced susceptibility of thin Pseudomonas aeruginosa biofilms to hydrogen peroxide and monochloramine. *Journal of applied microbiology,* 88**,** 22-30.
COÊLHO, D. F., SATURNINO, T. P., FERNANDES, F. F., MAZZOLA, P. G., SILVEIRA, E. & TAMBOURGI, E. B. 2016. Azocasein substrate for determination of proteolytic activity: reexamining a traditional method using bromelain samples. *BioMed Research International,* 2016.
COELHO, P., OLIVEIRA, J., FERNANDES, I., ARAÚJO, P., PEREIRA, A. R., GAMEIRO, P. & BESSA, L. J. 2021. Pyranoanthocyanins Interfering with the Quorum Sensing of Pseudomonas aeruginosa and Staphylococcus aureus. *International journal of molecular sciences,* 22**,** 8559.
COOPERSTEIN, M. A. & CANAVAN, H. E. 2013. Assessment of cytotoxicity of (N-isopropyl acrylamide) and poly (N-isopropyl acrylamide)-coated surfaces. *Biointerphases,* 8**,** 19.
COREHTASH, Z. G., KHORSHIDI, A., FIROOZEH, F., AKBARI, H. & AZNAVEH, A. M. 2015. Biofilm formation and virulence factors among Pseudomonas aeruginosa isolated from burn patients. *Jundishapur journal of microbiology,* 8.
COSTERTON, J. 1984. The formation of biocide-resistant biofilms in industrial, natural, and medical systems. *Developments in Industrial Microbiology,* 25**,** 363-372.
D'ARGENIO, D. A., WU, M., HOFFMAN, L. R., KULASEKARA, H. D., DÉZIEL, E., SMITH, E. E., NGUYEN, H., ERNST, R. K., LARSON FREEMAN, T. J. & SPENCER, D. H. 2007. Growth phenotypes of Pseudomonas aeruginosa lasR mutants adapted to the airways of cystic fibrosis patients. *Molecular microbiology,* 64**,** 512-533.

DAI, L., WU, T.-Q., XIONG, Y.-S., NI, H.-B., DING, Y., ZHANG, W.-C., CHU, S.-P., JU, S.-Q. & YU, J. 2019. Ibuprofen-mediated potential inhibition of biofilm development and quorum sensing in Pseudomonas aeruginosa. *Life sciences,* 237**,** 116947.

DALMONT, H., PINPRAYOON, O. & SAUNDERS, B. R. 2008. Study of pH-responsive microgels containing methacrylic acid: effects of particle composition and added calcium. *Langmuir,* 24**,** 2834-2840.

DAS, T., KUTTY, S. K., KUMAR, N. & MANEFIELD, M. 2013. Pyocyanin facilitates extracellular DNA binding to Pseudomonas aeruginosa influencing cell surface properties and aggregation. *PLoS One,* 8**,** e58299.

DAVEY, M. E., CAIAZZA, N. C. & O'TOOLE, G. A. 2003. Rhamnolipid surfactant production affects biofilm architecture in Pseudomonas aeruginosa PAO1. *Journal of bacteriology,* 185**,** 1027-1036.

DAVIES, D. G., PARSEK, M. R., PEARSON, J. P., IGLEWSKI, B. H., COSTERTON, J. W. & GREENBERG, E. P. 1998. The involvement of cell-to-cell signals in the development of a bacterial biofilm. *Science,* 280**,** 295-298.

DE BENTZMANN, S., POLETTE, M., ZAHM, J.-M., HINNRASKY, J., KILEZTKY, C., BAJOLET, O., KLOSSEK, J.-M., FILLOUX, A., LAZDUNSKI, A. & PUCHELLE, E. 2000. Pseudomonas aeruginosa virulence factors delay airway epithelial wound repair by altering the actin cytoskeleton and inducing overactivation of epithelial matrix metalloproteinase–2. *Laboratory investigation,* 80**,** 209-219.

DE KIEVIT, T. R. & IGLEWSKI, B. H. 2000. Bacterial quorum sensing in pathogenic relationships. *Infection and immunity,* 68**,** 4839-4849.

DEKIMPE, V. & DEZIEL, E. 2009. Revisiting the quorum-sensing hierarchy in Pseudomonas aeruginosa: the transcriptional regulator RhlR regulates LasR-specific factors. *Microbiology,* 155**,** 712-723.

DELISA, M. P., WU, C.-F., WANG, L., VALDES, J. J. & BENTLEY, W. E. 2001. DNA microarray-based identification of genes controlled by autoinducer 2-stimulated quorum sensing in Escherichia coli. *Journal of bacteriology,* 183**,** 5239-5247.

DEZIEL, E., LEPINE, F., MILOT, S. & VILLEMUR, R. 2003. rhlA is required for the production of a novel biosurfactant promoting swarming motility in Pseudomonas aeruginosa: 3-(3-hydroxyalkanoyloxy) alkanoic acids (HAAs), the precursors of rhamnolipids. *Microbiology,* 149**,** 2005-2013.

DÖRING, G., OBERNESSER, H. & BOTZENHART, K. 1981. Extracellular toxins of Pseudomonas aeruginosa. II. Effect of two proteases on human immunoglobulins IgG, IgA and secretory IgA (author's transl). *Zentralblatt fur Bakteriologie. 1. Abt. Originale. A: Medizinische Mikrobiologie, Infektionskrankheiten und Parasitologie,* 249**,** 89-98.

DOROSHENKO, N., RIMMER, S., HOSKINS, R., GARG, P., SWIFT, T., SPENCER, H. L., LORD, R. M., KATSIKOGIANNI, M., POWNALL, D. & MACNEIL, S. 2018. Antibiotic functionalised polymers reduce bacterial biofilm and bioburden in a simulated infection of the cornea. *Biomaterials science,* 6**,** 2101-2109.

DÖSSEL, J., MEYER-HOFFERT, U., SCHRÖDER, J. M. & GERSTEL, U. 2012. Pseudomonas aeruginosa-derived rhamnolipids subvert the host innate immune response through manipulation of the human beta-defensin-2 expression. *Cellular microbiology,* 14**,** 1364-1375.

DOWNWARD, J. 2001. The ins and outs of signalling. *Nature,* 411**,** 759.

DUMAS, J.-L., DELDEN, C., PERRON, K. & KÃ¶HLER, T. 2006. Analysis of antibiotic resistance gene expression inPseudomonas aeruginosaby quantitative real-time-PCR. *FEMS Microbiology Letters,* 254**,** 217-225.

EICKHOFF, M. J. & BASSLER, B. L. 2018. SnapShot: bacterial quorum sensing. *Cell,* 174**,** 1328-1328. e1.

ELMASSRY, M. M., MUDALIAR, N. S., COLMER-HAMOOD, J. A., SAN FRANCISCO, M. J., GRISWOLD, J. A., DISSANAIKE, S. & HAMOOD, A. N. 2020. New markers for sepsis caused by Pseudomonas aeruginosa during burn infection. *Metabolomics,* 16**,** 1-16.

ENGEBRECHT, J., NEALSON, K. & SILVERMAN, M. 1983. Bacterial bioluminescence: isolation and genetic analysis of functions from Vibrio fischeri. *Cell,* 32**,** 773-781.

FLEITAS MARTÍNEZ, O., CARDOSO, M. H., RIBEIRO, S. M. & FRANCO, O. L. 2019. Recent advances in anti-virulence therapeutic strategies with a focus on dismantling bacterial membrane microdomains, toxin neutralization, quorum-sensing interference and biofilm inhibition. *Frontiers in cellular and infection microbiology,* 9**,** 74.

FOZARD, J. A., LEES, M., KING, J. R. & LOGAN, B. S. 2012. Inhibition of quorum sensing in a computational biofilm simulation. *Biosystems,* 109**,** 105-114.

FRANK, L. & DEMOSS, R. 1959. On the biosynthesis of pyocyanine. *Journal of bacteriology,* 77**,** 776.

FRØLUND, B., PALMGREN, R., KEIDING, K. & NIELSEN, P. H. 1996. Extraction of extracellular polymers from activated sludge using a cation exchange resin. *Water research,* 30**,** 1749-1758.

FUQUA, W. C., WINANS, S. C. & GREENBERG, E. P. 1994. Quorum sensing in bacteria: the LuxR-LuxI family of cell density-responsive transcriptional regulators. *Journal of bacteriology,* 176**,** 269-275.

GAGNIÈRE, J., RAISCH, J., VEZIANT, J., BARNICH, N., BONNET, R., BUC, E., BRINGER, M.-A., PEZET, D. & BONNET, M. 2016. Gut microbiota imbalance and colorectal cancer. *World journal of gastroenterology,* 22**,** 501.

GARCÍA-CONTRERAS, R., MAEDA, T. & WOOD, T. K. 2013. Resistance to quorum-quenching compounds. *Applied and environmental microbiology,* 79**,** 6840-6846.

GARRETT, T. R., BHAKOO, M. & ZHANG, Z. 2008. Bacterial adhesion and biofilms on surfaces. *Progress in natural science,* 18**,** 1049-1056.

GIRARD, G. & BLOEMBERG, G. V. 2008. Central role of quorum sensing in regulating the production of pathogenicity factors in Pseudomonas aeruginosa.

GONZALEZ, M. R., FLEUCHOT, B., LAUCIELLO, L., JAFARI, P., APPLEGATE, L. A., RAFFOUL, W., QUE, Y.-A. & PERRON, K. 2016. Effect of human burn wound exudate on Pseudomonas aeruginosa virulence. *Msphere,* 1**,** e00111-15.

GORELOV, A., DU CHESNE, A. & DAWSON, K. 1997. Phase separation in dilute solutions of poly (N-isopropylacrylamide). *Physica A: Statistical Mechanics and its Applications,* 240**,** 443-452.

GRANDCLÉMENT, C., TANNIÈRES, M., MORÉRA, S., DESSAUX, Y. & FAURE, D. 2016. Quorum quenching: role in nature and applied developments. *FEMS microbiology reviews,* 40**,** 86-116.

GREEN, M., APEL, A. & STAPLETON, F. 2008. Risk factors and causative organisms in microbial keratitis. *Cornea,* 27**,** 22-27.

GURINA, T. S. & SIMMS, L. 2020. Histology, Staining.

HALL, S., MCDERMOTT, C., ANOOPKUMAR-DUKIE, S., MCFARLAND, A. J., FORBES, A., PERKINS, A. V., DAVEY, A. K., CHESS-WILLIAMS, R., KIEFEL, M. J. & ARORA, D. 2016. Cellular effects of pyocyanin, a secreted virulence factor of Pseudomonas aeruginosa. *Toxins,* 8**,** 236.

HAMOOD, A. N., GRISWOLD, J. & COLMER, J. 1996. Characterization of elastase-deficient clinical isolates of Pseudomonas aeruginosa. *Infection and immunity,* 64**,** 3154-3160.

HARRISON, F., MURULI, A., HIGGINS, S. & DIGGLE, S. P. 2014. Development of an ex vivo porcine lung model for studying growth, virulence, and signaling of Pseudomonas aeruginosa. *Infection and immunity,* 82**,** 3312-3323.

HAUSER, A. R. 2009. The type III secretion system of Pseudomonas aeruginosa: infection by injection. *Nature Reviews Microbiology,* 7**,** 654-665.

HAZAN, L., TARNIEWICZ, J., RAMONET, M., LAURENT, O. & ABBARIS, A. 2016. Automatic processing of atmospheric CO 2 and CH 4 mole fractions at the ICOS Atmosphere Thematic Centre. *Atmospheric Measurement Techniques,* 9**,** 4719-4736.

HE, W., MA, Y., GAO, X., WANG, X., DAI, X. & SONG, J. Application of Poly (N-isopropylacrylamide) as Thermosensitive Smart Materials. Journal of Physics: Conference Series, 2020. IOP Publishing, 012063.

HENSE, B. A., KUTTLER, C., MÜLLER, J., ROTHBALLER, M., HARTMANN, A. & KREFT, J.-U. 2007. Does efficiency sensing unify diffusion and quorum sensing? *Nature Reviews Microbiology,* 5**,** 230.

HENTZER, M., RIEDEL, K., RASMUSSEN, T. B., HEYDORN, A., ANDERSEN, J. B., PARSEK, M. R., RICE, S. A., EBERL, L., MOLIN, S. & HØIBY, N. 2002. Inhibition of quorum sensing in

Pseudomonas aeruginosa biofilm bacteria by a halogenated furanone compound. *Microbiology,* 148**,** 87-102.
HEURLIER, K., DÉNERVAUD, V. & HAAS, D. 2006. Impact of quorum sensing on fitness of Pseudomonas aeruginosa. *International journal of medical microbiology,* 296**,** 93-102.
HOLLAND, M. J. 2002. Transcript abundance in yeast varies over six orders of magnitude. *Journal of Biological Chemistry,* 277**,** 14363-14366.
HOPKINS, S., CARTER, S., SWANSON, L., MACNEIL, S. & RIMMER, S. 2007. Temperature-dependent phagocytosis of highly branched poly (N-isopropyl acrylamide-co-1, 2 propandiol-3-methacrylate) s prepared by RAFT polymerization. *Journal of Materials Chemistry,* 17**,** 4022-4027.
HU, R., YUAN, K., ZHOU, J., ZHANG, Y., ZHENG, J., ZHAO, Y., HUANG, X. & JIN, X. 2021. Influence of Pseudomonas autoinducer N-3-oxododecanoyl homoserine lactone on human corneal epithelial cells. *Experimental Biology and Medicine,* 246**,** 426-435.
HUSAIN, F. M., ANSARI, A. A., KHAN, A., AHMAD, N., ALBADRI, A. & ALBALAWI, T. H. 2019. Mitigation of acyl-homoserine lactone (AHL) based bacterial quorum sensing, virulence functions, and biofilm formation by yttrium oxide core/shell nanospheres: Novel approach to combat drug resistance. *Scientific Reports,* 9.
HUSCHKA, R., NEUMANN, O., BARHOUMI, A. & HALAS, N. J. 2010. Visualizing light-triggered release of molecules inside living cells. *Nano letters,* 10**,** 4117-4122.
JACK, A. A., KHAN, S., POWELL, L. C., PRITCHARD, M. F., BECK, K., SADH, H., SUTTON, L., CAVALIERE, A., FLORANCE, H. & RYE, P. D. 2018. Alginate oligosaccharide-induced modification of the lasI-lasR and rhlI-rhlR quorum-sensing systems in Pseudomonas aeruginosa. *Antimicrobial agents and chemotherapy,* 62**,** e02318-17.
JACOBSEN, J. N., ANDERSEN, A. S. & KROGFELT, K. A. 2012. Impact of Pseudomonas aeruginosa quorum sensing on cellular wound healing responses in vitro. *Scandinavian journal of infectious diseases,* 44**,** 615-619.
JAROSZ, L. M., OVCHINNIKOVA, E. S., MEIJLER, M. M. & KROM, B. P. 2011. Microbial spy games and host response: roles of a Pseudomonas aeruginosa small molecule in communication with other species. *PLoS pathogens,* 7**,** e1002312.
JEFFERY MARANO, R., JANE WALLACE, H., WIJERATNE, D., WILLIAM FEAR, M., SAN WONG, H. & O'HANDLEY, R. 2015. Secreted biofilm factors adversely affect cellular wound healing responses in vitro. *Scientific reports,* 5**,** 1-11.
JI, X., LU, Q., SUN, X., ZHAO, L., ZHANG, Y., YAO, J., ZHANG, X. & ZHAO, H. 2022. Dual-Active Au@ PNIPAm Nanozymes for Glucose Detection and Intracellular H2O2 Modulation. *Langmuir*.
JIANG, Q., CHEN, J., YANG, C., YIN, Y. & YAO, K. 2019. Quorum sensing: a prospective therapeutic target for bacterial diseases. *BioMed Research International,* 2019.
JIRICNY, N., MOLIN, S., FOSTER, K., DIGGLE, S. P., SCANLAN, P. D., GHOUL, M., JOHANSEN, H. K., SANTORELLI, L. A., POPAT, R. & WEST, S. A. 2014. Loss of social behaviours in populations of Pseudomonas aeruginosa infecting lungs of patients with cystic fibrosis. *PloS one,* 9**,** e83124.
JONES, S., YU, B., BAINTON, N. A., BIRDSALL, M., BYCROFT, B., CHHABRA, S., COX, A., GOLBY, P., REEVES, P. & STEPHENS, S. 1993. The lux autoinducer regulates the production of exoenzyme virulence determinants in Erwinia carotovora and Pseudomonas aeruginosa. *The EMBO journal,* 12**,** 2477-2482.
K BHARDWAJ, A., VINOTHKUMAR, K. & RAJPARA, N. 2013. Bacterial quorum sensing inhibitors: attractive alternatives for control of infectious pathogens showing multiple drug resistance. *Recent patents on anti-infective drug discovery,* 8**,** 68-83.
KALIA, V. C., RAJU, S. C. & PUROHIT, H. J. 2011. Genomic analysis reveals versatile organisms for quorum quenching enzymes: acyl-homoserine lactone-acylase and-lactonase. *The open microbiology journal,* 5**,** 1.
KANAMARU, K., KANAMARU, K., TATSUNO, I., TOBE, T. & SASAKAWA, C. 2000. SdiA, an Escherichia coli homologue of quorum-sensing regulators, controls the expression of virulence factors in enterohaemorrhagic Escherichia coli O157: H7. *Molecular microbiology,* 38**,** 805-816.

KANTHAKUMAR, K., CUNDELL, D., JOHNSON, M., WILLS, P., TAYLOR, G., COLE, P. & WILSON, R. 1994. Effect of salmeterol on human nasal epithelial cell ciliary beating: inhibition of the ciliotoxin, pyocyanin. *British journal of pharmacology,* 112**,** 493.

KARIMINIK, A., BASERI-SALEHI, M. & KHEIRKHAH, B. 2017. Pseudomonas aeruginosa quorum sensing modulates immune responses: an updated review article. *Immunology letters,* 190**,** 1-6.

KAUFMANN, G. F., PARK, J. & JANDA, K. D. 2008. Bacterial quorum sensing: a new target for anti-infective immunotherapy. *Expert opinion on biological therapy,* 8**,** 719-724.

KEARNS, D. B. 2010. A field guide to bacterial swarming motility. *Nature Reviews Microbiology,* 8**,** 634.

KHARAZMI, A. 1991. Mechanisms involved in the evasion of the host defence by Pseudomonas aeruginosa. *Immunology letters,* 30**,** 201-205.

KIM, C. S., GATSIOS, A., CUESTA, S., LAM, Y. C., WEI, Z., CHEN, H., RUSSELL, R. M., SHINE, E. E., WANG, R. & WYCHE, T. P. 2020. Characterization of Autoinducer-3 Structure and Biosynthesis in E. coli. *ACS central science,* 6**,** 197-206.

KIM, M. K., INGREMEAU, F., ZHAO, A., BASSLER, B. L. & STONE, H. A. 2016. Local and global consequences of flow on bacterial quorum sensing. *Nature microbiology,* 1**,** 15005.

KOCH, B., LILJEFORS, T., PERSSON, T., NIELSEN, J., KJELLEBERG, S. & GIVSKOV, M. 2005. The LuxR receptor: the sites of interaction with quorum-sensing signals and inhibitors. *Microbiology,* 151**,** 3589-3602.

KÖHLER, T., GUANELLA, R., CARLET, J. & VAN DELDEN, C. 2010. Quorum sensing-dependent virulence during Pseudomonas aeruginosa colonisation and pneumonia in mechanically ventilated patients. *Thorax,* 65**,** 703-710.

KONG, K.-F., VUONG, C. & OTTO, M. 2006. Staphylococcus quorum sensing in biofilm formation and infection. *International Journal of Medical Microbiology,* 296**,** 133-139.

KOSTAKIOTI, M., HADJIFRANGISKOU, M. & HULTGREN, S. J. 2013. Bacterial biofilms: development, dispersal, and therapeutic strategies in the dawn of the postantibiotic era. *Cold Spring Harbor perspectives in medicine,* 3**,** a010306.

KOSTYLEV, M., KIM, D. Y., SMALLEY, N. E., SALUKHE, I., GREENBERG, E. P. & DANDEKAR, A. A. 2019. Evolution of the Pseudomonas aeruginosa quorum-sensing hierarchy. *Proceedings of the National Academy of Sciences,* 116**,** 7027-7032.

KRAVCHENKO, V. V., KAUFMANN, G. F., MATHISON, J. C., SCOTT, D. A., KATZ, A. Z., GRAUER, D. C., LEHMANN, M., MEIJLER, M. M., JANDA, K. D. & ULEVITCH, R. J. 2008. Modulation of gene expression via disruption of NF-κB signaling by a bacterial small molecule. *Science,* 321**,** 259-263.

KRISHNAN, V. V. 2019. Molecular thermodynamics using nuclear magnetic resonance (NMR) spectroscopy. *Inventions,* 4**,** 13.

KUNGWATCHAKUN, D. & IRIE, M. 1988. Photoresponsive polymers. Photocontrol of the phase separation temperature of aqueous solutions of poly-[N-isopropylacrylamide-co-N-(4-phenylazophenyl) acrylamide]. *Die Makromolekulare Chemie, Rapid Communications,* 9**,** 243-246.

LAARMAN, A. J., BARDOEL, B. W., RUYKEN, M., FERNIE, J., MILDER, F. J., VAN STRIJP, J. A. & ROOIJAKKERS, S. H. 2012. Pseudomonas aeruginosa alkaline protease blocks complement activation via the classical and lectin pathways. *The Journal of Immunology,* 188**,** 386-393.

LANG, S. & WAGNER, F. 2017. Structure and properties of biosurfactants. *Biosurfactants and biotechnology.* Routledge.

LANSBURY, L., LIM, B., BASKARAN, V. & LIM, W. S. 2020. Co-infections in people with COVID-19: a systematic review and meta-analysis. *Journal of Infection,* 81**,** 266-275.

LARI, A. R., HONAR, H. B. & ALAGHEHBANDAN, R. 1998. Pseudomonas infections in Tohid burn center, Iran. *Burns,* 24**,** 637-641.

LASARRE, B. & FEDERLE, M. J. 2013. Exploiting quorum sensing to confuse bacterial pathogens. *Microbiol. Mol. Biol. Rev.,* 77**,** 73-111.

LATIFI, A., FOGLINO, M., TANAKA, K., WILLIAMS, P. & LAZDUNSKI, A. 1996. A hierarchical quorum-sensing cascade in Pseudomonas aeruginosa links the transcriptional activators LasR and RhIR (VsmR) to expression of the stationary-phase sigma factor RpoS. *Molecular microbiology,* 21**,** 1137-1146.

LATIFI, A., WINSON, M. K., FOGLINO, M., BYCROFT, B. W., STEWART, G. S., LAZDUNSKI, A. & WILLIAMS, P. 1995. Multiple homologues of LuxR and LuxI control expression of virulence determinants and secondary metabolites through quorum sensing in Pseudomonas aeruginosa PAO1. *Molecular microbiology,* 17**,** 333-343.

LAU, G. W., HASSETT, D. J., RAN, H. & KONG, F. 2004. The role of pyocyanin in Pseudomonas aeruginosa infection. *Trends in molecular medicine,* 10**,** 599-606.

LAZDUNSKI, A. M., VENTRE, I. & STURGIS, J. N. 2004. Regulatory circuits and communication in Gram-negative bacteria. *Nature Reviews Microbiology,* 2**,** 581.

LEBEER, S., DE KEERSMAECKER, S. C., VERHOEVEN, T. L., FADDA, A. A., MARCHAL, K. & VANDERLEYDEN, J. 2007. Functional analysis of luxS in the probiotic strain Lactobacillus rhamnosus GG reveals a central metabolic role important for growth and biofilm formation. *Journal of bacteriology,* 189**,** 860-871.

LEE, J. & ZHANG, L. 2015a. The hierarchy quorum sensing network in Pseudomonas aeruginosa. *Protein & cell,* 6**,** 26-41.

LEE, J. & ZHANG, L. 2015b. The hierarchy quorum sensing network in Pseudomonas aeruginosa.

LESIC, B., LÉPINE, F., DÉZIEL, E., ZHANG, J., ZHANG, Q., PADFIELD, K., CASTONGUAY, M.-H., MILOT, S., STACHEL, S. & TZIKA, A. A. 2007. Inhibitors of pathogen intercellular signals as selective anti-infective compounds. *PLoS pathogens,* 3**,** e126.

LEWENZA, S., CONWAY, B., GREENBERG, E. & SOKOL, P. A. 1999. Quorum sensing in Burkholderia cepacia: identification of the LuxRI homologs CepRI. *Journal of Bacteriology,* 181**,** 748-756.

LI, H., LI, X., WANG, Z., FU, Y., AI, Q., DONG, Y. & YU, J. 2015. Autoinducer-2 regulates Pseudomonas aeruginosa PAO1 biofilm formation and virulence production in a dose-dependent manner. *BMC Microbiology,* 15.

LI, L., HE, Y., ZHAO, M. & JIANG, J. 2013. Collective cell migration: Implications for wound healing and cancer invasion. *Burns & trauma,* 1**,** 2321-3868.113331.

LIANG, C.-C., PARK, A. Y. & GUAN, J.-L. 2007. In vitro scratch assay: a convenient and inexpensive method for analysis of cell migration in vitro. *Nature protocols,* 2**,** 329-333.

LIU, Z., PAN, Y., LI, X., JIE, J. & ZENG, M. 2017. Chemical composition, antimicrobial and anti-quorum sensing activities of pummelo peel flavonoid extract. *Industrial crops and products,* 109**,** 862-868.

LU, Y.-T., ZENG, K., FUHRMANN, B., WOELK, C., ZHANG, K. & GROTH, T. 2022. Engineering of Stable Cross-Linked Multilayers Based on Thermo-Responsive PNIPAM-Grafted-Chitosan/Heparin to Tailor Their Physiochemical Properties and Biocompatibility. *ACS Applied Materials & Interfaces*.

LUO, J., DONG, B., WANG, K., CAI, S., LIU, T., CHENG, X., LEI, D., CHEN, Y., LI, Y. & KONG, J. 2017. Baicalin inhibits biofilm formation, attenuates the quorum sensing-controlled virulence and enhances Pseudomonas aeruginosa clearance in a mouse peritoneal implant infection model. *PLoS One,* 12**,** e0176883.

LUO, J., KONG, J.-L., DONG, B.-Y., HUANG, H., WANG, K., WU, L.-H., HOU, C.-C., LIANG, Y., LI, B. & CHEN, Y.-Q. 2016. Baicalein attenuates the quorum sensing-controlled virulence factors of Pseudomonas aeruginosa and relieves the inflammatory response in *P. aeruginosa*-infected macrophages by downregulating the MAPK and NFκB signal-transduction pathways. *Drug design, development and therapy,* 10**,** 183.

MA, H. & BRYERS, J. D. 2013. Non-invasive determination of conjugative transfer of plasmids bearing antibiotic-resistance genes in biofilm-bound bacteria: effects of substrate loading and antibiotic selection. *Applied microbiology and biotechnology,* 97**,** 317-328.

MACNEIL, S., SHEPHERD, J. & SMITH, L. 2011a. Production of tissue-engineered skin and oral mucosa for clinical and experimental use. *3D cell culture.* Springer.

MACNEIL, S., SHEPHERD, J. & SMITH, L. 2011b. Production of Tissue-Engineered Skin and Oral Mucosa for Clinical and Experimental Use. *Methods in Molecular Biology.* Humana Press.

MAEDA, T., GARCÍA-CONTRERAS, R., PU, M., SHENG, L., GARCIA, L. R., TOMÁS, M. & WOOD, T. K. 2012. Quorum quenching quandary: resistance to antivirulence compounds. *The ISME journal,* 6**,** 493-501.

MALCOLM, G. & ROWLINSON, J. 1957. The thermodynamic properties of aqueous solutions of polyethylene glycol, polypropylene glycol and dioxane. *Transactions of the Faraday Society,* 53**,** 921-931.

MALGAONKAR, A. & NAIR, M. 2019. Quorum sensing in Pseudomonas aeruginosa mediated by RhlR is regulated by a small RNA PhrD. *Scientific reports,* 9**,** 1-11.

MARCHANT, R. & BANAT, I. M. 2017. Protocols for measuring biosurfactant production in microbial cultures. *Hydrocarbon and lipid microbiology protocols: activities and phenotypes***,** 119-128.

MARTINELLI, D., GROSSMANN, G., SÉQUIN, U., BRANDL, H. & BACHOFEN, R. 2004. Effects of natural and chemically synthesized furanones on quorum sensing in Chromobacterium violaceum. *BMC microbiology,* 4**,** 1-10.

MASHBURN, L. M., JETT, A. M., AKINS, D. R. & WHITELEY, M. 2005. Staphylococcus aureus serves as an iron source for Pseudomonas aeruginosa during in vivo coculture. *Journal of bacteriology,* 187**,** 554-566.

MASTERTON, R., GALLOWAY, A., FRENCH, G., STREET, M., ARMSTRONG, J., BROWN, E., CLEVERLEY, J., DILWORTH, P., FRY, C. & GASCOIGNE, A. 2008. Guidelines for the management of hospital-acquired pneumonia in the UK: report of the working party on hospital-acquired pneumonia of the British Society for Antimicrobial Chemotherapy. *Journal of Antimicrobial Chemotherapy,* 62**,** 5-34.

MAVRODI, D. V., PEEVER, T. L., MAVRODI, O. V., PAREJKO, J. A., RAAIJMAKERS, J. M., LEMANCEAU, P., MAZURIER, S., HEIDE, L., BLANKENFELDT, W. & WELLER, D. M. 2010. Diversity and evolution of the phenazine biosynthesis pathway. *Applied and environmental microbiology,* 76**,** 866-879.

MCCLEAN, K. H., WINSON, M. K., FISH, L., TAYLOR, A., CHHABRA, S. R., CAMARA, M., DAYKIN, M., LAMB, J. H., SWIFT, S. & BYCROFT, B. W. 1997a. Quorum sensing and Chromobacterium violaceum: exploitation of violacein production and inhibition for the detection of N-acylhomoserine lactones. *Microbiology,* 143**,** 3703-3711.

MCCLEAN, K. H., WINSON, M. K., FISH, L., TAYLOR, A., CHHABRA, S. R., CAMARA, M., DAYKIN, M., LAMB, J. H., SWIFT, S., BYCROFT, B. W., STEWART, G. S. A. B. & WILLIAMS, P. 1997b. Quorum sensing and Chromobacterium violaceum: exploitation of violacein production and inhibition for the detection of N-acylhomoserine lactones. *Microbiology,* 143**,** 3703-3711.

MCGRATH, S., WADE, D. S. & PESCI, E. C. 2004. Dueling quorum sensing systems in Pseudomonas aeruginosa control the production of the Pseudomonas quinolone signal (PQS). *FEMS microbiology letters,* 230**,** 27-34.

MICHALSKA, M. & WOLF, P. 2015. Pseudomonas Exotoxin A: optimized by evolution for effective killing. *Frontiers in microbiology,* 6**,** 963.

MILES, A. A., MISRA, S. & IRWIN, J. 1938. The estimation of the bactericidal power of the blood. *Epidemiology & Infection,* 38**,** 732-749.

MOHAMMED SAKR, M., MOHAMED ANWAR ABOSHANAB, K., MABROUK ABOULWAFA, M. & ABDEL-HALEEM HASSOUNA, N. 2013. Characterization and complete sequence of lactonase enzyme from Bacillus weihenstephanensis isolate P65 with potential activity against acyl homoserine lactone signal molecules. *BioMed Research International,* 2013.

MOK, N., CHAN, S. Y., LIU, S. Y. & CHUA, S. L. 2020. Vanillin inhibits PqsR-mediated virulence in Pseudomonas aeruginosa. *Food & function,* 11**,** 6496-6508.

MORADALI, M. F., GHODS, S. & REHM, B. H. 2017. Pseudomonas aeruginosa lifestyle: a paradigm for adaptation, survival, and persistence. *Frontiers in cellular and infection microbiology,* 7**,** 39.

MOURA-ALVES, P., PUYSKENS, A., STINN, A., KLEMM, M., GUHLICH-BORNHOF, U., DORHOI, A., FURKERT, J., KREUCHWIG, A., PROTZE, J. & LOZZA, L. 2019. Host monitoring of quorum sensing during Pseudomonas aeruginosa infection. *Science,* 366**,** eaaw1629.

MULLER, M., LI, Z. & MAITZ, P. K. 2009. Pseudomonas pyocyanin inhibits wound repair by inducing premature cellular senescence: role for p38 mitogen-activated protein kinase. *Burns,* 35**,** 500-508.

MURRAY, E. J., DUBERN, J.-F., CHAN, W. C., CHHABRA, S. R. & WILLIAMS, P. 2022. A Pseudomonas aeruginosa PQS quorum-sensing system inhibitor with anti-staphylococcal activity sensitizes polymicrobial biofilms to tobramycin. *Cell Chemical Biology*.

NADAL JIMENEZ, P., KOCH, G., THOMPSON, J. A., XAVIER, K. B., COOL, R. H. & QUAX, W. J. 2012. The multiple signaling systems regulating virulence in Pseudomonas aeruginosa. *Microbiology and Molecular Biology Reviews,* 76**,** 46-65.

NAGANO, T., HAO, J.-L., NAKAMURA, M., KUMAGAI, N., ABE, M., NAKAZAWA, T. & NISHIDA, T. 2001. Stimulatory effect of pseudomonal elastase on collagen degradation by cultured keratocytes. *Investigative ophthalmology & visual science,* 42**,** 1247-1253.

NAIK, V. & MAHAJAN, G. 2013. Quorum sensing: a non-conventional target for antibiotic discovery. *Natural product communications,* 8**,** 1934578X1300801030.

NICKZAD, A. & DÉZIEL, É. 2014. The involvement of rhamnolipids in microbial cell adhesion and biofilm development–an approach for control? *Letters in applied microbiology,* 58**,** 447-453.

NIKAIDO, H. 1998. Multiple antibiotic resistance and efflux. *Current opinion in microbiology,* 1**,** 516-523.

NILFOROUSHZADEH, M. A., ASHTIANI, H. R. A., JAFFARY, F., JAHANGIRI, F., NIKKHAH, N., MAHMOUDBEYK, M., FARD, M., ANSARI, Z. & ZARE, S. 2017. Dermal fibroblast cells: biology and function in skin regeneration. *Journal of Skin and Stem Cell,* 4.

NORDMANN, P. & GUIBERT, M. 1998. Extended-spectrum beta-lactamases in Pseudomonas aeruginosa. *The Journal of antimicrobial chemotherapy,* 42**,** 128-131.

NOUMI, E., MERGHNI, A., M. ALRESHIDI, M., HADDAD, O., AKMADAR, G., DE MARTINO, L., MASTOURI, M., CEYLAN, O., SNOUSSI, M. & AL-SIENI, A. 2018. Chromobacterium violaceum and Pseudomonas aeruginosa PAO1: Models for evaluating anti-quorum sensing activity of Melaleuca alternifolia essential oil and its main component terpinen-4-ol. *Molecules,* 23**,** 2672.

O'LOUGHLIN, C. T., MILLER, L. C., SIRYAPORN, A., DRESCHER, K., SEMMELHACK, M. F. & BASSLER, B. L. 2013. A quorum-sensing inhibitor blocks Pseudomonas aeruginosa virulence and biofilm formation. *Proceedings of the National Academy of Sciences,* 110**,** 17981-17986.

OCHSNER, U. A. & REISER, J. 1995. Autoinducer-mediated regulation of rhamnolipid biosurfactant synthesis in Pseudomonas aeruginosa. *Proceedings of the National Academy of Sciences,* 92**,** 6424-6428.

OHMAN, D., CRYZ, S. & IGLEWSKI, B. 1980. Isolation and characterization of Pseudomonas aeruginosa PAO mutant that produces altered elastase. *Journal of Bacteriology,* 142**,** 836-842.

OSBORN, M., ROSEN, S., ROTHFIELD, L., ZELEZNICK, L. & HORECKER, B. 1964. Lipopolysaccharide of the Gram-Negative Cell Wall: Biosynthesis of a complex heteropolysaccharide occurs by successive addition of specific sugar residues. *Science,* 145**,** 783-789.

PANG, Z., RAUDONIS, R., GLICK, B. R., LIN, T.-J. & CHENG, Z. 2019. Antibiotic resistance in Pseudomonas aeruginosa: mechanisms and alternative therapeutic strategies. *Biotechnology advances,* 37**,** 177-192.

PAPENFORT, K. & BASSLER, B. L. 2016. Quorum sensing signal–response systems in Gram-negative bacteria. *Nature Reviews Microbiology,* 14**,** 576.

PARK, J., JAGASIA, R., KAUFMANN, G. F., MATHISON, J. C., RUIZ, D. I., MOSS, J. A., MEIJLER, M. M., ULEVITCH, R. J. & JANDA, K. D. 2007. Infection control by antibody disruption of bacterial quorum sensing signaling. *Chemistry & biology,* 14**,** 1119-1127.

PARK, P. W., PIER, G. B., PRESTON, M. J., GOLDBERGER, O., FITZGERALD, M. L. & BERNFIELD, M. 2000. Syndecan-1 shedding is enhanced by LasA, a secreted virulence factor of Pseudomonas aeruginosa. *Journal of Biological Chemistry,* 275**,** 3057-3064.

PARMELY, M., GALE, A., CLABAUGH, M., HORVAT, R. & ZHOU, W.-W. 1990. Proteolytic inactivation of cytokines by Pseudomonas aeruginosa. *Infection and immunity,* 58**,** 3009-3014.

PARSEK, M. R., VAL, D. L., HANZELKA, B. L., CRONAN JR, J. E. & GREENBERG, E. 1999. Acyl homoserine-lactone quorum-sensing signal generation. *Proceedings of the National Academy of Sciences,* 96**,** 4360-4365.

PASPARAKIS, G., COCKAYNE, A. & ALEXANDER, C. 2007. Control of bacterial aggregation by thermoresponsive glycopolymers. *Journal of the American Chemical Society,* 129**,** 11014-11015.

PATERSON, T. E., BARI, A., BULLOCK, A. J., TURNER, R., MONTALBANO, G., FIORILLI, S., VITALE-BROVARONE, C., MACNEIL, S. & SHEPHERD, J. 2020. Multifunctional copper-containing mesoporous glass nanoparticles as antibacterial and proangiogenic agents for chronic wounds. *Frontiers in Bioengineering and Biotechnology,* 8**,** 246.

PATTEM, J., SWIFT, T., RIMMER, S., HOLMES, T., MACNEIL, S. & SHEPHERD, J. 2021. Development of a novel micro-bead force spectroscopy approach to measure the ability of a thermo-active polymer to remove bacteria from a corneal model. *Scientific Reports,* 11**,** 1-11.

PEARSON, J. P., PASSADOR, L., IGLEWSKI, B. H. & GREENBERG, E. 1995. A second N-acylhomoserine lactone signal produced by Pseudomonas aeruginosa. *Proceedings of the National Academy of Sciences,* 92**,** 1490-1494.

PEARSON, J. P., VAN DELDEN, C. & IGLEWSKI, B. H. 1999. Active efflux and diffusion are involved in transport of Pseudomonas aeruginosa cell-to-cell signals. *Journal of bacteriology,* 181**,** 1203-1210.

PESCI, E. C., MILBANK, J. B. J., PEARSON, J. P., MCKNIGHT, S., KENDE, A. S., GREENBERG, E. P. & IGLEWSKI, B. H. 1999. Quinolone signaling in the cell-to-cell communication system of Pseudomonas aeruginosa.

PESCI, E. C., PEARSON, J. P., SEED, P. C. & IGLEWSKI, B. H. 1997. Regulation of las and rhl quorum sensing in Pseudomonas aeruginosa. *Journal of bacteriology,* 179**,** 3127-3132.

PIIPPONEN, M., LI, D. & LANDÉN, N. X. 2020. The immune functions of keratinocytes in skin wound healing. *International journal of molecular sciences,* 21**,** 8790.

PILETSKA, E. V., STAVROULAKIS, G., KARIM, K., WHITCOMBE, M. J., CHIANELLA, I., SHARMA, A., EBOIGBODIN, K. E., ROBINSON, G. K. & PILETSKY, S. A. 2010. Attenuation of Vibrio fischeri quorum sensing using rationally designed polymers. *Biomacromolecules,* 11**,** 975-980.

PILETSKA, E. V., STAVROULAKIS, G., LARCOMBE, L. D., WHITCOMBE, M. J., SHARMA, A., PRIMROSE, S., ROBINSON, G. K. & PILETSKY, S. A. 2011. Passive control of quorum sensing: prevention of Pseudomonas aeruginosa biofilm formation by imprinted polymers. *Biomacromolecules,* 12**,** 1067-1071.

PIRHONEN, M., FLEGO, D., HEIKINHEIMO, R. & PALVA, E. T. 1993. A small diffusible signal molecule is responsible for the global control of virulence and exoenzyme production in the plant pathogen Erwinia carotovora. *The EMBO journal,* 12**,** 2467-2476.

PLENDERLEITH, R., SWIFT, T. & RIMMER, S. 2014. Highly-branched poly (N-isopropyl acrylamide) s with core–shell morphology below the lower critical solution temperature. *Rsc Advances,* 4**,** 50932-50937.

PUNDIR, P., LIU, R., VASAVDA, C., SERHAN, N., LIMJUNYAWONG, N., YEE, R., ZHAN, Y., DONG, X., WU, X. & ZHANG, Y. 2019. A connective tissue mast-cell-specific receptor detects bacterial quorum-sensing molecules and mediates antibacterial immunity. *Cell host & microbe,* 26**,** 114-122. e8.

QU, J., CAI, Z., LIU, Y., DUAN, X., HAN, S., LIU, J., ZHU, Y., JIANG, Z., ZHANG, Y. & ZHUO, C. 2021. Persistent bacterial coinfection of a COVID-19 patient caused by a genetically adapted Pseudomonas aeruginosa chronic colonizer. *Frontiers in cellular and infection microbiology***,** 129.

QUAN, K., HOU, J., ZHANG, Z., REN, Y., PETERSON, B. W., FLEMMING, H.-C., MAYER, C., BUSSCHER, H. J. & VAN DER MEI, H. C. 2022. Water in bacterial biofilms: pores and channels, storage and transport functions. *Critical Reviews in Microbiology,* 48**,** 283-302.

RANDALL, M. J., JÜNGEL, A., RIMANN, M. & WUERTZ-KOZAK, K. 2018. Advances in the biofabrication of 3D skin in vitro: healthy and pathological models. *Frontiers in bioengineering and biotechnology,* 6**,** 154.

REDFIELD, R. J. 2002. Is quorum sensing a side effect of diffusion sensing? *Trends in microbiology,* 10**,** 365-370.

RIMMER, S., CARTER, S., RUTKAITE, R., HAYCOCK, J. W. & SWANSON, L. 2007. Highly branched poly-(N-isopropylacrylamide) s with arginine–glycine–aspartic acid (RGD)-or COOH-chain ends that form sub-micron stimulus-responsive particles above the critical solution temperature. *Soft Matter,* 3**,** 971-973.

ROBITAILLE, S., GROLEAU, M. C. & DÉZIEL, E. 2020. Swarming motility growth favours the emergence of a subpopulation of Pseudomonas aeruginosa quorum-sensing mutants. *Environmental microbiology,* 22**,** 2892-2906.

ROCHA, A. J., DE SOUZA MIRANDA, R., SOUSA, A. J. S. & DA SILVA, A. L. C. 2016. Guidelines for Successful Quantitative Gene Expression in Real-Time qPCR Assays. *Polymerase Chain Reaction for Biomedical Applications***,** 1.

ROUDASHTI, S., ZEIGHAMI, H., MIRSHAHABI, H., BAHARI, S., SOLTANI, A. & HAGHI, F. 2017. Synergistic activity of sub-inhibitory concentrations of curcumin with ceftazidime and ciprofloxacin against Pseudomonas aeruginosa quorum sensing related genes and virulence traits. *World Journal of Microbiology and Biotechnology,* 33**,** 1-8.

RUBY, E. G. 1996. Lessons from a cooperative, bacterial-animal association: the Vibrio fischeri–Euprymna scolopes light organ symbiosis. *Annual review of microbiology,* 50**,** 591-624.

RUFFIN, M. & BROCHIERO, E. 2019. Repair process impairment by Pseudomonas aeruginosa in epithelial tissues: major features and potential therapeutic avenues. *Frontiers in cellular and infection microbiology,* 9**,** 182.

RUMBAUGH, K. P., GRISWOLD, J. A., IGLEWSKI, B. H. & HAMOOD, A. N. 1999. Contribution of quorum sensing to the virulence ofpseudomonas aeruginosa in burn wound infections. *Infection and immunity,* 67**,** 5854-5862.

RUST, L., MESSING, C. R. & IGLEWSKI, B. H. 1994. [44] Elastase assays. *Methods in enzymology,* 235**,** 554-562.

SAINT-CRIQ, V., VILLERET, B., BASTAERT, F., KHEIR, S., HATTON, A., CAZES, A., XING, Z., SERMET-GAUDELUS, I., GARCIA-VERDUGO, I., EDELMAN, A. & SALLENAVE, J.-M. 2018. Pseudomonas aeruginosa LasB protease impairs innate immunity in mice and humans by targeting a lung epithelial cystic fibrosis transmembrane regulator–IL-6–antimicrobial–repair pathway. *Thorax,* 73**,** 49-61.

SAKURAGI, Y. & KOLTER, R. 2007. Quorum-sensing regulation of the biofilm matrix genes (pel) of Pseudomonas aeruginosa. *Journal of bacteriology,* 189**,** 5383-5386.

SAMBROOK, H. 1989. Molecular cloning: a laboratory manual. Cold Spring Harbor, NY.

SANTHAKUMARI, S. & RAVI, A. 2019. Targeting quorum sensing mechanism: an alternative anti-virulent strategy for the treatment of bacterial infections. *South African Journal of Botany,* 120**,** 81-86.

SAVLI, H., KARADENIZLI, A., KOLAYLI, F., GUNDES, S., OZBEK, U. & VAHABOGLU, H. 2003. Expression stability of six housekeeping genes: a proposal for resistance gene quantification studies of Pseudomonas aeruginosa by real-time quantitative RT-PCR. *Journal of medical microbiology,* 52**,** 403-408.

SCHAD, P. A. & IGLEWSKI, B. H. 1988. Nucleotide sequence and expression in Escherichia coli of the Pseudomonas aeruginosa lasA gene. *Journal of bacteriology,* 170**,** 2784-2789.

SCHAEFER, A. L., VAL, D. L., HANZELKA, B. L., CRONAN JR, J. E. & GREENBERG, E. P. 1996. Generation of cell-to-cell signals in quorum sensing: acyl homoserine lactone synthase activity of a purified Vibrio fischeri LuxI protein. *Proceedings of the National Academy of Sciences,* 93**,** 9505-9509.

SCHILD, H. G. 1992. Poly (N-isopropylacrylamide): experiment, theory and application. *Progress in polymer science,* 17**,** 163-249.

SCHLAGER, T., SADLER, J., WEBER, D., DONOWITZ, L. & LOHR, J. 1994. Hospital-acquired infections in pediatric burn patients. *Southern medical journal,* 87**,** 481-484.

SCHMITTGEN, T. D. A. L., K.J. 2008. Analyzing real-time PCR data by the comparative

CT method. *Nature Protocols,* 3(6)**,** pp.1101-1108.

SCHULTZ, D. R. & MILLER, K. D. 1974. Elastase of Pseudomonas aeruginosa: inactivation of complement components and complement-derived chemotactic and phagocytic factors. *Infection and immunity,* 10**,** 128-135.

SCHUMERS, J. M., FUSTIN, C. A. & GOHY, J. F. 2010. Light-responsive block copolymers. *Macromolecular rapid communications,* 31**,** 1588-1607.

SCHURCH, N. J., SCHOFIELD, P., GIERLIŃSKI, M., COLE, C., SHERSTNEV, A., SINGH, V., WROBEL, N., GHARBI, K., SIMPSON, G. G. & OWEN-HUGHES, T. 2016. How many

biological replicates are needed in an RNA-seq experiment and which differential expression tool should you use? *Rna,* 22**,** 839-851.
SCHUSTER, M. & GREENBERG, E. P. 2007. Early activation of quorum sensing in Pseudomonas aeruginosa reveals the architecture of a complex regulon. *Bmc Genomics,* 8**,** 1-11.
SCHUSTER, M., LOSTROH, C. P., OGI, T. & GREENBERG, E. P. 2003. Identification, timing, and signal specificity of Pseudomonas aeruginosa quorum-controlled genes: a transcriptome analysis. *Journal of bacteriology,* 185**,** 2066-2079.
SHEIKH, A. F., SHAHIN, M., SHOKOOHIZADEH, L., HALAJI, M., SHAHCHERAGHI, F. & GHANBARI, F. 2019. Molecular epidemiology of colistin-resistant Pseudomonas aeruginosa producing NDM-1 from hospitalized patients in Iran. *Iranian journal of basic medical sciences,* 22**,** 38.
SHEPHERD, J., DOUGLAS, I., RIMMER, S., SWANSON, L. & MACNEIL, S. 2009. Development of three-dimensional tissue-engineered models of bacterial infected human skin wounds. *Tissue Engineering Part C: Methods,* 15**,** 475-484.
SHEPHERD, J., SARKER, P., SWINDELLS, K., DOUGLAS, I., MACNEIL, S., SWANSON, L. & RIMMER, S. 2010. Binding bacteria to highly branched poly (N-isopropyl acrylamide) modified with vancomycin induces the coil-to-globule transition. *Journal of the American Chemical Society,* 132**,** 1736-1737.
SHEPHERD, J., SWIFT, T., CHANG, C.-Y., BOYNE, J. R., RIMMER, S. & MARTIN, W. H. 2019. Highly branched poly (N-isopropyl acrylamide) functionalized with an inducer molecule suppresses quorum sensing in Chromobacterium violaceum. *Chemical Communications,* 55**,** 9765-9768.
SINGH, P. K., PARSEK, M. R., GREENBERG, E. P. & WELSH, M. J. 2002. A component of innate immunity prevents bacterial biofilm development. *Nature,* 417**,** 552.
SMITH, J. L., FRATAMICO, P. M. & YAN, X. 2011. Eavesdropping by bacteria: the role of SdiA in Escherichia coli and Salmonella enterica serovar Typhimurium quorum sensing. *Foodborne pathogens and disease,* 8**,** 169-178.
SMITH, J. N. & AHMER, B. M. 2003. Detection of other microbial species by Salmonella: expression of the SdiA regulon. *Journal of Bacteriology,* 185**,** 1357-1366.
SOBERÓN-CHÁVEZ, G., LÉPINE, F. & DÉZIEL, E. 2005. Production of rhamnolipids by Pseudomonas aeruginosa. *Applied microbiology and biotechnology,* 68**,** 718-725.
STEINDLER, L. & VENTURI, V. 2007. Detection of quorum-sensingN-acyl homoserine lactone signal molecules by bacterial biosensors. *FEMS Microbiology Letters,* 266**,** 1-9.
STEWART, P. S. 1996. Theoretical aspects of antibiotic diffusion into microbial biofilms. *Antimicrobial agents and chemotherapy,* 40**,** 2517-2522.
STOREY, D. G., UJACK, E. E., RABIN, H. R. & MITCHELL, I. 1998. Pseudomonas aeruginosa lasR transcription correlates with the transcription of lasA, lasB, and toxA in chronic lung infections associated with cystic fibrosis. *Infection and immunity,* 66**,** 2521-2528.
STRATEVA, T. & MITOV, I. 2011. Contribution of an arsenal of virulence factors to pathogenesis of Pseudomonas aeruginosa infections. *Annals of microbiology,* 61**,** 717-732.
SUN, J., LAROCK, D. L., SKOWRONSKI, E. A., KIMMEY, J. M., OLSON, J., JIANG, Z., O'DONOGHUE, A. J., NIZET, V. & LAROCK, C. N. 2020. The Pseudomonas aeruginosa protease LasB directly activates IL-1β. *EBioMedicine,* 60**,** 102984.
SUN, Z., HE, X., BRANCACCIO, V. F., YUAN, J. & RIEDEL, C. U. 2014. Bifidobacteria exhibit LuxS-dependent autoinducer 2 activity and biofilm formation. *PLoS One,* 9**,** e88260.
SURETTE, M. G., MILLER, M. B. & BASSLER, B. L. 1999. Quorum sensing in Escherichia coli, Salmonella typhimurium, and Vibrio harveyi: a new family of genes responsible for autoinducer production. *Proceedings of the National Academy of Sciences,* 96**,** 1639-1644.
SWANSON, T., ANGEL, D., SUSSMAN, G., COOPER, R., HAESLER, E., OUSEY, K., CARVILLE, K., FLETCHER, J., KALAN, L. & KEAST, D. 2016. Wound infection in clinical practice: principles of best practice.
SWEM, L. R., SWEM, D. L., O'LOUGHLIN, C. T., GATMAITAN, R., ZHAO, B., ULRICH, S. M. & BASSLER, B. L. 2009. A quorum-sensing antagonist targets both membrane-bound and cytoplasmic receptors and controls bacterial pathogenicity. *Molecular cell,* 35**,** 143-153.

TAGLIALEGNA, A., LASA, I. & VALLE, J. 2016. Amyloid structures as biofilm matrix scaffolds. *Journal of bacteriology,* 198**,** 2579-2588.
TEIMOURI, A., YEUNG, P. & AGU, R. 2018. 2D vs. 3D cell culture models for in vitro topical (dermatological) medication testing. *Cell Culture.* IntechOpen.
TERATANATORN, P., HOSKINS, R., SWIFT, T., DOUGLAS, C. I., SHEPHERD, J. & RIMMER, S. 2017. Binding of bacteria to poly (N-isopropylacrylamide) modified with vancomycin: Comparison of behavior of linear and highly branched polymers. *Biomacromolecules,* 18**,** 2887-2899.
TEUFEL, P. & GÖTZ, F. 1993. Characterization of an extracellular metalloprotease with elastase activity from Staphylococcus epidermidis. *Journal of bacteriology,* 175**,** 4218-4224.
THOMAS, R. E. & THOMAS, B. C. 2021. Reducing biofilm infections in burn patients' wounds and biofilms on surfaces in hospitals, medical facilities and medical equipment to improve burn care: a systematic review. *International Journal of Environmental Research and Public Health,* 18**,** 13195.
TODER, D., FERRELL, S., NEZEZON, J., RUST, L. & IGLEWSKI, B. 1994. lasA and lasB genes of Pseudomonas aeruginosa: analysis of transcription and gene product activity. *Infection and immunity,* 62**,** 1320-1327.
TODER, D., GAMBELLO, M. & IGLEWSKI, B. 1991. Pseudomonas aeruginosa LasA: a second elastase under the transcriptional control of lasR. *Molecular microbiology,* 5**,** 2003-2010.
TOPA, S. H., PALOMBO, E. A., KINGSHOTT, P. & BLACKALL, L. L. 2020. Activity of cinnamaldehyde on quorum sensing and biofilm susceptibility to antibiotics in Pseudomonas aeruginosa. *Microorganisms,* 8**,** 455.
TRIPATHI, N. & SAPRA, A. 2020. Gram staining.
TULEVA, B. K., IVANOV, G. R. & CHRISTOVA, N. E. 2002. Biosurfactant production by a new Pseudomonas putida strain. *Zeitschrift für Naturforschung C,* 57**,** 356-360.
TÜMMLER, B. & KIEWITZ, C. 1999. Cystic fibrosis: an inherited susceptibility to bacterial respiratory infections. *Molecular medicine today,* 5**,** 351-358.
UROZ, S., DESSAUX, Y. & OGER, P. 2009. Quorum sensing and quorum quenching: the yin and yang of bacterial communication. *ChemBioChem,* 10**,** 205-216.
VADEKEETIL, A., ALEXANDAR, V., CHHIBBER, S. & HARJAI, K. 2016. Adjuvant effect of cranberry proanthocyanidin active fraction on antivirulent property of ciprofloxacin against Pseudomonas aeruginosa. *Microbial pathogenesis,* 90**,** 98-103.
VAN'T WOUT, E. F., VAN SCHADEWIJK, A., VAN BOXTEL, R., DALTON, L. E., CLARKE, H. J., TOMMASSEN, J., MARCINIAK, S. J. & HIEMSTRA, P. S. 2015. Virulence factors of Pseudomonas aeruginosa induce both the unfolded protein and integrated stress responses in airway epithelial cells. *PLoS pathogens,* 11**,** e1004946.
VASAVI, H. S., ARUN, A. B. & REKHA, P. D. 2014. Anti-quorum sensing activity of Psidium guajava L. flavonoids against Chromobacterium violaceum and Pseudomonas aeruginosa PAO1. *Microbiology and immunology,* 58**,** 286-293.
VELNAR, T., BAILEY, T. & SMRKOLJ, V. 2009. The wound healing process: an overview of the cellular and molecular mechanisms. *Journal of international medical research,* 37**,** 1528-1542.
WADAJKAR, A. S., KOPPOLU, B., RAHIMI, M. & NGUYEN, K. T. 2009. Cytotoxic evaluation of N-isopropylacrylamide monomers and temperature-sensitive poly (N-isopropylacrylamide) nanoparticles. *Journal of Nanoparticle Research,* 11**,** 1375-1382.
WAGNER, V. E., GILLIS, R. J. & IGLEWSKI, B. H. 2004. Transcriptome analysis of quorum-sensing regulation and virulence factor expression in Pseudomonas aeruginosa. *Vaccine,* 22**,** S15-S20.
WANG, Y.-W., REN, J.-H., XIA, K., WANG, S.-H., YIN, T.-F., XIE, D.-H. & LI, L.-H. 2012. Effect of mitomycin on normal dermal fibroblast and HaCat cell: an in vitro study. *Journal of Zhejiang University SCIENCE B,* 13**,** 997-1005.
WANG, Z., HOU, Z., WANG, P., CHEN, F. & LUO, X. 2022. CuS-PNIPAm nanoparticles with the ability to initiatively capture bacteria for photothermal treatment of infected skin. *Regenerative Biomaterials,* 9.
WATSON, W. T., MINOGUE, T. D., VAL, D. L., VON BODMAN, S. B. & CHURCHILL, M. E. 2002. Structural basis and specificity of acyl-homoserine lactone signal production in bacterial quorum sensing. *Molecular cell,* 9**,** 685-694.

WEI, Q. & MA, L. Z. 2013. Biofilm matrix and its regulation in Pseudomonas aeruginosa. *International journal of molecular sciences,* 14**,** 20983-21005.
WEINSTEIN, R. A. & MAYHALL, C. G. 2003. The epidemiology of burn wound infections: then and now. *Clinical infectious diseases,* 37**,** 543-550.
WELSH, M. A. & BLACKWELL, H. E. 2016. Chemical probes of quorum sensing: from compound development to biological discovery. *FEMS Microbiology Reviews,* 40**,** 774-794.
WERNER, S., KRIEG, T. & SMOLA, H. 2007. Keratinocyte–fibroblast interactions in wound healing. *Journal of investigative dermatology,* 127**,** 998-1008.
WHITCHURCH, C. B., TOLKER-NIELSEN, T., RAGAS, P. C. & MATTICK, J. S. 2002. Extracellular DNA required for bacterial biofilm formation. *Science,* 295**,** 1487-1487.
WHITEHEAD, N. A., BARNARD, A. M., SLATER, H., SIMPSON, N. J. & SALMOND, G. P. 2001. Quorum-sensing in Gram-negative bacteria. *FEMS microbiology reviews,* 25**,** 365-404.
WHITELEY, M., DIGGLE, S. P. & GREENBERG, E. P. 2017. Bacterial quorum sensing: the progress and promise of an emerging research area. *Nature,* 551**,** 313.
WHOOLEY, M. A. & MCLOUGHLIN, A. J. 1983. The protonmotive force in Pseudomonas aeruginosa and its relationship to exoprotease production. *Microbiology,* 129**,** 989-996.
WINSON, M. K., CAMARA, M., LATIFI, A., FOGLINO, M., CHHABRA, S. R., DAYKIN, M., BALLY, M., CHAPON, V., SALMOND, G. & BYCROFT, B. W. 1995. Multiple N-acyl-L-homoserine lactone signal molecules regulate production of virulence determinants and secondary metabolites in Pseudomonas aeruginosa. *Proceedings of the National Academy of Sciences,* 92**,** 9427-9431.
WINSTANLEY, C. & FOTHERGILL, J. L. 2009. The role of quorum sensing in chronic cystic fibrosis Pseudomonas aeruginosa infections. *FEMS microbiology letters,* 290**,** 1-9.
WOOD, T. L., GONG, T., ZHU, L., MILLER, J., MILLER, D. S., YIN, B. & WOOD, T. K. 2018. Rhamnolipids from Pseudomonas aeruginosa disperse the biofilms of sulfate-reducing bacteria. *NPJ biofilms and microbiomes,* 4**,** 1-8.
WU, C. & ZHOU, S. 1995. Laser light scattering study of the phase transition of poly (N-isopropylacrylamide) in water. 1. Single chain. *Macromolecules,* 28**,** 8381-8387.
XIAO, G., HE, J. & RAHME, L. G. 2006. Mutation analysis of the Pseudomonas aeruginosa mvfR and pqsABCDE gene promoters demonstrates complex quorum-sensing circuitry. *Microbiology,* 152**,** 1679-1686.
XU, F., BYUN, T., DUSSEN, H.-J. & DUKE, K. R. 2003. Degradation of N-acylhomoserine lactones, the bacterial quorum-sensing molecules, by acylase. *Journal of Biotechnology,* 101**,** 89-96.
YADAV, M. K., VIDAL, J. E., GO, Y. Y., KIM, S. H., CHAE, S.-W. & SONG, J.-J. 2018. The LuxS/AI-2 quorum-sensing system of Streptococcus pneumoniae is required to cause disease, and to regulate virulence-and metabolism-related genes in a rat model of middle ear infection. *Frontiers in cellular and infection microbiology,* 8**,** 138.
YAN, J. & BASSLER, B. L. 2019. Surviving as a community: antibiotic tolerance and persistence in bacterial biofilms. *Cell host & microbe,* 26**,** 15-21.
YANG, L., BARKEN, K. B., SKINDERSOE, M. E., CHRISTENSEN, A. B., GIVSKOV, M. & TOLKER-NIELSEN, T. 2007. Effects of iron on DNA release and biofilm development by Pseudomonas aeruginosa. *Microbiology,* 153**,** 1318-1328.
YATES, E. A., PHILIPP, B., BUCKLEY, C., ATKINSON, S., CHHABRA, S. R., SOCKETT, R. E., GOLDNER, M., DESSAUX, Y., CÁMARA, M. & SMITH, H. 2002. N-acylhomoserine lactones undergo lactonolysis in a pH-, temperature-, and acyl chain length-dependent manner during growth of Yersinia pseudotuberculosis and Pseudomonas aeruginosa. *Infection and immunity,* 70**,** 5635-5646.
YAYAN, J., GHEBREMEDHIN, B. & RASCHE, K. 2015. Antibiotic resistance of Pseudomonas aeruginosa in pneumonia at a single university hospital center in Germany over a 10-year period. *Plos one,* 10**,** e0139836.
YI, X.-J., WANG, Y. & FU-SHIN, X. Y. 2000. Corneal epithelial tight junctions and their response to lipopolysaccharide challenge. *Investigative ophthalmology & visual science,* 41**,** 4093-4100.
YOGEV, S., SHABTAY-ORBACH, A., NYSKA, A. & MIZRAHI, B. 2019. Local toxicity of topically administrated thermoresponsive systems: in vitro studies with in vivo correlation. *Toxicologic Pathology,* 47**,** 426-432.

ZHANG, A. & CHU, W.-H. 2017. Anti-quorum sensing activity of Forsythia suspense on Chromobacterium violaceum and Pseudomonas aeruginosa. *Pharmacognosy Magazine,* 13**,** 321.
ZHANG, J., ZHANG, Y.-Z., ZHAO, B.-H., ZHANG, K., LIANG, D.-B., WEI, J., WANG, X.-J., LI, J. & CHEN, G.-H. 2019. Effects of pH on AHL signal release and properties of ANAMMOX granules with different biomass densities. *Environmental Science: Water Research & Technology,* 5**,** 1723-1735.
ZHANG, L., MURPHY, P. J., KERR, A. & TATE, M. E. 1993. Agrobacterium conjugation and gene regulation by N-acyl-L-homoserine lactones. *Nature,* 362**,** 446-448.
ZHANG, X., WU, D. & CHU, C.-C. 2004. Synthesis and characterization of partially biodegradable, temperature and pH sensitive Dex–MA/PNIPAAm hydrogels. *Biomaterials,* 25**,** 4719-4730.
ZHAO, K., DU, L., LIN, J., YUAN, Y., WANG, X., YUE, B., WANG, X., GUO, Y., CHU, Y. & ZHOU, Y. 2018. Pseudomonas aeruginosa quorum-sensing and type VI secretion system can direct interspecific coexistence during evolution. *Frontiers in microbiology,* 9**,** 2287.
ZHAO, X., YU, Z. & DING, T. 2020. Quorum-sensing regulation of antimicrobial resistance in bacteria. *Microorganisms,* 8**,** 425.
ZHU, H., CONIBEAR, T. C., THURUTHYIL, S. J. & WILLCOX, M. D. 2008. Pseudomonas aeruginosa quorum-sensing signal molecules induce IL-8 production by human corneal epithelial cells. *Eye & contact lens,* 34**,** 179-181.
ZHU, J., CHAI, Y., ZHONG, Z., LI, S. & WINANS, S. C. 2003. Agrobacterium bioassay strain for ultrasensitive detection of N-acylhomoserine lactone-type quorum-sensing molecules: detection of autoinducers in Mesorhizobium huakuii. *Applied and Environmental Microbiology,* 69**,** 6949-6953.
ZULIANELLO, L., CANARD, C., KÖHLER, T., CAILLE, D., LACROIX, J.-S. & MEDA, P. 2006. Rhamnolipids are virulence factors that promote early infiltration of primary human airway epithelia by Pseudomonas aeruginosa. *Infection and immunity,* 74**,** 3134-3147.

Appendices

A- Chapter 2

Appendix 1 : polymers images

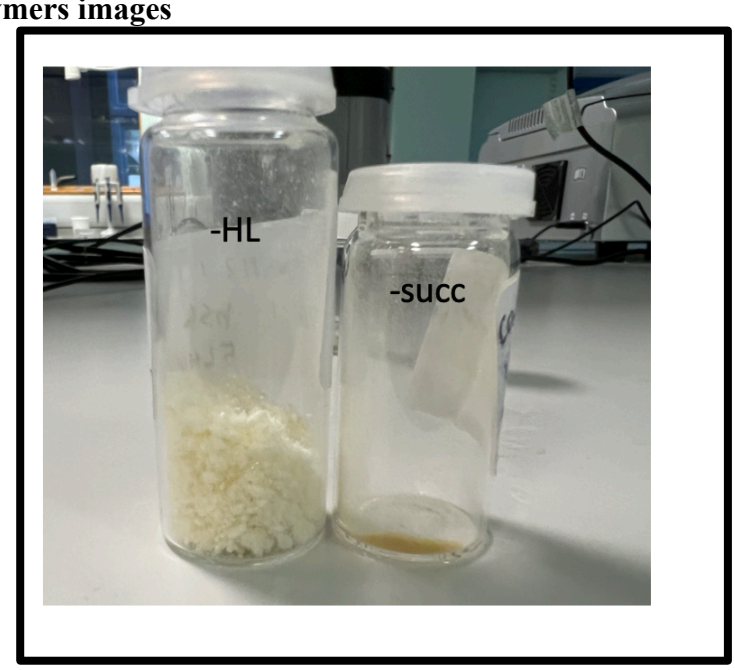

Appendix 2 : Agarose gel of extracted RNA to assess purity and quality. Red squares show RNA of good quality with clear 28S and 18S rRNA band visualization.

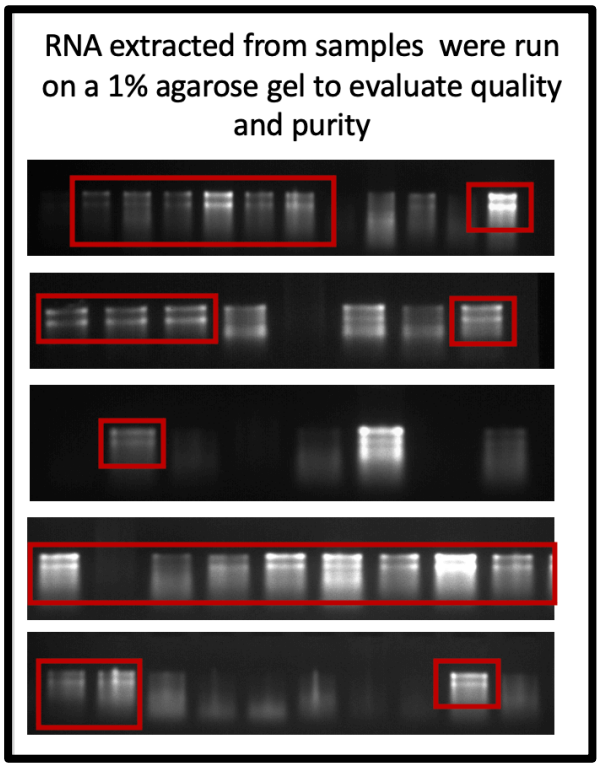

Appendix 3: A graph of different reference genes at different conditions (Treated and untreated) testing the stability of a several reference genes for the bacterium *C.violaceum* CV026. The endogenous gene with the shortest error bars was selected as this indicates that the CT value between treated and untreated treatments is not very large and

therefore the treatment does not target the endogenous gene and provides inaccurate results.

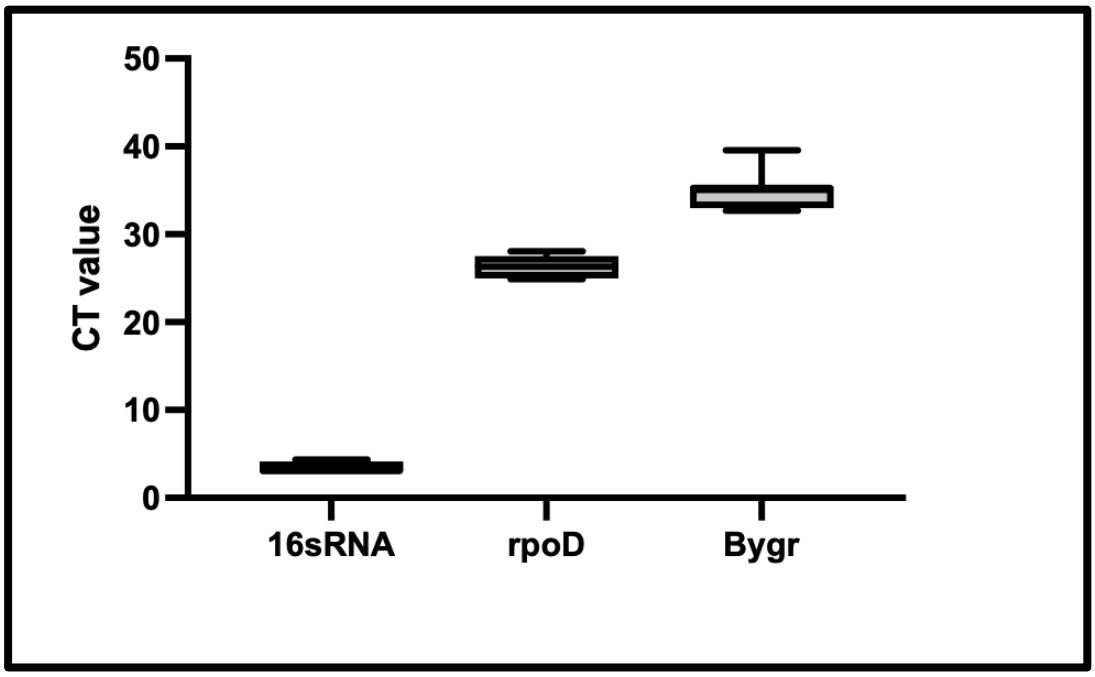

Appendix 4:

1- ANOVA result for results in (Figure 18, B)

ANOVA summary					
ANOVA table	SS	DF	MS	F (DFn, DFd)	P value
Treatment (between columns)	4.779	12	0.3982	F (12, 26) = 15.73	P<0.0001
Residual (within columns)	0.6582	26	0.02531		
Total	5.437	38			

2- ANOVA result for results in (Figure 20, A)

Two-way RM ANOVA	Matching: Both factors				
Source of Variation	% of total variation	P value	P value summary	Significant?	
Row Factor	1.778	0.2615	ns	No	
Column Factor	83.58	0.0023	**	Yes	
Row Factor x Column Factor	1.778	0.2615	ns	No	
Subject x Row Factor	2.066				
Subject x Column Factor	0.3808				
Subject	8.349				
ANOVA table	SS	DF	MS	F (DFn, DFd)	P value
Row Factor	0.07949	3	0.02650	F (3, 6) = 1.721	P=0.2615
Column Factor	3.737	1	3.737	F (1, 2) = 439.0	P=0.0023
Row Factor x Column	0.07949	3	0.02650	F (3, 6) =	P=0.2615

Factor				1.721	

B- Chapter 3

Appendix 5: An agarose gel of PCR products under different annealing temperatures of genes' primers was used in this project.

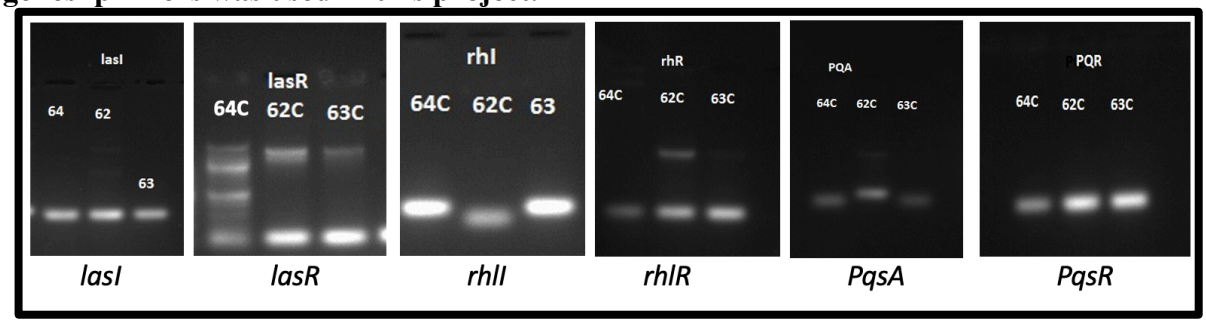

Appendix 6: A graph of different reference genes at different conditions (Treated and untreated) for testing the stability of a several reference genes for the bacterium *P.aeruginosa PAO1*.

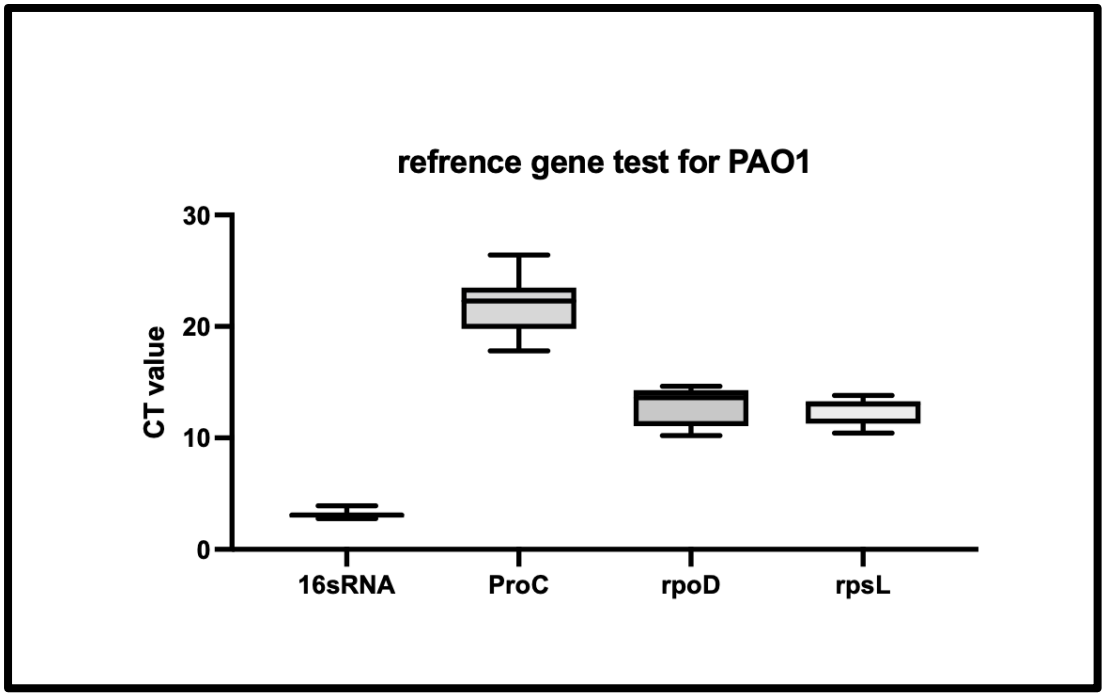

Appendix 7: Replicates of Biofilms grown on a glass coverslip for 18h with different concentration of fluorescence labelled HB-PNIPAM-HL. Scale = 100µm

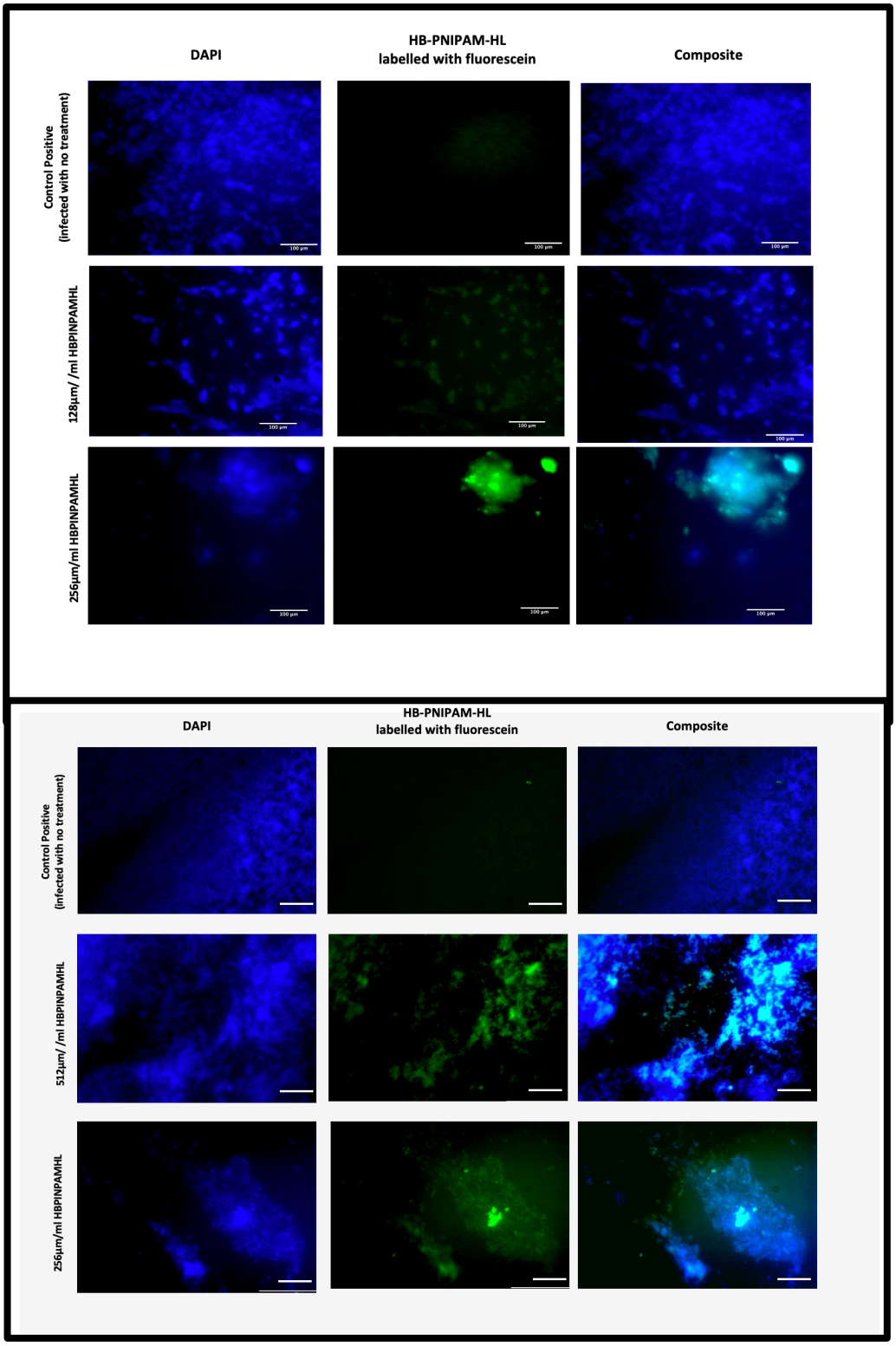
DAPI
HB-PNIPAM-HL
labelled with fluorescein
Composite
Control Positive
(infected with no treatment)
128µm/ /ml HBPINPAMHL
256µm/ml HBPINPAMHL
DAPI
HB-PNIPAM-HL
labelled with fluorescein
Composite
Control Positive
(infected with no treatment)
512µm/ /ml HBPINPAMHL
256µm/ml HBPINPAMHL

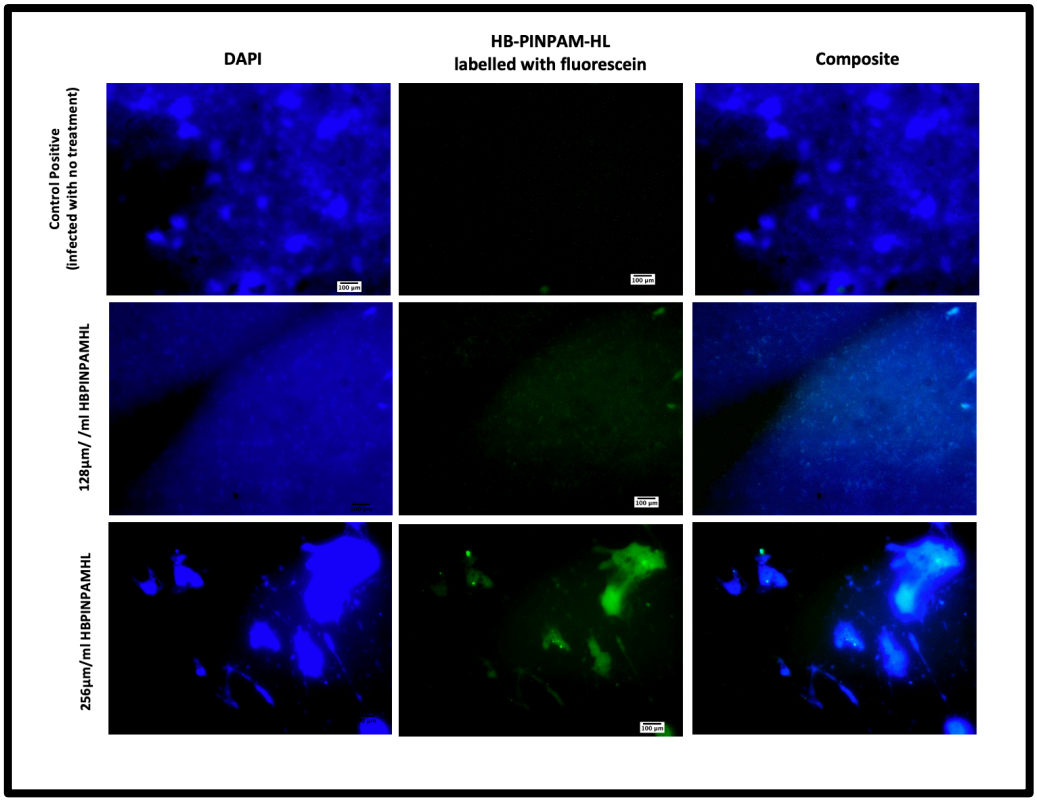

Appendix 8: An agarose gel (1%) of the RT-qPCR products after a run to examine product size in (bp).

Appendix 9: ANOVA report

A- Figure 27

3- Protease (Figure 27. A)

ANOVA summary					
ANOVA table	SS	DF	MS	F (DFn, DFd)	P value
Treatment (between columns)	0.2441	2	0.1221	F (2, 9) = 18.23	P=0.0007

Residual (within columns)	0.06026	9	0.006696		
Total	0.3044	11			

4- Elastase (Figure 27, C)

ANOVA summary					
ANOVA table	SS	DF	MS	F (DFn, DFd)	P value
Treatment (between columns)	5.157	2	2.579	F (2, 9) = 5.699	P=0.0252
Residual (within columns)	4.072	9	0.4524		
Total	9.229	11			

5- Rhamnolipids (Figure 27, E)

ANOVA summary					
ANOVA table	SS	DF	MS	F (DFn, DFd)	P value
Treatment (between columns)	0.9012	2	0.4506	F (2, 9) = 34.25	P<0.0001
Residual (within columns)	0.1184	9	0.01316		
Total	1.020	11			

6- Pyocyanin 18h and 24h (Figure 27, G)

Two-way ANOVA	Ordinary				
ANOVA table	SS	DF	MS	F (DFn, DFd)	P value
Interaction	5.269	2	2.635	F (2, 18) = 54.49	P<0.0001
Row Factor	7.305	2	3.653	F (2, 18) = 75.54	P<0.0001
Column Factor	4.788	1	4.788	F (1, 18) = 99.01	P<0.0001
Residual	0.8704	18	0.04835		

B- ANOVA result for results in (Figure 30, A and C)

1- QPCR for QS genes (Figure 29, A)

Two-way ANOVA	Ordinary				
ANOVA table	SS (Type III)	DF	MS	F (DFn, DFd)	P value
Interaction	0.2273	9	0.02525	F (9, 41) = 1.029	P=0.4341
Row Factor	0.3760	3	0.1253	F (3, 41) = 5.107	P=0.0043
Column Factor	3.263	3	1.088	F (3, 41) = 44.31	P<0.0001
Residual	1.006	41	0.02454		

2- QPCR for VFs genes (Figure 29, C)

Two-way ANOVA	Ordinary				
ANOVA table	SS	DF	MS	F (DFn, DFd)	P value
Interaction	0.3431	6	0.05719	F (6, 24) = 1.886	P=0.1247

Row Factor	0.6523	3	0.2174	F (3, 24) = 7.172	P=0.0013
Column Factor	2.813	2	1.406	F (2, 24) = 46.39	P<0.0001
Residual	0.7277	24	0.03032		

Appendix 10 diagnostic blots. For large-scale expression data such as RNA sequencing, normalisation methods are needed to obtain biological variations originating from the lower end of the detection limit

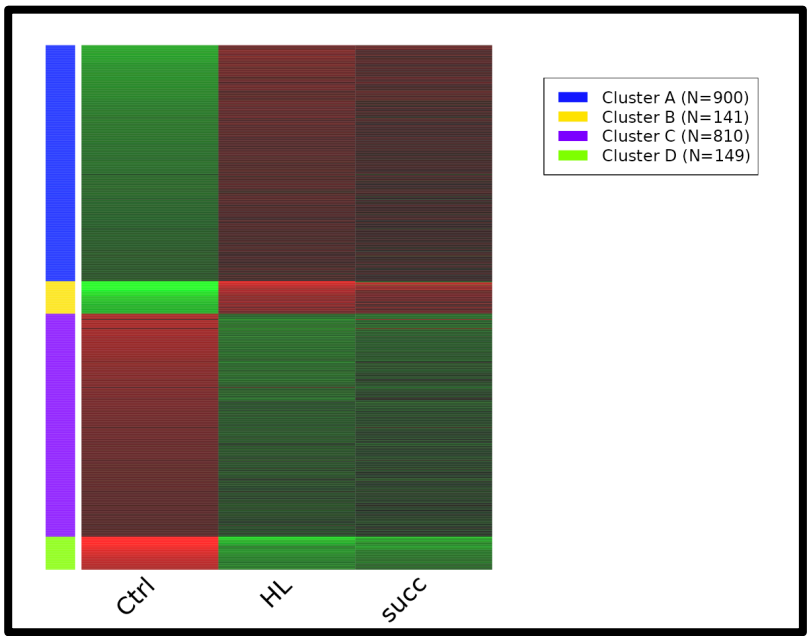

Appendix 11: Classification of up- and down-regulated genes in samples treated with HB-PNIPAM-HL or HB-PNIPAM -succ based on Kyoto Encyclopaedia of Genes and Genomes pathway prediction

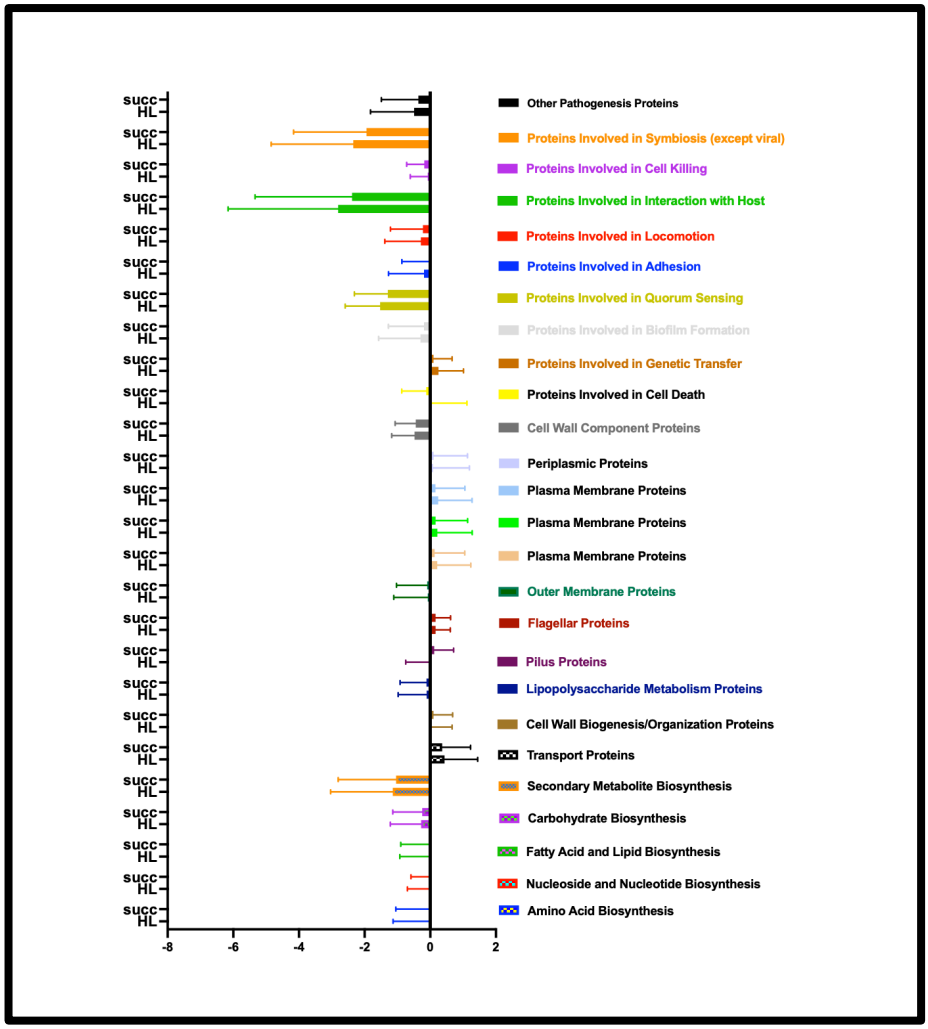

C- Chapter 4

Appendix 12: Screen shots that shows how wound healing assay images were analysed using ImageJ software

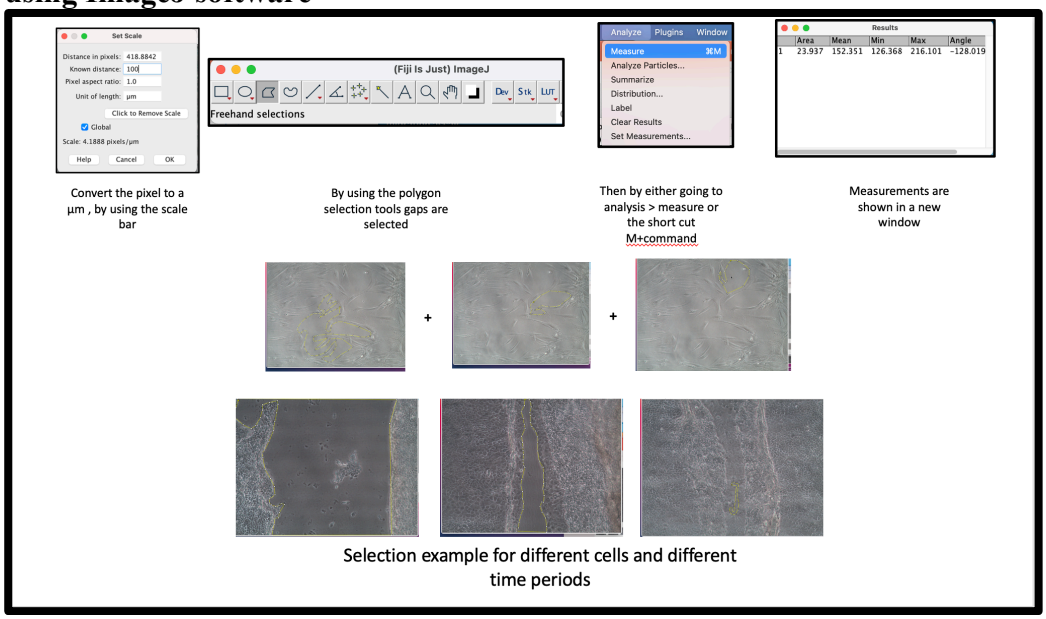

Appendix 13: ANOVA report

A- ANOVA result for results in (Figure 37, A and B)

1- Toxicity of HB-PNIPAM-HL and HB-PNIPAM-succ tested on immortalized human keratinocytes (HaCat)

ANOVA summary					
ANOVA table	SS	DF	MS	F (DFn, DFd)	P value
Treatment (between columns)	3012494708	5	602498942	F (5, 12) = 64.80	P<0.0001
Residual (within columns)	111570590	12	9297549		
Total	3124065298	17			

2- Toxicity of HB-PNIPAM-HL and HB-PNIPAM-succ tested on Human Dermal cells (HDF)

ANOVA summary					
ANOVA table	SS	DF	MS	F (DFn, DFd)	P value
Treatment (between columns)	3623992220	5	724798444	F (5, 12) = 135.3	P<0.0001
Residual (within columns)	64301654	12	5358471		
Total	3688293874	17			

B- ANOVA result for results in (Figure 38, B) and (Figure 39, B)

1- Wound healing assay for HDF after treatments with different concentrations of HB-PINPMA-HL and HB-PNIPAM-succ

ANOVA table	SS	DF	MS	F (DFn, DFd)	P value
Row Factor	46777	2	23388	F (1.032, 2.064) = 69.06	P=0.0129
Column Factor	8188	4	2047	F (1.759, 3.517) = 12.34	P=0.0265
Row Factor x Column Factor	9253	8	1157	F (1.455, 2.910) = 6.345	P=0.0880
Subject x Row Factor	1355	4	338.7		
Subject x Column Factor	1327	8	165.9		
Subject	87.07	2	43.53		
Residual	2917	16	182.3		

2- Wound healing assay for HaCat after treatments with different concentrations of HB-PINPMA-HL and HB-PNIPAM-succ

ANOVA table	SS	DF	MS	F (DFn, DFd)	P value
Row Factor	115994	1	115994	F (1, 4) = 425.6	P<0.0001

Column Factor	397.5	4	99.37	F (4, 16) = 0.1372	P=0.9661
Row Factor x Column Factor	1957	4	489.4	F (4, 16) = 0.7371	P=0.5801
Subject x Row Factor	1090	4	272.6		
Subject x Column Factor	11591	16	724.4		
Subject	819.1	4	204.8		
Residual	10622	16	663.9		

C- ANOVA result for results in (Figure 40, B) and (Figure 41, B)

1- The quantitively data from the M&M showing the CFU after 2h treatment with HB-PNIPAM-HL and -succ

ANOVA summary					
F	3.350				
P value	0.0276				
P value summary	*				
Significant diff. among means (P < 0.05)?	Yes				
ANOVA table	SS	DF	MS	F (DFn, DFd)	P value
Treatment (between columns)	17302591	4	4325648	F (4, 22) = 3.350	P=0.0276
Residual (within columns)	28405067	22	1291139		
Total	45707658	26			

2- The quantitively data from the M&M showing the CFU after 24h treatment with HB-PNIPAM-HL and -succ

ANOVA summary					
F	6.396				
P value	0.0002				
P value summary	***				
Significant diff. among means (P < 0.05)?	Yes				
ANOVA table	SS	DF	MS	F (DFn, DFd)	P value
Treatment (between columns)	38004869	6	6334145	F (6, 29) = 6.396	P=0.0002
Residual (within columns)	28720254	29	990354		
Total	66725123	35			

D- Chapter 5

Appendix 10: the CFU/mg of S.aureus recovered from a 3D skin model treated with 100 l supernatant of untreated P.aeruginosa or with the treated polymer HB-PNIPAM-HL at concentrations of 256 -512 μg/ml.

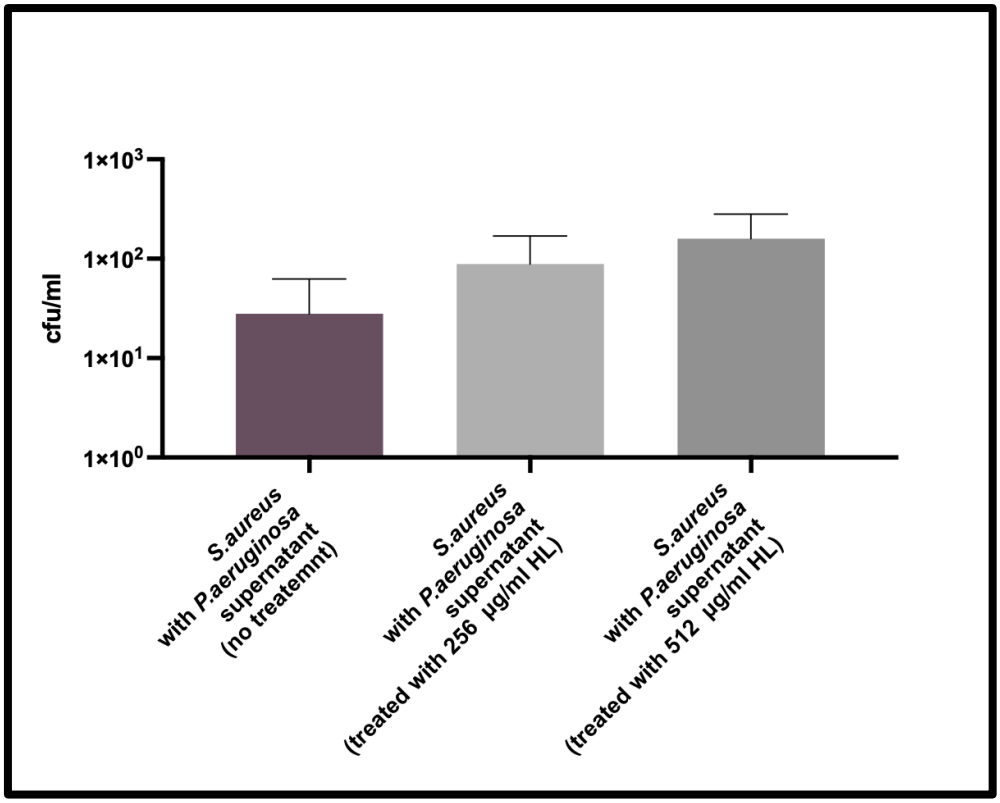
1×10^3
1×10^2
1×10^1
1×10^0
cfu/ml
S.aureus with P.aeruginosa supernatant (no treatemnt)
S.aureus with P.aeruginosa supernatant (treated with 256 µg/ml HL)
S.aureus with P.aeruginosa supernatant (treated with 512 µg/ml HL)